



**HAL**  
open science

# Sexual reproduction and chemical interactions in the parasite *Amoebophrya ceratii* infecting the dinoflagellate host *Scrippsiella acuminata*

Jérémy Szymczak

► **To cite this version:**

Jérémy Szymczak. Sexual reproduction and chemical interactions in the parasite *Amoebophrya ceratii* infecting the dinoflagellate host *Scrippsiella acuminata*. Systematics, Phylogenetics and taxonomy. Sorbonne Université; Friedrich-Schiller-Universität (Iéna, Allemagne), 2023. English. NNT : 2023SORUS650 . tel-04513753

**HAL Id: tel-04513753**

**<https://theses.hal.science/tel-04513753>**

Submitted on 20 Mar 2024

**HAL** is a multi-disciplinary open access archive for the deposit and dissemination of scientific research documents, whether they are published or not. The documents may come from teaching and research institutions in France or abroad, or from public or private research centers.

L'archive ouverte pluridisciplinaire **HAL**, est destinée au dépôt et à la diffusion de documents scientifiques de niveau recherche, publiés ou non, émanant des établissements d'enseignement et de recherche français ou étrangers, des laboratoires publics ou privés.



CNRS • SORBONNE UNIVERSITÉ  
Station Biologique  
de Roscoff



**Sorbonne Université**

École doctorale 227 « Sciences de la Nature et de l'Homme : Évolution et Écologie »  
Station Biologique de Roscoff, CNRS – Sorbonne Université / Adaptation et diversité en Milieu Marin (AD2M),  
UMR 7144 / Équipe Ecology of Marine Plankton (ECOMAP)

**Sexual reproduction and chemical interactions in the parasite  
*Amoebophrya ceratii* infecting the dinoflagellate host  
*Scrippsiella acuminata***

**Par Jérémy Szymczak**

Thèse de doctorat en Écologie Microbienne  
Dirigée par Laure Guillou, co-dirigée Georg Pohnert et co-encadrée par Marine Vallet

Présentée et soutenue publiquement le 14 décembre 2023

Devant un jury composé de :

Julia Kubanek, Rapportrice  
Professor, Georgia Institute of Technology, USA

Assaf Vardi, Rapporteur  
Professor, Weizmann Institute of Science, Israël

Flora Vincent, Examinatrice  
Researcher, EMBL Heidelberg, Germany

Erik Selander, Examineur  
Professor, University of Gothenburg, Sweden

Christophe Destombe, Examineur  
Professor, CNRS/SU – Station Biologique de Roscoff, France

Laure Guillou, Directrice de thèse  
Research director, CNRS/SU – Station Biologique de Roscoff, France

Georg Pohnert, Co-directeur de thèse  
Professor, Friedrich Schiller University Jena – Max Planck Institute for Chemical Ecology, Germany

Marine Vallet, Co-encadrante de thèse  
Researcher, Friedrich Schiller University Jena – Max Planck Institute for Chemical Ecology, Germany



*A Elina et Ezio,*





# Acknowledgements

I would like to thank Julia Kubanek, Assaf Vardi, Flora Vincent, Erik Selander and Christophe Destombe for agreeing to take part in the evaluation of my thesis work.

Merci à Laure de m'avoir transmis sa passion pour ce sujet pendant toutes ces années à Roscoff. Merci beaucoup de m'avoir accompagné jusqu'à la thèse, cette grande aventure scientifique et humaine. Merci de m'avoir encouragé à parfaire mon travail. Tu m'as aussi donné la liberté d'être créatif en science et de développer mes idées.

Thank you to Georg and Marine for opening the door to their laboratory in Germany and bringing chemical ecology to my subject. Thank you for your excellent supervision and for the wonderful time spent in the Jena laboratory. Thank you also for the warm welcome I received from the team. It's been a pleasure working with you and you've given me a tremendous amount of knowledge.

Thank you to Cécile Jauzein, Catharina Alves-de-Souza, Catherine Leblanc and Christophe Destombe for advising me during my thesis committee. Thank you for the wonderful scientific discussions.

Thank you to Ehsan Kayal, Erwan Corre and Catharina Alves-de-Souza for supervising my master's internship. These experiences were very enlightening and greatly contributed to the success of my thesis.

I would like to thank the many co-authors of my thesis and from other publications. Without you it would not have been possible to produce such a great work. I have learnt so much from working with you.

Merci Estelle Bigeard de m'avoir formé et aidé depuis le début (depuis janvier 2016). J'ai beaucoup appris grâce à toi.

Merci à tous les membres de l'équipe ECOMAP pour leur soutien. Je remercie Dominique M. et Martin G. pour leurs précieux conseils, j'ai beaucoup appris sur la cytométrie en flux. Je suis heureux d'avoir eu la chance de travailler avec vous.

Merci à tous les membres de la Station Biologique de Roscoff, aux collègues et aux amis pour leur soutien. Merci à Brigitte et à Paula qui font un travail formidable. Merci

également au personnel du Gulf Stream pour le service de qualité et l'accueil chaleureux.

Thanks to the DAAD for the travel grant. Merci au programme doctoral "IPV" pour la bourse de thèse. Merci à l'école doctorale 227 pour votre soutien, votre bonne humeur, vous êtes super !

Merci aux plateformes de la Station (METABOMER, MERIMAGE, RCC) qui m'ont aidé dans mon travail de thèse.

Mon aventure roscovite a commencé bien avant la thèse. Depuis mon premier stage dans l'équipe ECOMAP à la SBR en 2016 (ça fait donc environ 8 ans) j'ai croisé la route de beaucoup de personnes formidables. Laure A., Alexis, Héloïse, Marine M., vous étiez mes ami.es de la première heure ! Vous m'avez bien fait découvrir la vie étudiante de Roscoff et bien sûr vous m'avez donné envie de suivre vos pas et de poursuivre mes ambitions jusqu'à la thèse ! Et puis il y a eu PYM, Ulysse, Camille TB, Victor, Damien, Flo, Mathilde B., Emilie, Ewen, Martin avec qui j'ai passé d'excellents moments à la station mais aussi en dehors !

Merci aux membres (actuels et anciens) de l'équipe « PK » Flo, Fabienne, Anne-Claire, Aurélie, Laurence, Christian, Christophe, Sarah R., Sarah G., Adriana, Nathalie, Mathilde F., Greg, Céline, Iris, Momo, Pris, Ian, Colomban, Joost, Michele, Daniel, Léna, Katell, Thibaut (avec qui j'ai bien rigolé en 2016 et qui est toujours un ami aujourd'hui), Solène, Hugo, Margot, Théophile, Martina, Delphine, Clémence, Fred, et Dominique (Maître Cyto). Cette équipe est comme une grande famille, on s'y entraide et l'ambiance y est bonne.

En 2018, en IGM3, merci à Delphine et Guita pour ces super moments et belles discussions. (Vive le code !)

Merci à Charles et Fabrice pour les discussions scientifiques et plus encore et aussi pour m'avoir présenté à la troupe de Théâtre de Roscoff, avec qui j'ai passé de belles soirées.

Je tiens particulièrement à remercier Eléna K., Michaela D.L.C. et Julie L. pour leur travail au laboratoire, vous avez tous contribué à la réussite de ma thèse.

Avec des aller-retours à la station, j'ai croisé plusieurs bandes. Merci à Mariana pour ton soutien à toute épreuve. On s'est bien amusé avec Mariarita, Fabien, Nico, Lydia,

Valeria, Catherine, Rafael, Miguel et Marie W., Greg, Jukka, Cédric, Jasna, Cristina, Marieke.

Vielen Dank an Mimi, Vera, Liuba, Johann, Justus, Janine und O'Hanna für euren herzlichen Empfang in Jena. Thank you Guy as well. Thank you to my friend in Galway, Sofi !

Mes très cher ami.es « de thèse » m'ont fait me sentir bien à Roscoff : Lisa, Louison, Yasmine, Aurélien, Sam B., Roman, Aline, Emma, Erwan L., Momo G. et mon cousin Douglas. Sans vous, Roscoff aurait été bien vide. Sans oublier, Yacine, Jade C., Guillaume C. et Guillaume L.B., Clément, PG, Soph, Camilles P., Jana, Dan, Marianne, Liz, Sylvie, Charlotte B., Pélagie, et j'en oublie sûrement.

Merci à ma binôme de bureau Marine, merci pour être comme tu es, ne change pas. Tu es une personne au top. J'espère que nos chemins se croiseront à nouveau. J'espère que tu vas bien bronzer dans le Sud. Et aussi, merci à Rafaele, super collègue du bureau de la teuf ! Et merci pour ton aide avec la micro fluidique !

Et les « jeunes » de la station comme je vous appelle secrètement, ma « dernière bande » de copains : Pierre, Julie, Elisa, Heliaz, Antonin, Clarisse, Emile, Pauline, Sam O., Tanguy, Tanweer, Guilhem, Théo (lui moins jeune, si je peux me permettre). Merci X10 Julie pour ton aide et bonne humeur au labo. Merci Sonia pour ton soutien, tu m'as épaulé, ta présence est très précieuse pour moi. Merci infiniment.

My dear Singaporean friends la, Denise and Clarence, I am glad I have met you. I had an excellent summer 2023 with you Clarence in Roscoff!

Merci à mes ami.es de master OEM de l'UPMC, en particulier Alex, Valentin L., Ilan, Melissa, Felix, Guillaume, Etienne, Marie, Rémi, Marine, Marine, Pauline, Pierre, Salomé, Clara, Benjamin et tous les autres.

Mes ami.es de longue date, mes inqualifiables Tom, Viki, Diane, Benjamin, Lisa, Vivien, Juliette, Arthur, Valentin, Coralie, Emma, Sarah, Gilles, Flavy, merci pour votre soutien. Merci aussi à Marie W., Lucas, Diane W., Valentin S..

Merci à ma famille pour votre grand soutien, mes parents, ma sœur et mon beau-frère et leurs beaux enfants, mes grands-parents, mon oncle et mes tantes.



# Table of contents

<b>Acknowledgements</b> .....	<b>5</b>
<b>Table of contents</b> .....	<b>9</b>
<b>List of figures</b> .....	<b>13</b>
<b>General introduction</b> .....	<b>17</b>
I. Scientific background.....	17
Science in a burning world .....	17
Marine plankton.....	18
Functional roles and ecological relevance.....	20
Symbiosis .....	22
Chemical interaction.....	25
II. Objectives, biological model and structure of the thesis project.....	27
General questions .....	27
General objectives.....	28
III. Biological models used in this thesis.....	28
Myzozoa .....	28
Dinoflagellates.....	29
The parasite of the <i>Amoebophrya</i> genus.....	31
Life cycle of the parasite <i>A. ceratii</i> .....	35
Historical description of the <i>Amoebophrya</i> genus .....	37
Structure of the manuscript .....	39
IV. References .....	41
<b>Chapter 1: First evidence of sexual reproduction in a widespread protist parasite infecting marine dinoflagellates</b> .....	<b>49</b>
Context of the study.....	49
Authors contribution.....	49
Article 1: A sexual stage in a widespread dinoflagellate parasite.....	51
Abstract .....	52
Introduction.....	52
Material and Methods .....	54
Results .....	64
Discussion .....	76
Acknowledgments .....	81

References .....	82
Supplementary data .....	87
<b>Chapter 2 : Metabolome dynamics during intracellular dinoflagellate infection emphasizes the role of azelaic acid in host resistance.....</b>	<b>99</b>
Context of the study.....	99
Authors contribution.....	99
Article 2: Metabolome dynamics during intracellular dinoflagellate infection emphasizes the role of azelaic acid in host resistance.....	100
Abstract .....	100
Introduction.....	101
Materials and methods .....	104
Results .....	111
Discussion .....	121
Conclusion.....	126
Acknowledgments .....	126
References .....	127
Supplementary Data.....	129
<b>Chapter 3 : Chemotaxis of the dinoflagellate parasite towards the chemical cues of its host .....</b>	<b>131</b>
Context of the study.....	131
Authors contribution.....	131
Article 3: Chemotaxis of the dinoflagellate parasite towards the chemical cues of its host.....	132
Abstract .....	132
Introduction.....	132
Materials and methods .....	134
Results .....	139
Discussion .....	143
Conclusion.....	145
Acknowledgments .....	146
References .....	146
Supplementary Data.....	147
<b>General discussion .....</b>	<b>149</b>
Personal motivation and origin of the project.....	149
The progress of my PhD thesis: a journey filled with challenges and opportunities.....	150

The major discoveries I made during my thesis and perspectives. ....	153
Conclusions.....	155
References .....	157
<b>Thesis Supplementary Document 1 .....</b>	<b>159</b>
Dinophyceae can use exudates as weapons against the parasite Amoebophrya sp. (Syndiniales). ....	159
<b>Thesis Supplementary Document 2.....</b>	<b>171</b>
Use of flow cytometry (Novocyte Advanteon) to monitor the complete life cycle of the parasite Amoebophrya ceratii infecting its dinoflagellate host.....	171
<b>Thesis Supplementary Document 3 .....</b>	<b>189</b>
Comparative biology and ecology of apicomplexans and dinoflagellates: a unique meeting of minds and biology .....	189
<b>Thesis Supplementary Document 4 .....</b>	<b>199</b>
Amoebophrya ceratii .....	199
<b>Abstracts .....</b>	<b>207</b>
<b>Résumé.....</b>	<b>203</b>
<b>Résumé long en français .....</b>	<b>207</b>





# List of figures

## General Introduction

Figure 0-1: From Intergovernmental Panel On Climate Change, 2023. History of global temperature change and causes of recent warming. ....	17
Figure 0-2: From Sieburth et al., 1978. Distribution of different taxonomic-trophic compartments of plankton in a spectrum of size fractions, with a comparison of size range of nekton.....	19
Figure 0-3: From de Vargas et al., 2015. Illustration of key eukaryotic plankton lineages. ....	21
Figure 0-4: From Tipton et al., 2019. Biological interactions and the symbiotic relationship continuum.....	23
Figure 0-5: From Muñoz-Gómez and Slamovits, 2018. A schematic phylogeny of the Myzozoa. ....	30
Figure 0-6: From Gómez, 2012. Diversity of major lineages of dinoflagellates.....	32
Figure 0-7: Few representations of the Amoebophrya genus parasite in the past 150 years.....	34
Figure 0-8: From Chambouvet et al 2011. Interactions between Scrippsiella acuminata and Amoebophrya sp. life cycles.....	35
Figure 0-9: from Cachon and Cachon 1987. Diagram of the life cycle of Amoebophrya .....	38

## Chapter 1: First evidence of sexual reproduction in a widespread protist parasite infecting marine dinoflagellates

Figure 1- 1:The intracellular development of the parasite Amoebophrya ceratii within its host, Scrippsiella acuminata, as monitored using flow cytometry. ....	65
Figure 1- 2:Flow cytometry used to monitor spore populations, namely P1, P2, and P3, at various time points following inoculation. ....	67
Figure 1- 3: Transmission electron microscopy (TEM) was employed to examine P1 (left) and P2 (right) spores using various techniques.....	69
Figure 1- 4: Swimming behaviour of P1 and P2 spores.....	70
Figure 1- 5: Decision-support hierarchical model based on 149 infection experiments. ....	71
Figure 1- 6: Multivariate analysis of selected metabolites.....	73
Figure 1- 7: Analysis of sorted populations using flow cytometry. ....	75

### Supplementary data Chapter 1

Figure S1- 1: Release of dinospores from 35.5 to 39 hours. ....	87
Figure S1- 2: The different dinospore types released from single infected host cells. ....	88

Figure S1- 3: Bimodal distribution of cell sizes in a mixed population of dinospores, as assessed by confocal microscopy. ....	89
Figure S1- 4: Flow cytograms from the five replicates prior to their use in estimating swimming behavior. ....	89
Figure S1- 5: Swimming trajectories of P1 and P2. P1 swims straight forward, while P2 exhibits helical motion with a large loop. ....	90
Figure S1- 6: Evolution of dinospores and host used for infectivity tests in June 7th, 2021.....	90
Figure S1- 7: Dinospore populations (P1 at left and P2 at right) sorted by flow cytometry prior to their use for infectivity tests (on February 23th 2023). ....	91
Figure S1- 8: Ploidy level of mixed populations of dinospores as observed by flow cytometry. ....	91
Figure S1- 9: Mating pairs experiment using three strain of the same species (MALVII Clade 2 Sub-clade 4). ....	92
Figure S1- 10: Scheme displaying the metabolomics workflow. ....	93
Figure S1- 11: Carbon content (dinospores and bacteria) estimated in endometablome samples.....	94
Figure S1- 12: Cytograms of cultures used for the metabolomic analyses. ....	94
Figure S1- 13: Analyses conducted on selected metabolites. ....	95
Figure S1- 14: Gates used for sorting infected host cell (20 cells per well) for transcriptomic analyses. ....	96
Figure S1- 15: Gates used for sorting dinospores (10 cells per well) for transcriptomic analyses. ....	96
Figure S1- 16: Heatmap analyses of gene expression along the course of infection.....	97
Table S1- 1:Metadata linked to samples collected for electronic microscopy analyses. ....	87
Table S1- 2: Counts of bacteria and dinospores in samples collected for metabolomics analyses, and % of P1 dinospores compared to P2. ....	93
Table S1- 3: Gene orthologues in Amoebophrya genome A120 for genes involved in meiosis. ....	98

**Chapter 2: Metabolome dynamics during intracellular dinoflagellate infection emphasizes the role of azelaic acid in host resistance**

Figure 2- 1: The general workflow from the culture of infected hosts to metabolomic analysis and bioassay.....	104
Figure 2- 2: Linear regression between prevalence and the percentage of P1 dinospores produced (on the total number of dinospores) during sampling for metabolomics analyses. ....	113
Figure 2- 3: Multivariate distribution from PLS-DA.....	114
Figure 2- 4: Venn diagrams illustrating the count of significant increasing endometabolites along the infection course.....	116

Figure 2- 5: Venn diagrams illustrating the count of significant decreasing endometabolites along the infection course.....117

Figure 2- 6: : Intensities of DMSP (A) and azelaic acid (B) at the three stages of infection in all samples.....118

Figure 2- 7: Formal identification of the azelaic acid (left panel) and correlation between the relative intensity of azelaic acid at intermediate stage and prevalence (right panel). .....119

Figure 2- 8: Survival of dinospores P1 and P2+3 and growth of the host and its microbiota .....120

Table 2- 1: Metadata for endo- and exometabolomes: estimation of relevant parameters and cell densities during the course of infection in the biological replicates. ....112

Table 2- 2: List of exo-metabolites associated with production by infected hosts at a late stage of infection, according to ANOVA, with corresponding identification in the endo-metabolites. ....119

Table 2- 3: Effect of azelaic acid (at 0, 100, 200  $\mu$ M), host exudate (Hext) and parasite exudate (Pext) on the density of parasites and prevalence after 8 hours of infection (CARD-FISH counts) and prevalence after 24 hours (flow cytometry). .....121

**Chapter 3 : Chemotaxis of the dinoflagellate parasite towards the chemical cues of its host**

Figure 3- 1: Chemotactic index (Ic) from the ISCA. ....140

Figure 3- 2: Comparison of age of dinospores and the Ic of P1 type dinospores in the 1 mg / mL of host exometabolites treatment in the ISCA experiments .....141

Figure 3- 3: Toxicity assays .....142

Table 3- 1: List of experiments with the conditions and objectives with the ISCA....137



# General introduction

## I. Scientific background

### Science in a burning world

Human activities, particularly since the industrial revolution in the 1850's, have changed the atmospheric composition, notably the greenhouse gas levels, e.g. the carbon dioxide (CO<sub>2</sub>) level (Intergovernmental Panel On Climate Change, 2023). While greenhouse gases are perfectly useful in regulating the Earth's temperature and making it favourable to life, their increase are rapid, exceeding natural fluctuation that occur on geological scales.

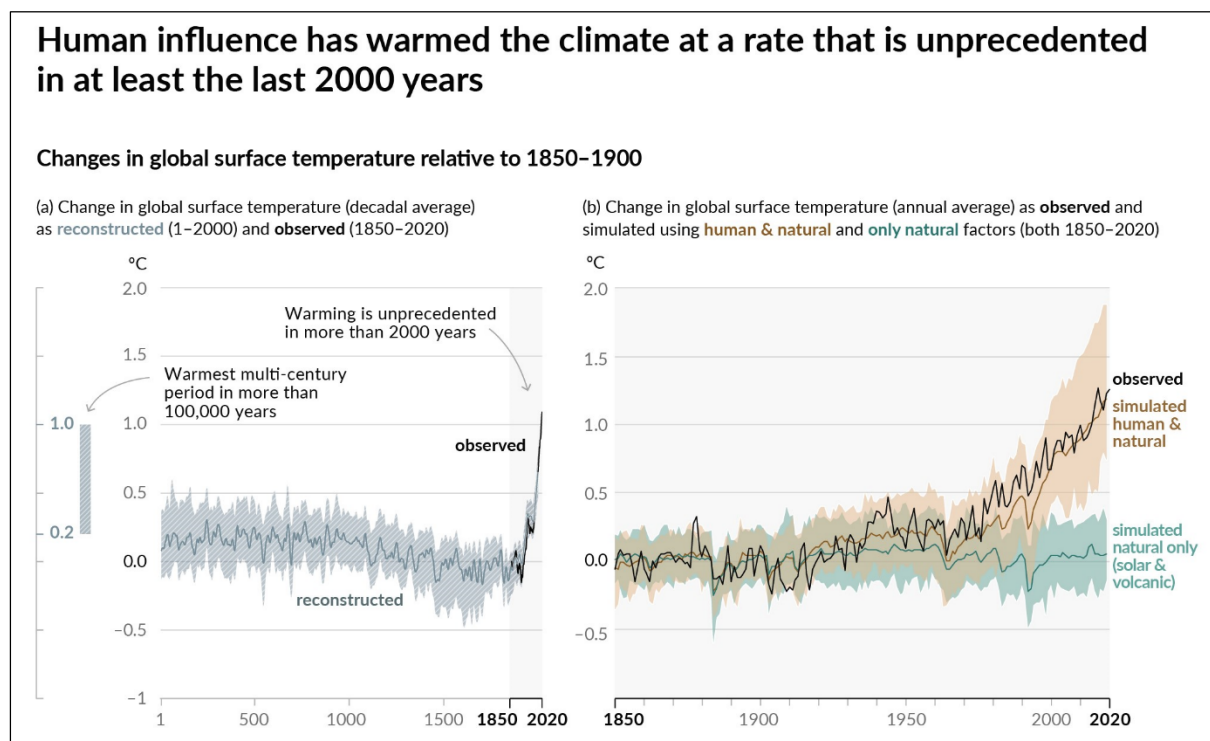


**Figure 0-1: From Intergovernmental Panel On Climate Change, 2023. History of global temperature change and causes of recent warming.**

Panel (a) Changes in global surface temperature reconstructed from paleoclimate archives (solid grey line, years 1–2000) and from direct observations (solid black line, 1850–2020), both relative to 1850–1900 and decadal averaged. The vertical bar on the left shows the estimated temperature (very likely range) during the warmest multi-century period in at least the last 100,000 years, which occurred around 6500 years ago during the current interglacial period (Holocene). The Last Interglacial, around 125,000 years ago, is the next most recent candidate for a period of higher temperature. These past warm periods were caused by slow (multi-millennial) orbital

## General Introduction

variations. The grey shading with white diagonal lines shows the very likely ranges for the temperature reconstructions. Panel (b) Changes in global surface temperature over the past 170 years (black line) relative to 1850–1900 and annually averaged, compared to Coupled Model Intercomparison Project Phase 6 (CMIP6) climate model simulations (see Box SPM.1) of the temperature response to both human and natural drivers (brown) and to only natural drivers (solar and volcanic activity, green). Solid coloured lines show the multi-model average, and coloured shades show the very likely range of simulations.

Increased CO<sub>2</sub> level ultimately raises the average atmosphere and ocean temperatures. Observations and modelling demonstrate that the current global atmosphere temperature is over one degree Celsius higher than the average temperature of the previous 2,000 years (Fig. 0-1). By cascading effect, the glaciers and sea ice formation and coverage are decreasing, water level is raising, the oceanic currents are modifying, the water stratification is increasing and the water chemistry is changing. As a result, the species distribution will be affected, and so will the biological interactions. Some species will move to new areas where they might survive, die or thrive; becoming non-indigenous species that could become invasive. Furthermore, human actions such as the discharge of ballast water, plastic pollution (Barnes, 2002; Guzzetti et al., 2018; Masó et al., 2003) and aquarium organisms could serve as sources of novel invasive species (Padilla and Williams, 2004). Invasive species are deleterious for local biodiversity equilibrium and are also the cause of large economical loss like in the USA with the zebra mussels (Strayer, 2009) or with the comb jelly fish *Mnemiopsis leidyi* in the Caspian Sea (Ivanov et al., 2000).

The impacts on the biosphere are so drastic that the changes might lead to the sixth mass extinction of species (Barnosky et al., 2011).

In order to better understand the consequences of human activities and anticipate the modifications of ecosystems, fundamental sciences aim to understand how ecosystems functioned in the past and how they function today. The ocean is a crucial environment for the Earth as well as all marine organisms.

### **Marine plankton**

The term plankton was created by the German marine biologist Victor Hensen in 1887, with Greek roots and could be translated as “marine drifter”. Indeed, plankton refers to

## General Introduction

all organisms present in the water column that move due to currents. Plankton is present in every drop of the ocean, from the bottom to the top, from the poorer to the richer waters. Planktonic organisms are highly diverse, highly polyphyletic, and very different in sizes, lifestyles and ecological roles. They also include many fixed, floating or swimming organisms that are, at some stage in their life cycle, planktonic. For instance, the eggs and larvae of many animals such as fish, molluscs, crustaceans and worms are planktonic and play an important role in the water column. To better categorize different types of plankton, it is common to sort them by size classes (Fig. 0-2) and by lifestyle (Sieburth et al., 1978). The Sieburth classification proposes a general classification of the planktonic organisms based on size (femto-, pico-, nano-, micro-plankton and so on), and traits as viro-, bacterio- myco and phyto-plankton. This classification, even not perfect, is still widely used in modern methods studying plankton. For instance, phytoplankton play a crucial role being primary producers, although this category also contains a lot of predators (myxotrophs).

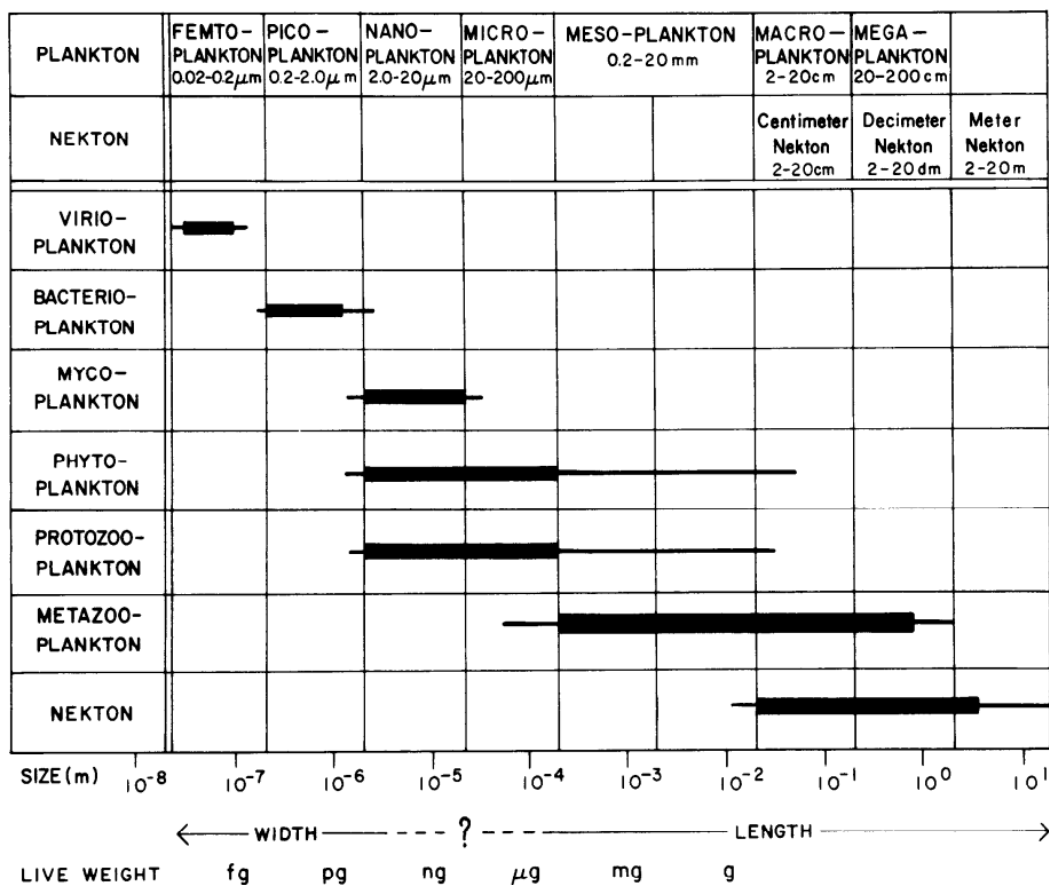


Figure 0-2: From Sieburth et al., 1978. Distribution of different taxonomic-trophic compartments of plankton in a spectrum of size fractions, with a comparison of size range of nekton.



## General Introduction

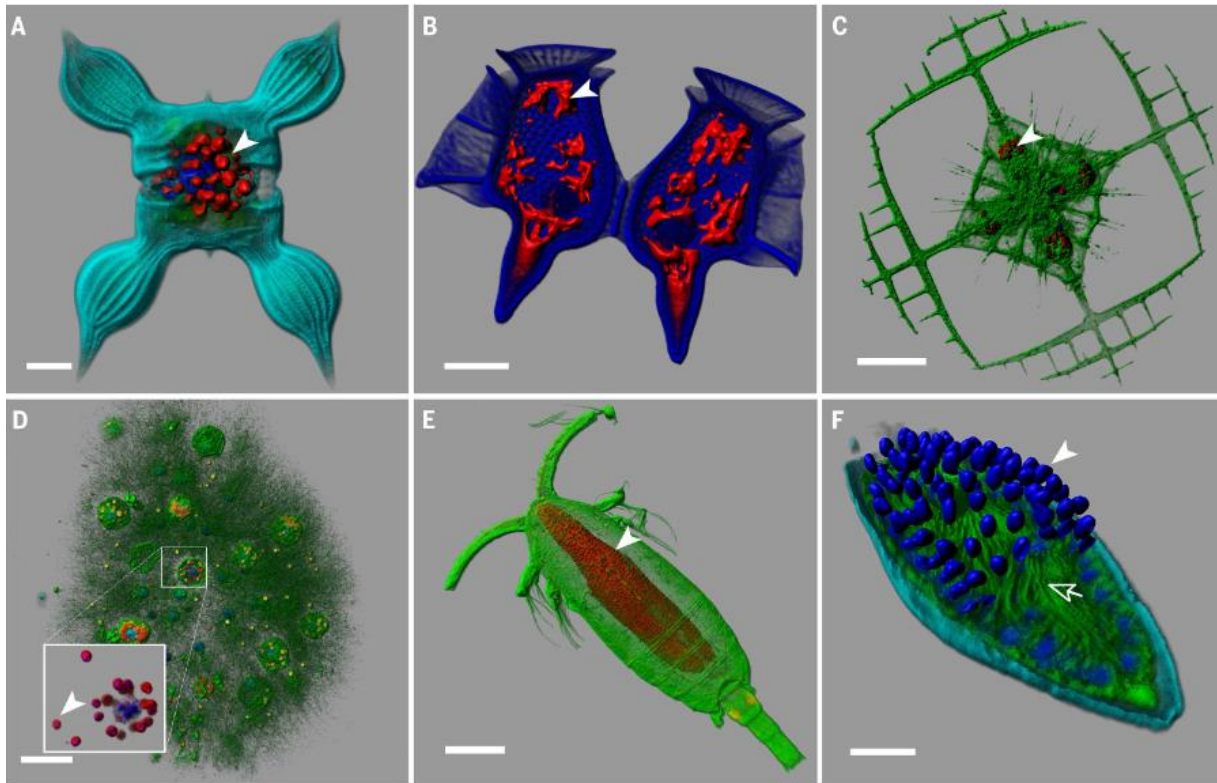
This is the case for numerous microalgae dinoflagellates. Some other mixotrophs are heterotroph hosts in symbiosis with a symbiont micro-alga as some radiolarians, e.g. acantharian (heterotroph) – *Phaeocystis* (photoautotroph) symbiosis (Fig. 0-3C). The classification of organisms according to their ecological traits and roles into 'functional groups' is a useful method for better understanding doing modeling and numerical ecology.

### **Functional roles and ecological relevance**

Among plankton, microbes (<100  $\mu\text{m}$  in size) are dominating. They play a key role in the oceans, and therefore on the planet (Falkowski et al., 2008). Marine microbes account for approximately two-thirds of the biomass, the rest consisting in plants and animals, including a large proportion of zooplankton (Bar-On and Milo, 2019). In terms of functional roles, microbes are also strongly involved in the trophic web and in biogeochemical cycles. For example, photosynthetic organisms are important for the carbon and oxygen cycles, producing  $\text{O}_2$  and using  $\text{CO}_2$ . Phytoplankton organisms are able to fix inorganic  $\text{CO}_2$  to produce biomass, using light energy. Even if they only represent less than one percent of the biomass, they produce about half of the net primary production on Earth (Field et al., 1998). Zooplankton grazes on the phytoplanktons and thus controls their population. In addition, some microbes are involved in the nitrogen cycle, mostly bacteria and archaea. The nitrogen fixers, also called diazotroph organisms, mainly cyanobacteria, are involved in the reduction of the  $\text{N}_2$  to ammonium, an important source of nitrogen for a lot of organisms. The nitrifiers oxidise ammonium producing nitrate. Whereas, the denitrifiers produce  $\text{N}_2$  or  $\text{N}_2\text{O}$  via the oxidation of ammonium or the reduction of nitrate. In addition to the carbon and nitrogen cycles, marine organisms are strongly involved in the phosphorus cycle, a crucial and abundant element for biology, moving it from inorganic to organic and bio-available forms. In contrast with these abundant elements, some organisms harbour rare elements, e.g. to form specific cellular "skeletons". As the radiolarians that produce shells made of strontium sulphate. Less rare but quite remarkable, diatoms produce frustule made of silicate and coccolithophores and foraminifera produces skeletons made of calcium carbonate. Finally, plankton depends on metal present in trace in the ocean to produce specific important cellular components like for example the

## General Introduction

chlorophyll a, the universal photosynthetic pigment, composed by an atom of magnesium. Among the trace metals useful for biological reaction, there are zinc,



magnesium, nickel, copper, and cadmium for example.

### Figure 0-3: From de Vargas et al., 2015. Illustration of key eukaryotic plankton lineages.

(A) Stramenopila; a phototrophic diatom *Chaetoceros bulbosus*, with its chloroplasts in red (arrowhead). Scale bar, 10  $\mu\text{m}$ . (B) Alveolata; a heterotrophic dinoflagellate *Dinophysis caudata* harboring kleptoplasts [in red (arrowhead)]. Scale bar, 20  $\mu\text{m}$  (75). (C) Rhizaria; an acantharian *Lithoptera* sp. with endosymbiotic haptophyte cells from the genus *Phaeocystis* [in red (arrowhead)]. Scale bar, 50  $\mu\text{m}$  (41). (D) Rhizaria; inside a colonial network of *Collodaria*, a cell surrounded by several captive dinoflagellate symbionts of the genus *Brandtodinium* (arrowhead). Scale bar, 50  $\mu\text{m}$  (33). (E) Opisthokonta; a copepod whose gut is colonized by the parasitic dinoflagellate *Blastodinium* [red area shows nuclei (arrowhead)]. Scale bar, 100  $\mu\text{m}$  (51). (F) Alveolata; a cross-sectioned, dinoflagellate cell infected by the parasitoid alveolate *Amoebophrya* (MALV-II). Each blue spot (arrowhead) is the nucleus of future free-living dinospores; their flagella are visible in green inside the mastigocoel cavity (arrow). Scale bar, 5  $\mu\text{m}$ . The cellular membranes were stained with DiOC6 (green); DNA and nuclei were stained with Hoechst (blue) [the dinoflagellate theca in (B) was also stained by this dye]. Chlorophyll autofluorescence is shown in red [except for in (E)]. An unspecific fluorescent painting of the cell surface (light blue) was used to reveal cell shape for (A) and (F). All specimens come from Tara Oceans samples preserved for confocal laser scanning fluorescent microscopy. Images were three-dimensionally reconstructed with Imaris (Bitplane).

## General Introduction

As biological activity in the oceans is fully involved in biogeochemical cycles, it is valuable to study the interactions between organisms. It is relevant to examine biotic interactions in marine plankton, as all organisms play a role in various ecological relationships, such as predator, prey, host, symbiont, competitor or other types of partner. For instance, despite the relatively recent discovery of the abundance of viruses in oceans (Bergh et al., 1989), they highly impact their hosts, and thus the entire ecosystem. Infected bacteria, representing up to 20 to 40% of total bacteria, exhibit modified metabolisms due to the integration of the viral genes (Howard-Varona et al., 2020).

## Symbiosis

Initially introduced by Anto De Barry in 1879 in his book “Die Erscheinung der Symbiose”, symbiosis was for a long time synonym of mutualism, but today this term includes more than one type of interaction. Today, the definition of symbiosis still lacks consensus among biologist (Bradford. D. Martin and Schwab, 2012 A; Bradford D. Martin and Schwab, 2012 B; Smith, 2001). However, symbiosis could be defined as followed: “a significant biological unilateral or bilateral relationship that is defined as a close (in terms of physical distance and interaction between host and symbiont) and long-lasting (generation after generation of host and symbiont in association) relationship between organisms” (Faust and Raes, 2012; Overstreet and Lotz, 2016; Tipton et al., 2019). The symbiosis type is defined by the level of mutual benefit that results from the relationship. This level can be represented as a continuum (Fig. 0-4) which is a dynamic, flexible and changing relationship between the host and the symbiont according to their individual physiological state and environment.

For instance, if both partners benefit from the interaction, the relationship is a mutualistic symbiosis. On the other hand, if only one partner benefits while the other neither gains nor loses, it is a commensal symbiosis. If the host suffers negative effects from the interaction, ranging from a minor disadvantage to the death of the host, it is a parasitic interaction. When the host's death is necessary at some point during the infection cycle, the parasite is known as a parasitoid. The cost or benefice for the host is variable and a symbiosis can shift from mutualistic to parasitic. This can be illustrated by the relationship between the dinoflagellate *Symbiodinium* and its jellyfish host:

## General Introduction

where horizontal transmission can lead to parasitic relationship whereas vertical transmission lead to symbiotic relationship (Sachs and Wilcox, 2006).

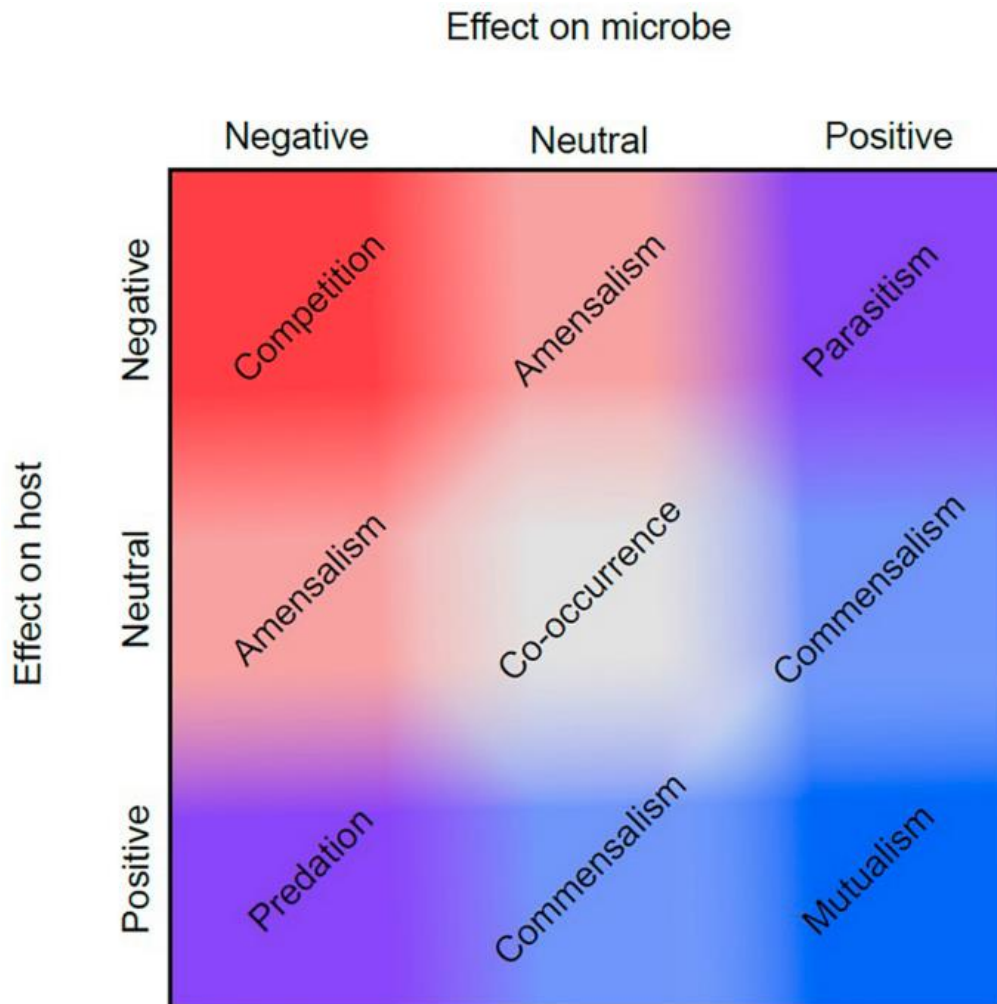


**Figure 0-4: From Tipton et al., 2019. Biological interactions and the symbiotic relationship continuum.**

Symbiotic relationships encompass multiple dimensions of effect, represented here on two axes. If a symbiosis has a positive (blue) effect for a microbe, and a negative (red) effect for the host, this is known as parasitism (top right corner). However, each type of symbiosis shown does not occupy a discrete factorial combination of positive and negative effects. Instead, some symbioses may have more positive or negative effects for a symbiont or host than others, and these may shift depending upon their environmental context as shown in the figure by the gradation of red and blue values between the two axes. For example, two different symbioses may both be mutualistic (mutually positive, bottom right), but one of those relationships may stray slightly more toward commensalism.

Parasitism is often underestimated because parasites are historically neglected, difficult to detect in their hosts, have complex life cycles, and their diversity is poorly known (Gómez and Nichols, 2013). However, parasitism could represent up to 50% of

## General Introduction

the lifestyles on Earth (Windsor, 1998). The omnipresence, as well as the impact on the host, renders parasites a major force in the trophic web. Often ignored in the studies of food webs, when parasites are added as consumer-resource, the metrics are drastically different as they are actually the dominant interaction. As a consequence, the consideration of parasite in food webs increase connectance (number of links per species) and relative nestedness (due to interaction between specialist species with only a subset of hosts, for example) and ultimately improves food web resistance to perturbation, e.g. introduction of invasive species (Lafferty et al., 2006). Indeed, parasitism should not be considered as solely a pest, but as an integrated role in the ecosystem (Poulin and Morand, 2000). In fact, the abundance of parasites has been proposed as a proxy to measure the health of ecosystems because they increase biodiversity, regulate the fitness of keystone species, and ultimately enhance the ecosystem's ecological resilience (Gómez and Nichols, 2013; Hudson et al., 2006; Wood and Johnson, 2015).

Several evolutionary models have been proposed to describe the interactions between hosts and parasites. Long term and close relationship between host and parasite allow co-evolution of the partners in a relatively short time scale, and co-speciation in a longer time scale (De Vienne et al., 2013). Virulent parasites spread faster and tend to be selected while resistant hosts are selected due to the higher mortality of the more sensitive ones. Both partners are under directional selection. This model is the evolutionary arm race dynamics. If the parasite population gains in virulence quicker than the host gains in resistance and thus reduces its abundance, the parasites can be negatively impacted due to a decreased host population. Then the impacted and so reduced parasite population can favour the host population, that in turn can quickly increase. Repeatedly, this scenario can cause population fluctuation like it is described in the Lotka-Volterra dynamics (Lotka, 1920; Volterra, 1928). The red Queen hypothesis is another model for co-evolution (Van Valen, 1973). This theory is based on the biotic selection pressures that cause perpetual need for the species to change to be maintained and this selection is fluctuating. Genetic variation is thus favoured and so antagonist relationship like for the host-parasite interaction, is a driver for maintenance of sexual reproduction and diversity. Sexual reproduction and change in ploidy level can also offer great advantage in resistance to parasite or virus. This is the case with the marine microalga *Emiliana huxleyi* that become insensitive to virus

## General Introduction

(giant phycodnaviruses) during the non-calcified haploid phase. This phenomenon is described as “Cheshire Cat” escape strategy by Miguel Frada et al. in 2008.

### **Chemical interaction**

Chemical ecology is the science that studies the chemical interactions between organisms themselves or between organisms and their environment. This field is expanding as chemical mediation appears to be a crucial vector of biotic interactions, being its universal language. As well, it leads to the discovery of new bioactive molecules, putatively interesting in crop disease management and medical applications (Poulin and Pohnert, 2019).

Chemical mediation is involved in successful reproduction during intraspecific chemical communication with pheromones, i.e. intraspecific infochemistry (Dicke and Sabelis, 1988). This the case in very different groups such as vertebrates (Brennan and Zufall, 2006), insects (Ayasse et al., 2001), and protists (Bardwell, 2005; Moeys et al., 2016). Chemical mediation could also be involved in prey finding (Vickers, 2000), predator detection (Lass and Spaak, 2003) or resource localization (Stocker et al., 2008).

Mostly discussed in plant biology, the chemically primed state is a specific biological state resulting from the reception of a stimulus that allows the receiver to increase its resistance to competitor or grazer and its abiotic stress resistance (Balmer et al., 2015; Conrath et al., 2006; Frost et al., 2008; Mauch-Mani et al., 2017). The primed state results from transcriptional and/or metabolomic modifications implemented in response to a stimulus.

The metabolome is the set of low molecular weight molecules (Færgestad et al., 2009; Fiehn, 2002) that plays a direct role for the cell or organism. It includes bioactive molecules such as secondary metabolites (i.e. metabolites not directly linked to survival but useful to increase fitness), also called natural products, often illustrated by plant toxins or sexual pheromones. The development of detection and identification techniques for microbial metabolites is important to study metabolomes.

The chemical ecology of marine protists is developing with the recent advances in chemical defence, allelopathy, bacteria-algae interaction, or discovery of pheromones

## General Introduction

(Kuhlisch and Pohnert, 2015). Chemical cues are dissolved in water, and unlike air, at low scale (under 1 mm) water is viscous and the propagation of molecules differs (Guasto et al., 2011). Chemical gradient around the cells of the emitter indicates to the potential receivers a direction through a gradient (Stocker, 2012). The surrounding micro-environment of the marine protists contain molecules produced by the cell in significant concentrations that decrease rapidly with the distance to the cell, forming a chemical gradient. This spherical volume around the cell is called the phycosphere defined by “the region immediately surrounding a phytoplankton cell that is enriched in organic molecules exuded by the cell into the surrounding water” (Smriga et al., 2016). The phycosphere is a crucial area of exchange for the microbiome and its host which mirrored the rhizosphere concept between terrestrial plant roots and beneficial microorganisms (Smriga et al., 2016).

To illustrate the role of chemical mediation, here some examples of chemical interaction between marine protists. The bloom-forming phytoplankton *Phaeocystis* shows different strategies when confronted with different grazers. In the presence of chemical cues from one of its larger grazers (a copepod), *Phaeocystis* downsizes its colony to favour the formation of a unicellular form, preventing grazing by the copepod. Conversely, when exposed to chemical cues from one of its smaller grazers (a ciliate), the colonies tend to enlarge to prevent grazing by this type of grazer (Long et al., 2007; Tang, 2003).

The bloom-forming, toxin producer, dinoflagellate *Alexandrium* increases by 2.5-fold its production of toxin in presence of a grazer (a copepod) (Selander et al., 2006). The use of a metabolomic tools served to characterise the chemical mediators responsible for this signal, the copepodamides (Grebner et al., 2019). It was later demonstrated that copepodamides also increase the production of amnesic shellfish toxin and induced a modification of the chain length in the preyed diatom *Skeletonema marinoi* (Grebner et al., 2019).

More studies provide information about the parasite-alga interactions. *Parvilucifera infectans* triggers the formation of temporary cysts of the dinoflagellate host *Alexandrium ostenfeldii* (Toth et al., 2004). The sporangium of the parasite *Parvilucifera sinerae* is a dormancy stage that is activated in the presence of its host *Alexandrium minutum*, and reacts similarly in presence of dimethylsulphide (DMS)

## General Introduction

(Garcés et al., 2013). The gene transcription of the host *Alexandrium fundyense* is modified in presence of signals from the parasite *Amoebophrya ceratii*. For example, an up-regulation of the genes involved in energy production from photosynthesis, ATP synthesis through glycolysis and fatty acid production, calcium-mediated signal transduction, and ROS production was observed (Lu et al., 2016). Toxin production by the dinoflagellates *Alexandrium minutum* or *Scrippsiella donghaiensis* reduces the level of infection of surrounding dinoflagellates host (such as *Scrippsiella acuminata*) by *Amoebophrya ceratii* (Long et al., 2021).

Chemical signalling is also used for intra-specific interaction in marine protists. For example, the mating of the diatom *Seminavis robusta* depends on the production of a pheromone (Moeys et al., 2016) which was identified as di-L-prolyl diketopiperazine using metabolomic tools (Gillard et al., 2013).

## II. Objectives, biological model and structure of the thesis project

### General questions

The importance of parasitic symbiotic interactions lies in the fundamental role they play in exerting pressure on hosts, shaping relationships between different organisms and influencing evolutionary responses. At the organism level, the metabolome undergoes constant changes over time and is tightly linked to the physiological state, making the measurement of metabolomic changes a critical method for understanding the mechanisms underlying biotic interactions. This study emphasizes its importance. Knowing that marine parasites deserve more attention, the general question of this thesis is:

What is the role of host and parasite metabolites in their interactions in the marine plankton?



### **General objectives**

Although marine parasites are recognized as key organisms in the ecosystem, their biology remains incompletely understood. There are knowledge gaps concerning the free-living parasite stage, its sexual reproduction, and its capacity to locate compatible hosts. We hypothesize that sexual reproduction plays a significant role in the interaction with the host. Additionally, we suggest that a multitude of metabolites are involved in the interaction process. Finally, the parasite possesses a mechanism to locate its host based on molecules. In this context, this thesis project aims to better understand:

- 1) the life cycle of the parasite and in particular the phenotypes, genes expression and metabolomic profiles of the free-living stage;
- 2) the dynamics of host metabolites during parasite infection and the distinction between metabolites associated with parasite development and those associated with putative host defence;
- 3) how the parasite free-living stage can reach the host cell using chemical gradient.

In this context, the model organisms used are two dinoflagellates, the parasitoid *Amoebophrya ceratii* (*Syndiniales*) infecting the bloom-forming phototrophic host *Scrippsiella acuminata*. For this project, we have employed laboratory culture experimentation techniques.

## III. Biological models used in this thesis

### **Myzozoa**

The group of interest in this study are Myzozoa, which include dinoflagellates, Perkinsea, as well as Apicomplexa (Fig. 0-5) Myzozoa are ecologically very successful on Earth. Indeed, Apicomplexa is a group of very impactful parasites, infecting all animals on earth, including humans, composed of, at least, 6,000 species (Adl et al., 2007). They have a complex life cycle, involving sometimes intermediate hosts, i.e. heteroxenous life cycle. They possess specialised organelles at the apical end of the cell, called the apical complex (hence the name Apicomplexa), used for the invasion

## General Introduction

of the host and in some cases for locomotion. One of the most important examples is *Plasmodium* spp., notorious for causing malaria, which, according to the World Malaria Report 2022 (World Health Organization, <https://www.who.int/>), causes about 620,000 deaths and more than 240 million cases annually. Other Apicomplexa organisms cause many other diseases, such as the genera *Theileria*, *Babesia*, and *Eimeria*, which affect domestic animals, such as cattle, and humans. A final example of an Apicomplexa parasite is the gregarines, another large group consisting of terrestrial and aquatic (marine and freshwater) parasites that infect a wide range of hosts, but mainly invertebrates, and in the marine environment, crustaceans, tunicates, worms and oysters. Their life cycle is, generally, composed of a unique host, i.e. monoxenous life cycle. New groups have been described as part of the alveolates as the chromerids, colponemids and the acavonemids (Tikhonenkov et al., 2014). Very interestingly, the two species of chromerids, *Chromera velia* (Moore et al., 2008) and *Vitrella brassicaformis* (Oborník et al., 2012) are photosynthetic organisms unlike their close relative, the apicomplexa. The study of these species helps to better understand the evolution of Myzozoans and, for example, helps to understand the presence of the remarkable vestigial plastid, called apicoplast, within Apicomplexa (McFadden et al., 1996). Indeed, this plastid is non-photosynthetic and derives from a series of loss. Nonetheless, this organelle remains essential and important for the synthesis of fatty acids, isoprenoid, iron-sulphur cluster and haem (Lim and McFadden, 2010). Interestingly, anti-plant-like molecules can block the function of the apicoplast and thus constitute antimalarial drugs.

## Dinoflagellates

Dinoflagellates are morphologically characterised by the presence of two flagella, a transversal and a longitudinal, and of flat vesicles below the membrane that sometimes contain solid plates containing cellulose and forms theca in the case of the armoured (or thecate) species. The dinoflagellates without rigid plate are unarmoured or also called naked, or athecate. Dinoflagellates harbour a vast morphological diversity, as shown in Figure 0-6. In the “core” dinoflagellates, the chromosomes are constantly condensed and lack classical histone proteins: this type of nucleus is called dinocaryon.

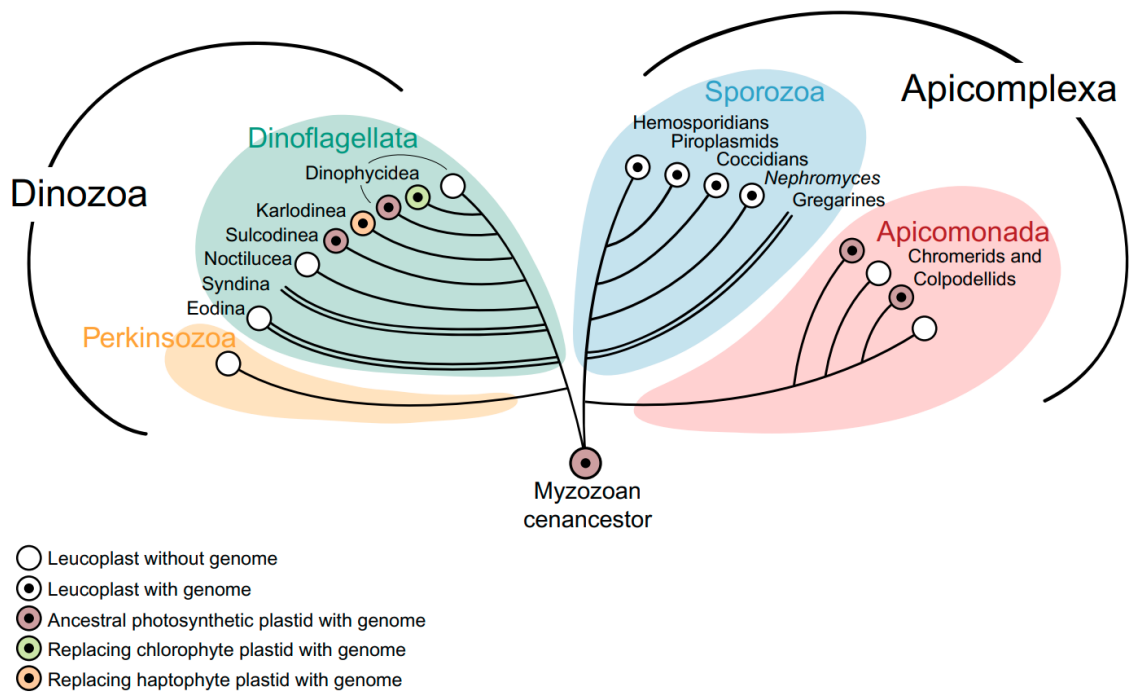


**Figure 0-5: From Muñoz-Gómez and Slamovits, 2018. A schematic phylogeny of the Myxozoa.**

The diagram summarises and synthesises the phylogenetic relationships among myxozoans based on Adl et al. (2012), Votýpka, Modrý, Oborník, Šlapeta, and Lukeš (2016), Janouškovec et al. (2015, 2017), and Cavalier-Smith (2017). For dinozoans, the evolutionary taxonomic scheme and taxon names of Cavalier-Smith (2017) are adopted. For apicomplexans, informal names are used for the particular major lineages discussed within the text, but Cavalier-Smith (2017) is followed for taxa above the parvphylum level. The distribution of plastids and their genomes is shown by different combinations of coloured and inside circles. Dinophytes with barely reduced ochrophyte endosymbionts (dinotoms), as well as cryptophyte-derived kleptoplastids in the dinophyte *Dinophysis* are not shown. The aplastidic myxozoans *Cryptosporidium* and *Haematodinium* are phylogenetically contained within gregarines and *Syndina*, respectively. Double branches denote paraphyly.

According to [algaebase.org](http://algaebase.org) (in May 2023), the superclass Dinoflagellata includes about 3,850 species. An outline of the dinoflagellates branches can be found in Figure 0-6. Most of them are marine (82%) but they have colonised all aquatic environments including freshwater (rivers and lakes) and brackish waters with important variations in salinity i.e. estuaries (Gómez, 2012). They show a wide diversity of lifestyles: half of the described species are photosynthetic organisms, sometime photosymbionts of corals, jellyfish, and other protists, others are micro- (size from 20 to 200  $\mu\text{m}$ ) and nano- (size from 2 to 20  $\mu\text{m}$ ) predators of bacteria and/or other nano-protists (Gómez,

## General Introduction

2012). Most, if not all phototrophic species are mixotrophic (Gómez, 2012). Dinoflagellates predominantly reproduce by asexual clonal division, but are able to reproduce sexually under certain conditions, as shown in Figure 0-8. Some species can perform bioluminescence, such as *Noctiluca scintillans*, *Pyrocystis lunula* or *Lingulodinium polyedra* (Valiadi and Iglesias-Rodriguez, 2013).

They are known to produce bioactive molecules, e.g. toxins, that can cause diseases for human and great economic loss (Zingone and Oksfeldt Enevoldsen, 2000) and this is one reason for which they have been intensively studied in ecology (Cousseau et al., 2020).

### **The parasite of the *Amoebophrya* genus**

The parasite strain used in this project belongs to the *Amoebophrya ceratii* species complex. *Amoebophrya* genus belongs to the Syndiniales, branch visible in Figure 0-6 (or Syndinid, or Syndiniophyceae, synonymous with Marine alveolates or MALVs), a complex group placed at the base of the dinoflagellates. Syndiniales is a group of exclusive parasites infecting a large range of host animals, such as crustacean (crab, langoustine, lobster), appendicular, copepods, fish eggs, and protists (micro-predator and photosynthetic) (Cachon and Cachon, 1987). *Amoebophrya* spp. are parasites of other protists such as radiolarian, ciliates and other dinoflagellates (Cachon, 1964; Coats, 1999). *Amoebophrya* spp. are widespread, from the coastal ocean and fjords, the open ocean, from the surface to the deep ocean, and some are present around the hydrothermal vents or in the oxygen minimum zone (Guillou et al., 2008). They have been detected at low cell concentration and low prevalence (proportion of infected host) even in one of the most oligotrophic areas of the ocean, i.e. the eastern part of the Mediterranean Sea (Siano et al., 2011). Moreover, those parasites were described to participate in the decline of blooming hosts with prevalence up to 50% (Chambouvet et al., 2008). *A. ceratii* is able to infect non-toxic but also toxic dinoflagellates such as *Alexandrium catenella* (Taylor, 1968), *Alexandrium fundyense* (Velo-Suárez et al., 2013) and *Alexandrium minutum* (Chambouvet et al., 2008).

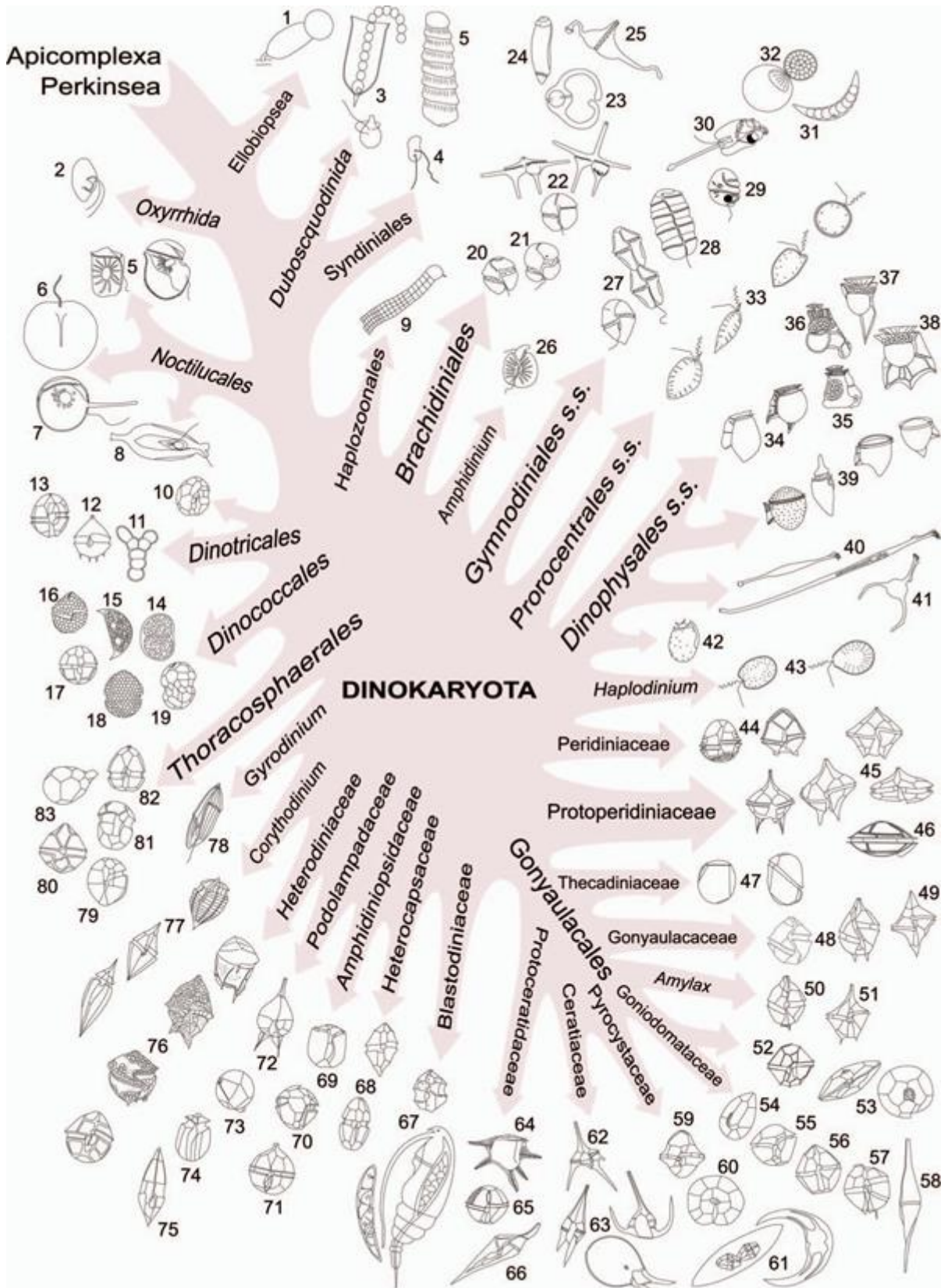


**Figure 0-6: From Gómez, 2012. Diversity of major lineages of dinoflagellates.**

1. Ellobiopsis; 2. Oxyrrhis; 3. Duboscquella; 4. Syndinium; 5. Kofoidinium; 6. Noctiluca; 7. Spatulodinium; 8. Scaphodinium; 9. Haplozoon; 10. Crypthecodinium; 11. Dinotrix; 12. Peridinium quinquecorne; 13. Durinskia; 14. Phytodinium; 15. Cystodinium; 16.

## General Introduction

Borghiella; 17. Sphaerodinium; 18. Biecheleria. 19. Symbiodinium; 20. Takayama; 21. Karlodinium; 22. Brachidinium; 23. Pseliodinium; 24. Torodinium; 25. Gynogonadinium; 26. Amphidinium; 27. Gymnodinium; 28. Polykrikos; 29. Warnowia; 30. Erythrospidinium; 31. Dissodinium; 32. Chytriodinium; 33. Prorocentrum s.s.; 34. Dinophysis; 35. Citharistes; 36. Histioneis; 37. Parahistioneis; 38. Ornithocercus; 39. Phalacroma; 40. Amphisolenia; 41. Triposolenia; 42. Sinophysis; 43. Exuviaella/Haplodinium; 44. Peridinium s.s.; 45. Protoperidinium s.s.; 46. Diplopsalis; 47. Thecadinium; 48. Gonyaulax; 49. Spiraulax; 50. Lingulodinium; 51. Amylax; 52. Goniodyma; 53. Gambierdiscus; 54. Ostreopsis; 55. Coolia; 56. Alexandrium; 57. Pyrodinium; 58. Centrodinium; 59. Fragilidium; 60. Pyrophacus; 61. Pyrocystis; 62. Ceratium; 63. Neoceratium; 64. Ceratocorys; 65. Protoceratium; 66. Schuettiella; 67. Blastodinium; 68. Heterocapsa; 69. Amphidiniopsis; 70. Herdmania; 71. Archaeoperidinium; 72. Podolampas; 73. Blepharocysta; 74. Roscoffia; 75. Lessardia; 76. Heterodinium; 77. Corythodinium; 78. Gyrodinium; 79. Hemidinium; 80. Glenodinium; 81. Pfiesteria; 82. Scrippsiella; 83. Oodinium.

Based on environmental DNA (i.e. ribosomal DNA sequencing), these species are included within Syndiniales, including MALV-II, being notable representatives (Fig. 0-2E and 2F) (de Vargas et al., 2015; Lima-Mendez et al., 2015). Studies of the interactions between planktonic protists show that parasitism is predominantly represented by the groups Dinoflagellata, Perkinsidea and Syndiniales, with half of the latter represented by *Amoebophrya* (Bjorbækmo et al., 2020).

There are 7 described species (complexes) of *Amoebophrya*:

- *Amoebophrya acanthometrae* Koeppen, 1894, infecting acantharea,
- *Amoebophrya ceratii* (Koeppen) J.Cachon, 1964, infecting many dinoflagellates species,
- *Amoebophrya grassei* Cachon, 1964, infecting the parasites *Oodinium poucheti* and *O. acanthometrae* (dinoflagellates), making *A. grassei* hyperparasitic,
- *Amoebophrya leptodisci* Cachon, 1964, infecting the heterotrophic dinoflagellate *Pratjetella medusoides*,
- *Amoebophrya stycholonchae* Koeppen, 1894, infecting sticholonche (radiolarians),
- *Amoebophrya tintinni* Cachon, 1964, infecting the tintinnid *Xystonella lohmanni* (ciliates),



## General Introduction

- *Amoebophrya rosei* Cachon, 1964, infecting chaetognathes (predatory marine worms) and *Abylopsis tetragona*, an apostome parasite of siphonophores making *A. rosei* hyperparasitic.

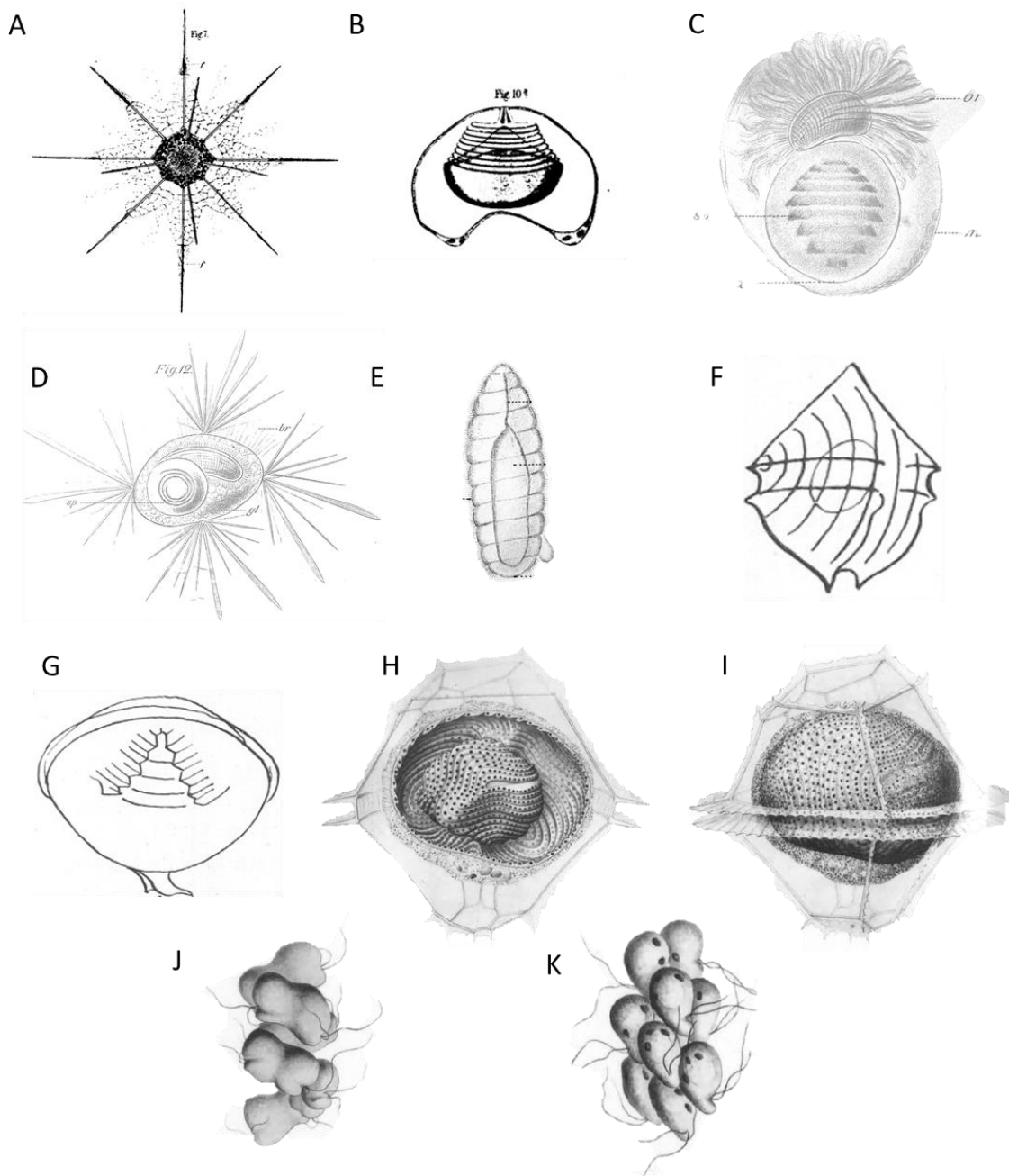


**Figure 0-7: Few representations of the Amoebophrya genus parasite in the past 150 years.**

(A) *Acanthometra serrata* and its (B) “nucleus” published by R. Hertwig in 1879. Published by H. Fol in 1883 (C) side view and (D) top view of *Stichonlonche zanclea* with the “spiral body” and (E) the “hatched spiral body”. Later, N. Koeppen in 1894 will

## General Introduction

describe that the nucleus with the spiral shape is actually the parasite *A. acanthometrae* in its host *A. serrata* and *A. sticholonche* in its host *S. zanclea*. The “hatched spiral body” is actually the parasite vermiform. In 1925, Marie V. Lebour sketched a diagram of *Amoebophrya* sp. infecting cells of (F) *Diplopsalis lenticula* and (G) *Peridinium* sp. In 1964, J. Cachon illustrated (H) transverse section and (I) in toto *Amoebophrya ceratii* infecting a dinoflagellate; (J) and (K) fraction of an elongated vermiform of *A. ceratii*.

### Life cycle of the parasite *A. ceratii*

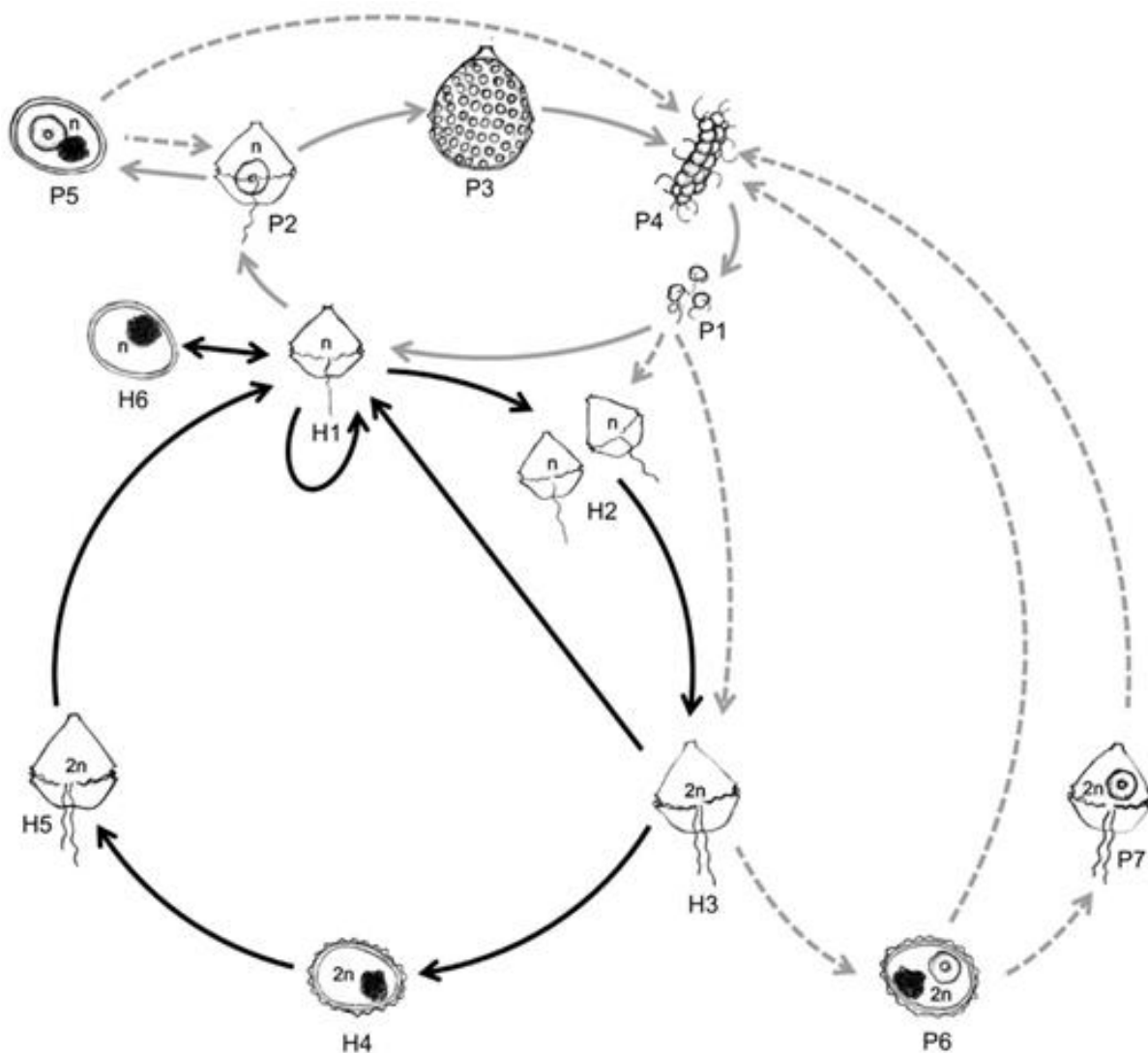


**Figure 0-8: From Chambouvet et al 2011. Interactions between *Scrippsiella acuminata* and *Amoebophrya* sp. life cycles.**

Black arrows indicate *S. acuminata* life cycle with haploid vegetative cells (H1), gametes (H2), diploid planozygote (H3), diploid calcified resting cyst (H4), diploid planomeiocyte (H5), and haploid non-calcified cyst (H6). *Amoebophrya* sp. life cycle (lines in grey) with the free-living stage of the parasite (dinospores, P1), able to infect



## General Introduction

vegetative cells of *S. acuminata* (P2), mature trophont of *Amoebophrya* (typical beehive stage, P3), and the vermiform stage (P4). The parasite was additionally detected in non-calcified (P5) and calcified cysts (P6) of its host. Dotted lines illustrated uncertain routes for the parasite. For examples, infected non-calcified (P5) and calcified (P6) cysts eventually give rise to infected vegetative cells (P2) and infected planomeiocyte (P7) respectively or directly to the vermiform stage (P4) and dinospores (P1).

The parasite alternates between a free-living and an intracellular stage. The infectious motile stage, the dinospore (P1 in Fig. 0-8), infects its host by entering the cell. When attached to the surface of the host, the dinospore loses its flagella and takes on a slug-like appearance and then enters the cell. A parasitophorous vacuole surrounds the parasite, separating from the host cytoplasm. The strains of parasite and host used in this project move to the host nucleus where the infection first takes place. The first stage of the infection is the feeding stage called the trophont stage (P2 in Fig. 0-8) where the parasite is osmotroph (Decelle et al., 2022). During its host's infection (trophont and sporont stage), the parasite maintains the activity of its chloroplasts and possibly of its mitochondria. Thus, *Amoebophrya* engages in kleptoplastidy by exploiting the host's cellular energy production derived from photosynthesis (Kayal et al., 2020). During the trophont stage the parasite grows. Then rapid divisions of the nucleus transform the cell into a syncytium. With this, a cavity inside the parasite is formed called the mastigocoel (Fig. 0-9D) where the flagella grow and shape the parasite into the typical and recognisable beehive, becoming the reproductive stage of the parasite, the sporont. At the end of the infection of the host, the sporont reverses (Fig. 0-9E), the mastigocoel is no longer a cavity and the flagella are on the outer surface of a temporary multicellular form called vermiform (P4 on Fig. 0-8 and Fig. 0-9F). This form is a free-living stage, motile, and involved in the dispersion of the future infectious stage with a limited lifespan. The vermiform elongates (g in Fig. 0-9) and, later, breaks into newly produced individual dinospores (Fig. 0-9H and 0-9I). The parasite eventually infects host vegetative cells (P2 in Fig. 0-8) but also gametes (H2 in Fig. 0-8), and diploid planozygotes (H3 in Fig. 0-8). It might enter a period of dormancy with its host and can survive for several months, typically during periods of low host abundance (Chambouvet et al., 2011). Sexual reproduction has been described in dinoflagellates, as illustrated in the Figure 0-8 alongside the host, whereas it remains hypothetical in *Amoebophrya*.

### **Historical description of the *Amoebophrya* genus**

In 1935, Berthe Biecheler and Edouard Chatton (Chatton and Biecheler, 1935) described that in 1879, R. Hertwig mistook the parasite sporont for the host nucleus in the radiolarian *Acanthometra serrata* (Fig. 0-7B), later assigned to *Amoebophrya acanthometrae* by N. Koeppen in 1894. In 1883, H. Fol also mistook the parasite sporont (Fig. 0-9C and 0-9D) but this time for the spermatophore, called “spiral body” at that time, in the radiolarian *Sticholonche zanclea*. This parasite will be assigned to *Amoebophrya sticholonche* also by N. Koeppen in 1894. In the same publication, B. Biecheler and E. Chatton highlighted that Korotneff was the first in 1891 to identify the parasitic nature of the structures later identified as sporont. In addition, in 1897 Borgert was the first to describe the parasite life cycle and interestingly, the vocabulary used at that time to describe the parasite was from zoology with for example the sentence (translated from French) “Young individuals have a gastrula with full invagination”. At the time of *Amoebophrya*'s initial description, it posed a challenge to the taxonomic assignment due to the presence of a multicellular stage (the vermiform) and metamorphoses.

General Introduction

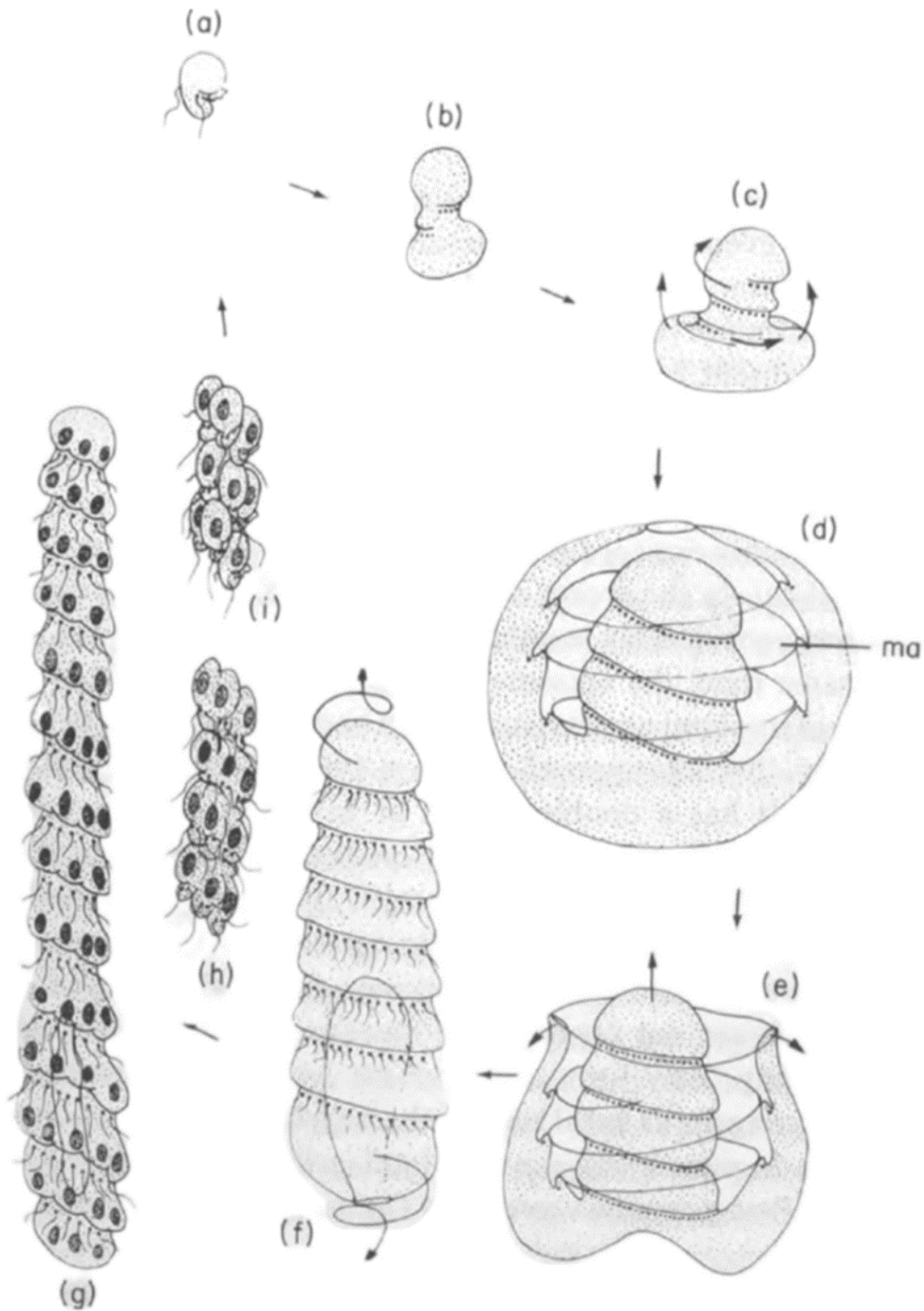


**Figure 0-9: from Cachon and Cachon 1987. Diagram of the life cycle of *Amoebophrya***

(a) dinospore; (b, c, d) invagination of the growing intracellular trophont (Ma = mastigocoel); (e, f) evagination of the trophont phagocytosis of the host and formation of a worm-shaped organism, the 'vermiform'; (g) lengthening of the vermiform; (i, h) formation of the swarmers.

## **Structure of the manuscript**

Chapter 1: First evidence of sexual reproduction in a widespread protist parasite infecting marine dinoflagellates

For the first time, we observed in culture several phenotypes of free living stage dinospores of *A. ceratii*. In other Syndiniales species, varying zoospore morphologies have already been observed, differing in size. Here, we characterised the role of the different *A. ceratii* dinospore morphotypes using laboratory culture techniques. We followed the life cycles and infection dynamics to compare the infectivity, cell production, lifespan of the morphotypes. We used transcriptomic to compare gene expression of different cell types (host and parasite) and metabolomics to compare chemical composition of different morphotypes.

Chapter 2: Metabolome dynamics during intracellular dinoflagellate infection emphasizes the role of azelaic acid in host resistance

In this chapter, we compared the endometabolomes and exometabolomes of infected host cultures at the initial, intermediate and final stages of infection. We identified particular metabolites at specific stages and suggested that some metabolites may be involved in host resistance. We selected azelaic acid and carry out bioassay to evaluate its role during the infection.

Chapter 3: Chemotaxis of the dinoflagellate parasite towards the chemical cues of its host

Dinospores are motile cells whose role is to infect a host cell. However, in the natural environment, their hosts are diluted in the water column. We suggest that dinospores are able to detect and locate host cells to initiate infection. This is the first results

## General Introduction

concerning the chemotaxis of a Syndiniales. We tested the swimming behaviour of dinospores in contact with host chemical extract in microfluidics devices.

### General discussion: Challenges, perspectives and conclusions of my thesis

This section traces the evolution of my thesis topic over the course of the project and outlines the initial objectives. The main results are connected, while new scientific questions and persistent gaps in knowledge are identified. I close the section with a discussion of the implementation of the *A. ceratii* model, containing suggested future research perspectives and avenues.

### Thesis supplementary documents:

- Thesis supplementary documents 1 : journal article in collaboration with IFREMER of Brest (France) team DYNECO (dynamics of coastal ecosystems). This study examines the impact of *Alexandrium minutum*, a toxin-producing dinoflagellate, on the host-parasite combination of *S. acuminata*-*A.ceratii*. Although the toxic effect has no influence on the host *S. acuminata*, it decreases the density of parasite dinospores and reduces infection. Therefore, the toxin appears to benefit the sensitive, non-toxin-producing host, even though *A. minutum* and *S. acuminata* are putative competitors.

Long, M., Marie, D., Szymczak, J., Toullec, J., Bigeard, E., Sourisseau, M., Le Gac, M., Guillou, L., Jauzein, C., 2021. Dinophyceae can use exudates as weapons against the parasite *Amoebophrya* sp. (Syndiniales). ISME COMMUN. 1, 34. <https://doi.org/10.1038/s43705-021-00035-x>

- Thesis supplementary documents 2: detailed protocol developed for this thesis project to identify and count host and parasite at different stages of infection using flow cytometry.

## General Introduction

Szymczak, J., Bigeard, E., Guillou, L., 2023. Use of flow cytometry (Novocyte Advanteon) to monitor the complete life cycle of the parasite *Amoebophrya ceratii* infecting its dinoflagellate host. [www.protocols.io](http://www.protocols.io)

- Thesis supplementary documents 3: report of the Jacques Monod conference entitled 'From Parasites to Plankton and Back: Comparative Biology and Ecology of Apicomplexans and Dinoflagellates' in the "Trends Talk" section of the journal *Trend in Parasitology*.

Waller, R.F., Alves-de-Souza, C., Cleves, P.A., Janouškovec, J., Kayal, E., Krueger, T., Szymczak, J., Yamada, N., Guillou, L., 2022. Comparative biology and ecology of apicomplexans and dinoflagellates: a unique meeting of minds and biology. *Trends in Parasitology* 38, 1012–1019. <https://doi.org/10.1016/j.pt.2022.09.010>

- Thesis supplementary documents 4: : one-page description of the *Amoebophrya ceratii* in the "Parasite of the month" section of the journal *Trend in Parasitology*.

Guillou, L., Szymczak, J., Alves-de-Souza, C., 2023. *Amoebophrya ceratii*. *Trends in Parasitology* 39, 152–153. <https://doi.org/10.1016/j.pt.2022.11.009>

## IV. References

Adl, S.M., Leander, B.S., Simpson, A.G.B., Archibald, J.M., Anderson, O.Roger., Bass, D., Bowser, S.S., Brugerolle, G., Farmer, M.A., Karpov, S., Kolisko, M., Lane, C.E., Lodge, D.J., Mann, D.G., Meisterfeld, R., Mendoza, L., Moestrup, Ø., Mozley-Standridge, S.E., Smirnov, A.V., Spiegel, F., 2007. Diversity, Nomenclature, and Taxonomy of Protists. *Systematic Biology* 56, 684–689. <https://doi.org/10.1080/10635150701494127>

Ayasse, M., Paxton, R.J., Tengö, J., 2001. Mating behavior and chemical communication in the order Hymenoptera. *Annu. Rev. Entomol.* 46, 31–78. <https://doi.org/10.1146/annurev.ento.46.1.31>

Balmer, A., Pastor, V., Gamir, J., Flors, V., Mauch-Mani, B., 2015. The 'prime-ome': towards a holistic approach to priming. *Trends in Plant Science* 20, 443–452. <https://doi.org/10.1016/j.tplants.2015.04.002>

## General Introduction

- Bardwell, L., 2005. A walk-through of the yeast mating pheromone response pathway. *Peptides* 26, 339–350. <https://doi.org/10.1016/j.peptides.2004.10.002>
- Bar-On, Y.M., Milo, R., 2019. The Biomass Composition of the Oceans: A Blueprint of Our Blue Planet. *Cell* 179, 1451–1454. <https://doi.org/10.1016/j.cell.2019.11.018>
- Bergh, Ø., Børsheim, K.Y., Bratbak, G., Heldal, M., 1989. High abundance of viruses found in aquatic environments. *Nature* 340, 467–468. <https://doi.org/10.1038/340467a0>
- Bjorbækmo, M.F.M., Evenstad, A., Røsæg, L.L., Krabberød, A.K., Logares, R., 2020. The planktonic protist interactome: where do we stand after a century of research? *The ISME Journal* 14, 544–559. <https://doi.org/10.1038/s41396-019-0542-5>
- Brennan, P.A., Zufall, F., 2006. Pheromonal communication in vertebrates. *Nature* 444, 308–315. <https://doi.org/10.1038/nature05404>
- Cachon, J., 1964. Contribution à l'étude des péridiniens parasites. *Cytologie, cycles évolutifs. Ann. Sci. Nat. Zool.* 1–158.
- Cachon, J., Cachon, M., 1987. Chapter 13. Parasitic dinoflagellates. In: F. J. R. Taylor (ed.). *The Biology of Dinoflagellates*. Blackwell Scientific Publications, Oxford 571–610.
- Cavalier-Smith, T., 2018. Kingdom Chromista and its eight phyla: a new synthesis emphasising periplastid protein targeting, cytoskeletal and periplastid evolution, and ancient divergences. *Protoplasma* 255, 297–357. <https://doi.org/10.1007/s00709-017-1147-3>
- Chambouvet, A., Alves-de-Souza, C., Cueff, V., Marie, D., Karpov, S., Guillou, L., 2011. Interplay Between the Parasite *Amoebophrya* sp. (Alveolata) and the Cyst Formation of the Red Tide Dinoflagellate *Scrippsiella trochoidea*. *Protist* 162, 637–649. <https://doi.org/10.1016/j.protis.2010.12.001>
- Chambouvet, A., Morin, P., Marie, D., Guillou, L., 2008. Control of Toxic Marine Dinoflagellate Blooms by Serial Parasitic Killers. *Science* 322, 1254–1257. <https://doi.org/10.1126/science.1164387>
- Chatton, E., Biecheler, B., 1935. Les *Amoebophrya* et les *Hyalosaccus*; leur cycle évolutif. L'ordre nouveau des Coelomastigines dans les Flagellés. *C. R. Acad. Sci., Paris* 200, 505–507.
- Coats, D.W., 1999. Parasitic Life Styles of Marine Dinoflagellates. *J Eukaryotic Microbiology* 46, 402–409. <https://doi.org/10.1111/j.1550-7408.1999.tb04620.x>
- Conrath, U., Beckers, G.J.M., Flors, V., García-Agustín, P., Jakab, G., Mauch, F., Newman, M.-A., Pieterse, C.M.J., Poinssot, B., Pozo, M.J., Pugin, A., Schaffrath, U., Ton, J., Wendehenne, D., Zimmerli, L., Mauch-Mani, B., 2006. Priming: Getting Ready for Battle. *MPMI* 19, 1062–1071. <https://doi.org/10.1094/MPMI-19-1062>

- Cousseau, A., Siano, R., Probert, I., Bach, S., Mehiri, M., 2020. Marine dinoflagellates as a source of new bioactive structures, in: *Studies in Natural Products Chemistry*. Elsevier, pp. 125–171. <https://doi.org/10.1016/B978-0-12-817905-5.00004-4>
- de Vargas, C., Audic, S., Henry, N., Decelle, J., Mahe, F., Logares, R., Lara, E., Berney, C., Le Bescot, N., Probert, I., Carmichael, M., Poulain, J., Romac, S., Colin, S., Aury, J.-M., Bittner, L., Chaffron, S., Dunthorn, M., Engelen, S., Flegontova, O., Guidi, L., Horak, A., Jaillon, O., Lima-Mendez, G., Luke, J., Malviya, S., Morard, R., Mulot, M., Scalco, E., Siano, R., Vincent, F., Zingone, A., Dimier, C., Picheral, M., Searson, S., Kandels-Lewis, S., Tara Oceans Coordinators, Acinas, S.G., Bork, P., Bowler, C., Gorsky, G., Grimsley, N., Hingamp, P., Iudicone, D., Not, F., Ogata, H., Pesant, S., Raes, J., Sieracki, M.E., Speich, S., Stemmann, L., Sunagawa, S., Weissenbach, J., Wincker, P., Karsenti, E., Boss, E., Follows, M., Karp-Boss, L., Krzic, U., Reynaud, E.G., Sardet, C., Sullivan, M.B., Velayoudon, D., 2015. Eukaryotic plankton diversity in the sunlit ocean. *Science* 348, 1261605–1261605. <https://doi.org/10.1126/science.1261605>
- Decelle, J., Kayal, E., Bigeard, E., Gallet, B., Bougoure, J., Clode, P., Schieber, N., Templin, R., Hehenberger, E., Prensier, G., Chevalier, F., Schwab, Y., Guillou, L., 2022. Intracellular development and impact of a marine eukaryotic parasite on its zombified microalgal host. *ISME J* 16, 2348–2359. <https://doi.org/10.1038/s41396-022-01274-z>
- Dicke, M., Sabelis, M.W., 1988. Infochemical Terminology: Based on Cost-Benefit Analysis Rather than Origin of Compounds? *Functional Ecology* 2, 131. <https://doi.org/10.2307/2389687>
- Færgestad, E.M., Langsrud, Ø., Høy, M., Hollung, K., Sæbø, S., Liland, K.H., Kohler, A., Gidskehaug, L., Almergren, J., Anderssen, E., Martens, H., 2009. 4.08 - Analysis of Megavariate Data in Functional Genomics, in: Brown, S.D., Tauler, R., Walczak, B. (Eds.), *Comprehensive Chemometrics*. Elsevier, Oxford, pp. 221–278. <https://doi.org/10.1016/B978-044452701-1.00011-9>
- Falkowski, P.G., Fenchel, T., Delong, E.F., 2008. The Microbial Engines That Drive Earth's Biogeochemical Cycles. *Science* 320, 1034–1039. <https://doi.org/10.1126/science.1153213>
- Farhat, S., Le, P., Kayal, E., Noel, B., Bigeard, E., Corre, E., Maumus, F., Florent, I., Alberti, A., Aury, J.-M., Barbeyron, T., Cai, R., Da Silva, C., Istace, B., Labadie, K., Marie, D., Mercier, J., Rukwavu, T., Szymczak, J., Tonon, T., Alves-de-Souza, C., Rouzé, P., Van de Peer, Y., Wincker, P., Rombauts, S., Porcel, B.M., Guillou, L., 2021. Rapid protein evolution, organellar reductions, and invasive intronic elements in the marine aerobic parasite dinoflagellate *Amoebophrya* spp. *BMC Biol* 19, 1. <https://doi.org/10.1186/s12915-020-00927-9>
- Fiehn, O., 2002. Metabolomics — the link between genotypes and phenotypes, in: Town, C. (Ed.), *Functional Genomics*. Springer Netherlands, Dordrecht, pp. 155–171. [https://doi.org/10.1007/978-94-010-0448-0\\_11](https://doi.org/10.1007/978-94-010-0448-0_11)



- Field, C.B., Behrenfeld, M.J., Randerson, J.T., Falkowski, P., 1998. Primary Production of the Biosphere: Integrating Terrestrial and Oceanic Components. *Science* 281, 237–240. <https://doi.org/10.1126/science.281.5374.237>
- Frost, C.J., Mescher, M.C., Carlson, J.E., De Moraes, C.M., 2008. Plant Defense Priming against Herbivores: Getting Ready for a Different Battle. *Plant Physiol.* 146, 818–824. <https://doi.org/10.1104/pp.107.113027>
- Garcés, E., Alacid, E., Reñé, A., Petrou, K., Simó, R., 2013. Host-released dimethylsulphide activates the dinoflagellate parasitoid *Parvilucifera sinerae*. *The ISME Journal* 7, 1065–1068. <https://doi.org/10.1038/ismej.2012.173>
- Gillard, J., Frenkel, J., Devos, V., Sabbe, K., Paul, C., Rempt, M., Inzé, D., Pohnert, G., Vuylsteke, M., Vyverman, W., 2013. Metabolomics Enables the Structure Elucidation of a Diatom Sex Pheromone. *Angewandte Chemie International Edition* 52, 854–857. <https://doi.org/10.1002/anie.201208175>
- Gómez, A., Nichols, E., 2013. Neglected wild life: Parasitic biodiversity as a conservation target. *International Journal for Parasitology: Parasites and Wildlife* 2, 222–227. <https://doi.org/10.1016/j.ijppaw.2013.07.002>
- Gómez, F., 2012. A quantitative review of the lifestyle, habitat and trophic diversity of dinoflagellates (Dinoflagellata, Alveolata). *Systematics and Biodiversity* 10, 267–275. <https://doi.org/10.1080/14772000.2012.721021>
- Grebner, W., Berglund, E.C., Berggren, F., Eklund, J., Harðadóttir, S., Andersson, M.X., Selander, E., 2019. Induction of defensive traits in marine plankton—new copepodamide structures. *Limnology and Oceanography* 64, 820–831. <https://doi.org/10.1002/lno.11077>
- Guasto, J.S., Rusconi, R., Stocker, R., 2011. *Fluid Mechanics of Planktonic Microorganisms* 30.
- Guillou, L., Viprey, M., Chambouvet, A., Welsh, R.M., Kirkham, A.R., Massana, R., Scanlan, D.J., Worden, A.Z., 2008. Widespread occurrence and genetic diversity of marine parasitoids belonging to *Syndiniales* ( *Alveolata* ). *Environmental Microbiology* 10, 3349–3365. <https://doi.org/10.1111/j.1462-2920.2008.01731.x>
- Howard-Varona, C., Lindback, M.M., Bastien, G.E., Solonenko, N., Zayed, A.A., Jang, H., Andreopoulos, B., Brewer, H.M., Glavina Del Rio, T., Adkins, J.N., Paul, S., Sullivan, M.B., Duhaime, M.B., 2020. Phage-specific metabolic reprogramming of virocells. *ISME J* 14, 881–895. <https://doi.org/10.1038/s41396-019-0580-z>
- Hudson, P.J., Dobson, A.P., Lafferty, K.D., 2006. Is a healthy ecosystem one that is rich in parasites? *Trends in Ecology & Evolution* 21, 381–385. <https://doi.org/10.1016/j.tree.2006.04.007>
- Janouškovec, J., Gavelis, G.S., Burki, F., Dinh, D., Bachvaroff, T.R., Gornik, S.G., Bright, K.J., Imanian, B., Strom, S.L., Delwiche, C.F., Waller, R.F., Fensome, R.A., Leander, B.S., Rohwer, F.L., Saldarriaga, J.F., 2017. Major transitions in dinoflagellate evolution unveiled by phylotranscriptomics. *Proc. Natl. Acad. Sci. U.S.A.* 114. <https://doi.org/10.1073/pnas.1614842114>

- Janouškovec, J., Tikhonenkov, D.V., Burki, F., Howe, A.T., Kolísko, M., Mylnikov, A.P., Keeling, P.J., 2015. Factors mediating plastid dependency and the origins of parasitism in apicomplexans and their close relatives. *Proc. Natl. Acad. Sci. U.S.A.* 112, 10200–10207. <https://doi.org/10.1073/pnas.1423790112>
- Kayal, E., Alves-de-Souza, C., Farhat, S., Velo-Suarez, L., Monjol, J., Szymczak, J., Bigeard, E., Marie, D., Noel, B., Porcel, B.M., Corre, E., Six, C., Guillou, L., 2020. Dinoflagellate Host Chloroplasts and Mitochondria Remain Functional During *Amoebophrya* Infection. *Front. Microbiol.* 11, 600823. <https://doi.org/10.3389/fmicb.2020.600823>
- Kuhlisch, C., Pohnert, G., 2015. Metabolomics in chemical ecology. *Natural Product Reports* 32, 937–955. <https://doi.org/10.1039/C5NP00003C>
- Lafferty, K.D., Dobson, A.P., Kuris, A.M., 2006. Parasites dominate food web links. *Proceedings of the National Academy of Sciences* 103, 11211–11216. <https://doi.org/10.1073/pnas.0604755103>
- Lass, S., Spaak, P., 2003. Chemically induced anti-predator defences in plankton: a review. *Hydrobiologia* 491, 221–239. <https://doi.org/10.1023/A:1024487804497>
- Lim, L., McFadden, G.I., 2010. The evolution, metabolism and functions of the apicoplast. *Phil. Trans. R. Soc. B* 365, 749–763. <https://doi.org/10.1098/rstb.2009.0273>
- Lima-Mendez, G., Faust, K., Henry, N., Decelle, J., Colin, S., Carcillo, F., Chaffron, S., Ignacio-Espinosa, J.C., Roux, S., Vincent, F., Bittner, L., Darzi, Y., Wang, J., Audic, S., Berline, L., Bontempi, G., Cabello, A.M., Coppola, L., Cornejo-Castillo, F.M., d'Ovidio, F., De Meester, L., Ferrera, I., Garet-Delmas, M.-J., Guidi, L., Lara, E., Pesant, S., Royo-Llonch, M., Salazar, G., Sánchez, P., Sebastian, M., Souffreau, C., Dimier, C., Picheral, M., Searson, S., Kandels-Lewis, S., Tara Oceans coordinators, Gorsky, G., Not, F., Ogata, H., Speich, S., Stemann, L., Weissenbach, J., Wincker, P., Acinas, S.G., Sunagawa, S., Bork, P., Sullivan, M.B., Karsenti, E., Bowler, C., De Vargas, C., Raes, J., 2015. Determinants of community structure in the global plankton interactome. *Science* 348, 1262073. <https://doi.org/10.1126/science.1262073>
- Long, J.D., Smalley, G.W., Barsby, T., Anderson, J.T., Hay, M.E., 2007. Chemical cues induce consumer-specific defenses in a bloom-forming marine phytoplankton. *Proceedings of the National Academy of Sciences* 104, 10512–10517. <https://doi.org/10.1073/pnas.0611600104>
- Long, M., Marie, D., Szymczak, J., Toullec, J., Bigeard, E., Sourisseau, M., Le Gac, M., Guillou, L., Jauzein, C., 2021. Dinophyceae can use exudates as weapons against the parasite *Amoebophrya* sp. (Syndiniales). *ISME COMMUN.* 1, 34. <https://doi.org/10.1038/s43705-021-00035-x>
- Lu, Y., Wohlrab, S., Groth, M., Glöckner, G., Guillou, L., John, U., 2016. Transcriptomic profiling of *Alexandrium fundyense* during physical interaction with or exposure to chemical signals from the parasite *Amoebophrya*. *Molecular Ecology* 25, 1294–1307. <https://doi.org/10.1111/mec.13566>

- Mauch-Mani, B., Baccelli, I., Luna, E., Flors, V., 2017. Defense Priming: An Adaptive Part of Induced Resistance 30.
- McFadden, G.I., Reith, M.E., Munholland, J., Lang-Unnasch, N., 1996. Plastid in human parasites. *Nature* 381, 482–482. <https://doi.org/10.1038/381482a0>
- Moeys, S., Frenkel, J., Lembke, C., Gillard, J.T.F., Devos, V., Van den Berge, K., Bouillon, B., Huysman, M.J.J., De Decker, S., Scharf, J., Bones, A., Brembu, T., Winge, P., Sabbe, K., Vuylsteke, M., Clement, L., De Veylder, L., Pohnert, G., Vyverman, W., 2016. A sex-inducing pheromone triggers cell cycle arrest and mate attraction in the diatom *Seminavis robusta*. *Sci Rep* 6, 19252. <https://doi.org/10.1038/srep19252>
- Moore, R.B., Oborník, M., Janouškovec, J., Chrudimský, T., Vancová, M., Green, D.H., Wright, S.W., Davies, N.W., Bolch, C.J.S., Heimann, K., Šlapeta, J., Hoegh-Guldberg, O., Logsdon, J.M., Carter, D.A., 2008. A photosynthetic alveolate closely related to apicomplexan parasites. *Nature* 451, 959–963. <https://doi.org/10.1038/nature06635>
- Muñoz-Gómez, S.A., Slamovits, C.H., 2018. Plastid Genomes in the Myzozoa, in: *Advances in Botanical Research*. Elsevier, pp. 55–94. <https://doi.org/10.1016/bs.abr.2017.11.015>
- Oborník, M., Modrý, D., Lukeš, M., Černotíková-Stříbrná, E., Cihlář, J., Tesařová, M., Kotabová, E., Vancová, M., Prášil, O., Lukeš, J., 2012. Morphology, Ultrastructure and Life Cycle of *Vitrella brassicaformis* n. sp., n. gen., a Novel Chromerid from the Great Barrier Reef. *Protist* 163, 306–323. <https://doi.org/10.1016/j.protis.2011.09.001>
- Poulin, R., Morand, S., 2000. The Diversity of Parasites. *The Quarterly Review of Biology* 75, 277–293. <https://doi.org/10.1086/393500>
- Poulin, R.X., Pohnert, G., 2019. Simplifying the complex: metabolomics approaches in chemical ecology. *Anal Bioanal Chem* 411, 13–19. <https://doi.org/10.1007/s00216-018-1470-3>
- Selander, E., Thor, P., Toth, G., Pavia, H., 2006. Copepods induce paralytic shellfish toxin production in marine dinoflagellates. *Proc Biol Sci* 273, 1673–1680. <https://doi.org/10.1098/rspb.2006.3502>
- Siano, R., Alves-de-Souza, C., Foulon, E., Bendif, E.M., Simon, N., Guillou, L., Not, F., 2011. Distribution and host diversity of Amoebophryidae parasites across oligotrophic waters of the Mediterranean Sea. *Biogeosciences* 8, 267–278. <https://doi.org/10.5194/bg-8-267-2011>
- Sieburth, J.McN., Smetacek, V., Lenz, J., 1978. Pelagic ecosystem structure: Heterotrophic compartments of the plankton and their relationship to plankton size fractions 1. *Limnol. Oceanogr.* 23, 1256–1263. <https://doi.org/10.4319/lo.1978.23.6.1256>
- Smriga, S., Fernandez, V.I., Mitchell, J.G., Stocker, R., 2016. Chemotaxis toward phytoplankton drives organic matter partitioning among marine bacteria. *Proc Natl Acad Sci USA* 113, 1576–1581. <https://doi.org/10.1073/pnas.1512307113>

- Stocker, R., 2012. Marine Microbes See a Sea of Gradients. *Science* 338, 628–633. <https://doi.org/10.1126/science.1208929>
- Stocker, R., Seymour, J.R., Samadani, A., Hunt, D.E., Polz, M.F., 2008. Rapid chemotactic response enables marine bacteria to exploit ephemeral microscale nutrient patches. *Proceedings of the National Academy of Sciences* 105, 4209–4214. <https://doi.org/10.1073/pnas.0709765105>
- Sunagawa, S., Acinas, S.G., Bork, P., Bowler, C., Eveillard, D., Gorsky, G., Guidi, L., Iudicone, D., Karsenti, E., Lombard, F., Ogata, H., Pesant, S., Sullivan, M.B., Wincker, P., Vargas, C. de, 2020. Tara Oceans: towards global ocean ecosystems biology. *Nature Reviews Microbiology* 18, 428–445. <https://doi.org/10.1038/s41579-020-0364-5>
- Tang, K.W., 2003. Grazing and colony size development in *Phaeocystis globosa* (Prymnesiophyceae): the role of a chemical signal. *J Plankton Res* 25, 831–842. <https://doi.org/10.1093/plankt/25.7.831>
- Taylor, F.J.R., 1968. Parasitism of the Toxin-Producing Dinoflagellate *Gonyaulax catenella* by the Endoparasitic Dinoflagellate *Amoebophrya ceratii*. *J. Fish. Res. Bd. Can.* 25, 2241–2245. <https://doi.org/10.1139/f68-197>
- Tikhonenkov, D.V., Janouškovec, J., Mylnikov, A.P., Mikhailov, K.V., Simdyanov, T.G., Aleoshin, V.V., Keeling, P.J., 2014. Description of *Colponema vietnamica* sp.n. and *Acavomonas peruviana* n. gen. n. sp., Two New Alveolate Phyla (*Colponemidia* nom. nov. and *Acavomonidia* nom. nov.) and Their Contributions to Reconstructing the Ancestral State of Alveolates and Eukaryotes. *PLoS ONE* 9, e95467. <https://doi.org/10.1371/journal.pone.0095467>
- Tipton, L., Darcy, J.L., Hynson, N.A., 2019. A Developing Symbiosis: Enabling Cross-Talk Between Ecologists and Microbiome Scientists. *Front. Microbiol.* 10, 292. <https://doi.org/10.3389/fmicb.2019.00292>
- Toth, G.B., Norén, F., Selander, E., Pavia, H., 2004. Marine dinoflagellates show induced life-history shifts to escape parasite infection in response to water-borne signals. *Proc. R. Soc. Lond. B* 271, 733–738. <https://doi.org/10.1098/rspb.2003.2654>
- Valiadi, M., Iglesias-Rodriguez, D., 2013. Understanding Bioluminescence in Dinoflagellates—How Far Have We Come? *Microorganisms* 1, 3–25. <https://doi.org/10.3390/microorganisms1010003>
- Velo-Suárez, L., Brosnahan, M.L., Anderson, D.M., McGillicuddy, D.J., 2013. A Quantitative Assessment of the Role of the Parasite *Amoebophrya* in the Termination of *Alexandrium fundyense* Blooms within a Small Coastal Embayment. *PLoS ONE* 8, e81150. <https://doi.org/10.1371/journal.pone.0081150>
- Vickers, N., 2000. Mechanisms of animal navigation in odor plumes. *The Biological Bulletin* 198, 203–212. <https://doi.org/10.2307/1542524>
- Votýpka, J., Modrý, D., Oborník, M., Šlapeta, J., Lukeš, J., 2016. Apicomplexa, in: Archibald, J.M., Simpson, A.G.B., Slamovits, C.H., Margulis, L., Melkonian, M., Chapman, D.J., Corliss, J.O. (Eds.), *Handbook of the Protists*. Springer

International Publishing, Cham, pp. 1–58. [https://doi.org/10.1007/978-3-319-32669-6\\_20-1](https://doi.org/10.1007/978-3-319-32669-6_20-1)

- Windsor, D.A., 1998. Controversies in parasitology, Most of the species on Earth are parasites. *International Journal for Parasitology* 28, 1939–1941. [https://doi.org/10.1016/S0020-7519\(98\)00153-2](https://doi.org/10.1016/S0020-7519(98)00153-2)
- Wood, C.L., Johnson, P.T., 2015. A world without parasites: exploring the hidden ecology of infection. *Frontiers in Ecology and the Environment* 13, 425–434. <https://doi.org/10.1890/140368>
- Zingone, A., Oksfeldt Enevoldsen, H., 2000. The diversity of harmful algal blooms: a challenge for science and management. *Ocean & Coastal Management* 43, 725–748. [https://doi.org/10.1016/S0964-5691\(00\)00056-9](https://doi.org/10.1016/S0964-5691(00)00056-9)
- Faust, K., Raes, J., 2012. Microbial interactions: from networks to models. *Nat Rev Microbiol* 10, 538–550. <https://doi.org/10.1038/nrmicro2832>
- Martin, Bradford D., Schwab, E., 2012. Current Usage of Symbiosis and Associated Terminology. *IJB* 5, p32. <https://doi.org/10.5539/ijb.v5n1p32>
- Martin, B. D., Schwab, E., 2012. Symbiosis: “Living together” in chaos. *Studies in the History of Biology* 4(4), 7–25.
- Sachs, J.L., Wilcox, T.P., 2006. A shift to parasitism in the jellyfish symbiont *Symbiodinium microadriaticum*. *Proc. R. Soc. B.* 273, 425–429. <https://doi.org/10.1098/rspb.2005.3346>
- Smith, D.C., 2001. Symbiosis research at the end of the millenium. *Hydrobiologia* 461, 49–54. <https://doi.org/10.1023/A:1012765114474>
- Tipton, L., Darcy, J.L., Hynson, N.A., 2019. A Developing Symbiosis: Enabling Cross-Talk Between Ecologists and Microbiome Scientists. *Front. Microbiol.* 10, 292. <https://doi.org/10.3389/fmicb.2019.00292>
- Overstreet, R.M., Lotz, J.M., 2016. Host–Symbiont Relationships: Understanding the Change from Guest to Pest, in: Hurst, C.J. (Ed.), *The Rasputin Effect: When Commensals and Symbionts Become Parasitic*, *Advances in Environmental Microbiology*. Springer International Publishing, Cham, pp. 27–64. [https://doi.org/10.1007/978-3-319-28170-4\\_2](https://doi.org/10.1007/978-3-319-28170-4_2)

# Chapter 1: First evidence of sexual reproduction in a widespread protist parasite infecting marine dinoflagellates

## Context of the study

The life cycle of the widespread dinoflagellate *Amoebophrya ceratii* has been well described (Cachon 1964). In brief, the dinospore, which is the free-living stage, invades the host cell and initiates the endo-cellular stage of infection. The parasite trophont feeds on the host's content and subsequently reproduces, leading to the mature sporont exiting the host cell. The newly produced dinospores aggregate and form a structured colony with a worm-like appearance called vermiform. The structure elongates until fragmentation and production of the individual dinospores, which form the new generation of infectious parasitic cells. Our understanding of the life cycle of this parasite has been enhanced by employing advanced methods such as flow cytometry, cell sorting, single cell transcriptomics, confocal microscopy, electron microscopy and behavioural monitoring. In particular, we have formulated a robust proposition on the sexual reproduction of the parasite, which was previously only hypothetical.

## Authors contribution

In this first chapter, I demonstrated the existence of non-infectious dinospores by monitoring the dynamics of infection in laboratory cultures using flow cytometry. The study was designed by Laure Guillou and myself. I carried out the host and parasite cultures with the help of Estelle Bigeard, I performed the flow cytometry monitoring (classical and cell sorting) to test infectivity, ploidy level, mating pairs between strains. I also did the sample preparation for microscopy with the help of Marie Walde (for data acquisition) and Sophie Le Panse (who took all the TEM negative stain images and

## Chapter 1

most of the TEM sections) and sample preparation for metabolomics. With the support of Marine Vallet, I performed the metabolomics extractions and we analysed the samples. Georg Pohnert helped with the design of the metabolomics experiment and the analysis. Johan Decelle and Estelle Bigeard performed the sample preparation and the TEM (after cryopreservation). Silvain Pinaud and Arthur Talman, with the help of Mickael Le Gac, Estelle Bigeard, Martin Gachenot and Laure Guillou, conducted cell sorting and transcriptomics. Laure Guillou, Eshan Kayal, Silvain Pinaud and Arthur Talman provided the gene expression analysis. Irene Romero Rodriguez and Mickael Le Gac, with the help of Cécile Jauzein, carried out the swimming behaviour experiments and analysis. Cecile Jauzein did the experiment to estimate the spore production per host. Catharina Alves-de-Souza performed the numerical analysis of the conditions related to P2 spore formation and prepared some figures.



## Article 1: A sexual stage in a widespread dinoflagellate parasite

Jeremy Szymczak<sup>1</sup>, Silvain Pinaud<sup>2</sup>, Irene Romero Rodriguez<sup>3</sup>, Marie Walde<sup>1</sup>, Ehsan Kayal<sup>4</sup>, Catharina Alves-de-Souza<sup>5,6</sup>, Estelle Bigeard<sup>1</sup>, Martin Gachenot<sup>7</sup>, Cécile Jauzein<sup>3</sup>, Mickael Le Gac<sup>3</sup>, Johan Decelle<sup>8</sup>, Sophie Le Panse<sup>9</sup>, Georg Pohnert<sup>10</sup>, Marine Vallet<sup>10</sup>, Arthur Talman<sup>2</sup>, Laure Guillou<sup>1</sup>

<sup>1</sup> Sorbonne Université, CNRS, UMR7144 Adaptation et Diversité en Milieu Marin, Ecology of Marine Plankton (ECOMAP), Station Biologique de Roscoff SBR, 29680, Roscoff, France

<sup>2</sup> MIVEGEC, Université de Montpellier, IRD, CNRS, Montpellier, France

<sup>3</sup> Ifremer, DYNECO Pelagos, Plouzané, France

<sup>4</sup> Department of Ecology, Evolution and Organismal Biology, Iowa State University, Ames, IA, USA

<sup>5</sup> Department of Oceanography, Faculty of Natural Sciences and Oceanography, University of Concepción, Concepción, Chile

<sup>6</sup> COPAS Coastal Oceanographic Research Center, University of Concepción, Chile

<sup>7</sup> Sorbonne Université, CNRS, FR2424 RECYF, Station Biologique de Roscoff SBR, 29680, Roscoff, France

<sup>8</sup> Laboratoire Physiologie Cellulaire et Végétale, Univ. Grenoble Alpes, CNRS, CEA, INRAE, IRIG-DBSCI-LPCV, 38000 Grenoble, France.

<sup>9</sup> Sorbonne Université, CNRS, FR2424 MERIMAGE, Station Biologique de Roscoff SBR, 29680, Roscoff, France

<sup>10</sup> Institute for Inorganic and Analytical Chemistry, Friedrich Schiller University Jena, Germany

<sup>11</sup> Max Planck Fellow Group Plankton Community Interaction, Max Planck Institute for Chemical Ecology, Jena, Germany



### **Abstract**

While most unicellular parasites primarily reproduce asexually, they usually possess a sexual phase associated with increased genetic variability and the ability to respond to environmental variation. Nonetheless, sexual reproduction is seldom observed in most parasitic species. In this study, we demonstrate the existence of specialized spores dedicated to sexual reproduction in the marine protist *Amoebophrya*, which parasitizes planktonic dinoflagellates. The inability to infect a new host is a notable characteristic of these sex spores when compared to infective spores, along with their larger size, unique swimming behaviour, shorter lifespan, and distinct metabolite production. Transcriptome analysis of these spores reveals a significant expression of ortholog genes associated with meiosis and DNA replication, suggesting their involvement in sexual reproduction. The production of these sexual spores exhibits intergenerational variability and remains unaffected by host factors such as density, age, and the initial host-parasite ratio. We further show that a given infected host cell typically generates either one of the two spore types, indicating a developmental decision within each infected host.

By using a decision-support hierarchical model, we identify the density of infective spores within the culture from which the parasite inoculum was obtained (n-1 generation) as critical explanatory variables for the production of sexual spores. We suggest that a density-dependent signal, operating among infective free-living spores of one generation, may induce sexual reproduction during the host infection, producing sexual spores in the subsequent generation. Altogether, we identify the first example of a sexual cell type and the environmental conditions required to induce sexual commitment in Syndiniales.

### **Introduction**

The discovery of novel marine alveolate (MALV) lineages in marine planktonic communities through culture-independent techniques, specifically MALV groups I and II (Díez et al., 2001a; López-García et al., 2001; Moon-van der Staay et al., 2001, de Vargas et al. 2015), has raised questions regarding the functional roles of these diverse microbial groups. These lineages represent polyphyletic early branching and poorly described dinoflagellates (Strassert et al. 2017), except for a few species identified

within the dinoflagellate order Syndiniales (Guillou et al. 2008). MALVs encompass a wide diversity of marine parasites able to infect a broad range of hosts, from unicellular organisms like dinoflagellates, ciliates, and radiolarians to metazoans such as crustaceans and fish. Unlike most other dinoflagellates, MALVs that have been studied so far lack both theca and chloroplasts (John et al. 2019, Kayal et al. 2020), and they have nuclei that never form a dinokaryon (Cachon 1964). Within their host, the trophic stage (trophont) precedes a multinucleate sporulating stage (sporont) formed by iterative division. At this stage, their condensed chromosomes exhibit a typical V-shaped structure, with the apex of the V permanently attached to the nuclear membrane. Sporulation ultimately produces motile spores (i.e., “dinospores”) released into the water, featuring two flagella arranged in the typical dinoflagellate fashion.

Within MALV lineages, various spore types are typically produced, often distinguished by their size (micro vs. macro spores). However, the nature of these spore types is mostly uncharted. These spore types were consistently described across different MALV lineages, regardless of the specific lineage or host they infect. For instance, in a study by Skovgaard et al. (2005) involving the infection of copepods by the parasite *Syndinium* (MALV Group IV), the release of three distinct spore types was observed, each originating from a different infected host. These authors concluded that the same parasitic species produced these different spore types by analysing SSU rDNA sequences and noting the close similarity of ITS1 and ITS2 sequences. In the case of *Ichthyodinium chaberi* (MALV Group I), a parasite affecting embryos and early larvae of fish, Shadrin et al. (2015) again reported that a given infected host produced a unique spore type. Additionally, these authors concluded that spore dimorphism can be explained by the number of divisions: small spores, presumably the invasive stage, are formed after three divisions, while large macrospores, with an unknown function, are formed after two divisions. Following the infection of the tintinnid *Eutintinnus pectinis* by the parasite *Euduboscquella cachoni* (MALV Group I), as reported by Coats in 1988, infected hosts released a unique spore type. While most dinoflagellates are haploid during their vegetative life, resting cysts traditionally originate from diploid zygotes and serve as a mechanism to withstand adverse environmental conditions (Bravo and Figueroa, 2014; Steidinger and Jangen, 1997).

Here, we sought to elucidate the ontology of spore types in MALVs. To achieve this, we explored spore populations produced within a clonal culture of *Amoebophrya ceratii*

(MALV group II), a widely distributed marine planktonic parasite that infects other dinoflagellates. In this species, several spore types are produced and can be isolated by flow cytometry. We deployed a range of tools, including microscopy, behavioural analysis, metabolite profiling, and gene expression analysis, to gain a deeper understanding of the functional roles of these spore populations. Additionally, we sought to understand the parameters that influence the production of one spore type over the other and to map the developmental bifurcation leading to either cell type.

### **Material and Methods**

#### *Culture conditions*

The experiments were conducted using cultures of *Amoebophrya* sp. (refer to the complex species of *A. ceratii* in Cachon 1964), strain A120 (RCC4398), belonging to MALVII-Clade 2 [ribotype 4, following classification by Guillou et al. (2008) and Cai et al. (2020)], infecting the dinoflagellate host *Scrippsiella acuminata* strain ST147 (RCC1627). Mating types were explored by crossing strain A120 against two other *Amoebophrya* strains from the same ribotype, specifically A42 (RCC4395) and A48 (RCC4396) (Cai et al. 2020). All strains are available at the Roscoff Culture Collection (<https://www.roscoff-culture-collection.org/>).

F/2 media was prepared with Red Sea Salt (Red Sea Company) diluted with milliQ water to achieve a salinity of 27 PSU (Bigéard, 2022).

Stock cultures of both host and parasites were grown at 21°C in 50-mL vented flasks (Culture One) under continuous light conditions at an intensity of 100  $\mu\text{Einstein m}^2 \text{s}^{-1}$ . Cultures were transferred twice a week, with a volume ratio of 1:4 for the host:medium and parasite:host.

Except when specified, parasite cultures were synchronized previous to experiments, as described in Bigéard, 2019. Briefly, old spores from the cultures were removed which resulted in all newly released spores being of the same age. To do so, infected hosts at the beginning of infection (7-10 hours following parasite inoculation) were gently collected by gravity filtration on 5-10  $\mu\text{m}$  nylon filters (Merck Millipore). Afterward, the filters with the host cells were rinsed on the same support device using

## Chapter 1

sterile culture medium to ensure the removal of the remaining old spores, and the cells retained on the filter were then collected and diluted into fresh medium in a new flask.

### *Cell counts and cell sorting by flow cytometry*

The infection dynamic was followed using a NovoCyte Advanteon flow cytometer (ACEA Biosciences, San Diego, CA) equipped with blue and violet lasers (488 and 405 nm, respectively). The dinoflagellate host *S. acuminata* was detected based on its chlorophyll autofluorescence determined under 488 nm excitation. In comparison, the parasite *Amoebophrya ceratii* A120 (both spores and infected hosts) was detected based on its natural bright green autofluorescence when excited under 405 nm. Specific details regarding the flow cytometry configuration and setup can be found in Szymczak et al., 2023. Parasite prevalence was established based on the percentage of infected hosts. The abbreviation for green fluorescence under violet (405 nm) laser is “Green-V-H”, for green fluorescence under blue (488 nm) laser is “Green-B-H”, for red fluorescence under blue (488 nm) laser is “Chlo-B-H”.

For bacterial counts (considered in metabolomics analyses), 500  $\mu$ L aliquots were fixed with grade II glutaraldehyde (Merck Sigma, 0.25% final concentration) for 15 minutes and then stored at  $-80$  °C until analysis. Upon thawing, DNA was stained using SYBR Green-I at a final dilution of 1/50,000, following the protocol outlined by Marie et al. (2000). Stained bacteria were detected under 488 nm excitation.

Various populations of spores (called P1, P2 and P3), as well as hosts at different stages of infection, were sorted by flow cytometer for microscopy analyses, ploidy level determination, infectivity assessment, and transcriptomic analyses. For that, we used Aurora CS (Cytex, California, USA) equipped with three lasers (405, 488, and 640 nm). Culture medium was used as sheath liquid for most experiments, while sterile PBS 1X was employed for transcriptomic analyses. Different spore populations were gated using the 405 nm laser (green autofluorescence) and FSC. For microalgal cell populations (uninfected and infected host cells), two successive gating strategies were used. The whole microalgal population was initially gated using the red autofluorescence under 488 nm excitation against FSC. Subsequently, a second gating strategy allowed for sorting host cells at different stages of the infection cycle, from the green fluorescence signal of the parasite measured under 405 nm excitation.

## Chapter 1

A flow rate of 45  $\mu\text{L}/\text{min}$  was used throughout all sorting procedures to maintain single-cell purity.

### *Estimation of spore production per host*

We isolated about 50 individual infected host cells 24 hours post-inoculation, using an inverted microscope (Carl Zeiss Axio Observer 3,  $\times 100$  magnification) and bright-field observations. These cells were carefully picked using flame-drawn Pasteur pipettes and transferred to separate wells within a 96-well plate. The plate was kept under the same environmental conditions as the stock cultures and was sampled 1 or 2 days after isolating the host cells. For each well sampled, the total volume of the well (about 100  $\mu\text{L}$ ) was analysed by flow cytometry in order to assess the flow cytometry signature and quantity of produced spores.

### *Confocal microscopy*

Samples were fixed in a combination of paraformaldehyde (Electron Microscopy Sciences, ref. 15714, 1% final conc.) and EM grade glutaraldehyde (Sigma-Aldrich G5882; Merck, Germany; 0.25% final conc.) (Kiernan JA, 2000) during 15 min at 4°C and mounted into chambered cover glasses (Nunc Lab-Tek II; Merck, Germany). Cells were coated with a fluorescent surface label consisting of 0.1 mg  $\text{ml}^{-1}$  poly-L-lysine (PLL; Sigma-Aldrich P5899; Merck, Germany) conjugated with Alexa Fluor 546 (AF546SE, Invitrogen A20002; Thermo Fisher Scientific, MA, USA) (Colin et al 2017) Cells were then imaged directly inside the chambers.

3D confocal images were acquired on a motorized and inverted SP8 laser scanning confocal microscope (Leica Microsystem, Germany) equipped with 63x oil NA 1.4 immersion objective by a semi-automated two-step procedure (Walde et al., 2023). After manual detection of cell positions, multichannel fluorescence z-stacks of 155 individual cells in sub-sample 1 and 172 individual cells in sub-sample 2 were automatically recorded (AF546: Ex 552 nm / Em 570-590 nm). 3D volumes were rendered from the AF546 fluorescence signal of the surface cover with Imaris 3D image visualization and analysis software (Oxford Instruments, UK). After the normal distribution of the biovolumes (Shapiro–Wilk test) was validated, the 99% confidence interval was calculated (mean  $\pm$  2.576\*Standard deviation) to separate spore populations.

*Electron microscopy*

Samples collected for transmission electron microscopy (TEM) exclusively originated from cultures dominated by a single spore type (P1 or P2) or were sorted by cytometry (Table S1-1).

For TEM negative staining, 20  $\mu$ L of freshly released spore were deposited upon a thin carbon film grid and let settle for 20 minutes. Subsequently, grids were incubated for 2 minutes with three droplets of uranyl acetate and then carefully absorbed to remove negative stain excess.

For TEM sections, freshly released spore samples were incubated at 4°C for 24 hours in a fixative solution containing 25% glutaraldehyde, 0.4 M sodium cacodylate buffer (pH 7.4), and 10% NaCl. Samples were centrifuged at 4,000  $\times$ g for 10 min between incubations. Pellets were rinsed three times (10-15 minutes each) with a solution of 0.4 M sodium cacodylate buffer and 10% NaCl, followed by post-fixation at 4°C for 60 minutes in a solution of 1% osmium tetroxide buffered with 0.4 M sodium cacodylate and 10% NaCl, and rinsed three times (10-15 minutes each) using a solution of 10% NaCl and 0.4 M sodium cacodylate.

Samples were then dehydrated through an ethanol series (absolute anhydrous ethanol, Carlo Erba) once at 30% and 50% (10 minutes each), twice at 70% (20 minutes each), and three times at 90% and 100% (20 minutes each). Finally, they were rinsed thrice for 20 minutes in 100% alcohol. After dehydration, pellets were gradually impregnated at room temperature in different concentrations of Spurr resin (Delta Microscopies, France) diluted once in 25% and 50% ethanol (1 hour each), once in 75% (overnight), and three times in pure resin (2 days each). Finally, the pellets were embedded in 100% Spurr resin at 60°C for two days and sectioned using a diamond knife on a Leica Ultracut UCT ultramicrotome, followed by staining with uranyl acetate and lead citrate. Both negative stained grids and sections were examined and photographed using a JEOL JEM 1400 transmission electron microscope (JEOL, Japan) equipped with a Gatan ultrascan camera.

For TEM after cryofixation, spores were cryo-fixed using high-pressure freezing (HPM100, Leica), followed by freeze-substitution (EM ASF2, Leica) as in Decelle et al. 2022. The freeze substitution mix contained 1% of osmium tetroxide. Ultrathin sections of 60 nm thickness were mounted onto copper grids or slots coated with formvar and

## Chapter 1

carbon. Sections were stained in 1% uranyl acetate (10 min) and lead citrate (5 min). Micrographs were obtained using a Tecnai G2 Spirit BioTwin microscope (FEI) operating at 120 kV with an Orius SC1000 CCD camera (Gatan).

### *Swimming behaviour*

Freshly released spores containing a mix of P1 and P2 populations were used to assess the swimming behaviour of spores from five biological replicates (one a week). Spores were separated from their hosts by gravity filtration (5µm nylon filter) and their density was adjusted (by dilution in culture medium) to approximately 300,000 cells mL<sup>-1</sup>. Cells were deposited onto customized chambers made by adding a silicone polymer (Polydimethylsiloxane; PDSM) upon a glass slide (2.5 cm length × 1.3 cm width × 64 µm height = 20.8 µL<sup>3</sup>). They were observed at a ×100 magnification using an inverted microscope (Carl Zeiss Axio Observer 3) equipped with a Zeiss AxioCam 705 camera and a LED module for epifluorescence. The light source was used at only 10% of its maximal intensity. Spores were observed from their autofluorescence signal, visible using an excitation filter of 420 ± 20 nm and a long path emission filter with a cut-off exceeding 470 nm. Videos were recorded with a resolution of 2,464 × 2,056 pixels and a pixel size of 0.548 µm using the ZeissZen blue 3.6 software. Five movies were recorded for each replicate. Movements were tracked for 20 seconds, with a 35 ms exposure time per frame. The images were imported into ImageJ software, and the brightness and contrast were adjusted to facilitate automatic cell tracking. Cell tracking was performed using the trackpy package (version 0.5.0+3.g3b280ea) in Python, with the following parameters: a minimum size of 23 pixels for a single particle, a maximum displacement of 90 pixels between frames per particle, and a memory of 300 frames to track disappearing particles while maintaining their identification. The minimum mass, representing the expected brightness for a particle, was manually selected for each video based on the level of noise present. This method enabled the identification of the coordinates and size of each cell frame by frame. The R Statistical Software (version 4.1.2; R Core Team 2021) was used to calculate the following parameters: the percentage of particles in motion (particles moving at least 1.5 µm between two frames and at least 15 µm over the entire video), as well as, for each particle, the total distance, swimming time, average speed, and Euclidean distance of their movement. The total distance was estimated by summing up all the distances calculated between

two frames based on the particle's coordinates. Swimming time was calculated by multiplying the number of frames in which movement occurred by the exposure time. The average speed was obtained by dividing the total distance by the swimming time. Finally, the Euclidean distance was calculated using each particle's starting and ending coordinates. The distribution of these normalized cell sizes, which exhibited a bimodal pattern, was modelled using Gaussian Mixture Modelling implemented in the flexmix R package. Cells were then assigned to either P1 or P2 based on their size, using a posterior probability threshold of 0.99 or higher. Out of the 657 particles tracked, 254 were assigned to P1, and 155 were assigned to P2. The statistical analysis of the generated data was conducted using non-parametric Kruskal-Wallis tests in R. The quantification of the difference in moving particles between sub-populations was verified using a Fisher exact test, which also provided an odds ratio (OR) and its corresponding 95% confidence interval (CI).

### *Conditions related to P2 spores formation*

We conducted a series of 149 experiments to determine culturing conditions favouring the production of P2 spores. Conditions in each experiment related to host and spore densities as well as spore:host ratios used for inoculation are informed in dataset 1. For each experiment, cell counts for hosts (infected and uninfected) and spores (P1 and P2+P3) were obtained in the inoculum (mother culture from which spores were obtained for inoculation) and at different time steps after inoculation: T0, T24, and T48 (i.e., 0h, 24h and 48h after inoculation, respectively). A categorical variable was created based on P1 and P2 densities at T48: (1) "P1 high" =  $P1 > 500,000 \text{ cells mL}^{-1}$  and P2 accounting for  $\leq 40\%$  of total spores; (2) "P2 high" =  $P2 > 500,000 \text{ cells mL}^{-1}$  and P1 accounting for  $\leq 40\%$  of total spores; (3) "P1 and P2 high" = both P1 and P2  $> 500,000 \text{ cells mL}^{-1}$ ; (3) "P1 and P2 low" = both P1 and P2  $< 500,000 \text{ cells mL}^{-1}$ . This categorical variable was then contrasted against different conditions using a decision-support hierarchical model (i.e., "decision tree") using the R package 'party' and focusing in the conditions determined in the mother culture (i.e., P1 and P2 counts), T0 (i.e., host, P1, and P2 counts, P1: host and P2: host ratios), and T24 (i.e., parasite prevalence).



## Chapter 1

### *Test of infectivity*

A culture dominated by P2 (100% of total spores, the few P1 counted correspond to noise and not actual cells) at  $754,000 \text{ cells mL}^{-1}$  was obtained by chance during one of the experiments conducted to assess conditions leading related to P2 spores production (Experiment 42 to 46 in dataset 1). This P2-dominated culture was filtrated through a  $5 \mu\text{m}$  nylon filter, to remove remaining hosts. Then, we initiated infection at different spore: host ratios in single replicate (154: 1, 68: 1, 43: 1, 23: 1, and 14: 1) and using an exponentially growing host (3 days old) with a concentration of  $7,800 \text{ cells mL}^{-1}$ . At the same time, we conducted an infection experiment using P1 and P2 spore populations sorted by flow cytometry. These sorted spores were used to inoculate an exponentially growing host culture (3 days old,  $17,000 \text{ cells mL}^{-1}$ ) at a spore:host ratio of 10:1, with four replicates for both P1 and P2 spores. In all cases, cultures were incubated in 24-well plates, and the parasite prevalence was evaluated by flow cytometry at  $t=24$  hours.

### *Ploidy level*

The ploidy levels of the different spore populations were established following the procedure outlined by Marie et al. (2000). Briefly, nuclei were extracted by mixing  $50 \mu\text{L}$  of freshly produced spore with  $450 \mu\text{L}$  of 0.25X NIB buffer, containing SYBR Green-I at a final concentration of 1/5000.

### *Mating pairs between strains*

All strains were combined in pairs, and eventual cell fusion (syngamy) was monitored by flow cytometry. This experiment was performed twice (on August 28 and September 8, 2023). Spores were collected three days after host incubation by filtration through a  $5 \mu\text{m}$  nylon filter. Subsequently, these strains were combined into 5 ml plastic tubes to achieve an equivalent number of P2+P3 spores from each strain. Throughout this experiment, pairs and individual spore strains were monitored at hourly intervals for half a day, and 24 and 48 hours after the initial combination. For that,  $50 \mu\text{L}$  of the samples were sampled and analysed using flow cytometry.

### *UHPLC-HRMS profiling and data-dependent MS acquisition*

Two days after inoculation, 40 mL of spore cultures were vacuum-filtered using 25 mm GF/C microfiber filters (Whatman). The GF/C filters were transferred directly to 2 mL safe-lock Eppendorf tubes and extracted with 1.6 mL methanol (Sigma-Aldrich) through sonication for 15 minutes. The organic phases were transferred to new glass vials and dried using a Vacufuge plus vacuum concentrator (Eppendorf). The samples were prepared in 100  $\mu$ L of methanol:water (1:1, vol:vol) and centrifuged for 20 minutes at 14,000 g. Subsequently, 50  $\mu$ L of each sample was transferred to 1.5 mL glass vials with inserts, and 10  $\mu$ L per sample was pooled into a QC mix sample, excluding blanks. Additionally, 1  $\mu$ L of the internal standard L-fluorophenylalanine (55  $\mu$ M in water) was added to each sample, thus reaching a final concentration of 0.055 mM. QC blank samples were prepared by combining 10  $\mu$ L of each blank sample from extracts of the axenic medium into one vial. 10  $\mu$ L of all samples were injected into the UHPLC-HR-MS system, consisting of an UltiMate<sup>TM</sup> 3000 UHPLC Dionex coupled to a Q-Exactive Plus Orbitrap mass spectrometer (Thermo Fisher Scientific). Metabolite separation was achieved using a 12-minute gradient, starting with 100% aqueous phase (2% acetonitrile, 0.1% formic acid in water) and increasing the acetonitrile phase over 8 minutes until reaching 100%. This ratio was held for 3 min before switching back to 100% aqueous phase and equilibration for 1 min. The flow rate was set at 0.4 mL min<sup>-1</sup>, and the column oven temperature was maintained at 25°C. Mass spectrometry analysis was performed in positive and negative modes with a scan range of  $m/z$  75 to 1125 and a peak resolution of 70,000 for MS1 acquisition. Electrospray ionization was carried out with the following parameters: capillary temperature of 380°C, spray voltage of 3000 V, sheath gas flow of 60 arbitrary units, and auxiliary gas flow of 20 arbitrary units. For MS2 acquisition using ddMS TopN experiments, MS2 spectra were obtained at a peak resolution of 70,000 (NCE 15, 30, 45), using an AGC target set to  $3 \times 10^6$  and a maximum ion time set to 100 ms. The MS/MS spectra of precursor ions were obtained from the pooled QC sample using the abovementioned MS parameters and with an isolation window of  $m/z$  0.4.

### *Analysis of significant features and metabolites identification*

LC-MS runs were visualized using the Xcalibur software (Thermo Fisher Scientific). Metabolome analysis, data processing, and peak deconvolution were performed using

## Chapter 1

Compound Discoverer™ software 3.3 (Thermo Fisher Scientific) following a comparative untargeted metabolomics workflow. The raw data were imported for peak deconvolution and metabolite annotation. The mass tolerance for MS identification was set at 5 ppm, the minimum MS peak intensity was  $2 \times 10^5$ , and the intensity tolerance for the isotope search was 30%. The relative standard deviation was set to 50%. The selected labelled spectra were exported as .xlsx files, and the masses were searched in public mass lists (LipidsMaps, Natural Products Atlas, Thermo libraries). The raw dataset will be uploaded on MetaboLights [MTBLS6476]. The compound list was exported as a .csv file, and the intensities were normalized based on a normalization factor determined by the total carbon content. PCA was performed to compare the similarities of metabolites between cellular extracts of *Amoebophrya* spores using MetaboAnalyst 5.0 (Pang et al., 2021). The interquartile filter was applied for all processed datasets, and the intensities were log-transformed and Pareto-scaled. The identity of selected compounds was further confirmed using tandem mass spectrometry, and the MS/MS spectra were compared by spectral analysis and similarity search using CSI:FingerID in SIRIUS (Dührkop et al., 2015).

### *Smartseq2 sample preparation, library generation and sequencing*

For both the spores and the infected host, a total of 10 and 20 cells, respectively, were sorted into 96-well plates (Thermo), each well contained 4  $\mu$ L of lysis buffer (0.8% of RNase-free Triton-X (Fisher) in nuclease-free water (Ambion), 2.5 mM dNTPs (Life Technologies), 2.5  $\mu$ M of oligo(dT) (5'-AAGCAGTGGTATCAACGCAGAGTACTTTTTTTTTTTTTTTTTTTTTTTTTTTTTTTTTTT-3') and 2U of SuperRNAsin (Life Technologies)). Sorted populations are illustrated in the supplementary data 9. Reverse transcription and cDNA amplification were conducted as reported previously (Reid et al. 2018; Howick et al. 2019; Gomes et al. 2022). Sorted plates were spun at 1,000 g for 10 s and immediately placed on dry ice. Plates were heated at 72°C for 3 min. A reverse transcription mix, containing 1  $\mu$ M of LNA-oligonucleotide (5'-AGCAGTGGTATCAACGCAGAGTACATrGrG+G-3'; Qiagen), 6  $\mu$ M MgCl<sub>2</sub>, 1 M Betaine (VWR), 1X reverse transcription buffer, 50  $\mu$ M DTT, 0.5 U of SuperRNAsin (Invitrogen), and 0.5  $\mu$ L of Smartscribe reverse transcriptase (Takara), was added to the plates. The total volume of the reaction was 10  $\mu$ L. The following cycling conditions were used: a single incubation period at 42°C for 90 min, followed

## Chapter 1

by 10 cycles (42°C/2 min, 50°C/2 min), before a final incubation at 70°C for 15 min. A further PCR mix was added to the plates, containing 1X KAPA Hotstart HiFi Readymix (Roche Diagnostics France) and 2.5 µM of the ISO SMART primer (Picelli et al. 2014) and incubated using the following program: a single incubation at 98°C for 3 min, 30 cycles (98°C/20 s, 67°C/15 s, 72°C/6 min), a final incubation at 72°C for 5 min. Reactions were purified with 1X Agencourt Ampure beads (Beckman Coulter) according to the manufacturer's instructions. Amplified cDNA was eluted with 10 µL nuclease-free water (Ambion). The quality of a subset of cDNA samples was assessed with the high-sensitivity DNA chip (Agilent) with an Agilent 2100 Bioanalyser. Sequencing libraries were prepared using the Nextera XT 96 kit (Illumina) according to manufacturer recommendations but using quarter reactions. Dual indices set A and B were used (Illumina) for 192 different index combinations, for a total of 192 libraries. Libraries were pooled in two pools and cleaned up with Agencourt Ampure beads (Beckman Coulter) used at a 4:5 ratio. The quality of the libraries was assessed with the high-sensitivity DNA chip (Agilent) ran on an Agilent 2100 Bioanalyser. Both pools were combined and sequenced on a Hiseq 4000 with PE150 (Genewiz). FASTQ files were obtained after base calling and demultiplexing with Illumina's software. Nextera adapter sequences were trimmed with cutadapt (v3.4) using `cutadapt -a CTGTCTCTTATACACATCT -A AGATGTGTATAAGAGACAG --length 50` (Martin, 2011). A combined reference of A120 and its host *Scrippsiella acuminata* (Farhat et al., 2020) was created using bedtools (Quinlan and Hall, 2010) and indexed with HISAT2 (v2.2.1) (Kim et al. 2019). Reads were aligned to this indexed reference with HISAT2 using `hisat2 --max-intronlen 5000 -p 8 -q --very-sensitive`. SAM files were converted to BAM using `samtools-1.2 view -b` and sorted with `samtools-1.2 sort` (Li et al. 2009). Uniquely mapped reads were selected with Sambamba (Tarasov et al. 2015). BAMs were sorted with `samtools sort` and reads counted with `samtools view`. Cells were first filtered based on the number of transcripts detected > 250 and more than > 2,000 reads. After filtration, 126 transcriptomes were used for further analysis. Differential expression analysis was conducted in DESeq2 with default parameters (Love, Huber, and Anders 2014). Differentially expressed gene and log fold changes were visualized with the gplots package (v3.1.3) with `heatmap.2`.

### *Orthology*

We used the method described in (Decelle et al. 2022) to identify orthologues of sex-related genes. Briefly, reference proteins of interest listed in previous studies (Cai, 2019, Lin et al. 2022, Shah et al. 2020) were downloaded from the UniProtKB (<https://www.uniprot.org>) and VEuPathDB (<https://veupathdb.org/veupathdb/app>) databases (last access September 2023). These reference sequences were used as BLAST queries to identify homologs in the *Amoebophrya* genome (available here: <http://application.sb-roscoff.fr/blast/hapar/download.html>), and the identity of positive hits was confirmed by (1) reverse-BLAST to the UniProtKB database (<https://www.uniprot.org/blast/>; last access September 2023); (2) sequence search in InterPro (<http://www.ebi.ac.uk/interpro/>; last access September 2023); (3) domain search with Pfam 34.0 (<http://pfam.xfam.org/>; last access September 2023); (4) phylogeny performed on the NGPhylogeny.fr website (<https://ngphylogeny.fr/>) [Lemoine et al. 2019] where genes were aligned using mafft v.7 (Kato & Standley, 2013), alignments filtered using trimAl (Capella-Guierres et al. 2009), and Maximum Likelihood (ML) trees were constructed using FastTree v.2 with 1000 bootstraps for branch support (Price et al. 2009, 2010). The homology of genes was based on visual inspection of alignments using SeaView v.5.0.5 (Gouy et al. 2010) and of phylogenetic trees using FigTree v1.4.4 (<http://tree.bio.ed.ac.uk/software/figtree/>). The final set of homologous sequences were then aligned with mafft online (Kato et al. 2019), and the alignments were filtered with Gblocks v. 0.91b with the -b5=an option (Castresana 2000). Single gene phylogenetic trees were reconstructed for each alignment using RAxML v. 8.2.12 (Stamatakis 2014) with the -# 1000 -m PROTGAMMAIAUTO options. The latter phylogenetic analyses were performed on the ABiMS platform (<http://abims.sb-roscoff.fr/>) at the Station Biologique de Roscoff.

## **Results**

### *Infection cycle assessed by flow cytometry*

We comprehensively monitored the complete infection cycle of *Amoebophrya ceratii* within *Scrippsiella acuminata* using a flow cytometer. Infected and non-infected host cells were distinguished based on their differential signatures derived from flow cytometry (Fig. 1-1A-P), primarily characterized by an increasing level of green autofluorescence in infected cells by a factor of 100x compared to uninfected host cells

(Fig. 1-1E-H). We defined three stages: initial infection (same fluorescence as uninfected hosts), mid-infection (intermediate fluorescent gate, peaking ~ 31 hours post infection), and late infection (higher green fluorescence gate, until ~ 36 hours). The red autofluorescence under the 488 nm laser (associated with chlorophyll content from the host chloroplasts) remained constant during the mid-infection stage and exhibited a rapid reduction during late infections (Fig. 1-1I-L). An increase in forward scatter (FSC) by a factor of 1.5x was observed during the intracellular development of the parasite (Fig. 1-1M-P).

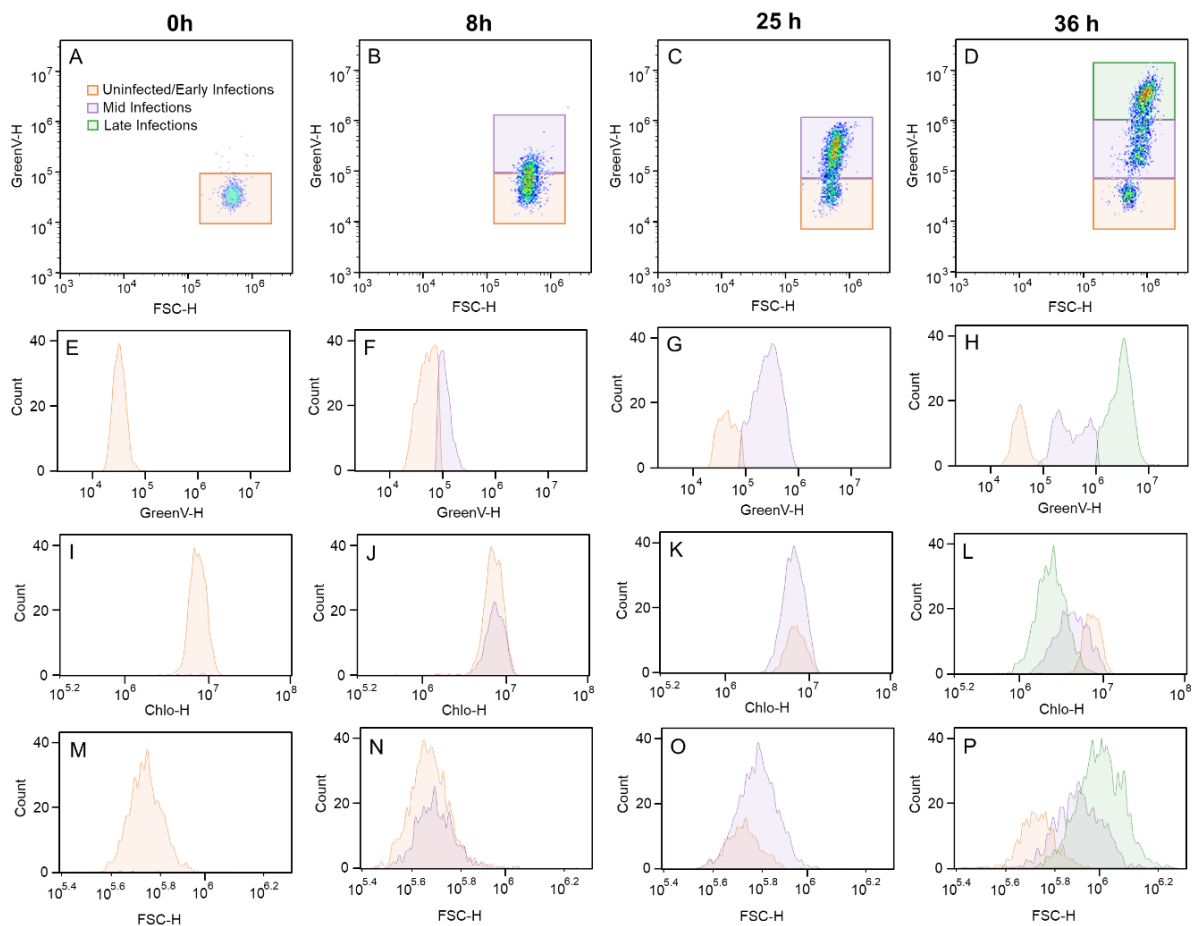


**Figure 1- 1:**The intracellular development of the parasite *Amoebophrya ceratii* within its host, *Scrippsiella acuminata*, as monitored using flow cytometry.

Three distinct stages of infection were highlighted: uninfected (or early infections), mid-infected, and late-infected, each represented by a different colour. The progression of infection was assessed at four-time points:  $t=0$ , 8, 25, and 36 hours after inoculation. A-D: Flow cytograms depicting green autofluorescence under 405 nm excitation (GreenV-H) related to forward scatter (FSC-H) at the specified time points. E-H: Histograms displaying green autofluorescence intensity (405 nm laser). I-L: Histograms displaying red autofluorescence under 488 nm excitation (chlorophyll content, Chlo-H). M-P: Histograms representing FSC, which provide information on cell size.

## Chapter 1

Distinct spore populations can be separated based on their flow cytometry signatures (Fig. 1-2), with two main populations of interest called P1 and P2 visible at 49 hours (Fig. 1-2A). P1 exhibiting lower green fluorescence (Fig. 1-2B) and FSC (Fig. 1-2C) as compared to P2. We tracked the fate of these populations through time (Fig. 1-2 C-I) and observed that whilst P1 remained relatively stable over time (with only a slight decrease in FSC and green fluorescence), P2 displayed a much more pronounced decrease in FSC and an increase in green fluorescence (Fig. 1-2 C-F), giving rise to a distinct population, named P3 hereafter (Fig. 1-2 G-H). The shift between P2 and P3 started around 73 hours after inoculation (Fig. 1-2K). During this transition, cytometric signatures revealed an overlap in the FSC between larger P1 and smaller P3, suggesting that the main distinguishing factor between them was their respective level of green autofluorescence. P2 spores were observed to be released first, 36 hours after inoculation and 1 h 30 min before P1 spores (Fig. S1-1, Fig. 1-2J). The differential release of P1 and P2 suggests that the two spore populations originated from distinct infected host cells. We analysed the spores released by single infected host cells to test this hypothesis. All but four infected host cells (Fig. S1-2) produced exclusively P1 or P2 spores (6 and 35 cells, respectively, out of a total of 45 sorted individuals). Notably, during this experiment, P1-producing hosts exhibited higher yield with an average of  $718 \pm 111$  spores released per host, compared to P2-producing hosts which released  $190 \pm 70$  spores. If we postulate that divisions were synchronous and each cell divided in two during the sporulation ( $y = 2^n$ ), the number of iterative divisions can be estimated to be around 10 and 8 generations, respectively.

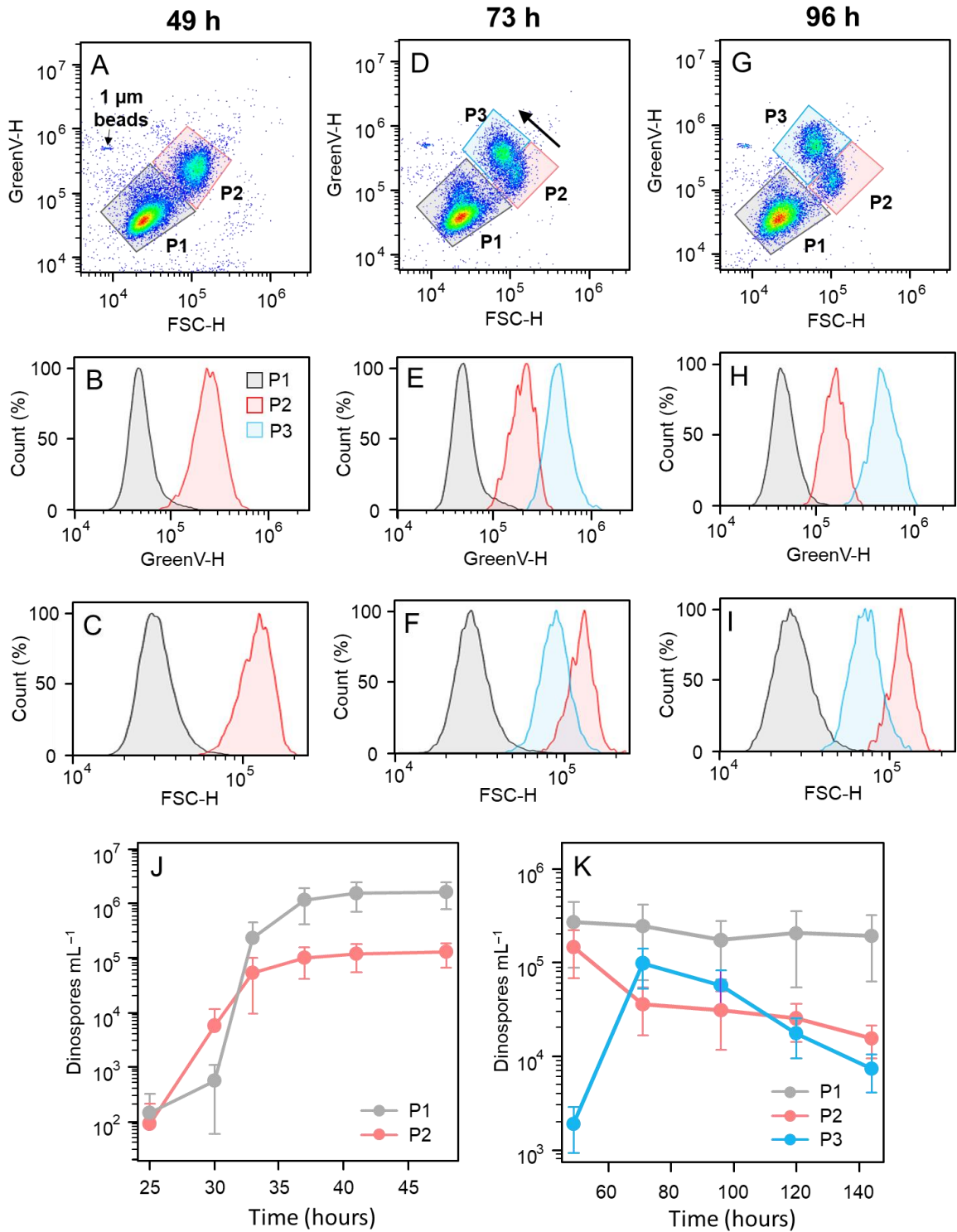


**Figure 1-2: Flow cytometry used to monitor spore populations, namely P1, P2, and P3, at various time points following inoculation.**

The sampling was performed at  $t=49$  (A-C), 73 (D-F), and 96 (G-I) hours after inoculation. First row (A, D, G): Flow cytograms illustrating the relationship between green autofluorescence and FSC (forward scatter). Second (B, E, H) and third rows (C, F, I): Histograms representing the normalised cell counts (in %) based on the green autofluorescence under 405 nm excitation and FSC, respectively. Last row (J, K): Spore counts, measured in cells per mL, tracked over time (hours).



### *Phenotypes of spores assessed by microscopy*

Two types of spores were distinguishable by epifluorescence microscopy based on their cell dimensions. Using confocal microscopy, we calculated biovolumes for P2 spores close to twice those estimated for P1 populations:  $27.2 \mu\text{m}^3 \pm 3 \mu\text{m}^3$  ( $n = 112$ ), and  $15.5 \mu\text{m}^3 \pm 2.5 \mu\text{m}^3$ , ( $n = 156$ ), respectively (Fig. S1-3). TEM negative staining of spore cells isolated by flow cytometry sorting indicated a mean length and width of  $1.84 \pm 0.23 \times 1.37 \pm 0.33 \mu\text{m}$  and  $2.9 \pm 0.41 \times 2.55 \pm 0.25$  for P1 and P2 spores, respectively. Both types had two flagella, one transversal bearing hairs and a smaller hair-less longitudinal one (Fig. 1-3A-B). The long flagellum is of nearly the same length between the two types of spores, measuring  $9.48 \pm 2.55 \mu\text{m}$  in P1 spores and  $10.46 \pm 2.27 \mu\text{m}$  in P2, respectively, displaying similar hairs. The smaller naked flagellum is challenging to observe, rarely observed by TEM in P1 spores and has an average size of  $2.11 \pm 1.34 \mu\text{m}$  in P2. TEM sections revealed distinct condensed chromatin in the nuclei of both P1 and P2 spores. In P1 spores, the chromatin forms a ring around the inner periphery of the nuclear envelope (Fig. 1-3C-D), whereas in P2, the chromatin is clearly separated into chromosomes (Fig. 1-3E-F). Only P1 spores possess an apical complex-like apparatus and trichocysts (Fig. 1-3C-D). The apical complex consists of various vesicles resembling dense granules and rhoptry-like structures. Further elucidation of this structure will necessitate 3D reconstruction due to its complexity. P2 spores were characterized by numerous lipid droplets in the cytoplasm (Fig. 1-3F).

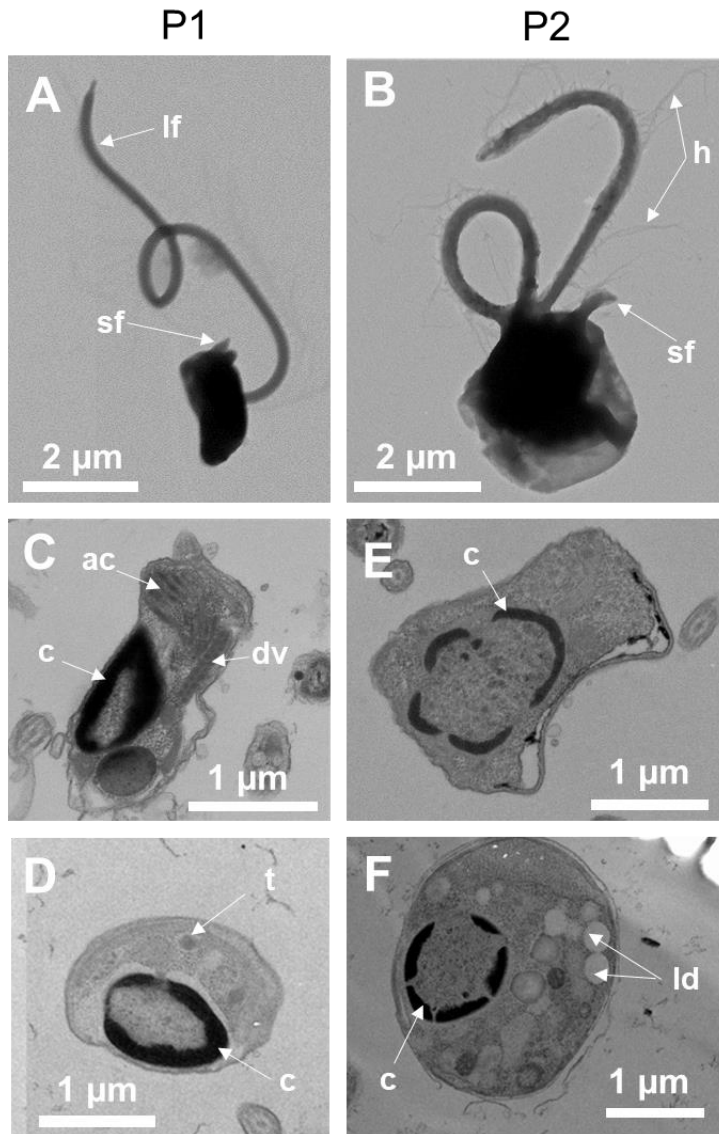


**Figure 1- 3: Transmission electron microscopy (TEM) was employed to examine P1 (left) and P2 (right) spores using various techniques.**

A-B: TEM negative staining, C-E: Thin section with chemical fixative, D-F: Thin section with cryofixation. ac: apical complex with vesicles, c: condensed chromatin, dv: dense vesicles, h: flagellar hairs, ld: lipid droplet, lf: long flagellum, sf: small flagellum, t: trichocyst.

In terms of swimming behaviour (Fig. S1-3), most spores did not swim under low violet light illumination when observed in the epifluorescence microscope. Only 9% (23 out of 254) of P1 and 37% (58 out of 155) of P2 exhibited movement among the recorded cells. P2 was nearly six times more likely to swim than P1 ( $p > 0.0001$ , odds ratio = 6.0, 95% CI: 3.4-10.8, Fisher-Exact Test). The two spore types displayed distinct swimming behaviours. While P1 swims straight forward, P2 exhibits helical motion with large loops (Fig. S1-4). P1 exhibited higher average speed compared to P2 (153.3  $\mu\text{m}$

$s^{-1}$  and  $105.7 \mu m s^{-1}$ , respectively,  $p = 0.0063$ , Kruskal-Wallis; Fig. 1-4A). However, P2 swimming time exceeded that of P1 (respectively 1.68 s and 0.93 s,  $p = 0.0007$ , Kruskal-Wallis; Fig. 1-4B). Consequently, P1 traveled shorter distances than P2 ( $50.4 \mu m$  and  $101.7 \mu m$ , respectively,  $p = 0.0069$ , Kruskal-Wallis; Fig. 1-4C). The Euclidean distance analysis further revealed that despite covering greater distances, P2 ended up closer to their starting point compared to P1 ( $15.6 \mu m$  and  $42.3 \mu m$ , respectively,  $p = 0.0009$ , Kruskal-Wallis; Fig. 1-4D), suggesting that P2 covered more surface.

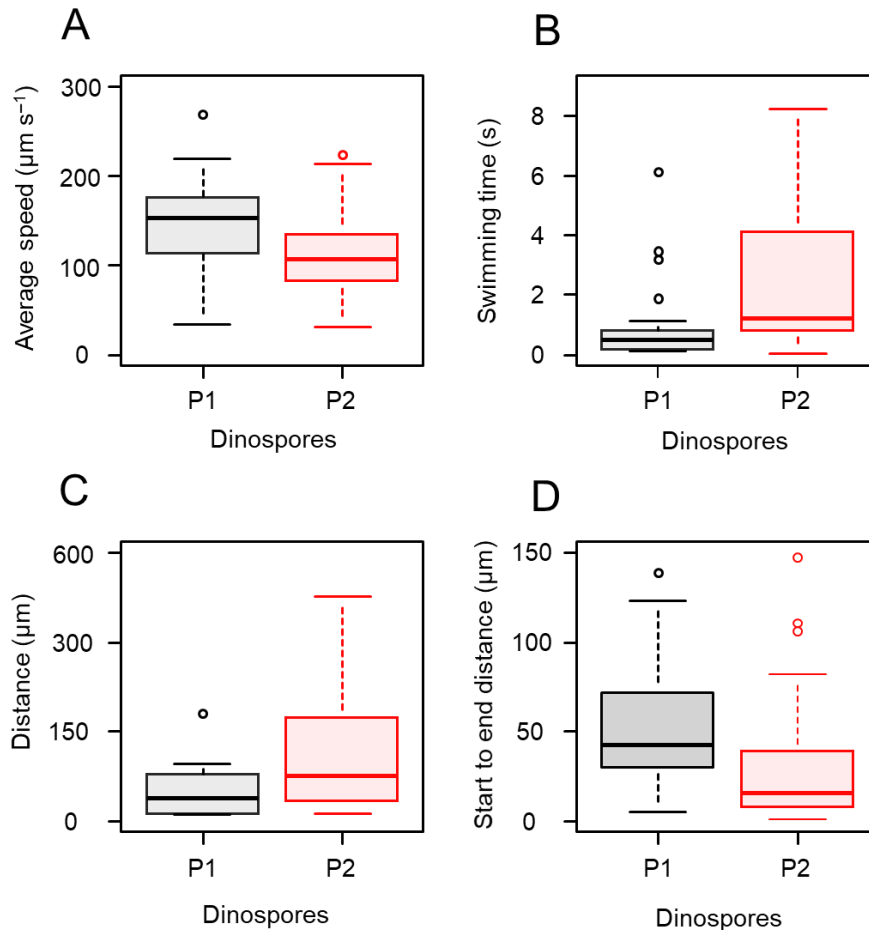


**Figure 1- 4: Swimming behaviour of P1 and P2 spores.**

A: average speed, B-Swimming time, C: distance covered, D: distance from the start to the end.

### *Exploring spore production*

Throughout our study we observed that P2 production was variable and not observed in every experiment. We therefore used a decision-support hierarchical model based on 149 infection experiments to assess culturing conditions affecting the densities and percentage of P1 and P2 at T47 (Fig. 1-5). This analysis indicated that the predominance of P2 production was typically favoured when the density of P1 spores

in the inoculum culture exceeded 1.66 million cells mL<sup>-1</sup> (n = 12, p < 0.001). In contrast, P1 densities in the inoculum culture lower than 190,000 cells mL<sup>-1</sup> results in both P1 and P2 low densities (>500,000 cells mL<sup>-1</sup>; n = 46, p < 0.001). When P1 densities in the inoculum culture were between 190,000 and 1.66 million cells mL<sup>-1</sup>, the density and proportion of the spore types were secondarily affected by the spore:host ratio at T0 (Fig. 1-5), with spore:host ratios lower than 7:1 leading to spore populations with both P1 and P2 at high densities (>500,000 cells mL<sup>-1</sup>; n = 16, p < 0.001), and spore:host ratios resulting either predominance of P1 or spore populations both with P1 and P2 low densities (n = 75, p < 0.001). Other tested parameters, such as the density and age of host at T0 were not related to either P1 or P2 production.

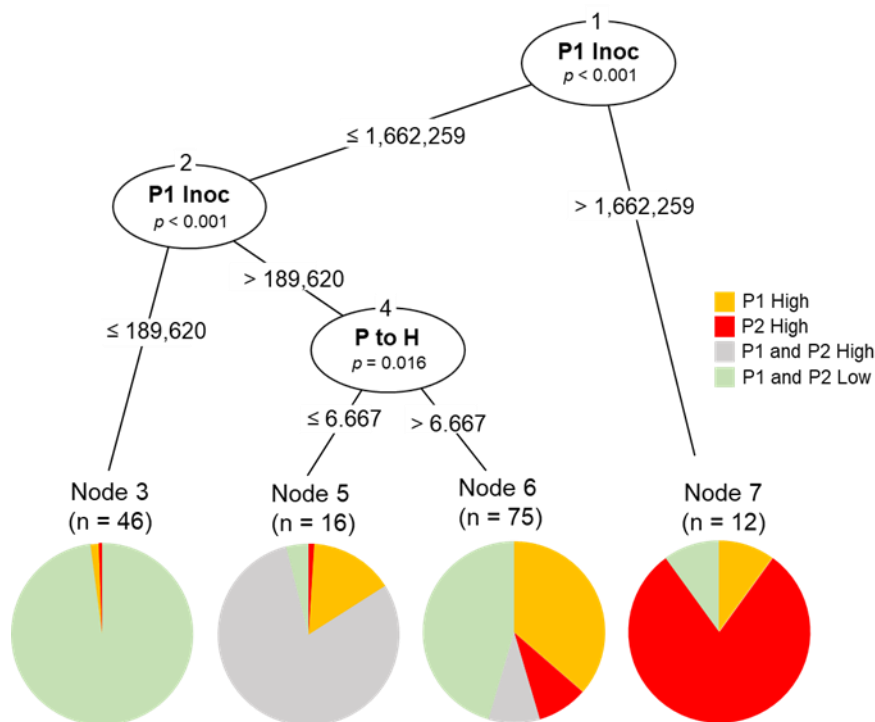


**Figure 1- 5: Decision-support hierarchical model based on 149 infection experiments.**

Production of spores was classified into four categories relative to cell density: (1) “P1 high” = P1 >500,000 cells mL<sup>-1</sup> and P2 accounting for ≤ 40% of total spores, (2) “P2 high” = P2 >500,000 cells mL<sup>-1</sup> and P1 accounting for ≤ 40% of total spores, (4) “P1 and P2 high” = both P1 and P2 > 500,000 cells mL<sup>-1</sup>, (4) “P1 and P2 low” = both P1 and P2 <500,000 cells mL<sup>-1</sup>. P1 Inoculum: density (cells mL<sup>-1</sup>) of P1 spores in the inoculum (i.e., mother cultures form which spores were obtained for inoculation); spore:host: ratio between spores and host at T0.

### *Infectivity, ploidy level, and mating type*

Using a pure culture of P2 spores (Fig. S1-6), we observed that no infection occurred over one week following inoculation, with all P2 spores transitioning to P3 45 hours after inoculation. In a second experiment using P1 and P2 populations sorted by flow cytometer and inoculated in exponentially growing hosts, P1-sorted cells resulted in 86% infected cells 50 hours post-inoculation whereas only 4.68% was obtained with P2-sorted spores. It is noteworthy that the P2 inoculum still contained a few P1 spores (P1:host ratio of 0.19, Fig. S1-7) , which could have caused the observed infections.

We further measured the ploidy levels of mixed populations of spores by flow cytometry, specifically those consisting of P1 with P2 and P1 with P3 (Fig. S1-8). The results revealed a remarkable similarity in DNA content for mixed populations of P1 with P2 or P1 with P3, with SYBR green fluorescence intensity (blue, 488 nm laser excitation) ratios of 1.17 and 1.18, respectively (Fig. S1-8). We concluded that P1, P2 and P3 had the same ploidy level.

To further assess if larger spores (P2) could act as gametes, three strains belonging to the same sub-cluster (MALVII Clade 2 subclade 4), purportedly of the same species (Cai et al. 2020), were crossed with strain A120 to investigate mating types within this species. We anticipated that the fused cells would be larger than their parental counterparts, and that if fusion occurred, novel, larger populations would emerge (larger FSC populations). However, no larger populations emerged in any of the mating tests conducted during the two experiments (Fig. S1-9).

### *Metabolites from exudates and endometabolome of Amoebophrya spores*

We comprehensively analysed metabolites (presented in Fig. S1-10), derived from exudates (exometabolome) and cells retained on filter (endometabolome) within cultures containing spores. Cell density data was recorded in Table S1-2 and the derived carbon content was depicted (Fig. S1-11). The cultures were primarily composed of either P1 or P2 spores at t=49 hours, or P3 spores at t=71 hours (Fig. S1-12). P2 and P3 spores exhibited similar metabolic profiles, as demonstrated by principal component analysis (PCA) for the endometabolome (Fig. 1-6A) and the exometabolome (Fig. S1-13). These spores clustered together, highlighting their metabolic similarity. Thus, P2 and P3 were grouped in the following analyses.

We identified substantial differences between P1 and the combined P2+P3 spores. Specifically, a curated selection of 44 metabolites showed distinct associations in P1 or P2+P3 spore cell extracts. Among the most significant metabolites that exhibited exclusive associations with either one of these categories in the endometabolome, five were uniquely identified in the P2+P3 extracts (Fig. 1-6B). Notably, two of these metabolites were also concurrently observed in the exometabolome, suggesting a potential extracellular secretion process of these components, although export has not been demonstrated.

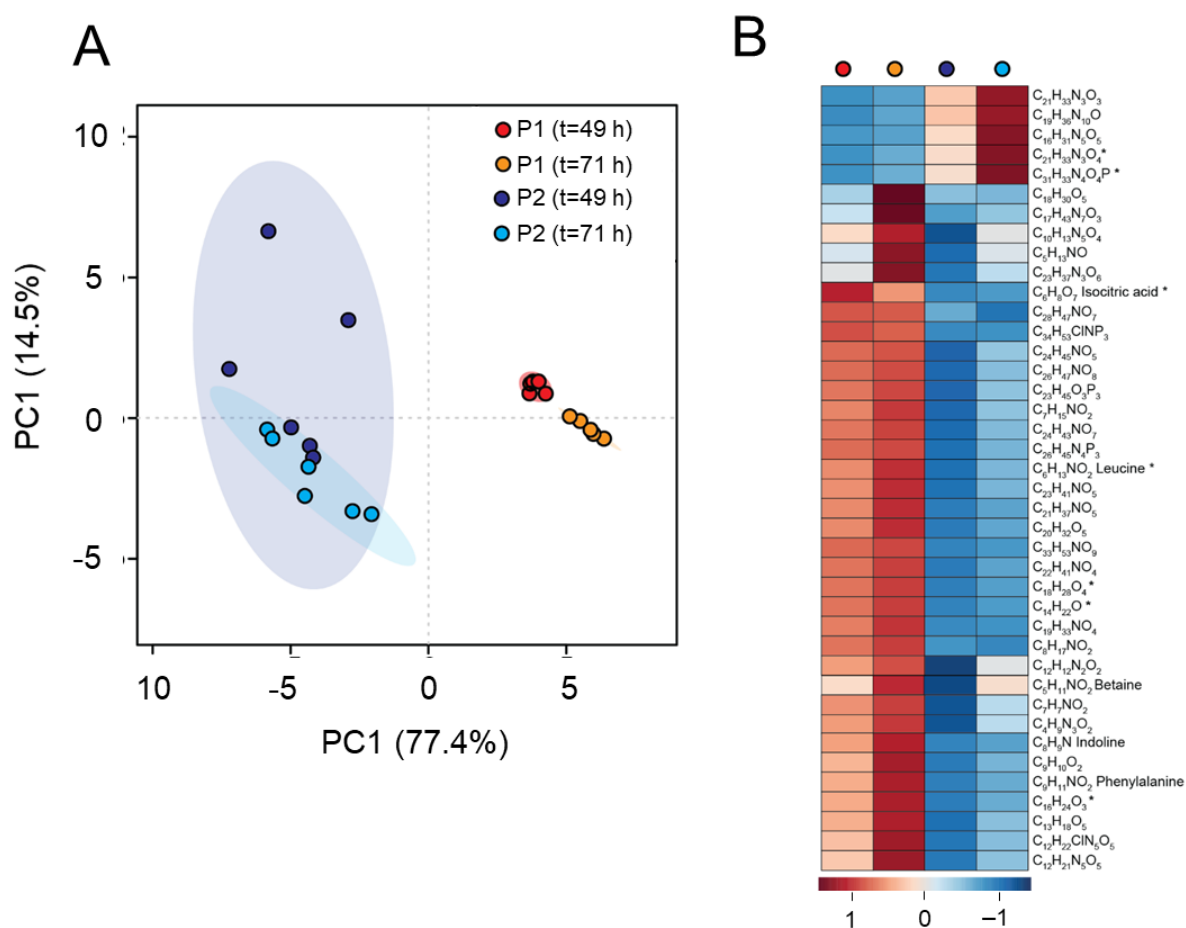


**Figure 1- 6: Multivariate analysis of selected metabolites**

A- Principal component analysis was conducted on the 44 selected metabolites specifically associated with spore cell exudate extract profiles at different age. B- The top 44 significant compounds discriminating the endometabolome profiles of P1 and P2 extracts were annotated. The intensities detected for the 44 metabolites were square root-transformed and Pareto-scaled, then displayed in the heatmap. \* Molecules also detected in the exometabolome (putatively secreted molecules). Only molecules that were unambiguously identified with a standard are named.

## Chapter 1

The remaining compounds were distinctly linked to P1 spores. Among those, we identified five molecules at the level 1 confidence accepted for metabolite (Schymanski et al. 2014), e.g.: isocitric acid, leucine, glycine betaine, indoline, and phenylalanine.

### *Gene expression patterns*

To gain a deeper insight into the characteristics of the different spore types, we conducted a transcriptomic analysis of pools of 20 sorted infected hosts at various stages of infection (Fig. S1-14), as well as pools of 10 P1, P2, or P3 spores (Fig. S1-15). Following *in silico* QCs, we obtained a transcriptomic dataset composed of 10 early-infected host cells (i1, on a total of 13), 20 mid-infected host cells (i2 or i3, on a total of 24), 10 late-infected host cells (i4, on a total of 12), 41 for P1 spores, 15 of P2 spores, and 30 of P3 spores (all pools retained for spores).

Mapping to a combined genome reference showed a progressive accumulation of parasite RNA within host cells as the infection advanced. In late-stage infections, host RNA represented up to ~25% of total reads (see Fig. 1-7A). Subsequently, we employed dimensionality reduction exclusively using transcript counts associated with the parasite. Principal component analysis (PCA) revealed that each stage had a distinct transcriptomic signature. The only exception was the overlap between mid-infected hosts (i2 and i3), and the remarkable similarity between P2 and P3 (Fig. 1-7B). As a result, both categories (i2+i3 and P2+P3) were grouped in subsequent analyses. Altogether, P1 and P2+P3 spores were markedly different. Based on a differential expression analysis, 2225 genes upregulated in P2+P3 compared to P1, whereas 252 genes were downregulated (adjusted p-value <  $10^{-10}$ , Dataset 2).

We thoroughly searched for orthologues associated with sexual reproduction in *Amoebophrya* sp. A120 genome. We identified 32 conserved meiotic genes (Table S1-3). Genes inventoried here encode for proteins involved in inducing meiosis, creating meiotic double-strand DNA breaks and subsequent meiotic DNA repair, crossing over, and cohesion of sister chromatids and homologous chromosomes. Remarkably, 21 of these genes were upregulated in P2+P3 and nearly absent in P1 (Fig 7C). Among these genes were SPO11 (Fig. 1-7D), HOP2, DMC1, and MND1, all of which have been confirmed as meiosis-specific in dinoflagellates (Lin et al., 2022). Additionally, we detected an ortholog of the gamete fusogen HAP2, which was exclusively in three P2 samples. We fail to identify orthologues for the nuclear fusion protein GEX1.

## Chapter 1

Furthermore, genes associated with DNA mismatch repair (Msh6, PMS1, MLH1, EXO1) and the cohesion complex (Smc1, Smc3, Smc4, RAD21) displayed heightened expression in P2 spores (Fig 7C). Interestingly, genes associated with sexual reproduction were already expressed in the last intracellular stages (i2/i3-i4) of infection (Fig 7C) suggesting that sexual reproduction may be already engaged in the intracellular phase.

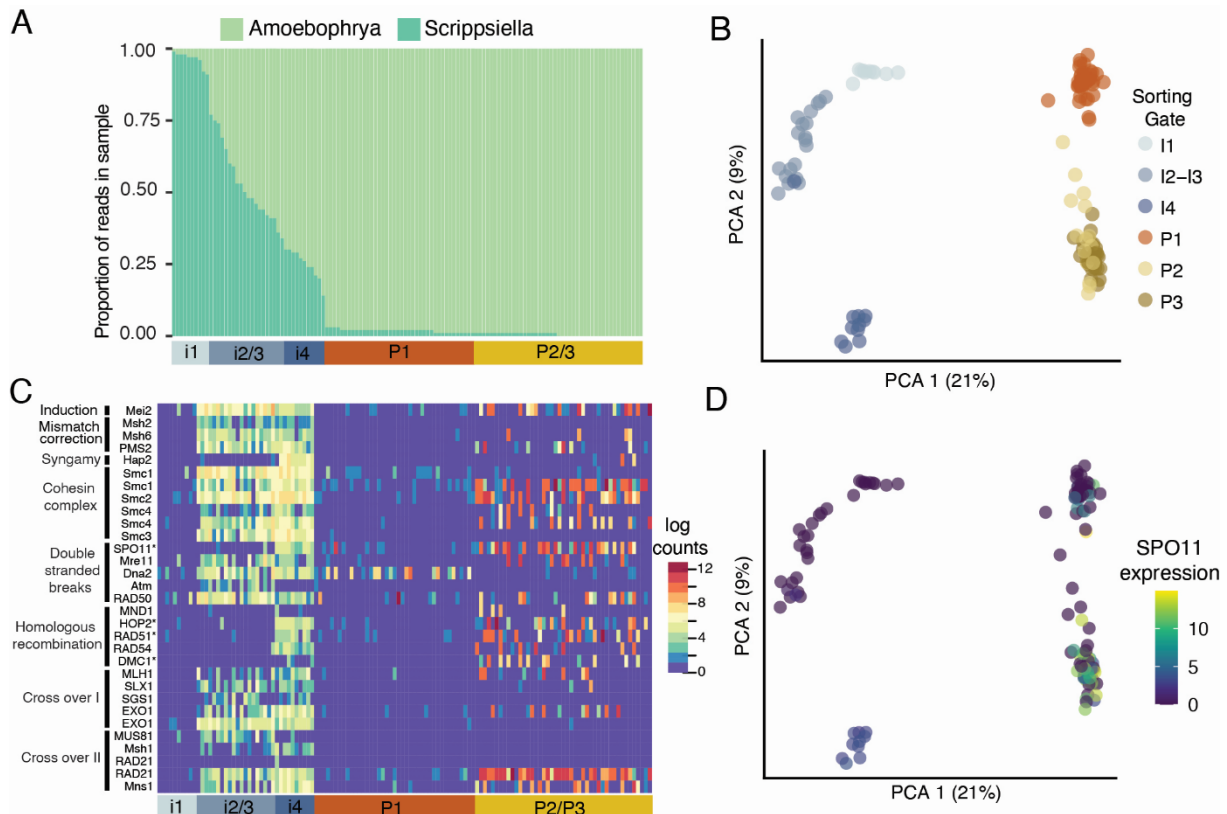


**Figure 1-7: Analysis of sorted populations using flow cytometry.**

A-Proportion of reads in sample (either the host *Scrippsiella acuminata* or the parasite *Amoebophrya ceratii*). B- Distribution of sample (PCA analysis). C-Heatmap of expression of genes involved in meiosis. D- One example of gene expression (SPO11, involved in meiosis) over sample (PCA analysis). i1, i2/3, i4: different stages of the intracellular development of the parasite at increasing time. P1, P2, P3: spore populations.

Several other pathways also exhibited differential expression in P2+P3 spores (Dataset 3). Notably, active DNA replication, an essential aspect of sexual reproduction, was supported by the upregulation of genes such as DNA primase, DNA polymerase (alpha and epsilon), topoisomerases I, II, and III, numerous helicases, and DNA replication licensing factor MCM(s) in P2+P3 spores (Fig. S1-16). Additionally,



## Chapter 1

RNA/DNA synthesis genes, including those associated with the pentose phosphate cycle (which aids in producing PRPP and IMP for purine synthesis), were also overexpressed (Fig. S1-16). This overexpression pattern extended to CTP synthase, which plays a pivotal role in pyrimidine production. The orchestration of chromosome organization was apparent in P2+P3 spores, with pronounced upregulation of genes such as DVNP, histones, proteins involved in kinetochore organization (NDC80, CDC20, EB1), tubulin, microtubules, and basal body-related genes (Fig. S1-16). These findings suggest dynamic modifications in chromosomal architecture.

In contrast, metabolic activity in P1 spores appeared subdued, with the notable exception of upregulated ribosomal proteins. These proteins play a crucial role in the initial stages of ribosome assembly and include small nucleolar ribonucleoproteins (snoRNPs) localized in the nucleolus, where ribosome biogenesis occurs, along with 12 other ribosomal proteins (Fig. S1-16), most of them also expressed in P2+ P3 spores.

## Discussion

MALVs (Marine Alveolates) remain an enigmatic group within marine plankton. Given the diversity and distribution of MALVs, resolving their life cycle is critical to comprehend their functional role in the oceans. In this study, we were able to finely investigate the timing of various life cycle stages in the dinoflagellate parasite *Amoebophrya* sp. (referring to the complex species *A. ceratii*) and highlight the multiple functional roles of the different spores produced.

The ground breaking elucidation of the infectious cycle of *Amoebophrya ceratii* was initially provided by Cachon in 1964. Our current research, monitored by more modern tools, aligns with this foundational understanding, confirming all previous observations and adding further insights into significant behavioural and phenotypical features. First, we described two main intracellular stages: low green fluorescence and high chlorophyll content (mid-infection), and high green fluorescence and low chlorophyll content (late infection). This observed shift taking place 31 hours after incubation may correspond to a critical transition occurring during the intracellular development of the parasite, marking the passage from the trophont to the sporulating stage.

## Chapter 1

The infection cycle unfolds rapidly, spanning less than two days, and is marked by a significant increase of size of the infected host cells by 1.5 times. The release of spores starts around 36 hours post-inoculation, yielding two distinct spore types, each displaying different flow cytometric signatures. Production of dimorphic spores was extensively documented in both *Amoebophrya* and nearly all Syndiniales species with well-studied life cycles. These spore types are commonly referred to as macro- and micro-spores, but their significance was not understood so far.

In this study, we significantly advance our understanding of the functional role of these spores. For instance, we demonstrate that the smaller morphotype exhibits extended viability and serves as the infectious propagule. This conclusion is supported by our infectivity experimental tests and a well-developed apical complex structure exclusively detected in this spore type, as observed in TEM. The apical complex is an organ system found in the Apicomplexa, enables the parasites to adhere to a host cell, extract its contents, or invade it (Guizetti and Frischknecht, 2021) P1 spores, in contrast to P2, were observed to exhibit a higher rate of immobility, which may explain their prolonged survival, given the energy-consuming nature of swimming. Additionally, P1 spores demonstrated a swifter forward-swarming motion, enhancing their capability to locate non-infected host cells. This swimming behaviour is unusual for dinoflagellates, as they are typically characterized by a helical trajectory. This unique trait in dinoflagellates results from the conjunction of a transversal flagellum that induces the cell to rotate along its length axis and a trailing longitudinal flagellum responsible for cell translation (Crenshaw, 1996; Fenchel, 2001). The reduction in the size of the transversal flagellum may, in part, contribute to the absence of the helical trajectory in P1.

We also show that the number of differentially expressed genes in P1 spores is generally reduced, except for the ribosomal structure. This is further corroborated by TEM section where P1 spores exhibited highly condensed chromatin surrounding the nucleus, which may result in decreased gene expression activity. In this context, pre-activation of the ribosomal pathway, especially involving small nucleolar ribonucleoproteins (snoRNPs) crucial for rRNA and other nucleolar RNA maturation, may serve as a precursor to protein synthesis activation in preparation for infecting a new host. Metabolomic analyses revealed five formally identified molecules in P1 spore: isocitric acid, leucine, glycine betaine, indoline, and phenylalanine. Notably, unlike phenylalanine, leucine cannot be synthesized *de novo* by *Amoebophrya* A120

(unpublished data). Our analysis further indicated that none of the genes involved in the metabolic pathways for synthesis, either isocitric acid or phenylalanine, were overexpressed in P1 spores, or P2. A significant portion of these compounds was thus likely acquired from the host or synthesized within the host. Isocitric acid is a key component of the Tricarboxylic Acid Cycle (TCA) or Krebs cycle, which plays a pivotal role in releasing stored energy through the oxidation of acetyl-CoA derived from carbohydrates, fats, and proteins. The accumulation of isocitric acid may potentially be a result of the incompleteness of the TCA cycle pathway in *Amoebophrya* (Decelle et al. 2022).

We show that larger spores (P2 + P3) are non-infective and involved in sexual reproduction. Sexual reproduction, which emerged approximately 2 billion years ago (Zimmer 2009), is not a universal trait among eukaryotes. However, it remains prevalent in many species. While most unicellular parasites primarily reproduce asexually, they possess the capability to switch to sexual reproduction as a means to enhance genetic diversity and sustain infectivity (Heitman et al., 2006). The screening of meiotic genes across various lineages became feasible due to the high conservation of these genes among a wide range of organisms, spanning animals, plants, and eukaryotic microorganisms (Malik et al. 2008). Consequently, it is not surprising to discover that the *Amoebophrya* genome contains nearly the complete set of tools for meiosis, including 32 conserved meiotic genes. Furthermore, the expression of genes associated with meiosis and metabolic pathways involved in DNA synthesis and replication during the late stages of infection, and the even higher expression observed in P2 spores, suggests their involvement in sexual reproduction.

The upregulation of meiotic genes in P2 spores may initially seem counterintuitive. In the traditional understanding of sexual reproduction in dinoflagellates, it involves the fusion of haploid gametes to generate a diploid, mobile planktonic zygote, eventually culminating in the formation of resting cysts in sediment. Importantly, meiosis in dinoflagellates occurs only after the germination of these resting cysts, following a period of dormancy lasting for weeks to several months (Taylor, 1990). Despite partial sequence homology, no direct link between genes and meiosis has been established in dinoflagellates so far. However, the overexpression of five core meiosis genes (SPO11, MND1, DMC1, HOP2, and MSH4) during the cyst germination of *S. acuminata* has been considered indirect evidence of their involvement in meiosis in

## Chapter 1

dinoflagellates (Lin et al. 2022). In *Amoebophrya*, the significant expression of all but one of these genes in P2 spores suggests their readiness to directly engage in meiosis without the need for cyst formation. The presence of condensed chromatin, organized into chromosomes, serves as an additional indicator of their preparedness for meiotic division, where compact chromosomes are essential for proper pairing and the initiation of meiotic reduction. In fact, it is known that meiosis can also occur directly after fusion, without the formation of resting cysts in dinoflagellates (Bravo and Figueroa, 2014; Kremp, 2013). or instance, recent reports have documented increased expression of meiosis genes during dinoflagellate blooms, leading to the conclusion that sexual reproduction also occurs outside the period of cyst germination (Lin et al. 2022).

P2 spores may function as gametes, poised for immediate meiosis following cell fusion. Flow cytometry analysis has demonstrated the transformation of P2 into P3 populations. Strikingly, both gene expression and metabolomic profiles of these two populations appear similar, highlighting the temporal succession and uniform nature of these two groups. Single-cell analysis would likely be the most suitable method to provide a more detailed understanding of the processes involved during the maturation of these spores. Here, the pooling of 10 cells for analysis may not provide the granularity required to dissect the intricacies of the maturation process.

If P2 spores are gametes, the observed phenotypic variations can be interpreted in the light of this hypothesis. For example, P2 spores moved more slowly than P1, covering larger distance and following a helical trajectory, which could increase the likelihood of encountering a compatible partner for fusion, as suggested by Persson et al. (2013). If this is true, the discovery of two unidentified molecules secreted by P2+P3 spores suggest they could function as pheromones, which could play a role in gamete recognition and fusion although this suggestion would require further validation.

Whereas P2+P3 spores could be gametes, our comprehension of the entire process of sexual reproduction in *Amoebophrya* is still partial. Our objective was to assess the potential of the formation of compatible mating pairs and shift of ploidy level, which should result from the cell fusion (i.e., syngamy). The homogenous ploidy levels, along with the absence of observable zygotic cells in our cultures nor through strain crossings, suggest an absence of fusion and zygote formation within a single

## Chapter 1

monoclonal strain. This observation strongly supports the notion that the strain is heterothallic, requiring interbreeding with a compatible strain for fusion, rather than relying on self-compatibility. This outcome leads us to propose that if P2 spores function as gametes, none of the three strains tested during this study were compatible. Alternatively, diploid stages in *Amoebophrya* cultures could be transient, preventing the accumulation of populations dense enough for detection via flow cytometry. In conclusion, although P2 is very likely involved in sexual reproduction, the exact timing of fusion, mating types, and meiosis remain elusive.

Our findings allow us to conclude that a single infected host cell predominantly produces a single spore morphotype. This phenomenon was previously documented in other Syndiniales species (e.g., *Syndinium*: Skovgaard et al. 2005, *Ichthyodinium*: Shadrin et al. 2015, *Euduboscquella*: Coats, 1988). As observed in *Ichthyodinium* by Shadrin et al. in 2015, the spore dimorphism found in *Amoebophrya ceratii* may depend on the number of iterative divisions during sporulation issuing from two distinct pathways of development (8 and 10 rounds of division for P2 and P1, respectively). Two fewer rounds of division could explain the larger cell size of P2 and their earlier production compared to P1. As P2 is released 1.5 hours before P1, we can estimate the duration of each of the two last replications to be about 45 minutes, although replication time may not be the same in each round. For instance, different replication times were reported for *Duboscquella melo* (Cachon 1964), nor for *Ichthyodinium chaberladii* (Shadrin et al. 2015).

Our decision hierarchical model suggested production of P2 spores may be environmentally determined in the previous generation, with the density of P1 spores in the donor culture as the primary factor influencing cell fate choice. Higher concentrations of infective spores in the water could lead to a notable reduction in host density within the water column, potentially jeopardizing the parasite's survival (Chambouvet et al., 2008). Shifting from an infectious cycle to sexual reproduction might alleviate stress on the host and engender new allele combinations conducive to adaptation. Two processes may be at play. First, a higher density of parasites may lead to higher rates of coinfection, which can favour the route for sexual reproduction during the intracellular development of parasites. Alternatively, the decision to generate either P1 or P2 may be made well before P1 enters host cells, potentially through molecular signalling of population density. The findings related to P1 spores

could draw parallels with observations in bacteria. Quorum sensing, a recognized mechanism in bacterial cell-to-cell communication, involves generating, detecting, and responding to extracellular signalling molecules called autoinducers (Sharma et al., 2020). This process empowers bacterial communities to collectively modulate their behaviour based on fluctuations in population density and species composition within the local environment. While further investigation is warranted, the molecules identified as secreted by P1 spores in our study hold considerable potential as autoinducers for future exploration in *Amoebophrya*.

We acknowledge that the conducted experiments here provide only a partial perspective on the phenomenon. There may be additional parameters at play that contribute to the observed outcomes. However, we made significant progress in recognizing the existence of sexual reproduction in MALVs (at least in *Amoebophrya*). Several crucial stages still demand further investigation, including the outcomes of fusion and the mating types of these parasites. Our interpretation has heavily relied on combining of microscopy, flow cytometry, metabolomics, and transcriptomics techniques. To gain deeper insights, we need to explore single-cell approaches and acquire sexually compatible strains.

### **Acknowledgments**

We warmly thank different platforms located at the Biological Station of Roscoff, namely Merimage for microscopic observations (confocal, TEM), the Roscoff Environmental Flow Cytometry and Microfluidics (RECYF) for Flow cytometry analyses, the Roscoff Culture Collection (RCC) for strain maintenance and distribution and the Mass spectrometry platform (METABOMER) for the advises and the material. This work was funded by the Agence Nationale de la Recherche ANR-21-CE02-0030-01 (ANR EPHEMER project), and promoted in the frame of the **GDR Phycotox**. MW was supported by a Benjamin Franklin Fellowship (project 464344344), GP and MV were supported by the CRC 1127/2 ChemBioSys (project 239748522), both from the Deutsche Forschungsgemeinschaft (DFG, German Research Foundation). We thank Julie Lepetit for her help during the experiments

## References

- Bigéard, E., 2022. F/2 medium at 27 PSU of salinity from Sea Red salts (preprint). <https://doi.org/10.17504/protocols.io.n92ldzyrxv5b/v1>
- Bigéard, E., 2019. Collect of Amoebophrya parasite (free-living stage) for genomic and transcriptomic analyses.
- Bravo, I., Figueroa, R., 2014. Towards an Ecological Understanding of Dinoflagellate Cyst Functions. *Microorganisms* 2, 11–32. <https://doi.org/10.3390/microorganisms2010011>
- Cachon, J., 1964. Contribution à l'étude des péridiniens parasites. Cytologie, cycles évolutifs. *Ann. Sci. Nat. Zool.* 1–158.
- Cai, R., 2019. Exploration de la diversité et du potentiel pour la reproduction sexuée au sein du complexe d'espèces *Amoebophrya ceratii* (Syndiniales), parasites de dinoflagellés marins (phdthesis). Sorbonne Université.
- Cai, R., Kayal, E., Alves-de-Souza, C., Bigéard, E., Corre, E., Jeanthon, C., Marie, D., Porcel, B.M., Siano, R., Szymczak, J., Wolf, M., Guillou, L., 2020. Cryptic species in the parasitic *Amoebophrya* species complex revealed by a polyphasic approach. *Scientific Reports* 10, 2531. <https://doi.org/10.1038/s41598-020-59524-z>
- Capella-Gutiérrez, S., Silla-Martínez, J.M., Gabaldón, T., 2009. trimAl: a tool for automated alignment trimming in large-scale phylogenetic analyses. *Bioinformatics* 25, 1972–1973. <https://doi.org/10.1093/bioinformatics/btp348>
- Castresana, J., 2000. Selection of Conserved Blocks from Multiple Alignments for Their Use in Phylogenetic Analysis. *Molecular Biology and Evolution* 17, 540–552. <https://doi.org/10.1093/oxfordjournals.molbev.a026334>
- Chambouvet, A., Morin, P., Marie, D., Guillou, L., 2008. Control of Toxic Marine Dinoflagellate Blooms by Serial Parasitic Killers. *Science* 322, 1254–1257. <https://doi.org/10.1126/science.1164387>
- Coats, D.W., 1988. *Duboscquella cachoni* sp. nov., a parasitic dinoflagellate lethal to its tintinnine host *Eutintinnus pectinis*.
- Colin, S., Coelho, L.P., Sunagawa, S., Bowler, C., Karsenti, E., Bork, P., Pepperkok, R., Vargas, C. de, 2017. Quantitative 3D-imaging for cell biology and ecology of environmental microbial eukaryotes. *eLife* 6, e26066. <https://doi.org/10.7554/eLife.26066>
- Crenshaw, H.C., 1996. A New Look at Locomotion in Microorganisms: Rotating and Translating. *Am Zool* 36, 608–618. <https://doi.org/10.1093/icb/36.6.608>
- de Vargas, C., Audic, S., Henry, N., Decelle, J., Mahe, F., Logares, R., Lara, E., Berney, C., Le Bescot, N., Probert, I., Carmichael, M., Poulain, J., Romac, S., Colin, S., Aury, J.-M., Bittner, L., Chaffron, S., Dunthorn, M., Engelen, S., Flegontova, O., Guidi, L., Horak, A., Jaillon, O., Lima-Mendez, G., Luke, J., Malviya, S., Morard, R., Mulot, M., Scalco, E., Siano, R., Vincent, F., Zingone, A., Dimier, C., Picheral, M., Searson, S., Kandels-Lewis, S., Tara Oceans Coordinators, Acinas, S.G., Bork, P., Bowler, C., Gorsky, G., Grimsley, N.,

- Hingamp, P., Iudicone, D., Not, F., Ogata, H., Pesant, S., Raes, J., Sieracki, M.E., Speich, S., Stemmann, L., Sunagawa, S., Weissenbach, J., Wincker, P., Karsenti, E., Boss, E., Follows, M., Karp-Boss, L., Krzic, U., Reynaud, E.G., Sardet, C., Sullivan, M.B., Velayoudon, D., 2015. Eukaryotic plankton diversity in the sunlit ocean. *Science* 348, 1261605–1261605. <https://doi.org/10.1126/science.1261605>
- Decelle, J., Kayal, E., Bigeard, E., Gallet, B., Bougoure, J., Clode, P., Schieber, N., Templin, R., Hehenberger, E., Prensier, G., Chevalier, F., Schwab, Y., Guillou, L., 2022. Intracellular development and impact of a marine eukaryotic parasite on its zombified microalgal host. *ISME J* 16, 2348–2359. <https://doi.org/10.1038/s41396-022-01274-z>
- Díez, B., Pedrós-Alió, C., Massana, R., 2001. Study of Genetic Diversity of Eukaryotic Picoplankton in Different Oceanic Regions by Small-Subunit rRNA Gene Cloning and Sequencing. *Applied and Environmental Microbiology* 67, 2932–2941. <https://doi.org/10.1128/AEM.67.7.2932-2941.2001>
- Dührkop, K., Shen, H., Meusel, M., Rousu, J., Böcker, S., 2015. Searching molecular structure databases with tandem mass spectra using CSI:FingerID. *Proceedings of the National Academy of Sciences* 112, 12580–12585. <https://doi.org/10.1073/pnas.1509788112>
- Fenchel, T., 2001. How Dinoflagellates Swim. *Protist* 152, 329–338. <https://doi.org/10.1078/1434-4610-00071>
- Gomes, A.R., Marin-Menendez, A., Adjalley, S.H., Bardy, C., Cassan, C., Lee, M.C.S., Talman, A.M., 2022. A transcriptional switch controls sex determination in *Plasmodium falciparum*. *Nature* 612, 528–533. <https://doi.org/10.1038/s41586-022-05509-z>
- Gouy, M., Guindon, S., Gascuel, O., 2010. SeaView Version 4: A Multiplatform Graphical User Interface for Sequence Alignment and Phylogenetic Tree Building. *Molecular Biology and Evolution* 27, 221–224. <https://doi.org/10.1093/molbev/msp259>
- Guillou, L., Viprey, M., Chambouvet, A., Welsh, R.M., Kirkham, A.R., Massana, R., Scanlan, D.J., Worden, A.Z., 2008. Widespread occurrence and genetic diversity of marine parasitoids belonging to *Syndiniales* (*Alveolata*). *Environmental Microbiology* 10, 3349–3365. <https://doi.org/10.1111/j.1462-2920.2008.01731.x>
- Guizetti, J., Frischknecht, F., 2021. Apicomplexans: A conoid ring unites them all. *PLOS Biology* 19, e3001105. <https://doi.org/10.1371/journal.pbio.3001105>
- Heitman, J., Filler, S.G., Edwards, J.E., Mitchell, A.P. (Eds.), 2006. *Molecular Principles of Fungal Pathogenesis*. ASM Press, Washington, DC, USA. <https://doi.org/10.1128/9781555815776>
- Howick, V.M., Russell, A.J.C., Andrews, T., Heaton, H., Reid, A.J., Natarajan, K., Butungi, H., Metcalf, T., Verzier, L.H., Rayner, J.C., Berriman, M., Herren, J.K., Billker, O., Hemberg, M., Talman, A.M., Lawniczak, M.K.N., 2019. The Malaria Cell Atlas: Single parasite transcriptomes across the complete *Plasmodium* life cycle. *Science* 365, eaaw2619. <https://doi.org/10.1126/science.aaw2619>
- John, U., Lu, Y., Wohlrab, S., Groth, M., Janouškovec, J., Kohli, G.S., Mark, F.C., Bickmeyer, U., Farhat, S., Felder, M., Frickenhaus, S., Guillou, L., Keeling, P.J.,



- Moustafa, A., Porcel, B.M., Valentin, K., Glöckner, G., 2019. An aerobic eukaryotic parasite with functional mitochondria that likely lacks a mitochondrial genome. *Sci. Adv.* 5, eaav1110. <https://doi.org/10.1126/sciadv.aav1110>
- Katoh, K., Rozewicki, J., Yamada, K.D., 2019. MAFFT online service: multiple sequence alignment, interactive sequence choice and visualization. *Briefings in Bioinformatics* 20, 1160–1166. <https://doi.org/10.1093/bib/bbx108>
- Katoh, K., Standley, D.M., 2013. MAFFT Multiple Sequence Alignment Software Version 7: Improvements in Performance and Usability. *Molecular Biology and Evolution* 30, 772–780. <https://doi.org/10.1093/molbev/mst010>
- Kayal, E., Alves-de-Souza, C., Farhat, S., Velo-Suarez, L., Monjol, J., Szymczak, J., Bigeard, E., Marie, D., Noel, B., Porcel, B.M., Corre, E., Six, C., Guillou, L., 2020. Dinoflagellate Host Chloroplasts and Mitochondria Remain Functional During Amoebozoa Infection. *Front Microbiol* 11. <https://doi.org/10.3389/fmicb.2020.600823>
- Kiernan, J.A., 2000. Formaldehyde, Formalin, Paraformaldehyde And Glutaraldehyde: What They Are And What They Do. *Microscopy Today* 8, 8–13. <https://doi.org/10.1017/S1551929500057060>
- Kim, D., Paggi, J.M., Park, C., Bennett, C., Salzberg, S.L., 2019. Graph-based genome alignment and genotyping with HISAT2 and HISAT-genotype. *Nat Biotechnol* 37, 907–915. <https://doi.org/10.1038/s41587-019-0201-4>
- Kremp, A., 2013. Diversity of dinoflagellate life cycles: facets and implications of complex strategies, in: Lewis, J.M., Marret, F., Bradley, L.R. (Eds.), *Biological and Geological Perspectives of Dinoflagellates*. Geological Society of London, p. 0. <https://doi.org/10.1144/TMS5.18>
- Li, H., Handsaker, B., Wysoker, A., Fennell, T., Ruan, J., Homer, N., Marth, G., Abecasis, G., Durbin, R., 1000 Genome Project Data Processing Subgroup, 2009. The Sequence Alignment/Map format and SAMtools. *Bioinformatics* 25, 2078–2079. <https://doi.org/10.1093/bioinformatics/btp352>
- Lin, S., Yu, L., Wu, X., Li, M., Zhang, Y., Luo, H., Li, H., Li, T., Li, L., 2022. Active meiosis during dinoflagellate blooms: A ‘sex for proliferation’ hypothesis. *Harmful Algae* 118, 102307. <https://doi.org/10.1016/j.hal.2022.102307>
- López-García, P., Rodríguez-Valera, F., Pedrós-Alió, C., Moreira, D., 2001. Unexpected diversity of small eukaryotes in deep-sea Antarctic plankton. *Nature* 409, 603–607. <https://doi.org/10.1038/35054537>
- Love, M.I., Huber, W., Anders, S., 2014. Moderated estimation of fold change and dispersion for RNA-seq data with DESeq2. *Genome Biology* 15, 550. <https://doi.org/10.1186/s13059-014-0550-8>
- Malik, S.-B., Pightling, A.W., Stefaniak, L.M., Schurko, A.M., Jr, J.M.L., 2008. An Expanded Inventory of Conserved Meiotic Genes Provides Evidence for Sex in *Trichomonas vaginalis*. *PLOS ONE* 3, e2879. <https://doi.org/10.1371/journal.pone.0002879>

- Marie, D., Simon, N., Guillou, L., Partensky, F., Vaultot, D., 2000. DNA/RNA Analysis of Phytoplankton by Flow Cytometry. *Current Protocols in Cytometry* 11, 11.12.1-11.12.14. <https://doi.org/10.1002/0471142956.cy1112s11>
- Martin, M., 2011. Cutadapt removes adapter sequences from high-throughput sequencing reads. *EMBnet.journal* 17, 10–12. <https://doi.org/10.14806/ej.17.1.200>
- Moon-van der Staay, S.Y., De Wachter, R., Vaultot, D., 2001. Oceanic 18S rDNA sequences from picoplankton reveal unsuspected eukaryotic diversity. *Nature* 409, 607–610. <https://doi.org/10.1038/35054541>
- Pang, Z., Zhou, G., Ewald, J., Chang, L., Hacariz, O., Basu, N., Xia, J., 2022. Using MetaboAnalyst 5.0 for LC–HRMS spectra processing, multi-omics integration and covariate adjustment of global metabolomics data. *Nat Protoc* 17, 1735–1761. <https://doi.org/10.1038/s41596-022-00710-w>
- Persson, A., Smith, B.C., Wikfors, G.H., Alix, J.H., 2013. Differences in swimming pattern between life cycle stages of the toxic dinoflagellate *Alexandrium fundyense*. *Harmful Algae* 21–22, 36–43. <https://doi.org/10.1016/j.hal.2012.11.005>
- Picelli, S., Faridani, O.R., Björklund, Å.K., Winberg, G., Sagasser, S., Sandberg, R., 2014. Full-length RNA-seq from single cells using Smart-seq2. *Nat Protoc* 9, 171–181. <https://doi.org/10.1038/nprot.2014.006>
- Price, M.N., Dehal, P.S., Arkin, A.P., 2010. FastTree 2 – Approximately Maximum-Likelihood Trees for Large Alignments. *PLOS ONE* 5, e9490. <https://doi.org/10.1371/journal.pone.0009490>
- Price, M.N., Dehal, P.S., Arkin, A.P., 2009. FastTree: Computing Large Minimum Evolution Trees with Profiles instead of a Distance Matrix. *Molecular Biology and Evolution* 26, 1641–1650. <https://doi.org/10.1093/molbev/msp077>
- Quinlan, A.R., Hall, I.M., 2010. BEDTools: a flexible suite of utilities for comparing genomic features. *Bioinformatics* 26, 841–842. <https://doi.org/10.1093/bioinformatics/btq033>
- Reid, A.J., Talman, A.M., Bennett, H.M., Gomes, A.R., Sanders, M.J., Illingworth, C.J.R., Billker, O., Berriman, M., Lawniczak, M.K., 2018. Single-cell RNA-seq reveals hidden transcriptional variation in malaria parasites. *eLife* 7, e33105. <https://doi.org/10.7554/eLife.33105>
- Schymanski, E.L., Jeon, J., Gulde, R., Fenner, K., Ruff, M., Singer, H.P., Hollender, J., 2014. Identifying Small Molecules via High Resolution Mass Spectrometry: Communicating Confidence. *Environ. Sci. Technol.* 48, 2097–2098. <https://doi.org/10.1021/es5002105>
- Shadrin, A.M., Simdyanov, T.G., Pavlov, D.S., Nguyen, T.H.T., 2015. Free-living stages of the life cycle of the parasitic dinoflagellate *Ichthyodinium chabelardi* Hollande et J. Cachon, 1952 (Alveolata: Dinoflagellata). *Dokl Biol Sci* 461, 104–107. <https://doi.org/10.1134/S0012496615020131>
- Shah, S., Chen, Y., Bhattacharya, D., Chan, C.X., 2020. Sex in Symbiodiniaceae dinoflagellates: genomic evidence for independent loss of the canonical

## Chapter 1

- synaptonemal complex. *Sci Rep* 10, 9792. <https://doi.org/10.1038/s41598-020-66429-4>
- Sharma, A., Singh, P., Sarmah, B.K., Nandi, S.P., 2020. Quorum sensing: its role in microbial social networking. *Research in Microbiology* 171, 159–164. <https://doi.org/10.1016/j.resmic.2020.06.003>
- Skovgaard, A., Massana, R., Balagué, V., Saiz, E., 2005. Phylogenetic Position of the Copepod-Infesting Parasite *Syndinium turbo* (Dinoflagellata, Syndinea). *Protist* 156, 413–423. <https://doi.org/10.1016/j.protis.2005.08.002>
- Steidinger, K.A., Jangen, K., 1997. Dinoflagellates, in: *Identifying Marine Phytoplankton*. Elsevier, pp. 387–584. <https://doi.org/10.1016/B978-012693018-4/50005-7>
- Szymczak, J., Bigeard, E., Guillou, L., 2023. Use of flow cytometry (Novocyte Advanteon) to monitor the complete life cycle of the parasite *Amoebophrya ceratii* infecting its dinoflagellate host. [www.protocols.io](http://www.protocols.io).
- Tarasov, A., Vilella, A.J., Cuppen, E., Nijman, I.J., Prins, P., 2015. Sambamba: fast processing of NGS alignment formats. *Bioinformatics* 31, 2032–2034. <https://doi.org/10.1093/bioinformatics/btv098>
- Taylor, F.J.R., 1990. Phylum Dinoflagellata, in: L. Margulis et al. (Eds.), *Handbook of Protozoology*, 24. pp. 419–437.
- Walde, M., Camplong, C., de Vargas, C., Baudoux, A.-C., Simon, N., 2023. Viral infection impacts the 3D subcellular structure of the abundant marine diatom *Guinardia delicatula*. *Frontiers in Marine Science* 9.
- Zimmer, C., 2009. On the Origin of Sexual Reproduction. *Science* 324, 1254–1256. <https://doi.org/10.1126/science.324.1254>

## Supplementary data

## 1- Supplementary information for flow cytometer: release of dinospores (Fig. S1-1)

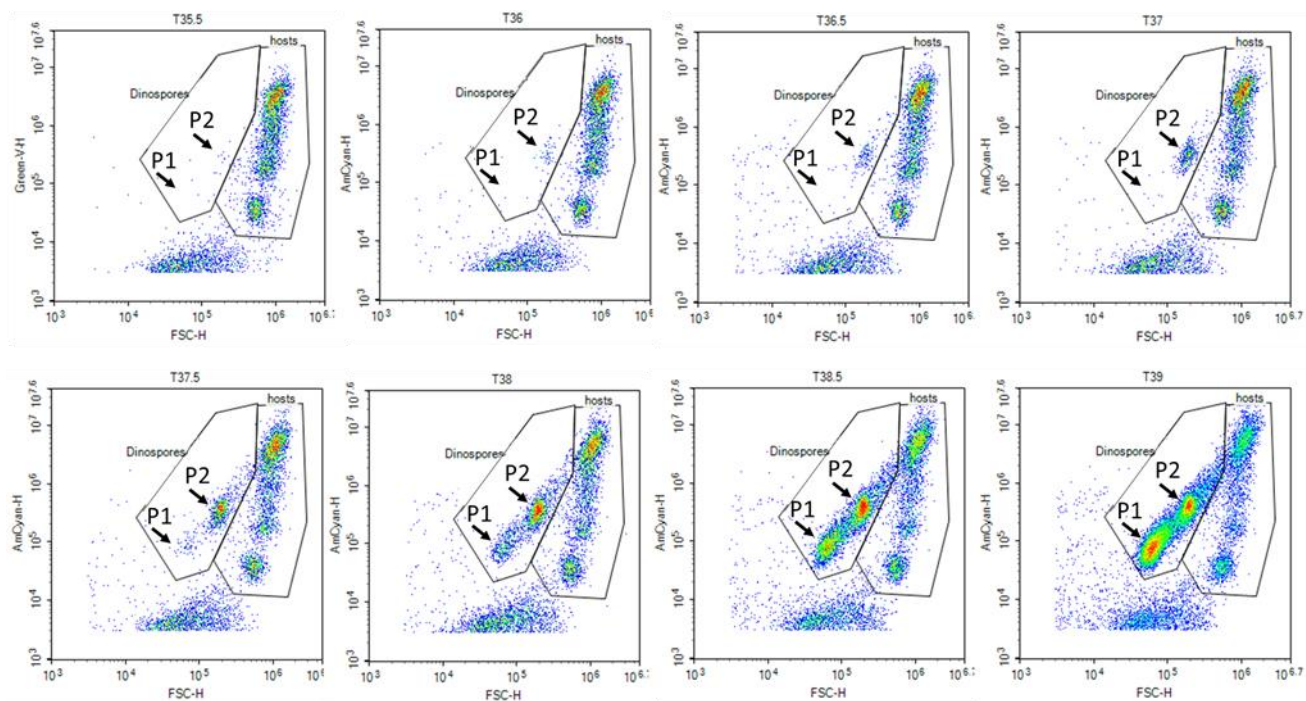


**Figure S1- 1: Release of dinospores from 35.5 to 39 hours.**

P2 populations were clearly visible at t=36 hours, whilst P1 populations were first observed at t=37.5 hours, so 1.5 hours after P2.

## 2- Supplementary information for electronic microscopy (Table S1-1)

**Table S1- 1: Metadata linked to samples collected for electronic microscopy analyses.**

Percentage of dinospores have been deduced from cell counts obtained by flow cytometry.

Date	Name	Type	Mode of collect	Culture age (in day)	P1 (%)	P2 (%)	P3 (%)
April 2022	Sample 3	Section	Sedimentation	3.5	93.4	2	4.5
November 2022	P2-n3	Section	Sorted by flow cytometry	3	0	100	0
april 2022	Sample 1	Negative staining	Sedimentation	3.5	92	4.4	2
april 2022	Sample 2	Negative staining	Sedimentation	3.5	66	26	6
6 July 2023	CN	Negative staining	Sedimentation	6.5	99	0	0.36
17 July 2023	P1	Negative staining	Sorted by flow cytometry	2	100	0	0
17 July 2023	P2	Negative staining	Sorted by flow cytometry	2	0	100	0

## Chapter 1

### 3- Supplementary information for the Analysis of dinospore types released from single infected host cells (Fig. S1-2)

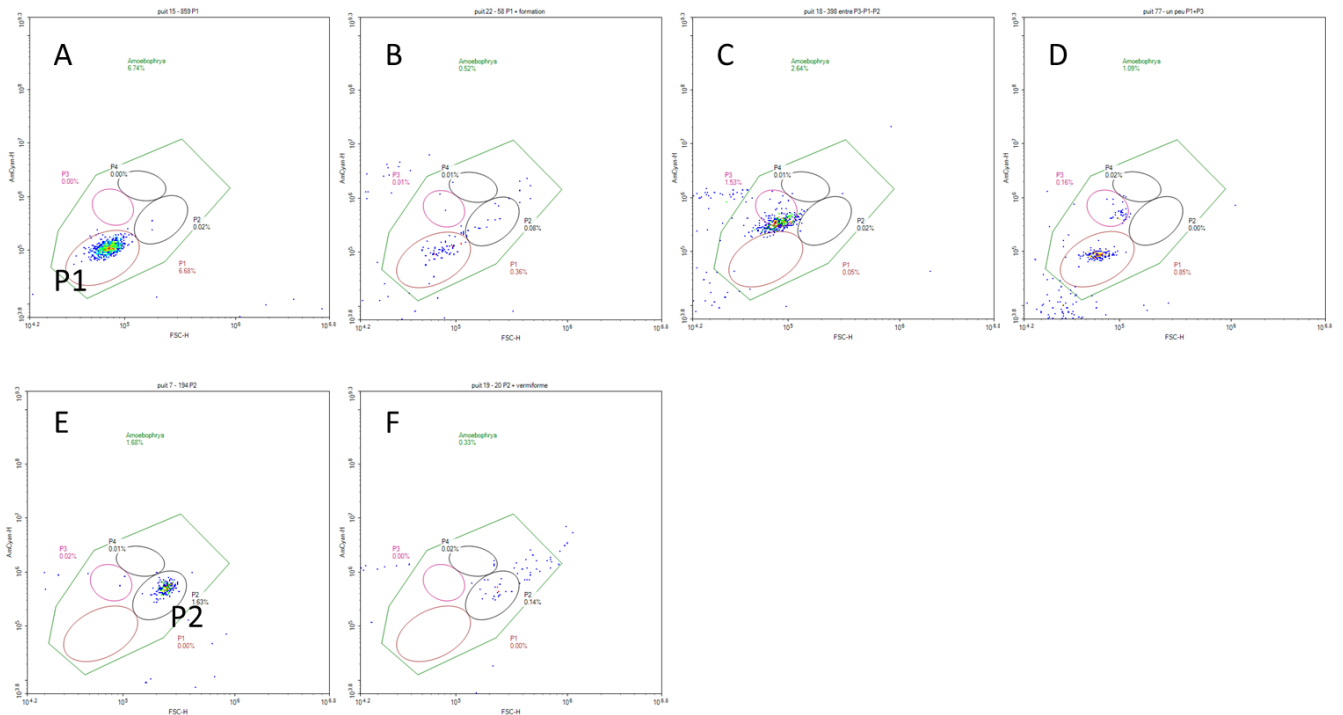


**Figure S1- 2: The different dinospore types released from single infected host cells.**

The results revealed that the majority of hosts produced either P1 (A) or P2 (E) dinospores, with 6 and 35 wells containing these respective types. Two wells contained a combination of intermediate forms that seemed to lead to the production of P1 (B) and P2 (F). This suggests a potential production pathway towards a final stage. If this interpretation is correct, it implies that the separation of sporonts into spores is asynchronous in Amoeboophrya. This spore separation happens after the release of the sporocyte, referred to as the vermiform stage. The vermiform stage is a multicellular and mobile stage that is directly released from the infected host and has a very short lifespan, typically ranging from a few minutes to a few hours. Each cell within this vermiform stage is capable of giving rise to one or several final spores. It's important to note that this stage remains relatively understudied and poorly understood. One well yielded a population with a similar forward scatter (FSC) as P1 but with higher green fluorescence (C), potentially belonging to a variant of P1. Another well produced a mixed population of normal P1 and P1 with higher green fluorescence (D), similar to the previous case.



# Chapter 1

## 4- Supplementary information for confocal microscopy (Fig. S1-3)

Confocal microscopy was employed to estimate the biovolumes of P1 and P2 dinospores from 3D image data. Cell volumes in two cultures of freshly released dinospores were compared, comprising approximately 88% P1 (sample 1) and 85% P2 (sample 2). Cell counts were determined using flow cytometry.

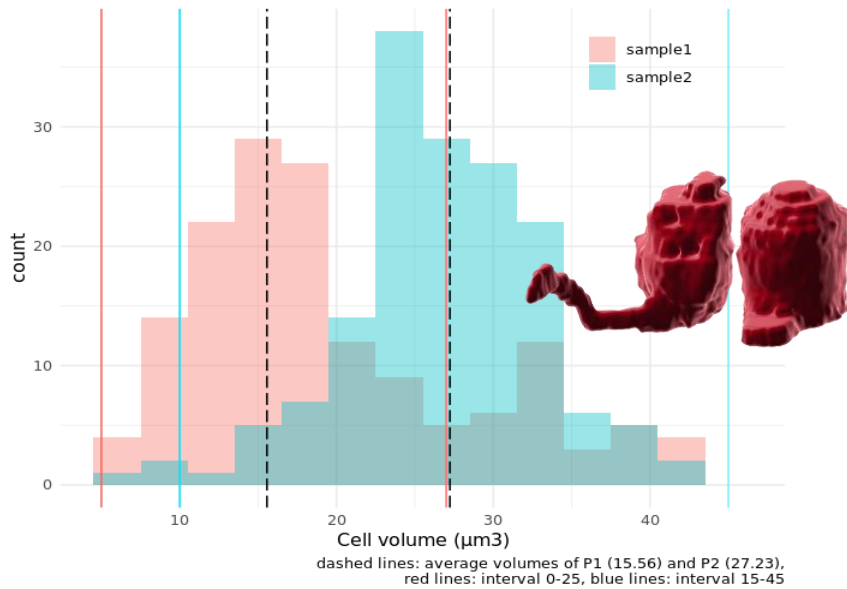


**Figure S1- 3: Bimodal distribution of cell sizes in a mixed population of dinospores, as assessed by confocal microscopy.**

## 5- Supplementary information for analysis of the swimming behavior (Fig. S1-4 and S1-5)

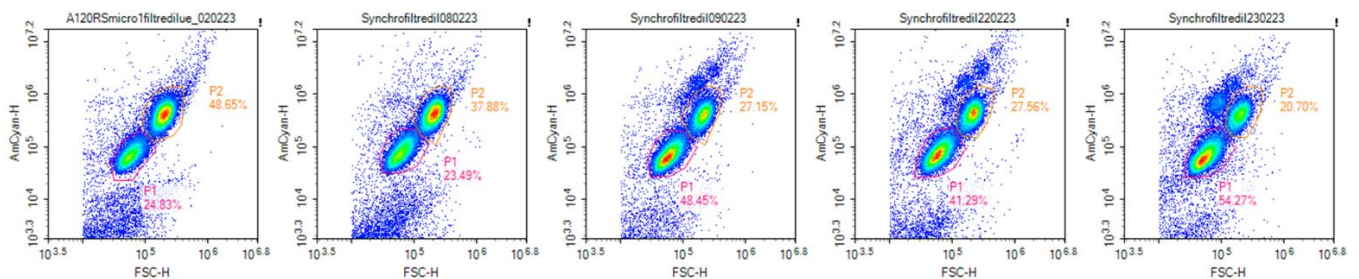


**Figure S1- 4: Flow cytograms from the five replicates prior to their use in estimating swimming behavior.**

The relative proportions of P1 and P2 are indicated in distinct windows

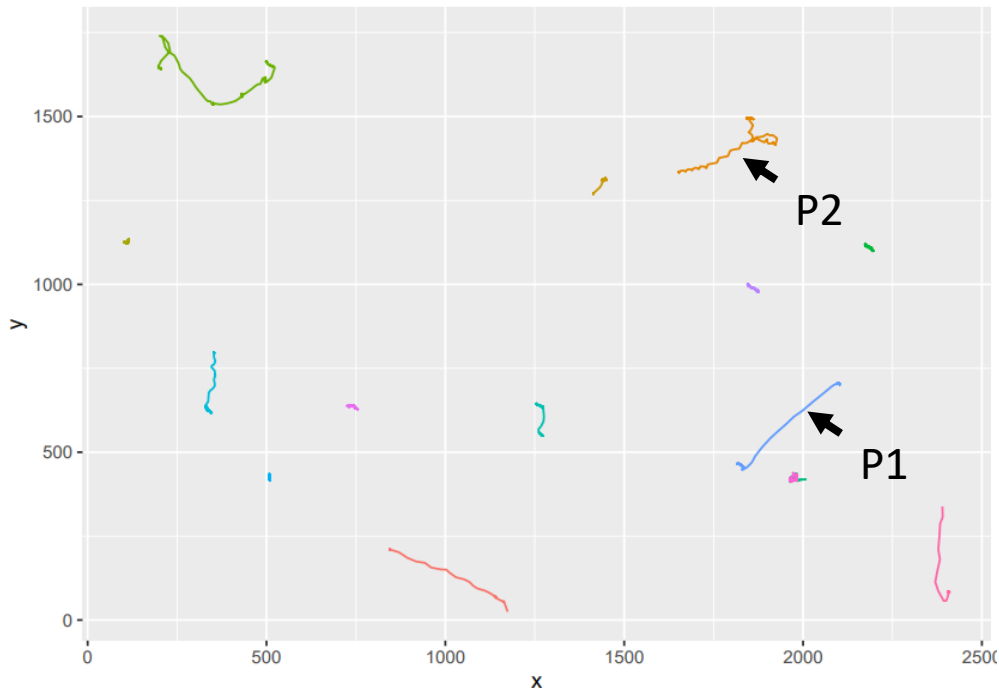


**Figure S1- 5: Swimming trajectories of P1 and P2. P1 swims straight forward, while P2 exhibits helical motion with a large loop.**

*6- Supplementary information for the infectivity tests (Fig. S1-6 and S1-7)*

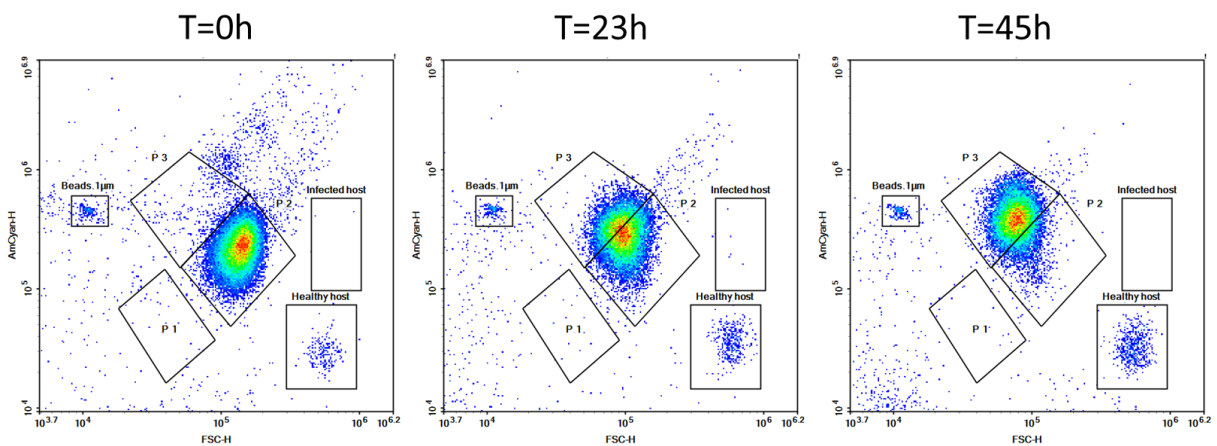


**Figure S1- 6: Evolution of dinospores and host used for infectivity tests in June 7th, 2021.**

The culture was composed exclusively of P2 dinospores. No infection was observed in host (followed during a week), while P2 population mainly transformed into P3 at t=45 hours.

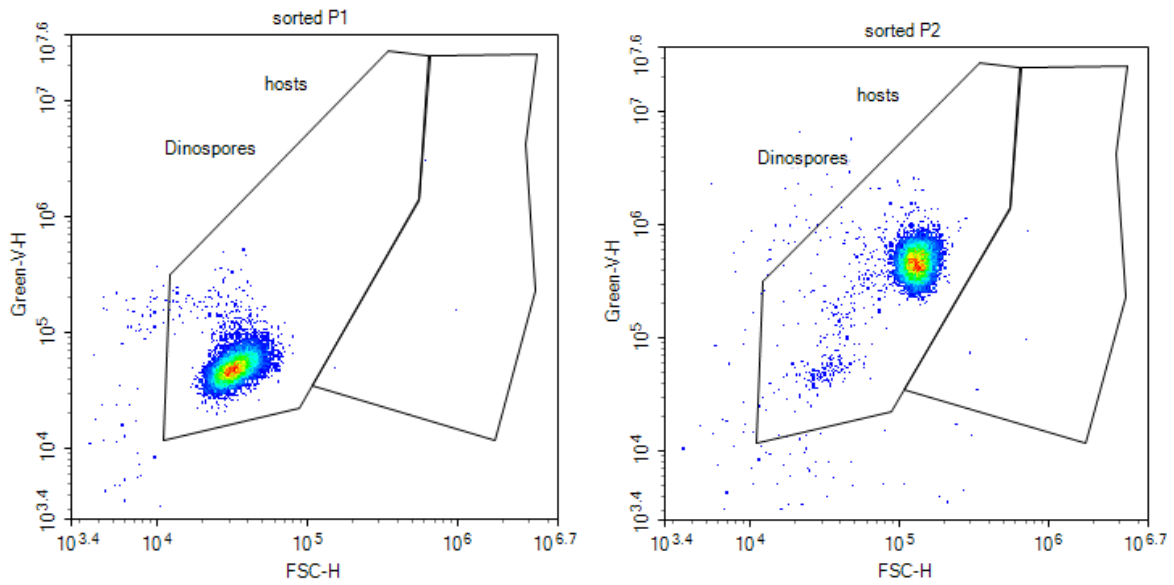


**Figure S1- 7: Dinospore populations (P1 at left and P2 at right) sorted by flow cytometry prior to their use for infectivity tests (on February 23th 2023).**

*7- Supplementary information for Analysis of the ploidy level (Fig. S8)*

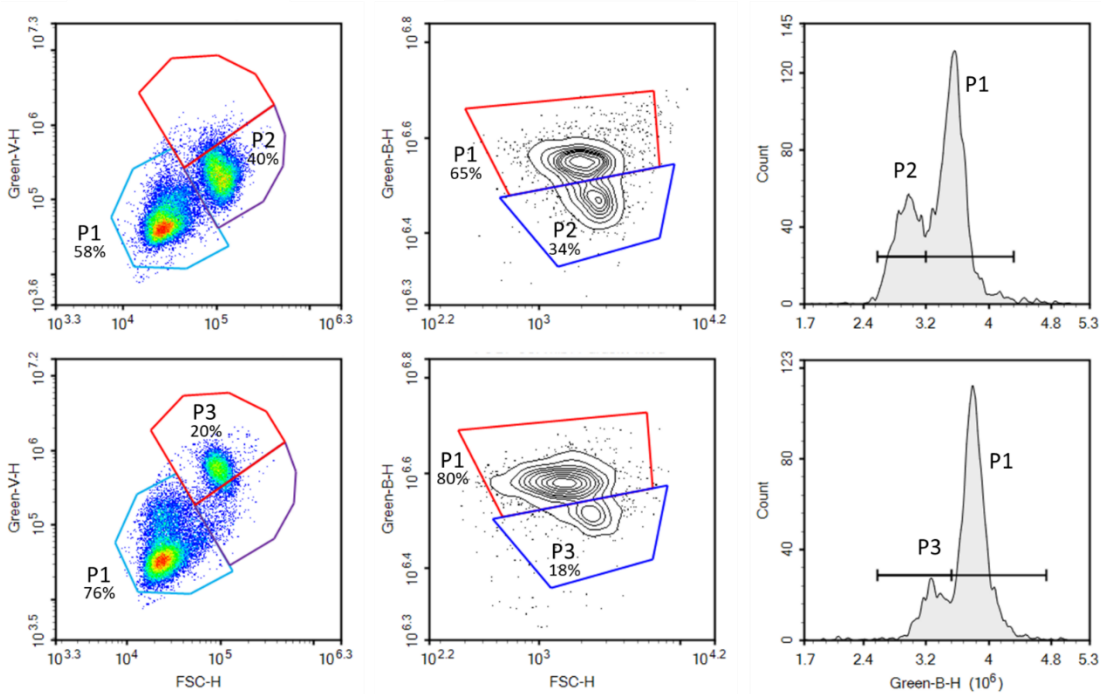


**Figure S1- 8: Ploidy level of mixed populations of dinospores as observed by flow cytometry.**

The left panel shows a density plot of the dinospore cultures, illustrating their distinct fluorescence (Green-V) and size characteristics (FSC-H). Moving to the middle panel, we observe a contour plot of extracted nuclei after NIB/2 + SYBR green I treatment. In this plot, the nuclei are differentiated based on the green fluorescence intensity after SYBR green I staining (Green-B-H) and size (FSC-H). The right panel displays the



## Chapter 1

same nuclei as shown in the middle panel, visualized on a histogram. This histogram is based on density (counts) and green fluorescence (Green-B-H). The upper layer represents a dinospore culture consisting of 58% P1 and 40% P2. The ratio of the P1 and P2 nuclei fluorescence is 1.17. The lower layer represents a dinospore culture comprising 76% P1 and 20% P3. The ratio of the P1 and P3 nuclei fluorescence is 1.18.

**Note:** The NIB/2 method theoretically ruptures the cell membrane, producing individual nuclei. Considering the considerable decrease in FSC values, we considered that the cells have ruptured and the nuclei have been individualized.

We can differentiate between the putative nuclei P1 and P2 or P3, according to their different size (FSC) and the slight variation in fluorescence. A ratio close to 1 for both P1/P2 and P1/P3 nuclei fluorescence indicates a similar level of ploidy for the three dinospore morphotypes. The results remained unaffected by a heating treatment of 70°C for 20 minutes (not shown).

### 8- Supplementary information for Mating pairs between strains (Fig. S1-9)

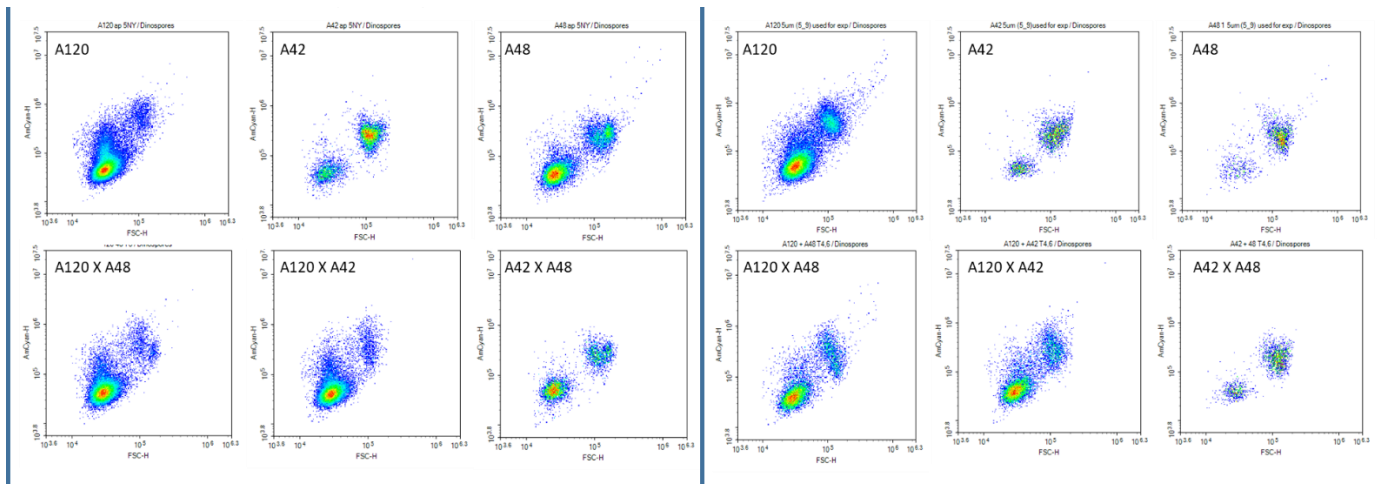


**Figure S1- 9: Mating pairs experiment using three strain of the same species (MALVII Clade 2 Sub-clade 4).**

Left: Experiment conducted the 29 of August 2023, Right: Experiment conducted the 8 of September 2023. Upper layer: individual strains, Lower layer: Mix strains after 6 and 4.5 hours (same result than for 24 and 48 hours). Three strains from MALV Group II clade 4, specifically A120, A42 (RCC4395), and A48 (RCC4396) (Cai et al. 2020), all infected the same host ST147, were paired to monitor eventual cell fusion during two replicated experiments. The expectation was that if fusion occurred, novel, larger populations would emerge (larger FSC). No large population was observed after mix.

## Chapter 1

The following data can be downloaded:

Dataset 1: Complete database used for statistical analyses (decision tree)

Dataset 2: Differentially expressed genes in P1 compared to P2+P3

Dataset 3: Gene orthologues in Amoebophrya genome A120 for genes involved into early development of the ribosomal structure, ADN & ARN synthesis and cell division

Download link : <https://tinyurl.com/suppthesis>

### 9- Supplementary information for Metabolomic analyses (Figs. S1-10-S13, Table S1-2)

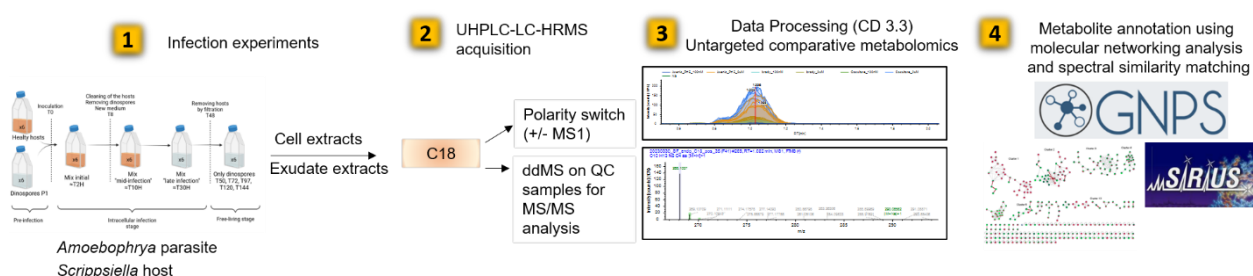
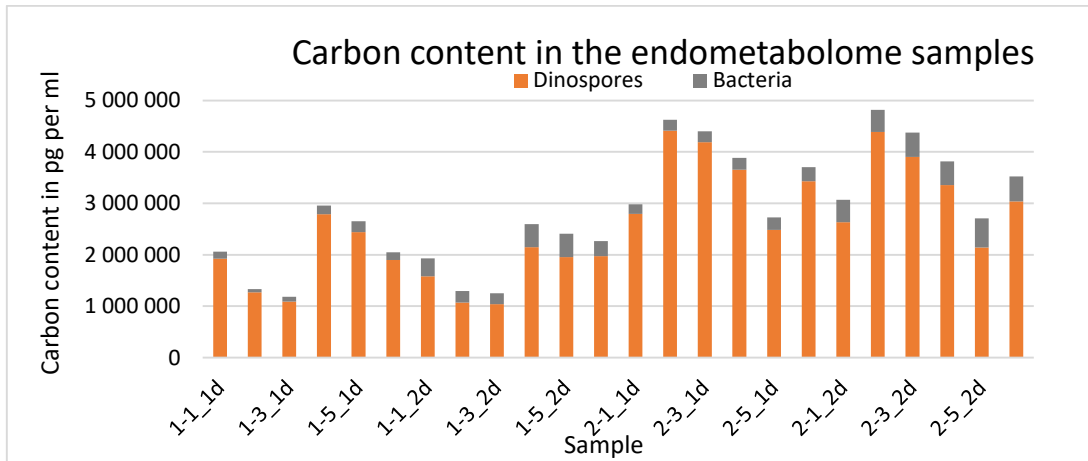


Figure S1- 10: Scheme displaying the metabolomics workflow.

Table S1- 2: Counts of bacteria and dinospores in samples collected for metabolomics analyses, and % of P1 dinospores compared to P2.

ID Endo	ID Exo	Experimentation- replicate_day of extraction after dinospores release	Bacteria density (in Cells/mL)	Bacteria retained of the filter (in Cells/mL)	P1 dinospores (in Cells/mL)	P2 dinospores (in Cells/mL)	P1/P2 ratio
JS_089	JS_096	1-1_1d	6 993 150	6 213 180	316 725	112 978	73,71
JS_090	JS_097	1-2_1d	7 709 520	6 922 380	569 496	109 710	83,85
JS_091	JS_098	1-3_1d	7 862 810	7 049 700	553 921	90 648	85,94
JS_092	JS_099	1-4_1d	8 446 790	7 652 180	438 947	123 077	78,10
JS_093	JS_100	1-5_1d	8 939 890	8 011 120	294 062	87 806	77,01
JS_094	JS_101	1-6_1d	9 960 300	9 123 860	310 015	217 519	58,77
JS_103	JS_110	1-1_2d	15 928 670	14 383 970	304 865	100 650	75,18
JS_104	JS_111	1-2_2d	15 667 910	14 178 340	571 174	103 883	84,61
JS_105	JS_112	1-3_2d	17 273 640	15 655 690	517 223	83 351	86,12
JS_106	JS_113	1-4_2d	16 751 780	15 142 070	396 259	120 145	76,73
JS_107	JS_114	1-5_2d	20 760 640	18 724 940	252 159	77 303	76,54
JS_108	JS_115	1-6_2d	17 896 030	16 071 670	264 915	202 266	56,71
JS_229	JS_236	2-1_1d	5 068 950	4 499 120	75 238	220 819	25,41
JS_230	JS_237	2-2_1d	1 975 970	1 933 640	156 350	39 266	79,93
JS_231	JS_238	2-3_1d	3 302 150	3 076 820	55 854	112 071	33,26
JS_232	JS_239	2-4_1d	6 008 870	5 694 460	183 925	244 735	42,91
JS_233	JS_240	2-5_1d	7 367 040	7 013 150	77 172	298 640	20,53
JS_234	JS_241	2-6_1d	5 630 200	5 026 490	181 059	110 983	62,00
JS_243	JS_250	2-1_2d	13 436 750	11 591 560	52 290	190 869	21,50
JS_244	JS_251	2-2_2d	8 566 900	7 359 490	128 770	36 258	78,03
JS_245	JS_252	2-3_2d	8 241 030	7 171 680	41 952	117 761	26,27
JS_246	JS_253	2-4_2d	17 139 440	14 793 360	142 989	187 640	43,25
JS_247	JS_254	2-5_2d	17 047 060	14 973 440	57 048	243 798	18,96
JS_248	JS_255	2-6_2d	10 754 920	9 599 650	186 522	117 437	61,36



**Figure S1- 11: Carbon content (dinospires and bacteria) estimated in endometablome samples.**

For bacteria, we used the carbon content of 30.2 fg C per cell (equivalent to 0.0302 pg C per cell) estimated for coastal bacterial assemblages (Fukuda et al., 1998). For *S. acuminata*, we used the following equation:  $=10^{(0.175+0.764 \cdot \text{LOG}_{10}(\text{Volume in } \mu\text{m}^3))} = 10^{(0.175+0.764 \cdot \text{LOG}_{10}(6861.23))} = 1276.47$  pgC per cell. (Menden-Deuer and Lessard, 2000). For dinospores, and according to Kayal et al. (2020), we employed the conversion factor from Borsheim and Bratbak (1987) for heterotrophic flagellates, which is 100 fgC per  $\mu\text{m}^3$  of bio-volume, and the biovolume estimated previously using confocal microscopy (P1 dinospore is  $15.56 \cdot 100 = 1565$  fgC per cell or 1,5pgC per cell, P2 dinospore is  $27.23 \cdot 100 = 2723$  fgC per cell or 2,7pgC per cell).

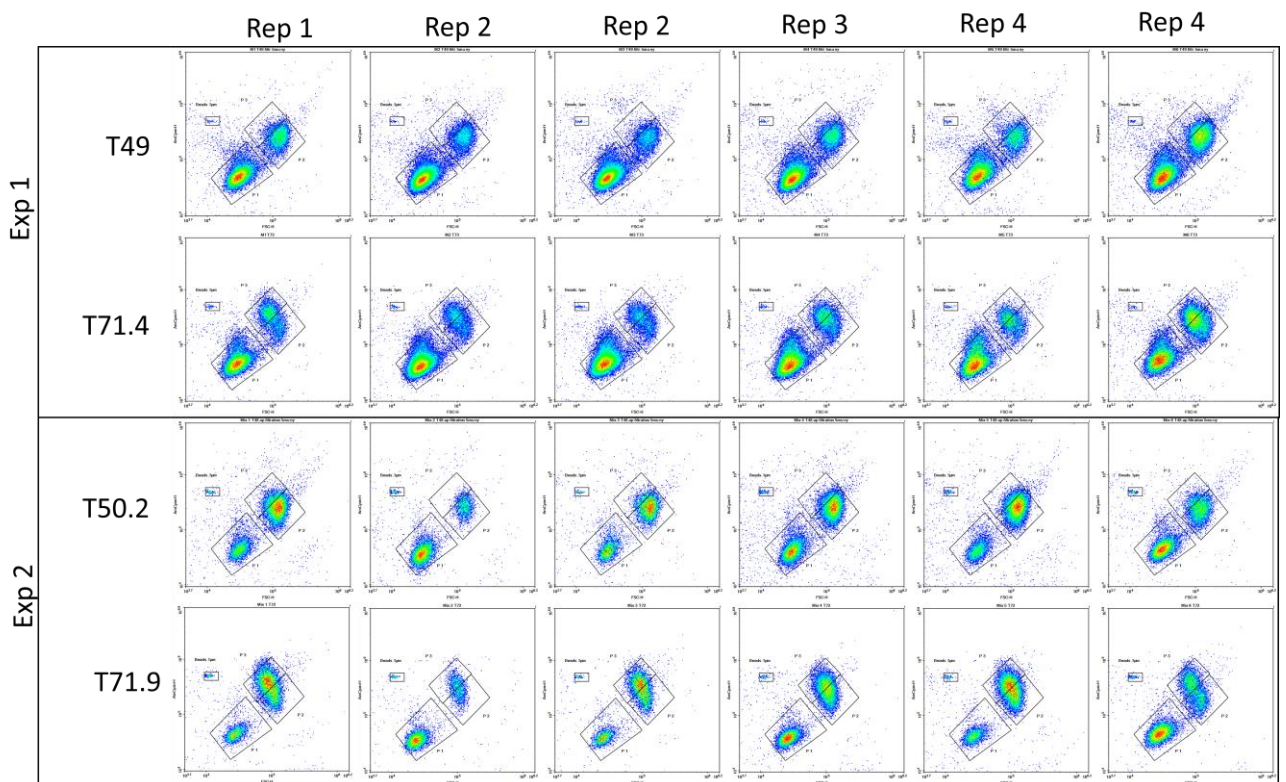


**Figure S1- 12: Cytograms of cultures used for the metabolomic analyses.**

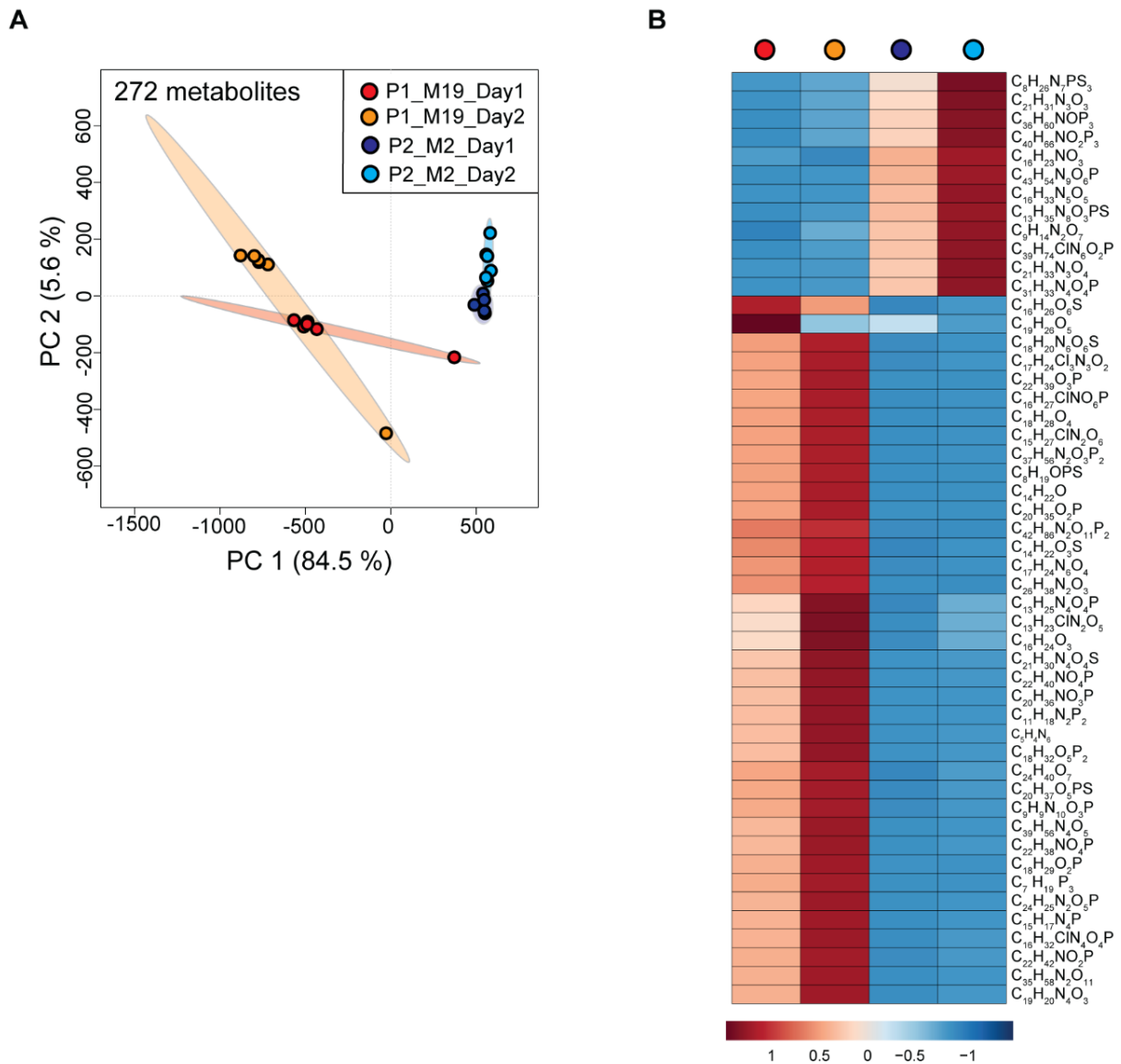


**Figure S1- 13: Analyses conducted on selected metabolites.**

A- Principal component analysis was conducted on the 272 selected metabolites specifically associated with P1 or P2 dinospore cell exudate extract profiles. B- Top 50 significant compounds discriminating the exometabolome profiles of P1 and P2 extracts were annotated. The intensities detected for the 50 metabolites were square root-transformed and Pareto-scaled, then displayed in the heatmap.

10- Supplementary information for Populations sorted by flow cytometry for the analysis of their gene expression (transcriptomic analyses) (Figs. S1-14-S16, Table S1-3)

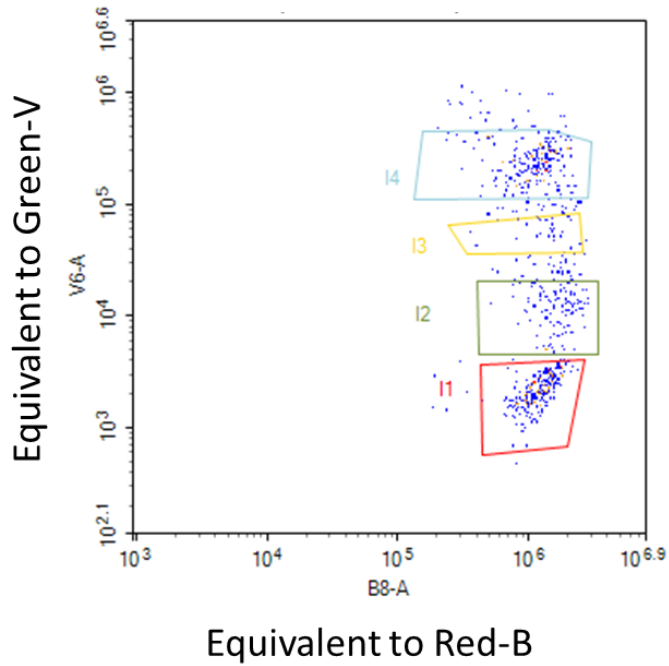


Figure S1- 14: Gates used for sorting infected host cell (20 cells per well) for transcriptomic analyses.

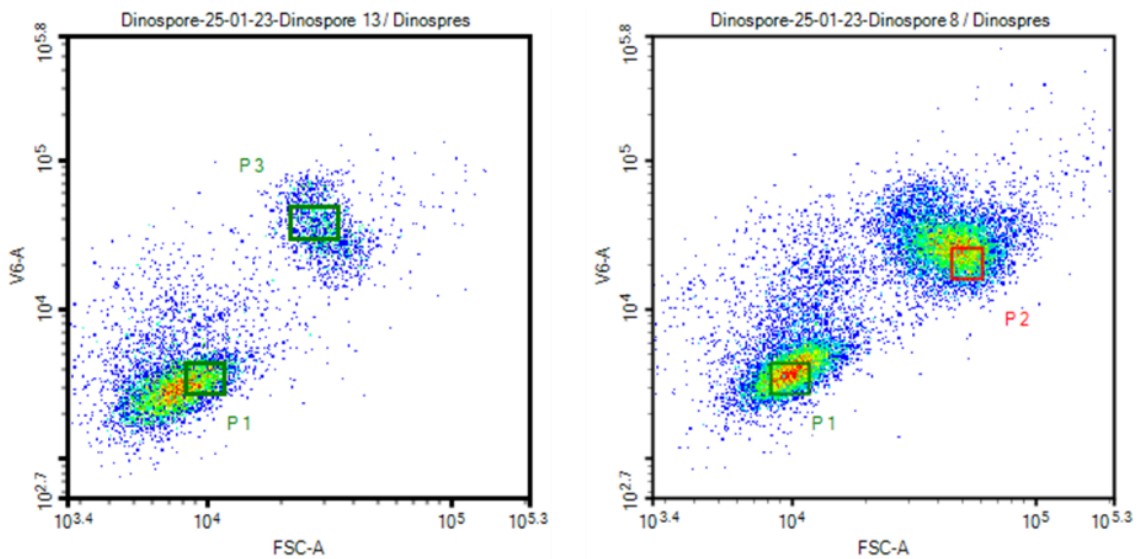
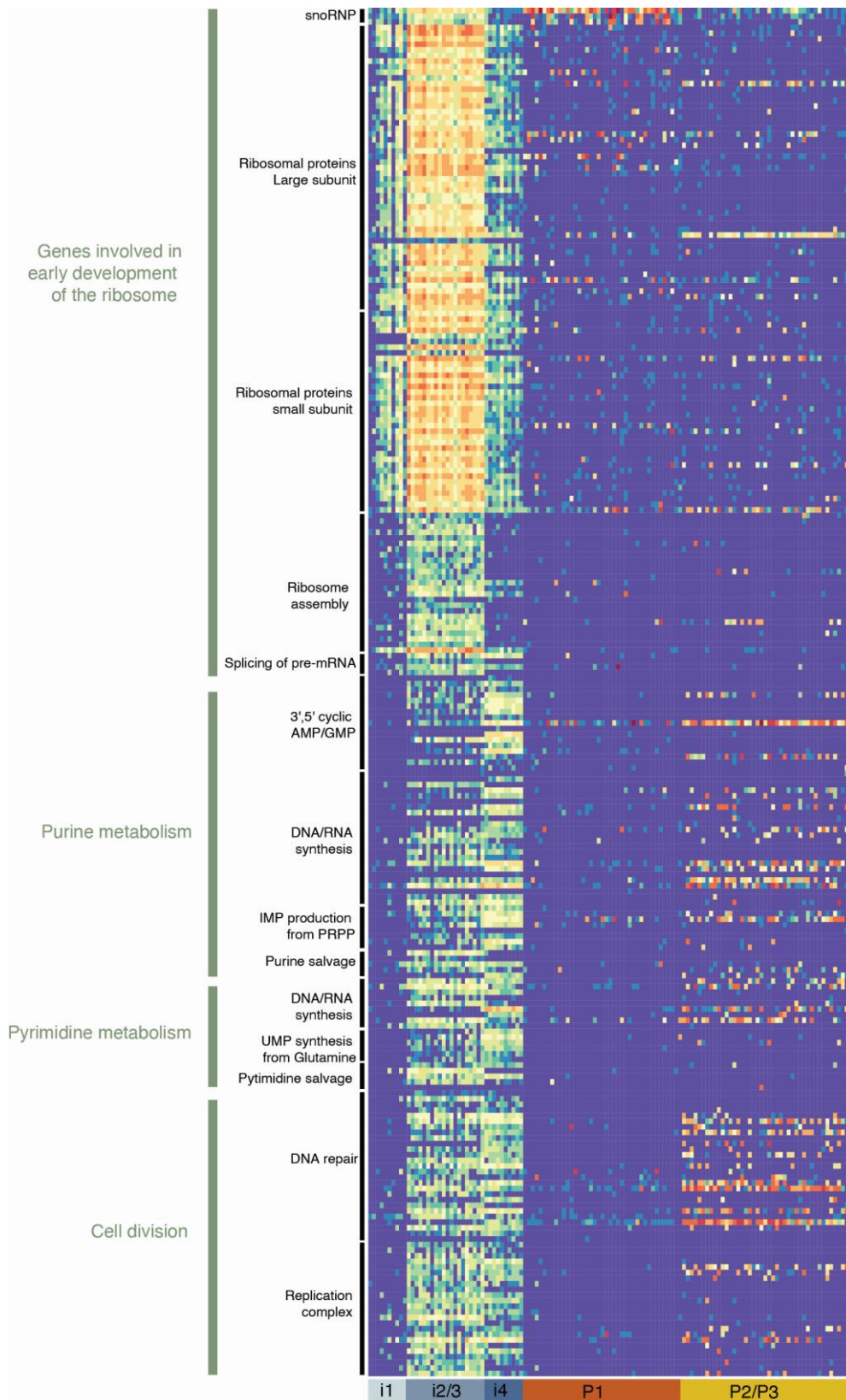


Figure S1- 15: Gates used for sorting dinospores (10 cells per well) for transcriptomic analyses.





**Figure S1- 16: Heatmap analyses of gene expression along the course of infection.**

(four stages of infection, namely i1, i2+i3, i4) and in dinospore populations (P1 or P2+P3) for selected metabolic pathways (genes involved in the earlier development of ribosomes, DNA and RNA synthesis, and cell replication).

## Chapter 1

**Table S1- 3: Gene orthologues in Amoebophrya genome A120 for genes involved in meiosis.**

REF: 1=Shah et al. 2020, 2=Cai et al. 2019, 3=Lin et al. 2022, 4=this study. \*meiosis-specific genes. ND=not detected

Processes	Name	Symbol	A120_Gene_ID	REF
Induction	switch from mitotic to meiotic	Meio, Mei2 (in vegetative cells after3)	GSA120T00008208001	4
Mismatch correction	DNA mismatch repair	Msh2 (in vegetative cells after3)	GSA120T00021256001	2
	DNA mismatch repair	Msh3	ND	2
	DNA mismatch repair	Msh6 (in vegetative cells after3)	GSA120T00017079001	2
	DNA mismatch repair (meiotic)	PMS1	ND	4
	DNA mismatch repair (meiotic)	PMS2 (in resting cysts after3)	GSA120T00014436001	4
Syngamy	Plasmogamy	Hap2* (in vegetative cells after3)	GSA120T00024727001	4
		GEX1*	ND in dinoflagellates	1
Cohesin complex		REC8	ND in dinoflagellates	1,2
	Cohesion complex	Smc1 (in resting cysts after3)	GSA120T00000722001	4
		Smc1 (in resting cysts after3)	GSA120T00021886001	4
		Smc2	GSA120T00011437001	4
		Smc4	GSA120T00003312001	4
		Smc4	GSA120T00003311001	4
		Smc3	GSA120T00016095001	4
		Smc5	ND in dinoflagellates	1
Smc6		ND in dinoflagellates	1	
SC formation		Hop1*	ND in dinoflagellates	1
		Red1*	ND in dinoflagellates	1
		Pch2*	ND in dinoflagellates	1
ZMM protein		Msh4* (in gametes after3)	ND	2
		Msh5* (in resting cysts after3)	ND	2
		Mer3*	ND	2
		Zip1	ND in dinoflagellates	1
		Zip2	ND in dinoflagellates	1
		Zip3	ND in dinoflagellates	1
Double strand breaks	Meiotic recombination protein	SPO11* (in germinating cysts after3)	GSA120T00013268001	2
	Meiotic recombination protein	Mre11 (in resting cysts after3)	GSA120T00000265001	4
		Dna2	GSA120T00007919001	4
		Atm	GSA120T00024825001	4
	Double strand breaks	RAD50 (in germinating cysts after3)	GSA120T00021321001	4
Homologous recombination	Stimulation of DMC1 activation	MND1* (in germinating cysts after3)	GSA120T00008837001	2
	Recombinase with specificity	HOP2* (in germinating cysts after3)	GSA120T0000161001	2
	DNA strand invasion	RAD51* (in resting cysts after3)	GSA120T00009824001	2
	Stimulation of RAD51 activation	RAD54 (in germinating cysts after3)	GSA120T00006516001	4
	Meiotic recombination protein	DMC1* (in germinating cysts after3)	GSA120T00010080001	2
Cross over I	DNA mismatch repair	MLH1 (in vegetative cells after3)	GSA120T00014170001	4
		MLH3	ND	4
		SLX1	GSA120T00019260001	4
		SLX4	ND	4
		SGS1	GSA120T00024235001	4
		EXO1	GSA120T00008768001	4
		EXO1	GSA120T00005899001	4
		MUS81	GSA120T00001489001	4
Cross over II		MMS4/EME1	ND	4
	Meiotically upregulated	Mug157 (in resting cysts after3)	ND	4
		Plant-Msh1	GSA120T00012118001	4
	Endonuclease	MustS2? (in germinating cysts after3)	ND	4
		Pms1 (in resting cysts after3)	GSA120T00014436001	4
	Cohesion complex	RAD21	GSA120T00017233001	2
		RAD21	GSA120T00009901001	2
	Control of meiotic division	Mns1	GSA120T00011473001	4

# **Chapter 2 : Metabolome dynamics during intracellular dinoflagellate infection emphasizes the role of azelaic acid in host resistance**

## **Context of the study**

The identification and rapid detection of different dinospore types and infection states in culture motivated the study of the metabolomic dynamics during the course of host infection. This study represents the first metabolomic investigation of this particular host-parasite combination. The initial aim was to compare different stages of infection and cultures characterised by different dinospore types. By varying infection rates and percentages of P1 and P2 produced by random or biological effects, we were able to hypothesise the role of certain metabolites associated with specific infection outcomes. To gain a deeper understanding of the role of the selected metabolite, we designed a bioassay to monitor its effect on infection or overall host-parasite dynamics. Our bioassay used azelaic acid as the metabolite of interest. Although the outcome of the bioassay is not as straightforward as expected, the design and implementation of this bioassay will certainly be useful for testing other promising metabolites in the future. In addition, the new metabolomics dataset will soon be available to the scientific community and will include putative new and undescribed compounds.

## **Authors contribution**

In this second chapter, I designed the study with the help of Laure Guillou and Marine Vallet. I carried out the sample cultivation and preparation. With the help of Marine Vallet, I performed the metabolomic extractions and we analysed the samples. With the help of Maria Anna Michaela De La Cruz, we did the bioassays and analysis. Laure Guillou and Marine Vallet with the contribution of Deo Florence Llacuna Onda and Georg Pohnert helped with the manuscript.



## Article 2: Metabolome dynamics during intracellular dinoflagellate infection emphasizes the role of azelaic acid in host resistance

Jeremy Szymczak<sup>1</sup>, Maria Anna Michaela De La Cruz<sup>2</sup>, Deo Florence Llacuna Onda<sup>2</sup>, Georg Pohnert<sup>3,4</sup>, Laure Guillou<sup>1</sup>, Marine Vallet<sup>3,4</sup>

<sup>1</sup>Sorbonne Université, CNRS, UMR7144 Adaptation et Diversité en Milieu Marin, Ecology of Marine Plankton (ECOMAP), Station Biologique de Roscoff SBR, 29680, Roscoff, France

<sup>2</sup>Microbial Oceanography Laboratory, The Marine Science Institute, Velasquez St., University of the Philippines, Diliman, 1101, Quezon City, Philippines

<sup>3</sup>Research Group Plankton Community Interaction, Max Planck Institute for Chemical Ecology, Jena, Germany

<sup>4</sup>Institute for Inorganic and Analytical Chemistry, Friedrich Schiller University Jena, Germany

### Keywords

Algae; Parasitism; Syndiniales; Amoebophrya; Metabolomics; High-resolution mass spectrometry; Azelaic acid

### Abstract

*Amoebophrya* spp. are widely distributed parasites that infect numerous marine dinoflagellates, including toxic species, and can even play a role in terminating algal blooms. These parasites undergo significant physiological changes during host infection, resulting in visible morphological and transcriptional modifications. However, our understanding of associated metabolic changes, such as metabolites accumulation or secretion, remain limited despite their potential roles in parasite virulence or host chemical defence.

## Chapter 2

In this study, we report clear-cut modifications in both endometabolites (internal metabolites) and exometabolites (potentially secreted metabolites) during host infection. We observe distinct metabolomic profiles at various infection stages, indicating that each stage has a specific metabolic composition. We identify certain metabolites that exhibited negative and positive correlations with the percentage of infected host cells and the proportion of a distinct dinospore type (P1 and P2). We hypothesize these molecules might be involved in host resistance or parasite development.

We tested this hypothesis through bioassays. When we pre-incubated the host with parasite exudate, we observed a reduction in infection prevalence 8 hours later but no effect after 24 hours. Additionally, we tested the impact of incubating the host with azelaic acid, a metabolite found to be negatively correlated with infection but positively with the production of spores involved in sexual reproduction. As a result, the percentage of hosts infected by a single parasite decreased with 200  $\mu\text{M}$  of this compound after 8 hours, with no effect detected after 24 hours. While these results raised methodological questions, they unquestionably provided insight into a potential defence mechanism the dinoflagellate host employs against the parasite.

### **Introduction**

Harmful Algal Blooms (HABs) result from the rapid proliferation and accumulation of opportunistic and often toxic microalgae, many of which belong to the dinoflagellate group (Hallegraeff, 1993). The increased frequency, intensity, and geographical spread of HABs in recent decades are primarily driven by anthropogenic nutrient enrichment, known as cultural eutrophication (Anderson et al. 2012).

Dinoflagellates, serving as hosts for various natural enemies, including parasites, encompass a wide range of pathogens. Parasitism is a common ecological strategy in the natural world, exerting substantial evolutionary pressures on both hosts and parasites (Poulin and Thomas, 1999). Understanding the factors that initiate, sustain, and limit these host-parasite associations is paramount.

## Chapter 2

Symbiotic interactions, including parasitism, mainly depend on what happens at the molecular level (Kafsack and Llinás, 2010; Kloehn et al., 2016). While genomics and transcriptomics provide valuable insights into genetic and transcriptional changes, metabolomics offers a real-time window into the biochemical alterations. The metabolome, comprising a dynamic collection of cellular metabolic products, includes various small molecules, each with a specific role as enzymatic substrates, products, or cofactors (Fiehn, 2002). Endometabolome uncover molecular strategies employed by intracellular parasites to manipulate their hosts or the host's defence mechanisms aimed at repelling invaders or limiting the parasite growth (Castro-Moretti et al., 2020). Moreover, the exometabolome can unveil bioactive molecules or messengers, some of which are active after their release into the water (Pohnert et al., 2007).

*Amoebophrya ceratii*, a member of the Syndiniales and equivalent to Marine ALVeolates Group II (MALV-II), specializes in parasitizing dinoflagellates. While the range of potential hosts may vary among strains, *Amoebophrya* species are highly specific to their hosts (Cai et al. 2020). They can control toxic dinoflagellate blooms in natural environments by infecting and killing host cells (Chambouvet et al., 2008, Velo-Suárez et al., 2013). As part of the marine planktonic ecosystem, MALV-II organisms are hyperdiverse pervasive components of the marine food web (de Vargas et al. 2015) and actively contribute to carbon export in the oceans (Guidi et al. 2016).

To date, all known Syndiniales parasites exhibit a biotrophic parasitic strategy, which means they refrain from killing their hosts during most of their intracellular development stages while still utilizing some of the host's physiological functions. In the case of an *Amoebophrya* infection, the host dinoflagellate's photosynthesis (and potentially its mitochondria) continues to function (Kayal et al. 2020, Decelle et al. 2022). During the infection, the transcriptome of the host is highly impacted (Lu et al. 2016, Faraht et al. 2018), as well as its cellular structure (Decelle et al. 2022). Within days, a single infected host can generate numerous small and large dinospores, each with distinct phenotypes and metabolomes. These dinospores have different sizes and typically have a lifespan of only a dozen days under laboratory conditions. This is discussed in Chapter 1 of this thesis.

This study explores the dynamics of the endo- and exometabolites during of infection of the photosynthetic dinoflagellate *Scrippsiella acuminata* by the parasite

## Chapter 2

*Amoebophrya ceratii*. This dynamic was performed along the parasite development in the host at initial, intermediate and late stage of infection. In addition to comparing the various infection stages, we examined how the infection rate, indicated as the percentage of infected cells, correlated with metabolite production. We retained one molecule for a bioassay to evaluate its role in the priming effect of the host and its influence on the success of the infection. This study marks the first exploration of the metabolomics of this particular pathosystem, complementing previous genomic and transcriptomic investigations done on the same strains (Farhat et al. 2021, Farhat et al. 2018) and contributing to a deeper understanding of the interaction dynamics between this widespread parasite and its host.

## Materials and methods

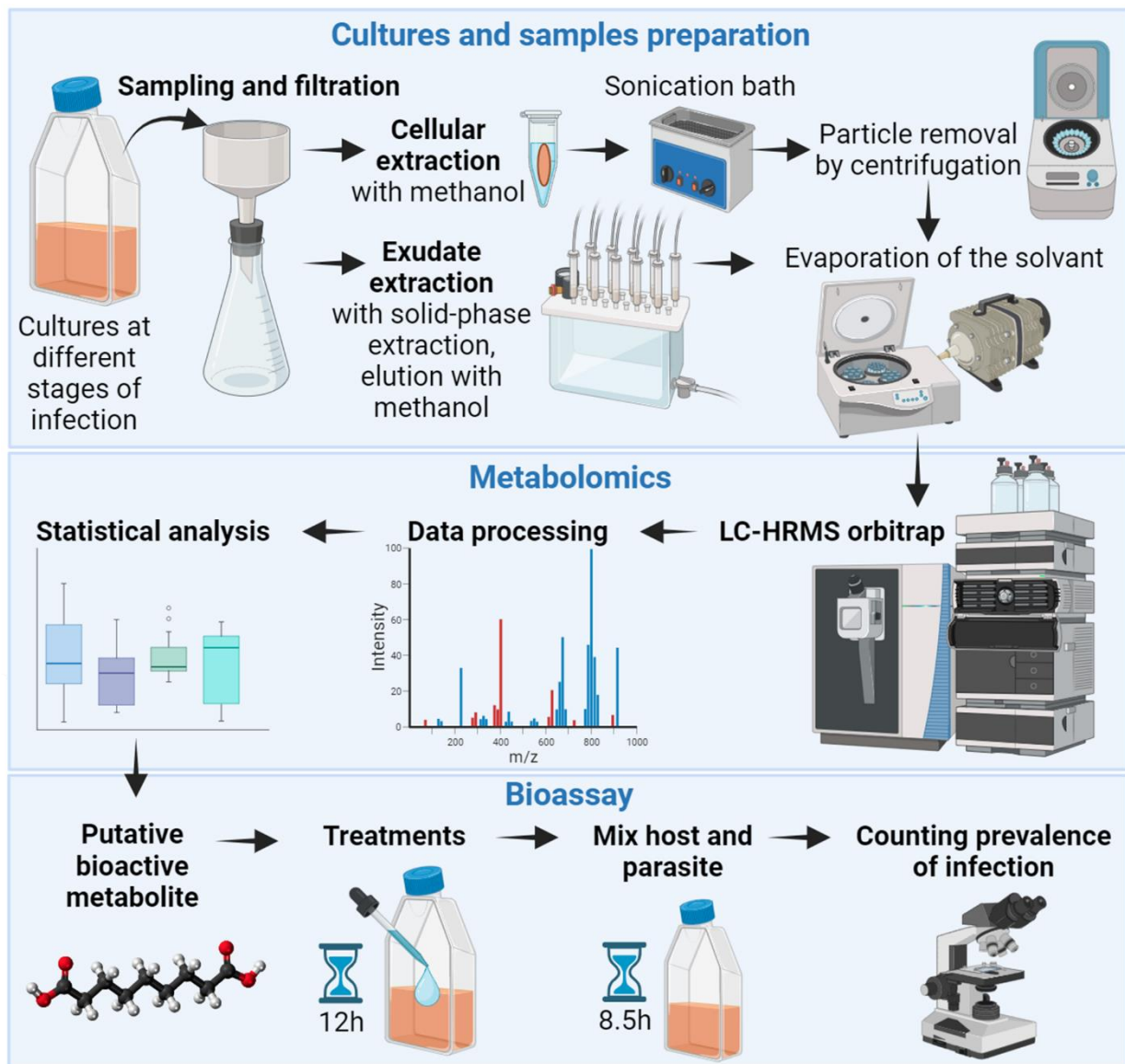


Figure 2- 1: The general workflow from the culture of infected hosts to metabolomic analysis and bioassay.

### Strains and cultivation procedure

We used the photosynthetic dinoflagellate, *Scrippsiella acuminata*, as host (strain ST147, RCC1627 <https://roscoff-culture-collection.org/rcc-strain-details/1627>) and the parasite *Amoebophrya ceratii* (strain A120, RCC4398 <https://roscoff-culture-collection.org/rcc-strain-details/4398>).

The host and the parasite were cultivated in F/2 medium, prepared using Red Sea Salt medium (Red Sea Company) to achieve a salinity of 27 PSU (Bigear, 2022). During preliminary tests conducted for bioassays, we used a different medium using natural

## Chapter 2

sea water from the Penzé estuary at a salinity of 27 PSU, kept about six months in the dark, filtered and autoclaved and enriched with F/2 medium (Guillard's (F/2) Marine Water Enrichment Solution, (Bigéard and Guillou, 2022)). The cultures were exposed to continuous light, equivalent to approximately  $100 \mu\text{Einstein m}^2 \text{s}^{-1}$  of light intensity, with a LED light source (EASY LED universal light 438 nm) and maintained at a temperature of 21°C. We opted to work with biological replicates instead of technical replicates. Thus, we divided an initial culture of hosts and a culture of parasites into six lineages, maintaining them as separate “host + parasite” pairs over multiple generations. The six pairs of host and parasite cultures were transferred twice weekly in vented flasks (CytoOne, Starlab). The host was transferred twice weekly by diluting the culture into sterile F/2 medium at a dilution ratio 1: 4 (host to medium, vol: vol). Infected host cultures were routinely transferred to healthy host cultures every 3-4 days to sustain the parasitic strains. The transfer was carried out using a volume ratio of 10: 1 (parasite: host) in 50 mL culture flasks.

### *Sample collection for metabolomic analyses*

The experiments were carried out twice: once at the fourth and once at the eighth generations of the maintained lineages. Metabolomic samples from both the endo and exometabolomes were extracted at various infection time points, specifically at the initial time (between 1.5 to 2 hours after inoculation), at the intermediate infection stage (between 10.5 to 11.5 hours after inoculation), and the late infection stage (between 25 to 28 hours after inoculation). This resulted in a total of 72 samples (six lineages x two generations x three-time points during infection x divided into two preparations: endo and exometabolomes).

Before starting the experiment, parasite cultures used for inoculation were filtered by gravity through a 5  $\mu\text{m}$  nylon membrane (Millipore) to remove infected and non-infected hosts. At the start of the experiment (T0h), 160 mL of these dinospores were mixed with 640 mL of hosts and incubated for eight hours. All experiments were conducted using vented culture flasks (CytoOne, Starlab) under conditions similar to those of the maintained lineages.

Subsequently, infected cultures were passed through a 5  $\mu\text{m}$  nylon membrane (Millipore), followed by two thorough rinses using fresh medium. Host cells retained on

## Chapter 2

the filter were then resuspended in 300 mL of sterile F/2 medium. This process was crucial for eliminating free parasites and enhancing the synchronization of infections.

### *Cell density estimated by flow cytometry*

The host (uninfected and infected) and parasite cells were counted by flow cytometry (Novocyte Advanteon, ACEA Biosciences), for the details, see Szymczak et al. 2023.

For bacterial counts, 500 µL aliquots were fixed with glutaraldehyde (0.25% final concentration) for a minimum of 15 minutes and then stored at -80°C until analysis. Upon thawing, samples were diluted twice in Tris buffer for a final 100x dilution, and DNA was stained using SYBR Green-I at a final dilution of 1/50,000, following the protocol outlined by Marie et al. 2000. The counts were conducted using flow cytometry with blue light excitation (488 nm).

Prevalence were estimated > 24 hours after inoculation, using counts obtained by flow cytometry and the following equation: prevalence of infection (Unit= percentage of infected cells): [infected host cells at intermediate + late stages] / [Uninfected + infected host cells at intermediate + late stages] \* 100

Cell counts and prevalence for the metabolomic experiment can be found in table 2-1.

### *Extraction of the cells from Amoebophrya-infected cultures of dinoflagellates*

Approximately 40 mL of the sample was gently filtered under a vacuum on a GF/C filter with a 25 mm diameter at each time point. The filter was then rapidly placed in a 2 mL Eppendorf tube containing 1.5 ml of cold methanol (HPLC grade) and kept at 20°C. The Eppendorf tubes containing the filter were sonicated for 30 minutes in an ultrasonic bath. Blanks consisted of extracts of 40 ml culture medium and solvent mixture.

Following sonication, the liquid extract was separated from the filter and any cell debris through three centrifugations, each lasting 10 minutes at 10,000 g. Subsequently, the supernatant was carefully transferred to a new 2 mL plastic tube. Once the extract was free from particles and debris, the solvent was evaporated at a temperature of 35°C using a SpeedVac system from Thermo scientific. This process was conducted in a glass tube to obtain dry extracts.

## Chapter 2

### *Extraction of the exudates from Amoebophrya-infected cultures of dinoflagellates*

Each filtrate produced during the filtration for the endometabolome was subjected to an additional filtration step using a 0.22  $\mu\text{m}$  PES syringe filter to ensure the removal of any remaining particles. The particle-free filtrate was extracted using the solid-phase extraction method (6cc OASIS HLB sorbent from Waters) with the following sequential steps: 1) conditioning (3 mL of methanol HPLC grade), 2) equilibration (3 mL of pure water), 3) sample extraction (about 35mL), 4) salt washing (4 mL of pure water), and 5) elution of the extract (3 mL of methanol). The eluted solvent was then evaporated at a temperature of 35°C using a SpeedVac (Thermo Fisher Scientific) in glass tubes to obtain dry extracts.

### *Sample preparation for LC-MS analysis*

To process the samples, 100  $\mu\text{L}$  of a methanol: water 1:1 ratio was added to each sample, followed by homogenization using a vortex. Samples were transferred to 1.5 mL Eppendorf tubes using a glass Pasteur pipette and centrifuged for 20 minutes at 14,000 g at 20°C. Subsequently, 50  $\mu\text{L}$  of the supernatant were transferred into a 1.5 mL glass vial with an insert, and 10  $\mu\text{L}$  was transferred in a QC pooled sample (quality control). Furthermore, 1  $\mu\text{L}$  of the internal standard L-fluoro-p-phenylalanine was added to each sample. This internal standard was prepared using 2,73 mM of water, resulting in a final concentration of 55  $\mu\text{M}$  in the 50  $\mu\text{L}$  final volume sample (final concentration of 0,055 mM). 10  $\mu\text{L}$  of the prepared samples were injected into a C18 column and analysed with the LC-MS. Blanks were prepared similarly to the experimental samples but were excluded from the QC pooled sample.

### *UHPLC-HRMS profiling and data-dependent MS acquisition*

Dried samples were prepared with 100  $\mu\text{L}$  methanol: water (1:1). 10  $\mu\text{L}$  of samples were injected on an Accucore C18 column (100  $\times$  2.1 mm, 2.6  $\mu\text{m}$ ), and metabolites were separated with a 10 min gradient. The UHPLC-HRMS method using a Q-Exactive Plus Orbitrap mass spectrometer (Thermo Fisher Scientific) was chosen with the same parameters as described in Vallet et al. 2019, except that analysis was conducted in polarity switch mode. The MS/MS spectra of all ions were recovered using full scan ddMS2 top N method with the Orbitrap system, performed on the QC sample in both polarities. The MS/MS was conducted within an isolation window of  $m/z$  0.4 at a peak



## Chapter 2

resolution of 140,000 and averaging the spectra recovered from the three collision energies (NCE 15, 35, 45). The samples have been randomised for the injection sequence. For technical reasons, samples 1-1 and 2-1 at initial stage and samples 1-1, 1-2 and 1-6 at late stages were not used for the analysis.

### *Raw data processing and metabolites annotation*

Raw data were imported in Compound Discoverer version 3.2 (Thermo Fisher Scientific) for peak picking, peak deconvolution, and annotation of chemical formula derived from the high-resolution isotopic pattern of the traces. QC normalization was performed using the standard values given by the metabolomics workflow, and the features from the blanks were marked with a threshold set to 100. The mass tolerance for MS identification was set at 5 ppm, the minimum MS peak intensity was  $2 \times 10^5$ , and the intensity tolerance for the isotope search was 30%. The relative standard deviation value was set to 50%. The selected labelled compounds were exported as .xlsx files, and their masses were searched in public mass lists (LipidsMaps, Natural Products Atlas, Thermo libraries). The data is currently being deposited in MetaboLights (project MTBLS5370).

### *Statistical analysis of the metabolomes with MetaboAnalyst*

Normalization based on equivalent carbon content of the cells was applied. The carbon content calculation is similar to chapter one. After processing the raw LC-MS data with Compound Discoverer, the statistical analysis was done with the MetaboAnalyst online tool (<https://www.metaboanalyst.ca/> version 5.0). 1903 endometabolites and 620 exometabolites were in two separate .csv files that contained normalized metabolites' peak intensities per sample.

For exometabolome profiling, carbon content estimation from all cells present in the samples was taken into account. For the endometabolome profiling, carbon content estimations were based on cells that were retained on the filter (this excluded part of bacteria that passed through the GF/C filter). We selected a square root transformation and a Pareto scaling on peak intensities. A permutation (1,000 permutations number) test with separation distance (B/W) was done to validate the use of the PLS-DA (p-value < 0.05) method.

## Chapter 2

To compare differences in metabolite production between stages, we initially employed the analysis of variance (One-way ANOVA) along with Fisher's LSD post-hoc tests, using a significance threshold of  $p\text{-value} < 0.05$ . Following this, among the significant metabolites in the ANOVA, the pattern analysis search tool was used to identify endometabolites that aligned with different scenarios. 1/ Increasing intensities along the infection stages: positive correlation with pattern 1-2-3 and negative correlation with pattern 1-0-0. 2/ Decreasing intensities along the infection stages: negative correlation with pattern 1-2-3 and positive correlation with pattern 1-0-0. In addition, the correlation analysis was used to highlight relationship between metabolites normalised intensities and the prevalence (estimated by flow cytometry between 24 hours after inoculation) and with percentages of P1 dinospores produced after dinospores release. The negative correlations correspond to relationship with low prevalence and P2 (the percentage is complementary to percentage of P1) respectively.

### *Bioassay with azelaic acid, host, and parasite exudates*

The analytical standard-grade azelaic acid (Sigma Aldrich) stock solution was prepared by dissolving the solid powder in sterilized pure water less than 48 hours before the experiment to create working solutions with a concentration 100 times higher than that used in the experiment. All concentrations were prepared using the same dilution of 1% (vol/vol). The cultures were mixed with pure water for the negative control without azelaic acid.

We initially conducted two sets of tests to assess the potential impact of azelaic acid: 1/ its effects on host growth and microbiota, and 2/ its influence on dinospore survival. For this purpose, one batch of host culture (4 days old) and one batch of parasites (4 days old) were each divided into four replicates. Each replicate was subjected to one of four distinct treatments, resulting in different final concentrations of azelaic acid: 0, 1 (for host and microbiome only), 10, and 100  $\mu\text{M}$ , final concentration. The culture volumes were maintained at 20 mL for the host and 5 mL for the dinospores, contained in vented flasks (CytoOne, Starlab), and incubated as previously described. Subsequently, samples were collected (300  $\mu\text{L}$  for parasites and 500  $\mu\text{L}$  for the host) from all flasks at different times.

## Chapter 2

In a distinct experiment, we examined the influence of azelaic acid on the infection process. We utilized four sets of host-parasite pairs, which had been independently maintained for 55 generations under identical culture conditions. In this experiment, the four host cultures (issued from the four pairs) was pre-incubated for 12 hours with five different treatments: 1) various concentrations of azelaic acid (0, 100, and 200  $\mu\text{M}$ , final concentration), 2) host exudates, and 3) parasite exudates. To prepare the host or parasite exudates, uninfected and infected cultures, both at 2.5 days old, were filtered using a 0.2  $\mu\text{m}$  syringe filter (Sterivex) and a 50 mL syringe using gentle pressure. The host density was approximately 17,000 cells per mL for the uninfected host exudate culture. For the parasite exudate, cultures containing dinospores mainly P1 in replicates 1, 2 and 3, mainly P2 in replicate 4, with total dinospores densities ranged from 600,000 to 1,200,000 cells per mL and with remaining host at all stages (infected and non-infected) with cell densities were about 7,000 to 14,000 per mL. At T0h, uninfected healthy host cells were collected using a 5  $\mu\text{m}$  porosity cellulose acetate syringe filter (Sartorius Minisart) via gravity filtration using a 5- $\mu\text{m}$  polycarbonate filter. The collected cells were resuspended using the appropriate exudates either from the host or the parasite to initiate the incubation. The cultures were kept under standard culture conditions throughout the 12-hour incubation period. Then, the host cultures from exudate incubation treatments were filtered using a 5  $\mu\text{m}$  pore size polycarbonate filter and resuspended in fresh culture medium to remove the exudates used for incubation. The mean host density across replicates and treatments was 14,190 cells per mL, with a standard deviation of 3,382.

After the first step of incubation of the host only, the host were inoculated with dinospores. A consistent P1-to-host cell ratio across all treatments were maintained to 8.7 (SD=1.8). The prevalence of infection was determined 24 hours after inoculation with flow cytometer. Additionally, the number of parasites infecting each host cell were counted, referred to as infection density, at an earlier stage, at T8.5h after inoculation, before sporulation occurred. CARD-FISH (Catalysed Reporter Deposition-Fluorescence in Situ Hybridization) was used for infection density count because direct microscopic count is possible unlike flow cytometry that measure a fluorescence intensity. The CARD-FISH protocol is outlined by Siano et al. 2011 using the ALV-01 probe described by Chambouvet et al. 2008. 100 to 150 host cells were counted for each sample and the cells were categorised into four groups: 1) Uninfected hosts, 2)

## Chapter 2

Hosts infected by one parasite, 3) Hosts infected by two parasites, and 4) Hosts infected by three or more parasites.

### Results

#### *Variability in the biological replicates used in the metabolomics experiment*

In the inoculum, cell density measurements within the host cultures, referred to as mother host cultures, we have consistently indicated cell densities ranging from 8,000 to 12,700 cells mL<sup>-1</sup> across replicates and generations (Table 2-1). At T0h, the ratio of P1 dinospores: host cell varies among samples, ranging from 1.92 to 12.34, 7.16 in average (SD=2.92). This variation arises because we used a volume-to-volume inoculum method to maintain consistent dilutions in all samples. Nevertheless, the prevalence, estimated through flow cytometry after 24 hours of incubation, remained consistently high, ranging from 68% to 95% in all samples except for one particular replicate with a prevalence of 23%.

However, the production of P1 dinospores, representing the infective form, exhibited substantial variability across generations and lineages, with values ranging from 41% to 88% of P1, as illustrated in Table 2-1.

## Chapter 2

Table 2- 1: Metadata for endo- and exometabolomes: estimation of relevant parameters and cell densities during the course of infection in the biological replicates.

Replicate names	Cultures before T0h			Conditions at initial stage (T0h)				
	Densities in cells/mL			Densities in cells/mL			Cells ratios per host	
	P1	P2	Hosts	P1	P2	Hosts	P1	P2
1-1	494 636	116 893	8 770	72 345	16 233	7 821	9.25	2.08
1-2	562 840	86 828	8 077	68 767	10 027	7 286	9.44	1.38
1-3	449 607	62 526	9 739	81 486	11 069	9 408	8.66	1.18
1-4	509 773	74 841	9 056	64 209	9 528	9 255	6.94	1.03
1-5	598 399	108 702	10 332	106 278	18 744	8 533	12.45	2.20
1-6	522 451	138 563	9 951	85 643	21 452	8 850	9.68	2.42
2-1	210 301	153 441	9 790	39 607	30 590	7 307	5.42	4.19
2-2	44 834	10 876	8 672	9 968	2 382	5 189	1.92	0.46
2-3	117 756	4 386	7 730	25 053	786	5 213	4.81	0.15
2-4	127 101	181 439	9 543	27 461	41 033	6 680	4.11	6.14
2-5	185 515	248 417	10 105	39 885	56 262	9 019	4.42	6.24
2-6	410 740	203 353	12 669	80 659	44 242	9 085	8.88	4.87

Replicate names	Prevalence in % at late stage (T24h)	Dinospores production after infection (T48h)	
		Number of dinospores	% of P1
1-1	88.2	170.0	77.95
1-2	89.9	161.1	86.40
1-3	92.6	171.3	88.82
1-4	93.5	153.1	82.51
1-5	95.3	125.2	84.02
1-6	93.7	146.5	65.41
2-1	71.1	139.4	28.43
2-2	23.0	556.9	80.77
2-3	76.6	139.1	37.87
2-4	68.2	182.5	47.49
2-5	79.9	135.1	24.09
2-6	89.3	113.4	64.00

The samples of the first experiment exhibited a high prevalence (92.2%) and a substantial production of P1 (80.8%). The samples in the second experiment showed a slightly lower prevalence (68.0%) and a lower production of P1 (47.1%). The sample 2-2 looked like an outlier with a low prevalence (23%) but with a high production of P1

(80.8%). Taken all together, there was no positive linear regression between prevalence and the production of P1 in our data (Fig. 2-2A) but when sample 2-2 was excluded, it was the case ( $R^2 = 0,67$ , Fig. 2-2B).

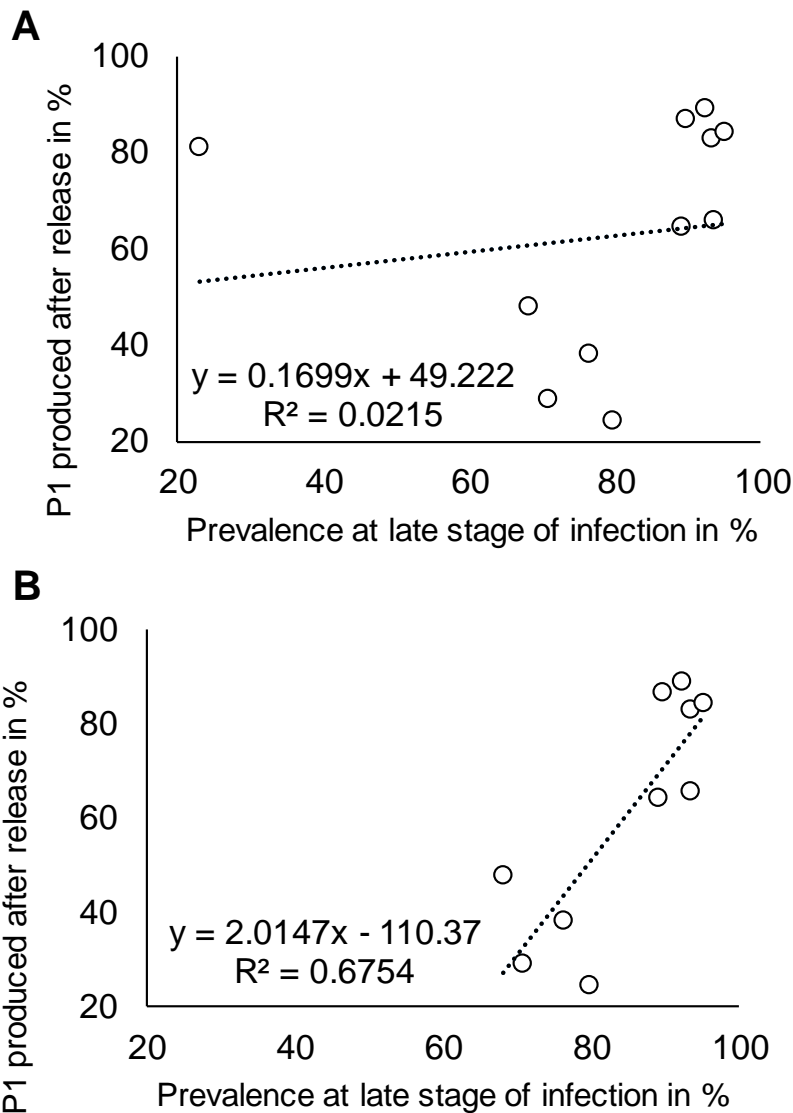


**Figure 2- 2: Linear regression between prevalence and the percentage of P1 dinospores produced (on the total number of dinospores) during sampling for metabolomics analyses.**

A: the sample 2-2 with the lowest prevalence is removed and the  $R^2$  is high B: all the samples were kept and the linear regression does not fit with a low  $R^2$ .

The infection dynamics appeared similar in all cases, indicating consistent sampling timing throughout infective progress. This consistency is supported by the recorded

## Chapter 2

cytometric signatures, which provide insights into the progression of the infection dynamics.

### *Analyses of the metabolome during infection*

After the data processing with Compound Discoverer 1,903 and 620 metabolites were obtained from the endometabolomes and the exometabolomes, respectively. Only a limited number of these metabolites were automatically annotated, 782 for the endometabolome and 200 for the exometabolome.

Both exo- and endometabolomes changed drastically over the infection, as illustrated by the PLS-DA. The initial and intermediate stages overlapped slightly in the analysis of endometabolomes and the intermediate and late stages partially overlapped in the analysis of exometabolomes (Fig. 2-3).

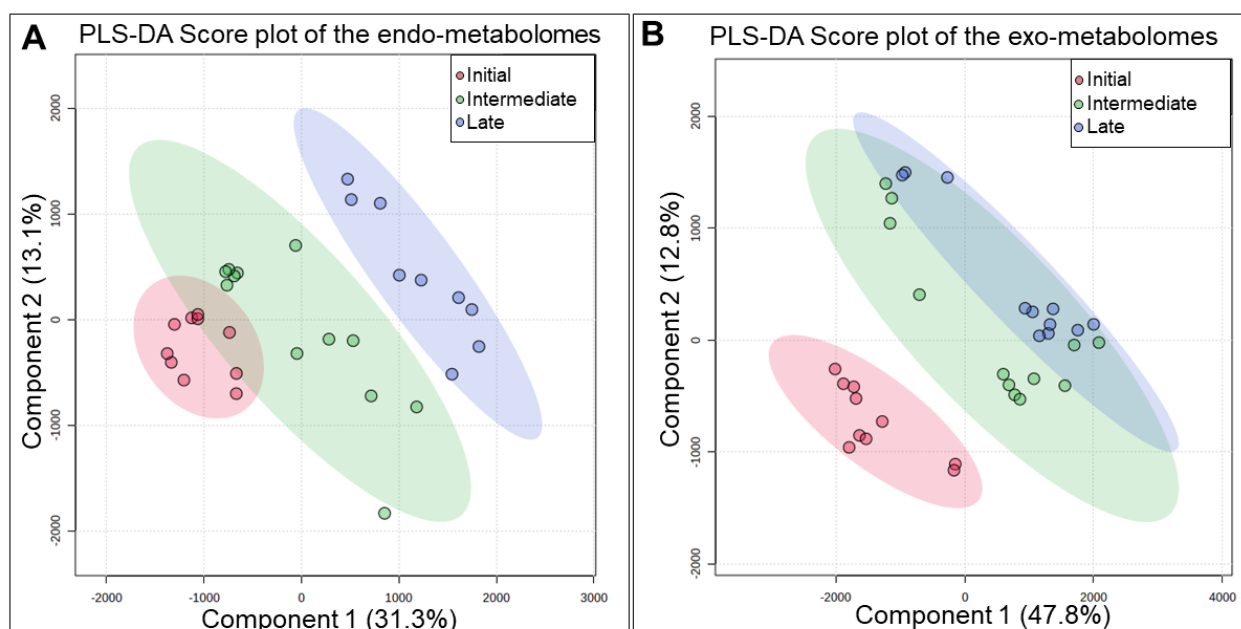


### **Figure 2- 3: Multivariate distribution from PLS-DA.**

Samples based on the intensities of the A: endometabolites and B: exometabolites. The coloured areas correspond to the 95% confidence regions.

These temporal differentiations were validated through the pattern search analysis, wherein 1,195 endometabolites (accounting for 62.8%) exhibited significant temporal patterns from the pattern analysis. Furthermore, the analysis of variance revealed significant differences between the various infection stages, providing an additional perspective. Indeed, 893 endometabolites (representing 47% of the total) and 214

## Chapter 2

exometabolites (34%) demonstrated statistical significance as determined by One-way ANOVA with Fisher's LSD post-hoc test, with a p-value less than 0.05.

Subsequently, 128 endometabolites and 442 endometabolites, as well as 57 exometabolites and 143 exometabolites, displayed significant correlations with the production of P1 dinospores and the prevalence, respectively. Most endometabolites (89.9%) exhibited negative correlations with both the prevalence and the percentage of P1, with approximately two-thirds demonstrating a temporal pattern.

The various Venn diagrams depict the significance between temporality, prevalence, and production of P1. 559 endometabolites had increasing intensity trends during infection, i.e. positive correlation with pattern 1-2-3 and negative pattern 1-0-0 and significant in the ANOVA. In common with the increasing metabolites, there were 21 endometabolites at intermediate stage (Fig. 2-4A) and 31 at late stage (Fig. 2-4B) with were positively correlated with the prevalence whereas 210 endometabolites at intermediate stage (Fig. 2-4A) and 115 endometabolites at late stage (Fig. 2-4B) with negative correlation. In addition, in common with the increasing metabolites, there were 19 endometabolites at intermediate or late stage with positively correlation with the percentage of P1 dinospores after release whereas there were 325 endometabolites with negatively correlated (Fig. 2-4C).



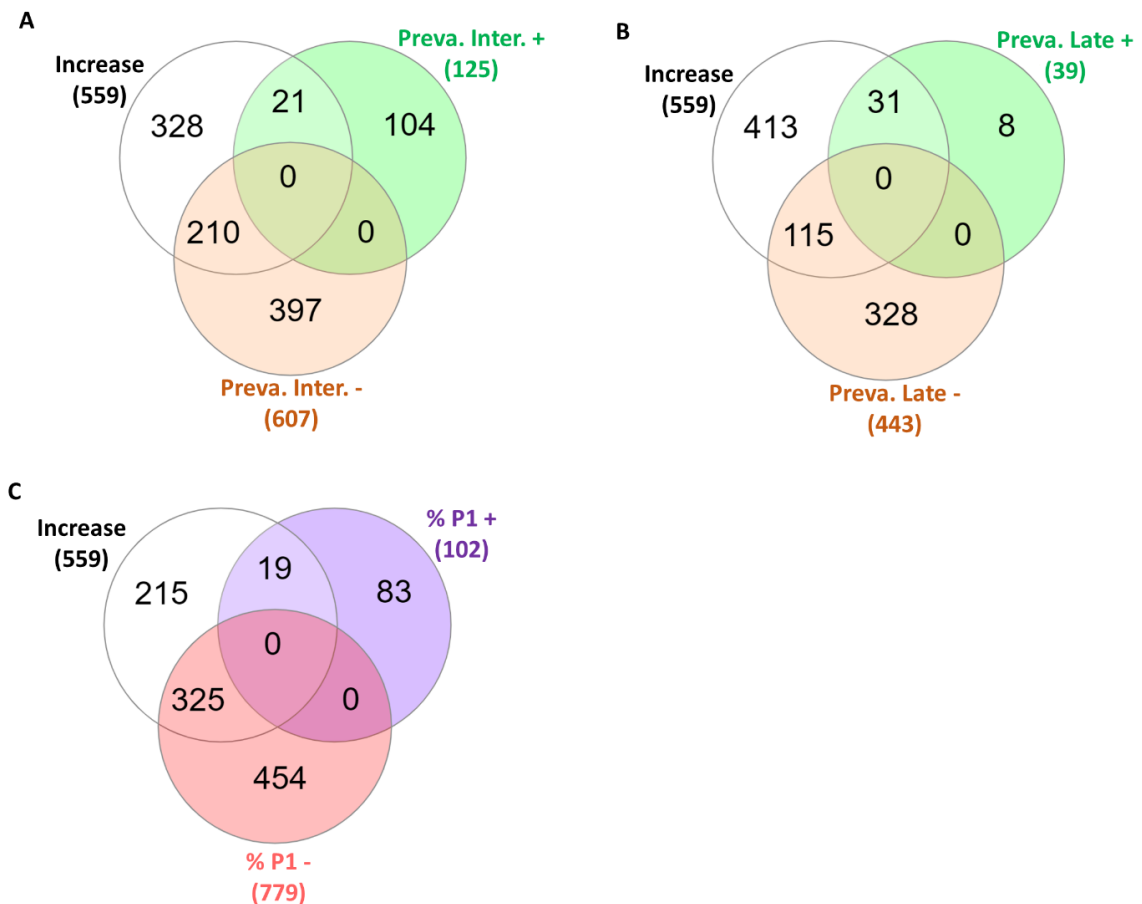


**Figure 2- 4: Venn diagrams illustrating the count of significant increasing endometabolites along the infection course**

which are also significant with the correlation (negative “-“ and positive “+”) with prevalence (“Preva.”) at intermediate (“Inter.”) stage (A) or late stage (B) and are also significant with the correlation (negative “-“ and positive “+”) with the percentage of P1 (“% P1”) dinospores after release (C).

Only 77 endometabolites had a decreasing intensity trends during infection, i.e. negative correlation with pattern 1-2-3 and positive correlation with pattern 1-0-0 and significant in the ANOVA. In common with the decreasing metabolites, there were 19 endometabolites at intermediate stage (Fig. 2-5A) and only 1 at late stage (Fig. 2-5B) with were positively correlated with the prevalence whereas 4 endometabolites at intermediate stage (Fig. 2-5A) and 31 endometabolites at late stage (Fig. 2-5B) with negative correlation. In addition, in common with the decreasing metabolites, there were 17 endometabolites at intermediate or late stage with positively correlation with the percentage of P1 dinospores after release whereas there were 11 endometabolites with negative correlation (Fig. 2-5C).

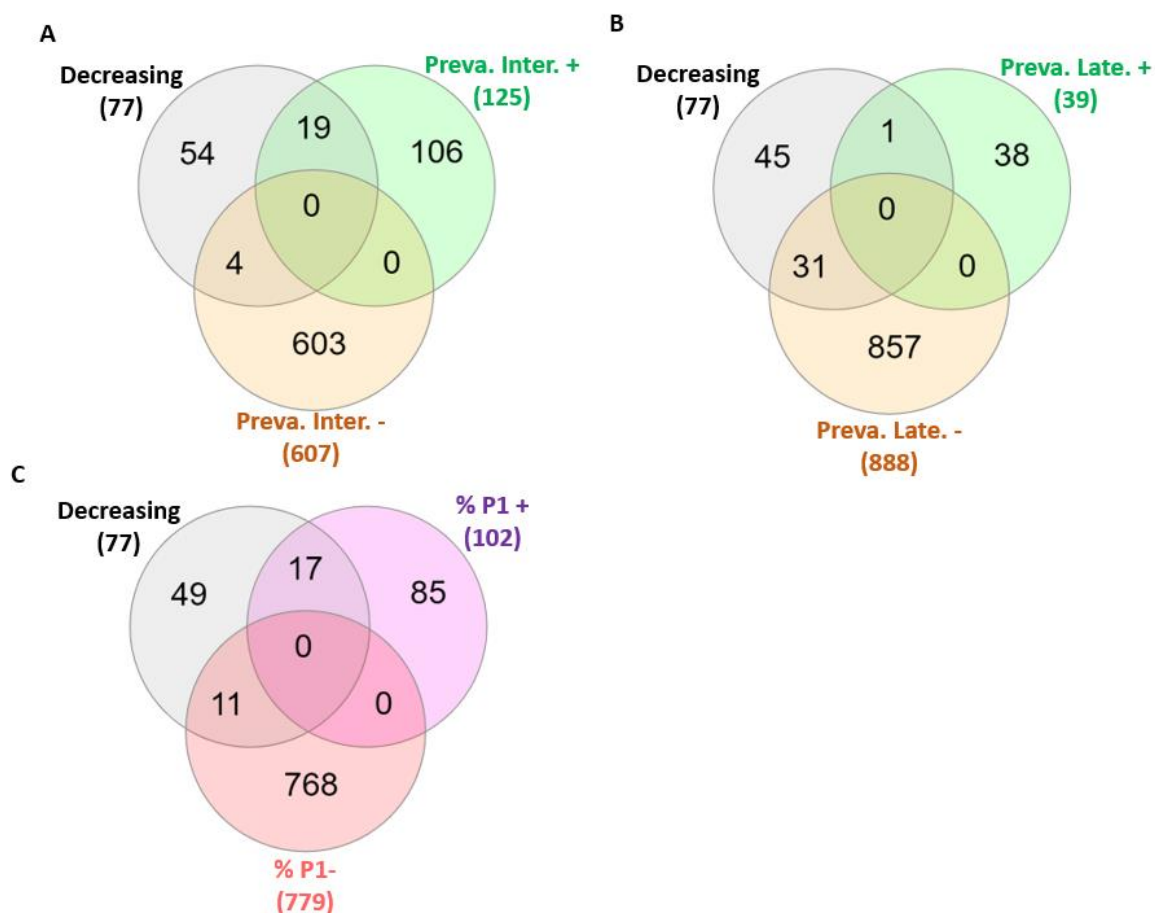


**Figure 2- 5: Venn diagrams illustrating the count of significant decreasing endometabolites along the infection course**

which are also significant with the correlation (negative “-“ and positive “+”) with prevalence (“Preva.”) at intermediate (“Inter.”) stage (A) or late stage (B) and are also significant with the correlation (negative “-“ and positive “+”) with the percentage of P1 (“% P1”) dinospores after release (C).

Among the metabolites having an annotation, we detected DMSP ( $C_5H_{10}O_2S$ ,  $m/z$  135.0474 for  $[M+H]^+$ ) and azelaic acid ( $C_9H_{16}O_4$ ,  $m/z$  187.0979 for  $[M-H]^-$ ). DMSP and azelaic acid were increasing with time during the infection according to the ANOVA (Fig. 2-6) and pattern analysis. In addition, DMSP was negatively correlated at initial and late stages with prevalence and negatively correlated at intermediate and late stage with the percentage of P1 dinospores produced. Azelaic acid was negatively correlated at initial and intermediate stages with prevalence and negatively correlated at intermediate and late stage with the percentage of P1 dinospores produced. Both metabolites were absent from the exometabolites list.

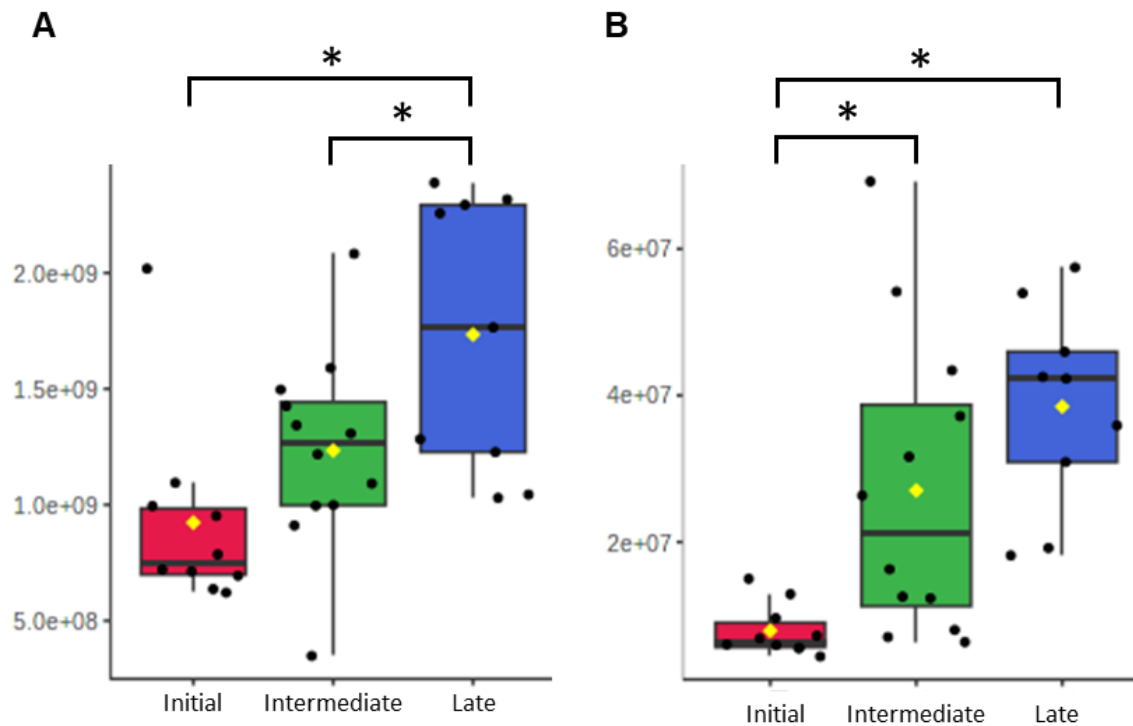


**Figure 2- 6: : Intensities of DMSP (A) and azelaic acid (B) at the three stages of infection in all samples.**

Asterisks indicate significant differences between stages according to ANOVA.

Out of the 257 exometabolomes analysed, only 142 exhibited correlations with both prevalence and the percentage of P1. Within this subset, 20 metabolites demonstrated a significant increase at the final stage compared to the initial and intermediate stages, as determined by the ANOVA analysis. Notably, we observed similar metabolites with matching chemical formulas and comparable retention time within the endometabolites that also displayed increasing trends over time (Table 2-2).

## Chapter 2

**Table 2- 2: List of exo-metabolites associated with production by infected hosts at a late stage of infection, according to ANOVA, with corresponding identification in the endo-metabolites.**

The results of the correlations analysis on the right side indicate the relationship with the percentage of P1 dinospores after release (“Corr. to %P1”) and the prevalence at late stage (“Corr. to prevalence”).

Putative exo-metabolites produced by infected host			Putative corresponding similar endo-metabolites				
Formula	Automatic annotation	RT	Formula	Automatic annotation	RT	Corr. to %P1	Corr. to prevalence
C13 H18 O3	(-)-6-Hydroxy-3-oxo-alpha-ionone	3.567	C13 H18 O3	(-)-6-Hydroxy-3-oxo-alpha-ionone	3.567	-	
C13 H18 O2	Cryptenol	4.746	C13 H18 O2	Cryptenol	3.273	-	
			C13 H18 O2	Cryptenol	4.746		-
C13 H20 O3	Violapyrone I	3.296	C13 H20 O3	Violapyrone I	3.274	-	-
			C13 H20 O3	Violapyrone I	3.781	-	-
C17 H26 O5	Botrydial	5.969	C17 H26 O5	3-O-Ethyllactarolide A	5.884		-
C13 H18 O2	4'-Hydroxymethyl-1-phenyl-n-hexan-1-one	3.294	C13 H18 O2	4'-Hydroxymethyl-1-phenyl-n-hexan-1-one	2.908		+

### *Identification of azelaic acid as a significant feature during the intracellular stage of Amoebophrya in the host cells*

Azelaic acid (C<sub>9</sub>H<sub>16</sub>O<sub>4</sub>, *m/z* 187.0979 for [M-H]<sup>-</sup>) was formally identified using spectral similarity matching with an analytical standard processed under similar conditions (Fig. 2-7). The production of this molecule negatively and linearly correlated with the parasite prevalence at intermediate stage of infection (R<sup>2</sup>= 0.75, Fig. 2-7).

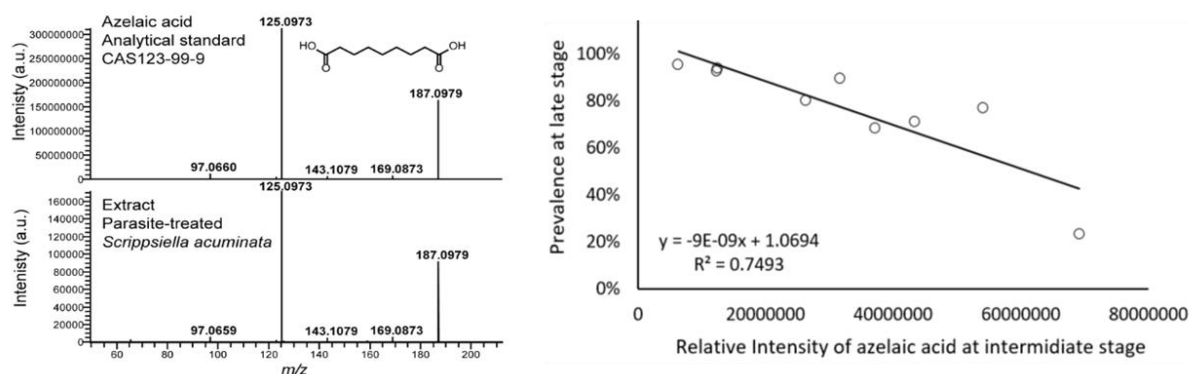


**Figure 2- 7: Formal identification of the azelaic acid (left panel) and correlation between the relative intensity of azelaic acid at intermediate stage and prevalence (right panel).**

Structural identification of the significant feature *m/z* 187.0979 for [M-H]<sup>-</sup> as azelaic acid by UHPLC-HRMS/MS was conducted by comparison of spectral information from endometabolome dataset and commercial standard.

## Chapter 2

Preliminary tests involving azelaic acid concentrations ranging from 0 to 100  $\mu\text{M}$  revealed no significant alterations in the growth of the host or its associated bacterial microbiota (Fig. 2-8C and 2-8D). Likewise, the presence of azelaic acid did not substantially affect the survival of the parasites (P1 and P2+3) (Fig. 2-8A and 2-8B).

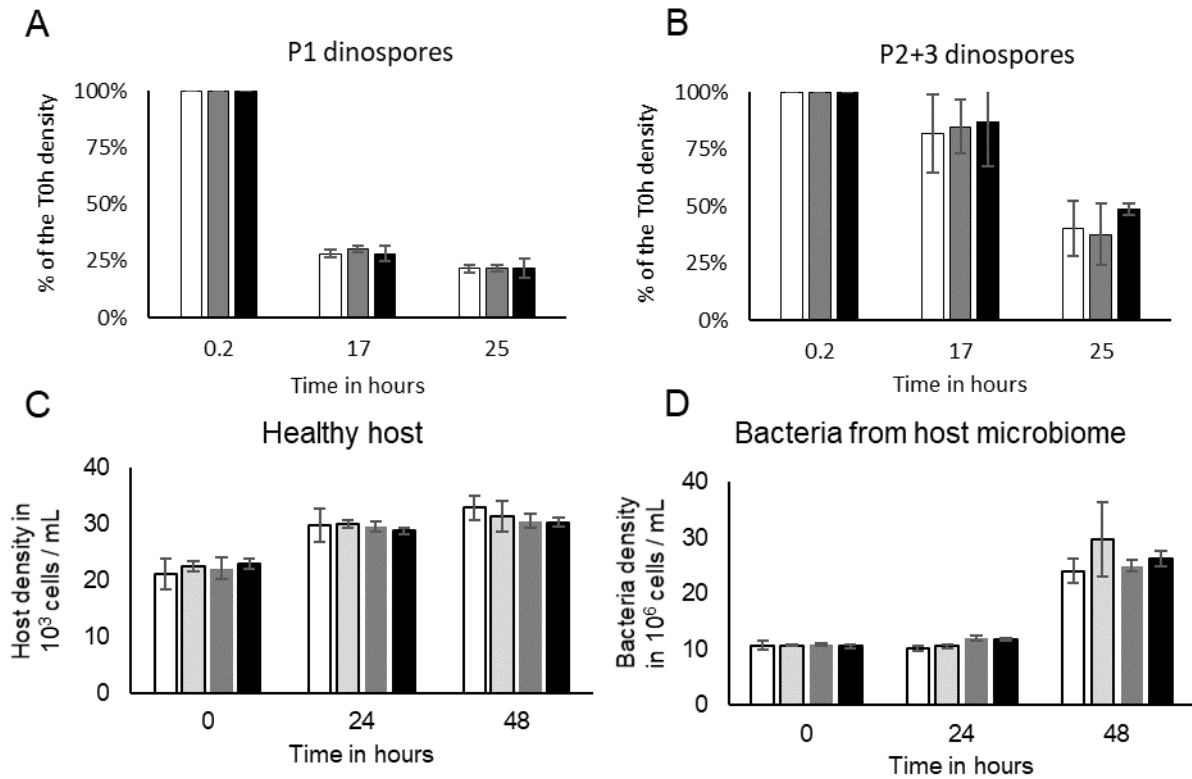


**Figure 2- 8: Survival of dinospores P1 and P2+3 and growth of the host and its microbiota.**

Host, parasites dinospores and bacteria densities followed over time (by flow cytometry) after incubation with different final concentrations of azelaic acid: 0  $\mu\text{M}$  (negative control, in white, addition of pure water only), 1  $\mu\text{M}$  in light grey, 10  $\mu\text{M}$  in darker grey and 100  $\mu\text{M}$  in black.

We subsequently investigated whether pre-incubating the host with azelaic acid for 12 hours before infection could affect the infection's fitness (Table 2-3). Two significant impacts on prevalence were observed after 8 hours of inoculation, determined by CARD-FISH. One was associated with using 200  $\mu\text{M}$  azelaic acid, and the other was linked to using the parasite exudate (Table 2-3). However, flow cytometry conducted 24 hours after incubation did not confirm these results. In the latter analysis, the prevalence remained consistently high, ranging from 68.69% to 74.47%, with no significant differences observed among treatments (Table 2-3). Production of P1 (expressed as a percentage of the total number of dinospores produced) was highly

## Chapter 2

variable over generation replicates and was actually dependent on the initial host x parasite pairs.

**Table 2- 3: Effect of azelaic acid (at 0, 100, 200  $\mu$ M), host exudate (Hext) and parasite exudate (Pext) on the density of parasites and prevalence after 8 hours of infection (CARD-FISH counts) and prevalence after 24 hours (flow cytometry).**

Means from four biological replicates, the p-value (p.val.) corresponds to the comparison (t.test) between the negative controls and the treatments. The samples “100  $\mu$ M” and “200  $\mu$ M” are compared to the “0  $\mu$ M”. The samples “host exudate” are also compared to the “0  $\mu$ M” and the samples “parasite exudate” are compared to “host exudate”. Significant p values are indicated in bold. The prevalences at T24h after inoculation and P1 and P2 productions measured with flow cytometry presented no significant difference (t.test) between the treatments.

Treatments	CARD-FISH												
	Non-infected	1 parasite			2 parasites			3 parasites or more			Prevalence		
	Mean in %	Mean in %	SD	t.test	Mean in %	SD	t.test	Mean in %	SD	t.test	Mean in %	SD	t.test
0 $\mu$ M	33.6%	29.5%	0.04		20.1%	0.06		16.8%	0.06		66.4%	0.16	
100 $\mu$ M	34.7%	28.7%	0.02	0.754	18.7%	0.04	0.719	17.8%	0.14	0.896	65.3%	0.17	0.927
200 $\mu$ M	54.6%	<b>17.3%</b>	0.03	<b>0.003</b>	16.6%	0.09	0.555	11.4%	0.15	0.525	45.4%	0.23	0.178
Hext	44.1%	22.4%	0.07	0.116	14.7%	0.06	0.251	18.8%	0.14	0.807	55.9%	0.12	0.331
Pext	62.1%	21.2%	0.05	0.787	9.1%	0.04	0.189	7.5%	0.05	0.188	<b>37.9%</b>	0.08	<b>0.048</b>

Treatments	Flow cytometer					
	Prevalence at late stage (T24h)		Dinospores production per infected host			
	Mean in %	SD	P1 cells	SD	P2 cells	SD
0 $\mu$ M	72.8%	4.27	158.9	94.4	126.9	15.6
100 $\mu$ M	74.5%	4.04	156.7	100.1	128.2	21.3
200 $\mu$ M	73.7%	5.95	159.5	109.0	145.5	17.2
Hext	71.9%	5.99	169.4	107.2	142.4	11.7
Pext	68.7%	4.41	177.8	108.9	156.8	9.4

## Discussion

Metabolomic analysis presents a significant opportunity to directly investigate the chemical communication between a host and its parasite. This encompasses the metabolites used by the parasite to gain control over its host and develop, as well as the defence strategies employed by the host. Therefore, this work aims to enhance our understanding of the production of these molecules overtime during an infectious cycle.

## Chapter 2

This project represents the second application of this methodology, following a previous study that focused on the free-living stage of the parasite (as detailed in the first chapter of this thesis). It should be noted that the dinospores analysed in the first chapter of this thesis were those produced during the experiments conducted in this second chapter.

In this non-targeted metabolomic approach, we made several methodological choices. First, we utilized synchronized cultures under standard culture conditions. With this cultivation method, the infection dynamics were well synchronized, and the infection times (duration of trophont and sporont stages) were relatively well preserved among the replicates. The synchronization involves the filtration of host cells to separate them from dinospores that have not yet initiated their infection. This crucial step eliminates the medium surrounding the cells after 8 hours of incubation. This fact adequately explains why the exometabolome exhibited substantial overlapping between intermediate and late stage (Fig. 2-3B).

Consequently, we decided to narrow our analysis to the changes observed between these two final time points, focusing exclusively on metabolites that accumulated in the medium and were potentially secreted by the uninfected/infected hosts. Secondly, we employed biological replicates instead of technical replicates (culture lineages), with each host x parasite cultures representing an independent pair maintained for four and eight generations before sampling. This strategy introduced heterogeneity, which has the advantage of providing variability in the signal. Consequently, the samples were consistent regarding host density and prevalence, but the initial concentration of P1 dinospores and the ratio varied.

### *Metabolites that correlated with time*

Compared to other omic analyses, metabolomics can be just as frustrating as transcriptomics, for example, due to the large number of metabolites and genes that remain unidentified, wrongly annotated, or just unknown. However, the primary signals captured by these two techniques converge: significant changes predominantly occur during the intracellular development of the parasites. Indeed, the specific multivariate distribution throughout time clearly illustrates substantial changes in the endometabolome, reflecting the progression of the infection. This highlights the pivotal

## Chapter 2

role of developmental stages as the primary driver behind the rapid shifts in the metabolome. Notably, this observation is in accordance with the findings of transcriptomic analyses conducted over time (Farhat et al. 2018)

Our first hypothesis was that metabolites accumulating during the intracellular development of the parasite and positively correlated with infection prevalence were likely involved in the parasite's infection process within the host. Conversely, metabolites picked at the early stages of the infection and associated with lower infection prevalence might be linked to the host's resistance and priming strategy (cell-to-cell communication). These scenarios were likely too simplistic as, in this study, most metabolites (559) accumulating over time (until the final stage) are negatively correlated with prevalence (307). This seemingly puzzling result can be explained in two ways. First, trophont (intermediate stage) and sporont stages (final stage) are likely metabolically distinct from each other, with only a few metabolites common to both stages that could accumulate over time. Most metabolites are likely produced and rapidly utilized by the parasite or its host. This hypothesis aligns with the biological transitions observed at the subcellular level during the infection (Decelle et al. 2022). For instance, a crucial transition occurs between the trophont and sporulation, supposedly corresponding to the intermediate and final stages (see chapter 1). In particular, the parasite can shift from osmotrophy and no cellular replication during the trophont stage to active replication and a shift for phagotrophy as soon as sporulation commences (Decelle et al., 2022). These transitions result in significant modifications, including in metabolic pathways involved in trophic mode and energetic metabolism.

Viewing the results from a different perspective, focusing on specific metabolic pathways, leads us to similar conclusions. For instance, as demonstrated, the host plastid and likely the mitochondrion remained functional during most of the intracellular development of the parasite, while the parasite rapidly digested the host nucleus (Kayal et al. 2020). These organelles are known to produce a significant amount of reactive oxygen species (ROS), which are highly toxic to organisms. In a previous study by Farhat et al. 2018, the parasite upregulated metabolic pathways involved in resistance against ROS during infection. The array of anti-ROS molecules is diverse, as documented by Hasanuzzaman et al. 2020. Surprisingly, molecules typically involved in ROS scavenging, such as ascorbic acid, glutathione, tocopherol, or carotenoids,



## Chapter 2

were not detected in our dataset, but this might be due to the restrictive selection of the extraction method and/or to the metabolomics approach. DMSP might also act as an antioxidant (Sunda et al., 2002). In our dataset, a metabolite has been automatically annotated as DMSP. This molecule accumulated over time was significant according to the one-way ANOVA test, and negatively correlated with prevalence in the endometabolome (absent from exometabolomes). However, we did not find any degradation products, such as methane sulphinic acid, dimethylsulphide, dimethylsulphoxide, and acrylate, which could indicate ROS scavenging, as described by Sunda et al. in 2002. The absence of these degradation products may be attributed to the limitations of the methodology employed, and further investigations using targeted methods may be needed to explore the presence of these molecules.

The second hypothesis explaining why most of the metabolites accumulating over time are negatively correlated with prevalence may relate to the correlation between the production of P1 dinospores and prevalence from this study. Many metabolites negatively correlated may be, in fact, more strongly associated with P2 production. We established in the first chapter of this thesis that P1 represents the infective stage of the parasite. At the same time, P2 is involved in sexual reproduction, with the exact location and process of meiosis remaining unclear. The production of P1 versus P2 is likely predetermined well before the parasite enters the host cell (see chapter 1), with each infected host cell producing either P1 or P2. Our results may indicate that the number of metabolites associated with P2 production was significantly higher than those associated with P1 production.

It is indeed true that one of the distinguishing features between these two types of spores is their size (larger in P2) and their cytoplasmic content, with P2 containing higher amount of reserve material. These reserves are essential for the potential formation of a resistance cyst after sexual reproduction, as seen in many dinoflagellates. There may, therefore, be a tendency for the accumulation of reserves in P2, a reduced property in P1. This could be explained by their different functional roles and survival strategies (fast infection for P1 versus sexual reproduction for P2). However, this assumption remains speculative and requires further empirical evidence. Exploring the identity of metabolites and their effect on host resistance and parasite infection in conjunction with P2 production could provide the beginning of an answer.

### *Effect of parasite exudate and azelaic acid in the infection*

One of these molecules was azelaic acid. Azelaic acid is known to function as a signalling molecule in plants' systemic acquired resistance (SAR). It triggers a cascade of reactions within plants (Parker, 2009; Jung et al., 2009), and its production requires reactive oxygen species (ROS) through the oxidation of C18 unsaturated fatty acids (El-Shetehy et al., 2015). In plant SAR mechanisms, azelaic acid is transported through the sap to trigger defence responses in distant parts of the plant. Strikingly, among phytoplankton, the production of azelaic acid by the diatom *Asterionellopsis glacialis* acts as a selective barrier for its microbiome. This compound promotes the growth of beneficial bacteria while inhibiting opportunistic microbial pathogens (Shibl et al., 2020).

Recognizing the significance of azelaic acid in positive and negative associations, we conducted bioassays to elucidate its role during *Amoebophrya* infection. Conducting in vitro bioassays is a complex undertaking. Initially, we ascertained that azelaic acid itself had no noticeable impact on host growth, and it did not reduce the survival of parasite dinospores. Subsequently, we hypothesized that supplementing the medium with azelaic acid for 12 hours might promote its accumulation within the host cell. We did not test this hypothesis in the current study. Later, we observed that employing this strategy did not significantly alter infection prevalence 24 hours after inoculation. The significant difference observed 8 hours after inoculation, using CARD-FISH and the highest final concentration of azelaic acid, was challenging to reconcile with the results obtained by flow cytometry. A first potential explanation is methodological, with the possibility of host cells being more fragile to the fixation depending on the infection level. However, such bias should be proportional and cannot explain the difference observed by itself. Another plausible explanation could be the disappearance of infected host cells between 8 and 24 hours. This phenomenon could be difficult to assess because uninfected host cells continue to divide in our cultures.

Similar observations were made when using the parasite exudate, including all the potential secreted molecules from both infected and uninfected hosts. No significant differences were observed after 24 hours when examined through flow cytometry, while a positive signal was detected after 8 hours using CARD-FISH. This second observation suggests that there might be a sensitivity issue and a methodological bias between the two techniques.

## Chapter 2

In conclusion, irrespective of our challenges, this study neither confirmed nor disproved the potential involvement of azelaic acid in the host's defence mechanisms. The design of this bioassay for this specific host and parasite is, however, useful for further experimentation, particularly with the molecules highlighted in the table 2-2.

### **Conclusion**

This study offers valuable insights into the molecular dynamics during the intracellular development of the parasite *Amoebophrya ceratii* within its host *Scrippsiella acuminata*. The metabolomic analysis uncovered hundreds of metabolites likely involved in the parasite's rapid growth and the intricate interplay between the parasite and its host. These include a multitude of unknown metabolites (not automatically annotated) and putative new compounds specific to *A. ceratii*. Due to the correlation between prevalence and P1 versus P2 production, separating these two parameters adequately in our statistical tests was challenging.

The azelaic acid bioassay demonstrated that this compound does not directly alter host growth or dinospore survival. Incubating the host with this compound before infection did not affect the final prevalence of the infection. Different experimental designs should be considered to uncover the potential effects of azelaic acid on this interaction.

This work illustrated the diversity of molecules produced during infection and highlighted the challenge of interpreting their trends, which are associated with the parasite's developmental stage. It underscores the difficulty of determining the role of these molecules in vitro.

### **Acknowledgments**

We warmly thank different platforms located at the Biological Station of Roscoff, namely the Roscoff Environmental Flow Cytometry and Microfluidics (RECYF) for Flow cytometry analyses, and the Roscoff Culture Collection (RCC) for strain maintenance and distribution. This work was funded by the Agence Nationale de la Recherche ANR-21-CE02-0030-01 (ANR EPHEMER project), and promoted in the frame of the **GDR Phycotox**. MW was supported by a Benjamin Franklin Fellowship (project 464344344), GP and MV were supported by the CRC 1127/2 ChemBioSys (project 239748522), both from the Deutsche Forschungsgemeinschaft (DFG, German Research Foundation).

## References

- Anderson, D.M., Cembella, A.D., Hallegraeff, G.M., 2012. Progress in Understanding Harmful Algal Blooms: Paradigm Shifts and New Technologies for Research, Monitoring, and Management. *Annu. Rev. Mar. Sci.* 4, 143–176. <https://doi.org/10.1146/annurev-marine-120308-081121>
- Bigéard, E., 2022. F/2 medium at 27 PSU of salinity from Sea Red salts (preprint). <https://doi.org/10.17504/protocols.io.n92ldzyrxv5b/v1>
- Bigéard, E., Guillou, L., 2022. F/2 medium added soil extract from estuary water at 27 PSU of salinity v1 (preprint). <https://doi.org/10.17504/protocols.io.dm6qpb9plzp/v1>
- Cai, R., Kayal, E., Alves-de-Souza, C., Bigéard, E., Corre, E., Jeanthon, C., Marie, D., Porcel, B.M., Siano, R., Szymczak, J., Wolf, M., Guillou, L., 2020. Cryptic species in the parasitic *Amoebophrya* species complex revealed by a polyphasic approach. *Scientific Reports* 10, 2531. <https://doi.org/10.1038/s41598-020-59524-z>
- Castro-Moretti, F.R., Gentzel, I.N., Mackey, D., Alonso, A.P., 2020. Metabolomics as an Emerging Tool for the Study of Plant–Pathogen Interactions. *Metabolites* 10, 52. <https://doi.org/10.3390/metabo10020052>
- Chambouvet, A., Morin, P., Marie, D., Guillou, L., 2008. Control of Toxic Marine Dinoflagellate Blooms by Serial Parasitic Killers. *Science* 322, 1254–1257. <https://doi.org/10.1126/science.1164387>
- de Vargas, C., Audic, S., Henry, N., Decelle, J., Mahe, F., Logares, R., Lara, E., Berney, C., Le Bescot, N., Probert, I., Carmichael, M., Poulain, J., Romac, S., Colin, S., Aury, J.-M., Bittner, L., Chaffron, S., Dunthorn, M., Engelen, S., Flegontova, O., Guidi, L., Horak, A., Jaillon, O., Lima-Mendez, G., Luke, J., Malviya, S., Morard, R., Mulot, M., Scalco, E., Siano, R., Vincent, F., Zingone, A., Dimier, C., Picheral, M., Searson, S., Kandels-Lewis, S., Tara Oceans Coordinators, Acinas, S.G., Bork, P., Bowler, C., Gorsky, G., Grimsley, N., Hingamp, P., Iudicone, D., Not, F., Ogata, H., Pesant, S., Raes, J., Sieracki, M.E., Speich, S., Stemann, L., Sunagawa, S., Weissenbach, J., Wincker, P., Karsenti, E., Boss, E., Follows, M., Karp-Boss, L., Krzic, U., Reynaud, E.G., Sardet, C., Sullivan, M.B., Velayoudon, D., 2015. Eukaryotic plankton diversity in the sunlit ocean. *Science* 348, 1261605–1261605. <https://doi.org/10.1126/science.1261605>
- Decelle, J., Kayal, E., Bigéard, E., Gallet, B., Bougoure, J., Clode, P., Schieber, N., Templin, R., Hehenberger, E., Prensier, G., Chevalier, F., Schwab, Y., Guillou, L., 2022. Intracellular development and impact of a marine eukaryotic parasite on its zombified microalgal host. *ISME J* 16, 2348–2359. <https://doi.org/10.1038/s41396-022-01274-z>
- El-Shetehy, M., Wang, C., Shine, M.B., Yu, K., Kachroo, A., Kachroo, P., 2015. Nitric oxide and reactive oxygen species are required for systemic acquired resistance in plants. *Plant Signaling & Behavior* 10, e998544. <https://doi.org/10.1080/15592324.2014.998544>

- Farhat, S., Florent, I., Noel, B., Kayal, E., Da Silva, C., Bigeard, E., Alberti, A., Labadie, K., Corre, E., Aury, J.-M., Rombauts, S., Wincker, P., Guillou, L., Porcel, B.M., 2018. Comparative Time-Scale Gene Expression Analysis Highlights the Infection Processes of Two *Amoebophrya* Strains. *Front. Microbiol.* 9. <https://doi.org/10.3389/fmicb.2018.02251>
- Farhat, S., Le, P., Kayal, E., Noel, B., Bigeard, E., Corre, E., Maumus, F., Florent, I., Alberti, A., Aury, J.-M., Barbeyron, T., Cai, R., Da Silva, C., Istace, B., Labadie, K., Marie, D., Mercier, J., Rukwavu, T., Szymczak, J., Tonon, T., Alves-de-Souza, C., Rouzé, P., Van de Peer, Y., Wincker, P., Rombauts, S., Porcel, B.M., Guillou, L., 2021. Rapid protein evolution, organellar reductions, and invasive intronic elements in the marine aerobic parasite dinoflagellate *Amoebophrya* spp. *BMC Biol* 19, 1. <https://doi.org/10.1186/s12915-020-00927-9>
- Fiehn, O., 2002. Metabolomics — the link between genotypes and phenotypes, in: Town, C. (Ed.), *Functional Genomics*. Springer Netherlands, Dordrecht, pp. 155–171. [https://doi.org/10.1007/978-94-010-0448-0\\_11](https://doi.org/10.1007/978-94-010-0448-0_11)
- Guidi, L., Chaffron, S., Bittner, L., Eveillard, D., Larhlimi, A., Roux, S., Darzi, Y., Audic, S., Berline, L., Brum, J.R., Coelho, L.P., Espinoza, J.C.I., Malviya, S., Sunagawa, S., Dimier, C., Kandels-Lewis, S., Picheral, M., Poulain, J., Searson, S., Tara Oceans Consortium Coordinators, Stemmann, L., Not, F., Hingamp, P., Speich, S., Follows, M., Karp-Boss, L., Boss, E., Ogata, H., Pesant, S., Weissenbach, J., Wincker, P., Acinas, S.G., Bork, P., De Vargas, C., Iudicone, D., Sullivan, M.B., Raes, J., Karsenti, E., Bowler, C., Gorsky, G., 2016. Plankton networks driving carbon export in the oligotrophic ocean. *Nature* 532, 465–470. <https://doi.org/10.1038/nature16942>
- Hallegraeff, G.M., 1993. A review of harmful algal blooms and their apparent global increase. *Phycologia* 32, 79–99. <https://doi.org/10.2216/i0031-8884-32-2-79.1>
- Hasanuzzaman, M., Bhuyan, M.H.M.B., Parvin, K., Bhuiyan, T.F., Anee, T.I., Nahar, K., Hossen, Md.S., Zulficar, F., Alam, Md.M., Fujita, M., 2020. Regulation of ROS Metabolism in Plants under Environmental Stress: A Review of Recent Experimental Evidence. *IJMS* 21, 8695. <https://doi.org/10.3390/ijms21228695>
- Jung, H.W., Tschaplinski, T.J., Wang, L., Glazebrook, J., Greenberg, J.T., 2009. Priming in Systemic Plant Immunity. *Science* 324, 89–91. <https://doi.org/10.1126/science.1170025>
- Kafsack, B.F.C., Llinás, M., 2010. Eating at the Table of Another: Metabolomics of Host-Parasite Interactions. *Cell Host & Microbe* 7, 90–99. <https://doi.org/10.1016/j.chom.2010.01.008>
- Kayal, E., Alves-de-Souza, C., Farhat, S., Velo-Suarez, L., Monjol, J., Szymczak, J., Bigeard, E., Marie, D., Noel, B., Porcel, B.M., Corre, E., Six, C., Guillou, L., 2020. Dinoflagellate Host Chloroplasts and Mitochondria Remain Functional During *Amoebophrya* Infection. *Front Microbiol* 11. <https://doi.org/10.3389/fmicb.2020.600823>
- Kloehn, J., Blume, M., Cobbold, S., Saunders, E., Dagley, M., McConville, M., 2016. Using metabolomics to dissect host–parasite interactions. *Current Opinion in Microbiology* 32, 59–65. <https://doi.org/10.1016/j.mib.2016.04.019>

## Chapter 2

- Lu, Y., Wohlrab, S., Groth, M., Glöckner, G., Guillou, L., John, U., 2016. Transcriptomic profiling of *Alexandrium fundyense* during physical interaction with or exposure to chemical signals from the parasite *Amoebophrya*. *Molecular Ecology* 25, 1294–1307. <https://doi.org/10.1111/mec.13566>
- Marie, D., Simon, N., Guillou, L., Partensky, F., Vaulot, D., 2000. DNA/RNA Analysis of Phytoplankton by Flow Cytometry. *CP Cytometry* 11. <https://doi.org/10.1002/0471142956.cy1112s11>
- Parker, J.E., 2009. The Quest for Long-Distance Signals in Plant Systemic Immunity. *Sci. Signal.* 2. <https://doi.org/10.1126/scisignal.270pe31>
- Pohnert, G., Steinke, M., Tollrian, R., 2007. Chemical cues, defence metabolites and the shaping of pelagic interspecific interactions. *Trends in Ecology & Evolution* 22, 198–204. <https://doi.org/10.1016/j.tree.2007.01.005>
- Poulin, R., Thomas, F., 1999. Phenotypic Variability Induced by Parasites: *Parasitology Today* 15, 28–32. [https://doi.org/10.1016/S0169-4758\(98\)01357-X](https://doi.org/10.1016/S0169-4758(98)01357-X)
- Shibl, A.A., Isaac, A., Ochsenkühn, M.A., Cárdenas, A., Fei, C., Behringer, G., Arnoux, M., Drou, N., Santos, M.P., Gunsalus, K.C., Voolstra, C.R., Amin, S.A., 2020. Diatom modulation of select bacteria through use of two unique secondary metabolites. *Proc Natl Acad Sci USA* 117, 27445–27455. <https://doi.org/10.1073/pnas.2012088117>
- Siano, R., Alves-de-Souza, C., Foulon, E., Bendif, E.M., Simon, N., Guillou, L., Not, F., 2011. Distribution and host diversity of Amoebophryidae parasites across oligotrophic waters of the Mediterranean Sea. *Biogeosciences* 8, 267–278. <https://doi.org/10.5194/bg-8-267-2011>
- Sunda, W., Kieber, D.J., Kiene, R.P., Huntsman, S., 2002. An antioxidant function for DMSP and DMS in marine algae. *Nature* 418, 317–320. <https://doi.org/10.1038/nature00851>
- Szymczak, J., Bigeard, E., Guillou, L., 2023. Use of flow cytometry (Novocyte Advanteon) to monitor the complete life cycle of the parasite *Amoebophrya ceratii* infecting its dinoflagellate host. [www.protocols.io](http://www.protocols.io).
- Vallet, M., Baumeister, T.U.H., Kaftan, F., Grabe, V., Buaya, A., Thines, M., Svatoš, A., Pohnert, G., 2019. The oomycete *Lagenisma coscinodisci* hijacks host alkaloid synthesis during infection of a marine diatom. *Nat Commun* 10, 4938. <https://doi.org/10.1038/s41467-019-12908-w>
- Velo-Suárez, L., Brosnahan, M.L., Anderson, D.M., McGillicuddy, D.J., 2013. A Quantitative Assessment of the Role of the Parasite *Amoebophrya* in the Termination of *Alexandrium fundyense* Blooms within a Small Coastal Embayment. *PLoS ONE* 8, e81150. <https://doi.org/10.1371/journal.pone.0081150>

### Supplementary Data

The results of the correlation test (metabolites) are available with this link :

<https://tinyurl.com/suppthesis>



# Chapter 3 : Chemotaxis of the dinoflagellate parasite towards the chemical cues of its host

## Context of the study

The encounter between the dinospores and the host is essential for the survival of the parasite. The swimming activity of the biflagellate dinospores is clear under the microscope. However, nothing is known about the chemotaxis of dinospores and whether such mechanisms exist. For the first time, we are investigating this using a microfluidic device, the *in situ chemotaxis assay* (ISCA), to test the chemo-attraction of dinospores towards the host chemical extraction form used medium and endo-cellular extract. Although the results are not yet definitive proof of chemotaxis towards the host, this study presents promising results for understanding the pre-initial stage of the infection cycle.

## Authors contribution

I designed the study and adapted the protocol with the help of Estelle Clerc, Jean-Baptiste Raina and Roman Stocker. Estelle Bigeard helped with the maintenance of the stains. I carried out the chemical extraction, the experiments (ISCA) and the data analysis. Laure Guillou helped with the manuscript and interpretation.



## Article 3: Chemotaxis of the dinoflagellate parasite towards the chemical cues of its host

Jeremy Szymczak<sup>1</sup>, Estelle Clerc<sup>2</sup>, Jean-Baptiste Raina<sup>3</sup>, Roman Stocker<sup>2</sup>, Estelle Bigeard<sup>1</sup>, Laure Guillou<sup>1</sup>

<sup>1</sup>Sorbonne Université, CNRS, UMR7144 Adaptation et Diversité en Milieu Marin, Ecology of Marine Plankton (ECOMAP), Station Biologique de Roscoff, 29680 Roscoff, France

<sup>2</sup>Environmental Microfluidics Group, Institute of Environmental Engineering, Department of Civil, Environmental and Geomatic Engineering, ETH Zürich, Zurich, Switzerland

<sup>3</sup>Climate Change Cluster, University of Technology Sydney, Ultimo 2007, NSW, Australia

### Abstract

The survival of an obligate parasite largely depends on its ability to find a suitable host. How parasites find their host is therefore critical to understand their ecology. Some parasites may find their hosts through chemotaxis, i.e. the ability of moving in response to chemical gradients. *Amoebophrya ceratii* is a common marine planktonic parasitoid that infects bloom-forming photosynthetic dinoflagellates. Most strains of this parasite have a narrow host range and rely on their hosts for survival, as they do not feed or reproduce outside the host. Here we evaluated the chemotactic ability of dinospores of a strain of *A. ceratii* infecting the red-bloom forming dinoflagellate *Scrippsiella acuminata*. We used the in situ chemotaxis assay (ISCA) to generate micro-gradients of host's chemicals. As a result, the dinospores showed moderate but significant chemotactic responses. This is the first step to understand how the parasite reach its host to initiate the infection.

### Introduction

Most zoosporic marine parasites release free-living swimmers into the water, where their rapid detection of preferred hosts within a complex planktonic community is crucial

for survival and overall fitness. Chemotaxis, i.e. the process of moving in response to chemical gradients, is an important strategy used by marine microbes (Clerc et al., 2022). However, chemotaxis in microalgae-parasite interactions remains poorly understood. Water-borne chemical signals released from the host can play roles in parasite release (Garcés et al., 2013). On the other hand, water-borne chemical signals released from a parasite can impact the host cyst formation as a defence mechanism against infection (Toth et al., 2004). Parasite exudate in contact with the host triggers modulations of the host transcriptome (Lu et al., 2014). This indicates that chemical communication exists and so that chemotaxis could allow the parasite to locate its host or for the host to enhance resistance within the surrounding populations.

In this study, we explored the chemotaxis capacity of the parasite *Amoebophrya ceratii*, an early-diverging, colourless marine dinoflagellate belonging to the Amoebophryidae (Syndiniales) or Marine Alveolates Group II (Guillou et al. 2008). *Amoebophrya ceratii* is a complex species comprising intracellular parasites that infect other dinoflagellates, especially those forming blooms (Chambouvet et al. 2008; Guillou et al., 2023). The parasite undergoes an alternating life cycle with an endocellular phase involving feeding (trophont stage) and sporulation inside the host cell (sporont stage). Once infection is complete, the parasite exits the host and forms individual swimming cells called dinospores, which actively search for new compatible hosts to infect.

Under laboratory conditions, a single infected host can produce approximately few hundred dinospores, measuring 2-5  $\mu\text{m}$  in size (Coats and Park 2002). Dinospores are motile biflagellate cells capable of surviving for up to ten days, but they are not expected to feed or reproduce. Strains of *Amoebophrya ceratii* produce dinospores with varying phenotypes (see thesis chapter 1). The smallest phenotype, P1, represents the infective form, while the larger P2 phenotype is non-infective and potentially involved in sexual reproduction. Our preliminary findings suggest that newly produced dinospores of *A. ceratii* have flow cytometry signatures that undergo rapid changes, indicating phenotypic modifications within hours to days (see thesis chapter 1). P2 phenotype increases in green fluorescence and decrease in size with time. The final resulting phenotype is called P3 but dinospores in between the P2-P3 gradient coexist and called P23 phenotype.

## Chapter 3

Our experimental approach involved evaluating the chemotactic ability of dinospores at different ages by exposing them to host endometabolites extract and exometabolites extract as potential chemoattractants, compared to fresh medium extract. To achieve this, we conducted laboratory experiments using the *in situ chemotaxis assay* or ISCA (Lambert et al. 2017). The ISCA is a small device comprising 4 rows of 5 wells, each connected to the outside dinospore cultures through a port (Lambert et al., 2017). These wells are filled with the host exo or endometabolites, which diffuses into the surrounding seawater during deployment, creating a chemical microplume above each well. Dinospores have the possibility to respond to this cue through chemotaxis, either swimming into the well if they are attracted or avoiding it in the case of a repellent effect. After deployment, the cells' chemotactic accumulation within each well can be quantified by using flow cytometry for enumeration of the cells in the wells. As our cultures are non-axenic, bacteria were also monitored.

### Materials and methods

#### *Strains and cultures*

The host and parasite cultures were maintained at 20°C. The culture medium is pure water, supplemented with red sea salt (Red Sea) to achieve a salinity of 27‰ and F/2 medium (Guillard's Marine Water Enrichment Solution, Sigma) for nutrients. The cultures were exposed to continuous light conditions, with an approximate intensity of  $100 \mu\text{E m}^{-2} \text{s}^{-1}$  under daylight fluorescent lamp (light bulb Sylvania Aquastar F18W/174). To transfer the host, the 3-4 days old culture was diluted in fresh medium to a ratio of 1/4 v-v. Similarly, the parasite culture was transferred by diluting the 3-4 days old parasite culture with the 3-4 days old host culture to a ratio of 1/4 v-v (parasite-host). The host strain used in this study was *Scrippsiella acuminata* ST147 (RCC1627, <https://roscoff-culture-collection.org/rcc-strain-details/1627>), a photosynthetic dinoflagellate. The parasitic strain used in this study was A120, (RCC4398 (<https://roscoff-culture-collection.org/rcc-strain-details/4398>)).

All the host extracts were processed using the same batch. For that, we prepared 1.1L of naïve (never been in contact with the parasite) healthy host ST147 in an exponential growth phase, with a density of 12 000 cells/mL. This culture was then filtered through

## Chapter 3

a 5 µm pore size nylon filter, for collecting either the endometabolites extract using the >5 µm fraction, and the exometabolites extract using the <5 µm fraction filtrated on a 0.22 µm filtration unit (Millipore).

Before each experiment, the parasite cultures were filtered through a 5 µm pore size nylon filter, the filtrate was collected and the remaining host cells and larger debris were discarded with the filter.

### *Host endometabolites extract*

The cells collected on the filter were resuspended in a fresh sterile culture medium, resulting in a new concentrated host culture of 190 mL at a concentration of 40,000 cells/mL. To extract metabolites from this concentrated host culture, a GF/C filter with a diameter of 25 mm was used to collect the cells. The filter was gently vacuum-filtered, and the collected material was placed in a tube containing 1.5mL of cold methanol (-20°C). This mixture was left overnight at -20°C. The next day, the tube was sonicated for 30 minutes in a sonication bath (Fisher brand). Subsequently the liquid extract was separated from the filter and cell debris through three rounds of centrifugations, each lasting 10 minutes at 10 000 g. The resulting supernatant was carefully transferred to a new 2 mL plastic tube. To obtain dry extracts the solvent was evaporated at 35°C using a glass tube and a vacuum concentrator (SpeedVac, Thermo Scientific). The glass tubes were weighed to determine the precise weight of the dry extracts. Samples were placed at -20°C for storage.

### *Host exometabolites extract*

The filtrate obtained previously was used to prepare the host exometabolites extract. For that it was further purification by passing it through a 0.22 µm filter (threaded Bottle Top Filter, Millipore) to remove any remaining particles. The resulting filtrate was stored at 4°C for 24 hours. Next, the stored filtrate was divided into ten fractions, and each fraction was subjected to solid-phase extraction using a 6cc OASIS HLB sorbent. The solid-phase extraction process involves several steps: conditioning with methanol (5 mL), equilibration with water (5 mL), extraction of sample (approximately 100 mL), salt washing with water (5 mL), and elution with methanol (5 mL). The ten resulting extracts were then pooled and further distributed into nine glass tubes (5.2 mL each) for homogenisation. To obtain dry extracts, the solvent was evaporated at 35°C using a

## Chapter 3

vacuum concentrator (SpeedVac, Thermo Scientific). The glass tubes were weighted to determine the precise weight of the dry extracts. Samples were stored -20°C until used.

### *ISCA*

The original and complete protocol for the use of the ISCA is available in a video format protocol (Clerc et al., 2020). For the ISCA, a fraction of the dinospore culture used for the ISCA was sampled and filtered through a 0.22 µm syringe filter to obtain a particle-free filtrate. This filtrate was then used to dissolve the dry extracts. To achieve this, 0.5 mL of filtrate per mg of extract was added to the tube, resulting in a solution with a concentration of 2 mg/mL. To enhance the solubilisation of the extract, the glass tube filled with the filtrate was sonicated in a sonication bath for 30 min and then further mixed for 5 min with a vortex. The mixture was then filtered again with a 0.22 µm syringe filter to remove any remaining particles. This chemoattractant mix now has a concentration of 2 mg/mL. For the chemotaxis experiments, the chemoattractant was successively diluted with the same parasite filtrate to produce the desired concentrations, which will be loaded into the wells of the ISCA. The negative control was the parasite filtrate only with no dilution of metabolites.

After securing the ISCA device at the bottom of a transparent sterile container, the wells were loaded with prepared chemoattractant solutions using a 27G needle and syringe. The different treatments in the ISCA were placed randomly in the different wells. The entire system was then placed in the usual incubator, alongside the other cultures. Subsequently, the dinospore culture was poured into the container, covering the ISCA platform with approximately 3 cm of liquid on top. A transparent cover was placed over the container. After one hour, the dinospore culture was carefully removed from the container using a 25 mL pipette without disturbing it, each well in the ISCA was sampled using a 27G needle and syringe. Cell densities for each well were measured using a flow cytometer (Szymczak et al., 2023). To enhance the identification and counting of the dinospores, the fresh sample (no fixative) was utilized for cell counting of both P1 and P2. Additionally, the bacteria count was conducted after fixing the samples with 1% glutaraldehyde, diluting them in TRIS buffer, and staining DNA with SYBR Green I.

**Table 3- 1: List of experiments with the conditions and objectives with the ISCA**

Experiments names	Chemoattractants tested	Age of the dinospores	Dinospores densities in cells/mL; percentage of P1	Objectives
Exp. A	Host filtrate extract (SPE)	42h	$1.3 \times 10^6$ 76%	Chemotaxis assay with dinospore culture and <b>healthy host exometabolites extract</b> at final concentrations of 0, $10^{-4}$ , $10^{-2}$ and 1 mg/mL
Exp. B	Host filtrate and fresh culture medium extracts (SPE)	46h	$6.35 \times 10^5$ 85%	Chemotaxis assay with dinospore culture and <b>healthy host exometabolites extract</b> and <b>fresh culture medium extract</b> at final concentrations of 0, $10^{-5}$ , $10^{-2}$ and 1 mg/mL
Exp. C	Host filtrate extract (SPE) and host cell extract	70h	$6.69 \times 10^5$ 99%	Chemotaxis assay with dinospore culture and <b>healthy host exometabolites extract</b> and <b>host cell extract</b> at final concentrations of 0, $10^{-2}$ , $10^{-1}$ and 1 mg/mL
Exp. D	Host filtrate extract (SPE)	36h	$4,5 \times 10^5$ 78%	Chemotaxis assay with dinospore culture and <b>healthy host exometabolites extract</b> at final concentrations of 0, $10^{-2}$ , $10^{-1}$ and 1 mg/mL

## Chapter 3

To calculate the chemotactic index ( $I_c$ ) for each treatment, we compute the mean of the ratios of the cell density in a well filled with metabolites compared to the mean density in the control wells, i.e. the 0 mg/ml treatment which is the filtrate of the tested parasite culture only. An  $I_c$  larger than one indicates the presence of attractive molecules in the treatment, while an  $I_c$  lower than one suggests that the treatment acted as a repellent or caused cell death. Significant difference between the control and the treatment are denoted by an asterisk (\*). The significance is determined using a two-sided T-test, with data assumed to be homoscedastic, and a p value < 0.05.

### *Toxicity assay*

The toxicity assay involved the combination of host extracts with a dinospore culture, with dinospores density being monitored over a 16 hours' period in triplicates in plastic culture tube. The dinospores culture was the same one used in experiment C (ISCA) because in this case,  $I_c$  lower than one were observed. The toxicity assay was done the following day the ISCA experiment. The extracts used for this assay were the same as those used for the ISCA assay, including host cell extract and exometabolites extract. The dry extracts were solubilised using a method similar to the chemoattractant preparation. They were dissolved in the filtrate (0.22  $\mu$ m PES syringe filter) of the dinospore culture, resulting in a stock solution at a concentration of 2 mg/mL extract. After sonication and mixing, the solution was filtered through a 0.22  $\mu$ m syringe filter. The experimental conditions for the toxicity assay were as follows:

- Negative control "0.4": The dinospore culture was mixed with the addition of 20% volume of its own culture filtrate
- Negative control "0.04": The dinospore culture was mixed with the addition of 2% volume of its own culture filtrate
- Endo 0.4: The dinospore culture was mixed with the addition of 20% volume of host endometabolites extract, which have a concentration equivalent to 2 mg/mL, resulting in a final concentration of 0.4 mg/mL in the culture
- Endo 0.04: The dinospore culture was mixed with the addition of 2% volume of host endometabolites extract, which have a concentration equivalent to 2 mg/mL, resulting in a final concentration of 0.04 mg/mL in the culture

## Chapter 3

- Exo 0.4: The dinospore culture was mixed with the addition of 20% volume of exometabolites extract, which have a concentration equivalent to 2 mg/mL, resulting in a final concentration of 0.4 mg/mL in the culture
- Exo 0.04: The dinospore culture was mixed with the addition of 2% volume of exometabolites extract, which have a concentration equivalent to 2 mg/mL, resulting in a final concentration of 0.04 mg/mL in the culture.

## Results

### *Chemotactic indexes and ISCA*

In Figure 3-1, the chemotactic index (Ic) results are presented with for distinct components: total dinospores counts are shown in white, dinospores P1 in light grey, dinospores P23 in darker grey, and the bacteria in black. The error bars represent the standard deviation (+/- SD) and the numbers displayed on the bars indicate the number of replicates.

We conducted four experiments on distinct dates, but all of them used the same preparation of endo- and exometabolites extracted from the same host batch. The parasite cultures were freshly collected; they were of different ages and were collected from different batches, except for experiment C and D, where the same batch of parasites was used with a one-day time difference.

P1 dinospores exhibited attraction to the host exometabolites once at  $10^{-5}$  mg/mL (experiment B) and three times at 1 mg/mL (experiment A, B, and C), while no effect was observed at this concentration in experiment D. Intermediate concentrations ( $10^{-4}$ ,  $10^{-2}$ , and  $10^{-1}$  mg/mL) had no effect. On the other hand, P23 dinospores were attracted only once at  $10^{-2}$  mg/mL during experiment B.

During experiment C, endometabolites tests showed no effect on dinospores at  $10^{-2}$  mg/mL but negatively affected P23 at  $10^{-1}$  and 1 mg/mL, and P1 at 1 mg/mL. In most tests, host metabolites had no effect on bacteria, or they provided antagonistic results. Specifically, Ic was lower than one once: experiment A, exometabolites at  $10^{-4}$  mg/mL and greater than one four times: exometabolites at 1 mg/mL during experiments B and D, endometabolites at 1 mg/mL during experiment C, and medium extract during experiment B.



Chapter 3

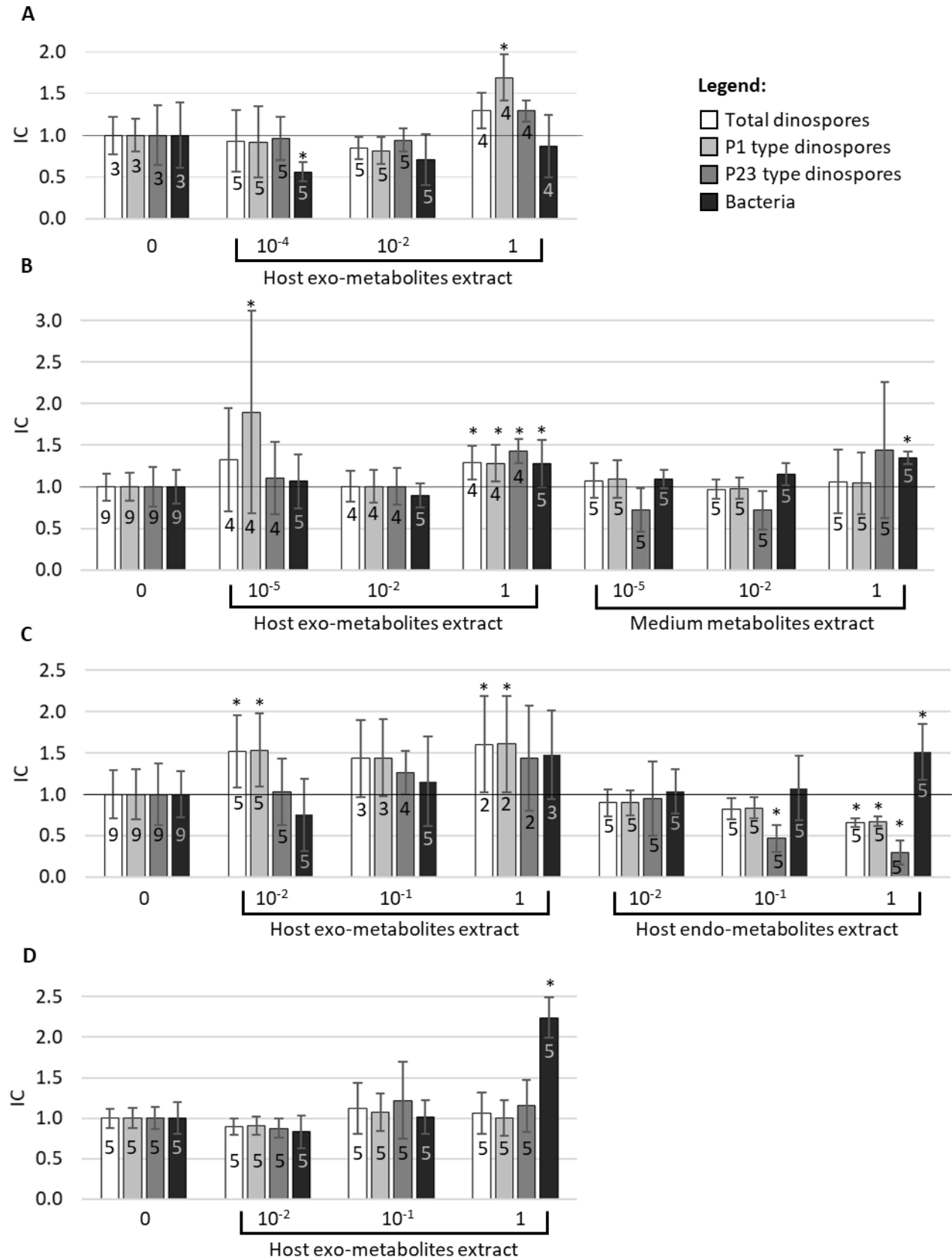


**Figure 3- 1: Chemotactic index (Ic) from the ISCA.**

The putative chemoattractants tested were healthy host endometabolites extract, healthy host exometabolites extracts and fresh culture medium extract at different

## Chapter 3

concentrations indicated below the bars in mg/mL. The parasite cultures contained a mix of both P1 and P23 types dinospores as well as the bacteria from the culture microbiome. The numbers of ISCA wells used for replication are indicated on each bar. The error bars are +/- standard deviation. The asterisks (\*) indicate significant difference compared with negative controls (0) according to t.test (p-value < 0.05). A. Host exometabolites tested at final concentrations of 0, 10<sup>-4</sup>, 10<sup>-2</sup> and 1 mg/mL. B. Host exometabolites and fresh culture medium tested at final concentrations of 0, 10<sup>-5</sup>, 10<sup>-2</sup> and 1 mg/mL. C. Host exometabolites and endometabolites tested at final concentrations of 0, 10<sup>-2</sup>, 10<sup>-1</sup> and 1 mg/mL. D. Host exometabolites tested at final concentrations of 0, 10<sup>-4</sup>, 10<sup>-2</sup> and 1 mg/mL.

The comparison of the  $I_c$  of P1 dinospores with the 1 mg/mL of host endometabolites results to significant difference between experiment A and D where the dinospores were 42h and 36h old respectively (Fig. 3-2). However, in experiment D, no chemotactic response was observed ( $I_c = 1$ ).

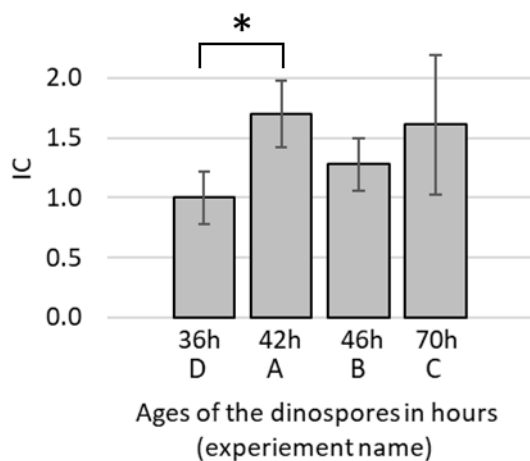


**Figure 3- 2: Comparison of age of dinospores and the  $I_c$  of P1 type dinospores in the 1 mg / mL of host exometabolites treatment in the ISCA experiments**

The asterisks (\*) indicates significant difference between indicated experiments, according to t.test (p-value < 0.05).

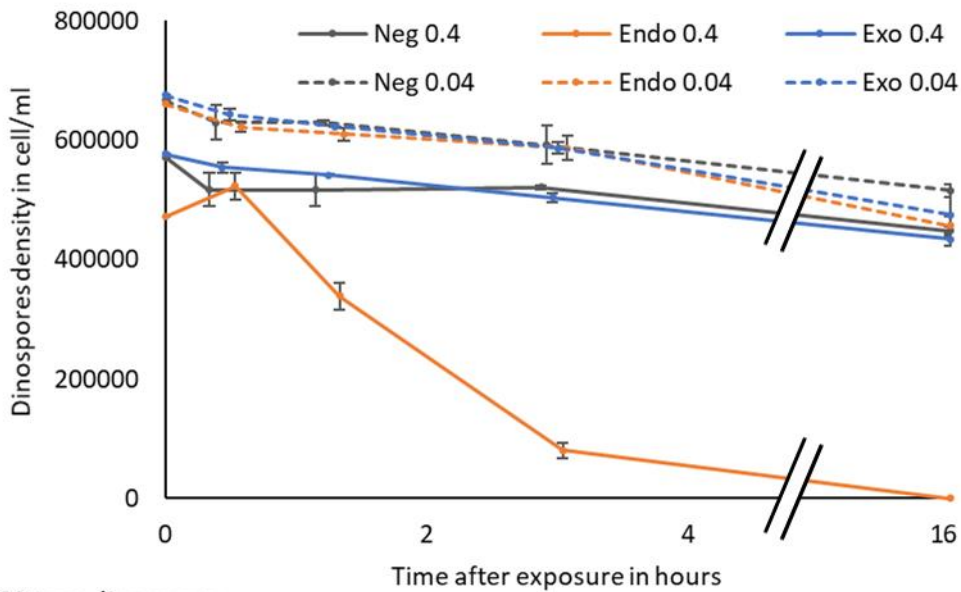
### *Toxicity assays of host extracts on dinospores*

Observations from previous experiments indicated that the host endometabolites had either no effect or a negative effect ( $I_c$  lower than one) on both P1 and P23 dinospores, raising suspicions of a potentially lethal effect on dinospores at certain concentrations. To investigate this hypothesis, we conducted a toxicity experiment using the host metabolites on a mixed culture of dinospores (with varying concentrations and ages) over a 16-hour period after mixing (Fig. 2-3). The results suggest that only the host endometabolites extract exhibit lethality, leading to a significant and rapid decline in cell density after a short period of contact. Specifically, P1 cells experience cell death at a concentration of 0.4 mg/mL, while P23 cells are affected at both 0.4 and 0.04

### Chapter 3

mg/mL. This suggests that P23 cells are even more sensitive to the host endometabolites extract compared to P1 cells.

#### A P1 type dinospores



#### B P23 type dinospores

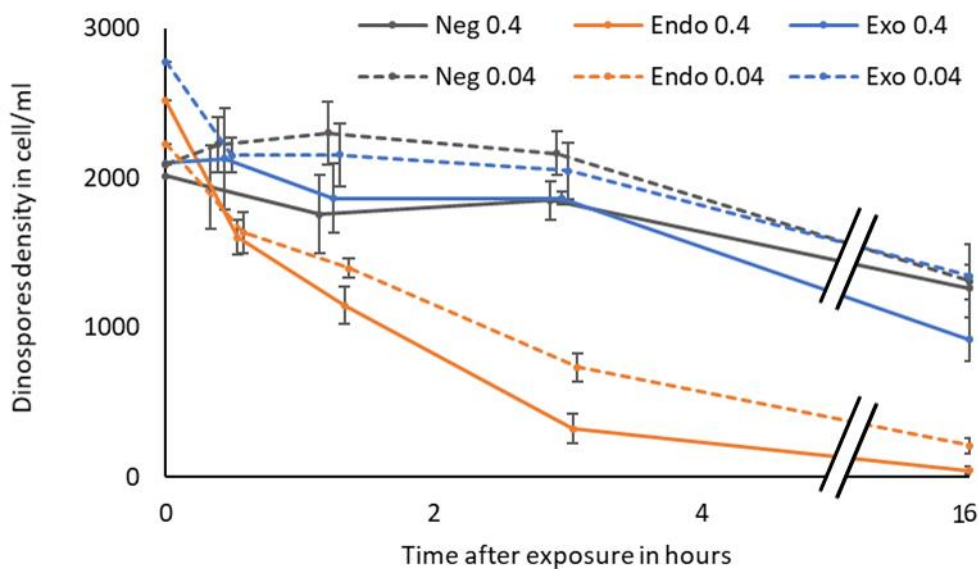


#### Figure 3- 3: Toxicity assays

A. dinospores P1 (upper panel) and B. P23 (lower panel) using of host exometabolites extract (Exo) in blue and host endometabolites (Endo) extract in orange, and compared to the dinospore's culture filtrate used as control (Neg) in black. Experimental tests were conducted in triplicates. The error bars are +/- the standard deviation. The curves represent the dinospore counts over time when mixed with various concentrations of substrates: solid line for the 5X dilution (0.4 mg/ml of extract) and dotted line for the 50X dilution of the stock solution (0.04 mg/ml of extract).

### Discussion

#### *Chemotaxis of the parasite towards the host signals*

The results of our study demonstrate significant variability in the  $I_c$  values, with both low and occasional high values up to 1.9 (Fig. 2-2). While the hypothesis of chemical attraction is not fully confirmed, it is not completely rejected either, suggesting that the interaction between the host exometabolites and dinospores is more complex than a simple on-off reaction.

To address potential sources of variability, we standardized the extraction of the host exometabolites from the same host culture. However, differences in parasite batches, age, and physiology could still contribute to the observed variations in responses. The observed phenotypical changes in P1 dinospore infectivity over time, as detected through flow cytometry, indicate a possible correlation between these changes and modifications in their chemotactic behaviour, warranting further investigation. Interestingly, we found that age of the dinospores does not show a simple correlation with the level of chemotactic behaviour in P1 dinospores when exposed to the host endometabolites (Fig. 2-2). This suggests that other physiological processes, not considered in our study, may play a crucial role in the chemotactic capacity of P1 dinospores, contributing to the observed variability in responses. Similar complex maturation systems have been observed in other models, such as human sperm, where capacitation is essential for chemotaxis during fertilization (Cohen-Dayag et al., 1995).

Methodological factors may also contribute to the variability in our results. The use of a single extraction method (SPE and elution with 100% methanol) to produce the host exometabolites chemoattractant could potentially exclude specific cues, leading to a partial representation of the exometabolites. Additionally, the resuspension method used for preparing the chemoattractant loaded in the wells may also exclude certain metabolites present in the dry extract. The choice of solvents and resuspension media may influence the outcome of the chemotactic assays. Furthermore, the observed high variability may also be influenced by the low concentration of dinospores, which might be close to the detection limit of the flow cytometer. At such low concentrations, statistical support for observed trends may be limited, leading to greater variability in the data.

## Chapter 3

Despite the challenges and sources of variability in our study, we consistently observed a chemical attraction for P1 dinospores compared to P23 dinospores, particularly at 1 mg/mL exometabolites concentrations. These findings confirm distinct behavioural differences between the two types, supporting the existence of phenotypic distinctions.

In a previous section (see thesis chapter 1), we observed significant variations in the swimming behaviour of P1 and P23 dinospores. P1 dinospores displayed directed swimming, while P23 dinospores exhibited a more random, dancing-like movement, resulting in shorter distances travelled by P23 dinospores. These differences in swimming behaviour may mechanistically contribute to the observed disparity in chemotactic responses between the two phenotypes. A longer incubation time in future experiments could provide valuable insights into this aspect. By allowing dinospores more time to interact with the host exometabolites, we may better understand how their distinct swimming behaviours influence their response to chemical attractants.

### *The effect of host cell extract on dinospores survival*

The  $IC_{50}$  and toxicity tests indicate that the host endometabolites content contains lethal molecules that can affect both P1 and P23 dinospores at a certain concentration. It appears that these molecules are generated within the host cell and are not actively exported outside, or if they are released, they become too diluted to exert a significant effect beyond the host cell. These molecules might be part of the host's resistance strategy against the parasitic infection.

The parasitic organism *Amoebophrya ceratii* has evolved a protective mechanism during its entry into the host cytoplasm. It forms a parasitophorous membrane that persists throughout its journey until it reaches the host nucleus, where the membrane is lost upon crossing the nuclear membrane. This strategy likely plays a critical role in the parasite's survival, helping it to withstand the impact of the lethal intracytoplasmic molecules produced by the host.

Alternatively, the intracellular molecules sensed by the dinospores could serve as triggers for initiating the infection process or inducing drastic phenotypical changes in the dinospores, such as dormancy or programmed cell death. These marked phenotypical changes might make the dinospores unsuitable for survival in the external

## Chapter 3

medium, which could explain their dependence on the host environment for continued survival.

In conclusion, the presence of lethal molecules in the host endometabolites content, the formation of a parasitophorous membrane by *Amoebophrya ceratii*, and the potential role of intracellular molecules in triggering infection and phenotypical changes in dinospores are intriguing observations. Further research is required to gain a comprehensive understanding of the underlying mechanisms driving these processes.

### *Chemotaxis of the bacteria towards the host signals*

Indeed, higher variability in bacterial attraction or repulsion responses to host metabolites was observed. These results are not surprising, especially when dealing with complex communities of bacteria. The diversity of bacteria in such communities can lead to a wide range of behavioural responses, contributing to the observed variability in experimental outcomes.

To gain a better understanding of the chemosensitivity of specific bacteria to host extracts, DNA/RNA based analyses can be valuable tools. Metabarcoding and QPCR allow for the identification and quantification of various bacterial species present in a sample based on specific genetic markers, such as 16S rRNA gene sequences. By analysing the species composition in response to different host extracts, researchers can discern which bacteria are more chemosensitive or responsive to particular host metabolites. This approach may reveal patterns in bacterial attraction or repulsion and shed light on how different bacterial species interact with the host endo- and exometabolites. Understanding the specific chemosensitivity of different bacteria can aid in deciphering the complex dynamics of host-parasite interactions and provide insights into the mechanisms underlying the observed variability in the experimental results.

### **Conclusion**

Despite the various challenges and methodological considerations, our study provides interesting evidence of potential higher chemical attraction of P1 dinospores compared to P23 dinospores to the host exometabolites. We also observed the lethality of the host endometabolites, which adds to our understanding of the host-parasite

## Chapter 3

interaction. Additionally, the variability in the bacterial community further highlights the complexity of the system.

To gain a deeper understanding of the underlying mechanisms driving potential chemotaxis, further research is needed. Addressing potential limitations in experimental design, such as increasing the density of dinospores and extending the incubation period, may help reduce the observed variability and provide more robust results. It is also important to consider that chemical sensing might be linked to rapid phenotypical changes in the dinospores, which were not monitored in this study. Therefore, exploring the correlation between the acquisition of the apical complex system and infectivity capacity with chemotaxis capacity could provide valuable insights into the dynamics of the system. In summary, our study opens up intriguing avenues for future research and emphasizes the need for comprehensive investigations into the chemotactic behaviour of dinospores and its underlying mechanisms. Addressing these questions will contribute to refining our understanding of the complex interactions between host exometabolites, bacterial community, and dinospore chemotaxis in the context of *Amoebophrya ceratii* parasitism.

### Acknowledgments

We warmly thank different platforms located at the Biological Station of Roscoff, namely the Roscoff Environmental Flow Cytometry and Microfluidics (RECYF) for Flow cytometry analyses, the Roscoff Culture Collection (RCC) for strain maintenance and distribution and the Mass spectrometry platform (METABOMER) for the advises and material. This work was funded by the Agence Nationale de la Recherche ANR-21-CE02-0030-01 (ANR EPHEMER project), and promoted in the frame of the **GDR Phycotox**. We also thank Eléna Kohler for her help during her internship with the team.

### References

- Chambouvet, A., Morin, P., Marie, D., Guillou, L., 2008. Control of Toxic Marine Dinoflagellate Blooms by Serial Parasitic Killers. *Science* 322, 1254–1257. <https://doi.org/10.1126/science.1164387>
- Clerc, E.E., Raina, J.-B., Lambert, B.S., Seymour, J., Stocker, R., 2020. In Situ Chemotaxis Assay to Examine Microbial Behavior in Aquatic Ecosystems. *JoVE* 61062. <https://doi.org/10.3791/61062-v>
- Clerc, E.E., Raina, J.-B., Peaudecerf, F.J., Seymour, J.R., Stocker, R., 2022. Survival in a Sea of Gradients: Bacterial and Archaeal Foraging in a Heterogeneous

- Ocean, in: Stal, L.J., Cretoiu, M.S. (Eds.), *The Marine Microbiome, The Microbiomes of Humans, Animals, Plants, and the Environment*. Springer International Publishing, Cham, pp. 47–102. [https://doi.org/10.1007/978-3-030-90383-1\\_2](https://doi.org/10.1007/978-3-030-90383-1_2)
- Coats, D.W., Park, M.G., 2002. Parasitism of Photosynthetic Dinoflagellates by Three Strains of *Amoebophrya* (dinophyta): Parasite Survival, Infectivity, Generation Time, and Host Specificity<sup>1</sup>. *Journal of Phycology* 38, 520–528. <https://doi.org/10.1046/j.1529-8817.2002.01200.x>
- Cohen-Dayag, A., Tur-Kaspa, I., Dor, J., Mashiach, S., Eisenbach, M., 1995. Sperm capacitation in humans is transient and correlates with chemotactic responsiveness to follicular factors. *Proc. Natl. Acad. Sci. U.S.A.* 92, 11039–11043. <https://doi.org/10.1073/pnas.92.24.11039>
- Garcés, E., Alacid, E., Reñé, A., Petrou, K., Simó, R., 2013. Host-released dimethylsulphide activates the dinoflagellate parasitoid *Parvilucifera sinerae*. *ISME J* 7, 1065–1068. <https://doi.org/10.1038/ismej.2012.173>
- Guillou, L., Szymczak, J., Alves-de-Souza, C., 2023. *Amoebophrya ceratii*. *Trends in Parasitology* 39, 152–153. <https://doi.org/10.1016/j.pt.2022.11.009>
- Guillou, L., Viprey, M., Chambouvet, A., Welsh, R.M., Kirkham, A.R., Massana, R., Scanlan, D.J., Worden, A.Z., 2008. Widespread occurrence and genetic diversity of marine parasitoids belonging to *Syndiniales* (*Alveolata*). *Environmental Microbiology* 10, 3349–3365. <https://doi.org/10.1111/j.1462-2920.2008.01731.x>
- Lambert, B.S., Raina, J.-B., Fernandez, V.I., Rinke, C., Siboni, N., Rubino, F., Hugenholtz, P., Tyson, G.W., Seymour, J.R., Stocker, R., 2017. A microfluidics-based in situ chemotaxis assay to study the behaviour of aquatic microbial communities. *Nat Microbiol* 2, 1344–1349. <https://doi.org/10.1038/s41564-017-0010-9>
- Lu, Y., Wohlrab, S., Glöckner, G., Guillou, L., John, U., 2014. Genomic Insights into Processes Driving the Infection of *Alexandrium tamarense* by the Parasitoid *Amoebophrya* sp. *Eukaryot Cell* 13, 1439–1449. <https://doi.org/10.1128/EC.00139-14>
- Szymczak, J., Bigeard, E., Guillou, L., 2023. Use of flow cytometry (Novocyte Advanteon) to monitor the complete life cycle of the parasite *Amoebophrya ceratii* infecting its dinoflagellate host. [www.protocols.io](http://www.protocols.io).
- Toth, G.B., Norén, F., Selander, E., Pavia, H., 2004. Marine dinoflagellates show induced life-history shifts to escape parasite infection in response to water-borne signals. *Proc. R. Soc. Lond. B* 271, 733–738. <https://doi.org/10.1098/rspb.2003.2654>

### Supplementary Data

The raw data and the calculation for ISCA are available with this link:

<https://tinyurl.com/suppthesis>





# General discussion

## Personal motivation and origin of the project

In 2016, I wanted to find out what fundamental research on marine plankton was like by doing an internship. I discovered the Biological Station of Roscoff and I literally fell in love with the *Amoebophrya* model. I learnt how to grow a collection of *Amoebophrya* and photosynthetic dinoflagellate host strains. I was also trained to use a microscope to observe natural samples of plankton (mainly protists) in order to identify and count the main local species. This first experience fully motivated my future choices. I decided to complement my knowledge of biology with a Master's degree in oceanography to learn more about the environment of marine organisms. I also decided to learn more and focus my research on the interactions of marine microbes. During my Master's degree, I did a first internship looking at host-parasite interactions in samples from off the coast of Chile, and a second internship reconstructing the metabolic pathways of *Amoebophrya ceratii* and a few dozen other alveolate species. Most importantly, I persisted with the study of *Amoebophrya* parasites. They are important players in the ocean, very few laboratories currently have strains, and the largest strain collection in the world is in Roscoff. Their natural green fluorescence is really fascinating; in addition to the red fluorescence of the host due to chlorophyll, it is a great way to understand the state of infection *in vivo*. Against the black background of the epifluorescence microscope, the dinospores, vermiforms, healthy and infected hosts are perfectly distinguishable. The host-parasite interaction is clearly visible, as is the growth of the parasite inside its host. The origin and role of this natural green fluorescence is unknown. Such a feature must have been selected for a good reason, but for now it remains a complete mystery. However, it is very convenient in the laboratory for maintaining the stain and this allows the complete life cycle to be followed by flow cytometry (see chapter one). Another remarkable aspect is how the parasite can keep its host alive while its biomass is converted into parasite biomass within a few hours. The parasite is able to use the energy machinery of the host while the host nucleus is completely digested and the parasite grows (Decelle et al. 2022). With flow cytometer, infected cells appear bigger (higher FSC) than the healthy hosts. This is the sign that the parasite expands and causes the host to enlarge. The red fluorescence from the chlorophyll in infected hosts, even at late stage, is relatively strong, just a bit

## General discussion

lower than healthy hosts. This is due to the fact that until the parasite is released, the chloroplasts are functional in the host (Kayal et al. 2020). The parasite exploits the host's energy production and, after killing it as the infected host swims to the final instant, the parasite is released in the proximity of compatible surrounding hosts.

In 2018, after graduation, I decided to write a PhD project under the supervision of Dr. Laure Guillou with who I had the opportunity to work in Roscoff since my first internship. In my new project, I wanted to learn new skills and have a strong scientific collaboration with a new research team. I wanted to conduct laboratory work and learn more about the *Amoebophrya*-host interaction. I focused my project on chemical interactions and chemical ecology and metabolomics became new challenges. Dr. Marine Vallet and Pr. Georg Pohnert in Jena, Germany, allowed me to learn how to use metabolomics to study host-parasite interactions in a new way in my thesis project.

### **The progress of my PhD thesis: a journey filled with challenges and opportunities.**

Initially, we planned to compare the interactions between several pairs. We selected two strains of photosynthetic dinoflagellates host of three types of parasites. Very rapidly, I realized that the amount of work to study only one parasite strain infecting one host strain was enough for an entire thesis project. In addition, a few months after I started my PhD in November 2019, the COVID-19 crisis hit the world and, I had to stop my laboratory experiments. At my return in 2020, it has been difficult to started again experiment because the cultures have to be produced relatively long before the experiment to get enough volume. During that time, however, I collaborated with Marc Long, Cecile Jauzein and collaborators in IFREMER of Brest (team DYNECO “dynamics of coastal ecosystems”) to explore the allelopathic effect of the toxic dinoflagellate *Alexandrium minutum* on the infection dynamics of *A. ceratii* infecting *Scrippsiella acuminata* (Long et al., 2021). We observed that *A. minutum* had a protective effect on *S. acuminata* by reducing the dinospores density. *A. ceratii* dinospores were sensitive to the toxin of *A. minutum* in contrast to its host *S. acuminata*. As a result, the presence of *A. minutum* reduced the parasite infection and finally benefit to *S. acuminata*. The results are presented in the scientific article in the thesis supplementary documents 1.

## General discussion

In 2021, after a chaotic year, I finally came back full time to the laboratory. At this moment, my objective was to optimise the culture condition in order to produce close to 100% prevalence in order to produce synchronous cultures for metabolomic analyses. In standard conditions, a certain proportion of the host do not get infected after the inoculation, and a second wave of infection is necessary to have 100% of host infected. Consequently, healthy and infected cells at different stages coexist in the culture flask. To obtain 100% of host infected at the first generation, I tested a combination of host and parasite of different ages as well as different host:parasite ratios. By doing that, I drastically increased the number of dinospore in the inoculum compared to the host, and I followed infections over several generations. Interestingly, in some cases, even with an enormous number of dinospores per host cell, I obtained no infection of the host. At that time, a new flow cytometer, the Novocyte Advanteon, with a better sensitivity, was acquired by the laboratory but most importantly, it was able to detect a wide range of size and fluorescence, as the host has a relatively larger size compared to dinospores unlike the previous one, the BD FACSAria III Cell Sorter. In addition, this flow cytometer was able to detect the red fluorescence and the green fluorescence, simultaneously. In the same cytogram, both host and parasite populations were visualised for the first time. It is now possible with flow cytometry to distinguish healthy from infected host and even possible to distinguish intermediate and late stage of infection, possibly corresponding to trophont stage (intermediate) and sporont stage (late), like it is discussed in chapter one. This is a very convenient method to obtain an infection prevalence: it takes one minute which is way quicker than the older traditional CARD-FISH method that takes about 24h with at least 5h of manipulation. To share this useful development of the flow cytometry method, I published a detailed protocol, which can be seen in the thesis supplementary (documents 2). For the first time, it was possible to visualise the parasite growth inside its host, and clearly visualised different dinospore populations, having different sizes and fluorescence intensities. The variety of dinospore sizes was considered as different stages of mitotic divisions following sporulation. Indeed, when the parasite is released, the vermiform is a colony-like of future dinospores and it was believed that the last parasite division occurred out of the host cell. I discovered that it was not the case: at least two dinospores existed with different final size and fluorescence. On the other hand, the host's green fluorescence gradually increases along the course of the

## General discussion

infection. When the hosts were highly green, these cells correlated with the dinospores production

In the case of the culture with a high dinospore-host ratio but with no infection, it was interesting to notice that only the larger and more fluorescent dinospores were present in the inoculum. After reporting and analysing other cases, I discovered that this specific morphotype was not infectious and has actually a different phenotype. These results motivated me to focus on the characterisation of the different dinospores phenotypes and deviate a little from my first PhD plan.

By chance, the laboratory acquired a new cell sorter flow cytometer, the Aurora CS Cytex in November 2022. This new instrument also allows to visualise a host-parasite culture, distinguishing the different cell types. The cell sorting was convenient for the confirmation of the identity of the different cell populations on the cytogram and allows to sort cells and their used for transcriptomic method to explore the gene expression of the different cell types (see chapter one). Due to technical limitations, we were unable to generate actual single cells but deposited 10 dinospores and 20 host cells per well. Nonetheless, we have intentions to improve the protocol and perform single cell transcriptomics at the end of 2023.

In 2022, I participated to the Jacques Monod conference entitled 'From Parasites to Plankton and Back: Comparative Biology and Ecology of Apicomplexans and Dinoflagellates' held in Roscoff. I found it quite interesting to bring together the scientific communities interested in marine parasites and those interested in human and animal parasites, both belonging to the same large phylogenetic group (Myzozoan). I presented my new thesis results to a large and very attentive audience. Also, I had the opportunity to assist in this conference coordinating and to contribute to a conference report article included in the supplement to this thesis (Thesis supplementary documents 3).

Finally, in 2022, I was invited to participate in producing a brief article outlining the essential features of this organism, or rather this species complex with all novel findings from these last 20 years, to raise awareness within the scientific community (Thesis supplementary documents 4).

**The major discoveries I made during my thesis and perspectives.**

About the sexual reproduction, Jean Cachon yet related in 1964 both polymorphisms and variations in size within dinospores. He also noticed that size differences are sometimes linked with the host sizes but did not explained completely this polymorphism. Cachon wrote that the most common dinospore has a roundish epitheca and an elongated hypotheca but some individuals have a spherical morphology. The variability described by Cachon could be due to the diversity of *A. ceratii* that is actually a species complex, since he was observing natural samples. Moreover, it is interesting to notice that the description of elongated and spherical dinospores by Cachon can correspond to P1 type dinospores that are more elongated and P2 type dinospore that are bigger and rounder. The description of different spore phenotypes also occurs in the parasite *Ichthyodinium* (MALV I) infecting fish egg/larva. Here, different morphotypes correspond to different stage of division (Shadrin et al., 2015). Also, in *Euduboscquella* (MALV I) infecting tintinnids, there are three types of spores and the syngamy of macro- and micro-spores has been observed (Coats et al 2012). However, the description of P1 and P2 in an *A. ceratii* monoclonal strain is novel. The role of P1 is clear with the infection of the host. In contrast to P1, P2 lacks apical complex-like according to TEM imaging and mixing P2 and the host does not cause any infection. In addition, P2 transcriptome is characterised by overexpression of genes related to meiosis and metabolic pathways linked to DNA synthesis and replication. The transcriptome and metabolome (from chapter one and two) results will be made available in online databases (to be deposited). In the light of all these elements, P2 is hypothesised to be involved in sexual reproduction like it is discussed in chapter one. However, we lack the ultimate proof for sexual reproduction. Unfortunately, we did not measure various levels of ploidy, neither higher in the instance of fused cells. Also, we did not observe actual cell fusion and/or bigger cells with additional flagella like it is observed in the case of the sexual reproduction in other dinoflagellates, where both of the two longitudinal flagella are retained. However, we supposed that *A. ceratii* is heterothallic because we did not observe fusing and 2N cells in clonal strains. Meanwhile even after mixing the strains with putative compatible dinospores, not fusion was observed. It could be due to the fact that laboratory conditions do not allow sexual reproduction even in the case of homothallism or because the stains we mixed were not compatible and/or the laboratory conditions

## General discussion

were not favourable. Further experimentation would really be worthwhile, under different conditions and with more combinations of strains. Infected host seems to produce either P1 or P2. The question is: at what point is the production of one dinospore type decided? The transcriptomes and metabolomes of the dinospores exhibit clear differences; can we track back these differences during the trophont and sporont stages? We are currently testing the experimental conditions presented in Chapter one to produced preferentially P2 dinospores. In December 2023, experiments will be conducted to sort infected single cells and analysed their transcriptome This approach should provide insight into the processes responsible for yielding either type.

In chapter two, I observed that the host incubated with parasite exudates might increase its resistance to *A. ceratii* knowing that more replication and different priming techniques must validate this hypothesis. The co-culture system would be a tool to monitor during several days the modification of the host sensitivity while continuously receiving exudates of an infected host culture from the opposite compartment. I personally tested a co-culture system with physical separation between two compartments made of a porous membrane blocking the cells but allowing the metabolites to flow (Paul et al., 2013). Even though this tool has finally not been used in this thesis, I have observed that this system is suitable for experimentations. Indeed, the host is able to grow and the parasite is able to infect the host. This is a promising tool to study priming effect on the host or on the parasite. A repertoire of metabolites produced along the infection was produced during my PhD. Plus, in our experimental condition, the samples are characterised by different level of prevalence and different percentages of produced P1 and P2. Those biological variability allows to formulate hypothesis on the role of some metabolites following different correlation between intensities and prevalence or percentage of P1. To test the putative role and activities, we developed bioassay with the metabolites azelaic acid. Even though more replications and some improvement would be needed to detect more clear effect, this protocol is suitable to test a series of putative bioactive metabolites already identified.

In chapter three, I observed that the parasite chemotaxis capacity seems to be involve in the host infection. If this capacity is true, the next step would be to identify the metabolite(s) involved. Are these molecules specific to the host strains or more

## General discussion

generalist? If P1 is able to detect the host, is P2 able to detect compatible cells to initiate sexual reproduction? To do so, experimentation with ISCA could be suitable (chapter three). The wells can be loaded with a large variety of diffusive molecules and putative host kairomones or parasite pheromones can be found in the metabolomes. Plus, lethal activity from the host cellular extract has been observed. To better understand the bioactivity and molecular interaction between the host and the parasite, the identification of those molecules is needed. An alternative method is the bioassay-guided fractionation where for example, the metabolites of a culture exudate with a biological activity is separated into multiple fractions and each fraction is tested. Additional separation steps of the active fraction(s) can be done until few or even only one chemical is present in the active fraction. However, this approach may be time-consuming and require a considerable amount of culture. Also, it is possible to obtain false positive and false negative (Houssen and Jaspars, 2012). Further comparative metabolomics investigations would assist in identifying metabolites for future bioassays.

## Conclusions

This study provides new insight into the biology of a widespread but still overlooked parasite. The description of different dinospores allows a better understanding of the life cycle of *Amoebophrya ceratii*, we have strong hypotheses on sexual reproduction, although the final proof is still needed. It would be beneficial to have full laboratory control over the production of P1 and P2 for future research, including the microscopic examination of P1, P2, and the more elusive P3, which has a short lifespan and lower density due to high mortality rate. Single-cell like transcriptomics and metabolomics of the host and parasite provide useful data, but limitations arise from the lack of gene and metabolite annotation. Further exploration can enhance our understanding.

This work opens up a number of perspectives. Previous research included genomic data (Cai et al., 2020; Farhat et al., 2021), while our study incorporates transcriptomics and metabolomics and lipidomics analyses are ongoing. A proteomics approach could potentially enhance our investigations. Indeed, proteins also play roles in bioactivity directly or being involved in secondary metabolites (Palazzotto and Weber, 2018). That's why, the study of proteins composition, production and regulation is useful to better understand species interaction.



## General discussion

For the study of *A. ceratii* in this project, we utilized the A120 strain. However, we also have a range of strains available for comparison at Roscoff, which could offer insight into the specificity of our findings. Our preliminary results suggest that a vast majority—if not all—of the strains produce P1, P2, and P3. In the presence of a homothallic strain, it would be possible to observe syngamy as direct evidence of sexual reproduction. Also, we observed that the saturation of the host with P1 dinospores that leads to an increased number of coinfection, might have an effect on the infection dynamics and the production of P2 dinospores. More experimentations need to be done to determine if sexual reproduction might occur in the host cell.

Field studies of this parasite in its natural environment are highly appealing. However, distinguishing *Amoebophrya* species or even subspecies of *A. ceratii* seems difficult as they are morphologically very similar. To address this issue, one possible approach is to use probes for CARD-FISH. Nevertheless, this method necessitates meticulous manipulation and can only be carried out on fixed samples.

New approach as the miniature microfluidics system also called lab-on-chip (LOC) is very promising for the exploration of marine protists (Hamon et al., 2015). The use of LOC demands less culture volume and less reagent in the case of bioassay. This can reduce the cost of the experiment but most importantly, LOC allow to work at single cell level. We could imagine to test bioactivity of selected exudate or metabolites on host or parasite cell and based on the phenotypical responses of behavioural response, select individuals and proceed to single cell transcriptomics of metabolomics to decipher the biological mechanisms. As well, the selection of particular cell based on specific responses can be interesting to acquire microscopic images to explore the associate cellular ultrastructure.

Finally, studying *A. ceratii* could provide insights into sexual reproduction, chemical communication, host interactions, and the modulation of virulence. Production of P2 has been found to decrease the overall percentage of infective parasites, and comparisons of naive versus primed hosts can shed light on host defence. There are still technical limitations, but the advancement of flow cytometry and microfluidics has enabled the removal of some of these obstacles and will continue to do so in the future.

## References

- Cachon, J., 1964. Contribution à l'étude des péridiniens parasites. Cytologie, cycles évolutifs. Ann. Sci. Nat. Zool. 1–158.
- Cai, R., Kayal, E., Alves-de-Souza, C., Bigeard, E., Corre, E., Jeanthon, C., Marie, D., Porcel, B.M., Siano, R., Szymczak, J., Wolf, M., Guillou, L., 2020. Cryptic species in the parasitic *Amoebophrya* species complex revealed by a polyphasic approach. Scientific Reports 10, 2531. <https://doi.org/10.1038/s41598-020-59524-z>
- Coats, D.W., Bachvaroff, T.R., Delwiche, C.F., 2012. Revision of the Family Duboscquellidae with Description of *Euduboscquella crenulata* n. gen., n. sp. (Dinoflagellata, Syndinea), an Intracellular Parasite of the Ciliate *Favella panamensis* Kofoid & Campbell, Journal of Eukaryotic Microbiology 59, 1–11. <https://doi.org/10.1111/j.1550-7408.2011.00588.x>
- Decelle, J., Kayal, E., Bigeard, E., Gallet, B., Bougoure, J., Clode, P., Schieber, N., Templin, R., Hehenberger, E., Prensier, G., Chevalier, F., Schwab, Y., Guillou, L., 2022. Intracellular development and impact of a marine eukaryotic parasite on its zombified microalgal host. ISME J 16, 2348–2359. <https://doi.org/10.1038/s41396-022-01274-z>
- Farhat, S., Le, P., Kayal, E., Noel, B., Bigeard, E., Corre, E., Maumus, F., Florent, I., Alberti, A., Aury, J.-M., Barbeyron, T., Cai, R., Da Silva, C., Istace, B., Labadie, K., Marie, D., Mercier, J., Rukwavu, T., Szymczak, J., Tonon, T., Alves-de-Souza, C., Rouzé, P., Van de Peer, Y., Wincker, P., Rombauts, S., Porcel, B.M., Guillou, L., 2021. Rapid protein evolution, organellar reductions, and invasive intronic elements in the marine aerobic parasite dinoflagellate *Amoebophrya* spp. BMC Biol 19, 1. <https://doi.org/10.1186/s12915-020-00927-9>
- Hamon, M., Dai, J., Jambovane, S., Hong, J.W., 2015. Microfluidic Systems for Marine Biotechnology, in: Kim, S.-K. (Ed.), Springer Handbook of Marine Biotechnology, Springer Handbooks. Springer, Berlin, Heidelberg, pp. 509–530. [https://doi.org/10.1007/978-3-642-53971-8\\_20](https://doi.org/10.1007/978-3-642-53971-8_20)
- Houssen, W.E., Jaspars, M., 2012. Isolation of marine natural products. Methods Mol Biol 864, 367–392. [https://doi.org/10.1007/978-1-61779-624-1\\_14](https://doi.org/10.1007/978-1-61779-624-1_14)
- Kayal, E., Alves-de-Souza, C., Farhat, S., Velo-Suarez, L., Monjol, J., Szymczak, J., Bigeard, E., Marie, D., Noel, B., Porcel, B.M., Corre, E., Six, C., Guillou, L., 2020. Dinoflagellate Host Chloroplasts and Mitochondria Remain Functional During *Amoebophrya* Infection. Front Microbiol 11. <https://doi.org/10.3389/fmicb.2020.600823>
- Long, M., Marie, D., Szymczak, J., Toullec, J., Bigeard, E., Sourisseau, M., Le Gac, M., Guillou, L., Jauzein, C., 2021. Dinophyceae can use exudates as weapons against the parasite *Amoebophrya* sp. (Syndiniales). ISME COMMUN. 1, 34. <https://doi.org/10.1038/s43705-021-00035-x>

## General discussion

- Palazzotto, E., Weber, T., 2018. Omics and multi-omics approaches to study the biosynthesis of secondary metabolites in microorganisms. *Current Opinion in Microbiology, Antimicrobials \* Microbial systems biology* 45, 109–116. <https://doi.org/10.1016/j.mib.2018.03.004>
- Paul, C., Mausz, M.A., Pohnert, G., 2013. A co-culturing/metabolomics approach to investigate chemically mediated interactions of planktonic organisms reveals influence of bacteria on diatom metabolism. *Metabolomics* 9, 349–359. <https://doi.org/10.1007/s11306-012-0453-1>
- Shadrin, A.M., Simdyanov, T.G., Pavlov, D.S., Nguyen, T.H.T., 2015. Free-living stages of the life cycle of the parasitic dinoflagellate *Ichthyodinium chabelardi* Hollande et J. Cachon, 1952 (Alveolata: Dinoflagellata). *Dokl Biol Sci* 461, 104–107. <https://doi.org/10.1134/S0012496615020131>

# Thesis Supplementary Document 1

Dinophyceae can use exudates as weapons against the parasite  
*Amoebophrya* sp. (Syndiniales).

Long, M., Marie, D., Szymczak, J., Toullec, J., Bigeard, E., Sourisseau, M., Le Gac,  
M., Guillou, L., Jauzein, C., 2021.

ISME COMMUN. 1, 34. <https://doi.org/10.1038/s43705-021-00035-x>

## ARTICLE OPEN



# Dinophyceae can use exudates as weapons against the parasite *Amoebophrya* sp. (Syndiniales)

Marc Long<sup>1</sup>✉, Dominique Marie<sup>2</sup>, Jeremy Szymczak<sup>2</sup>, Jordan Toullec<sup>1</sup>, Estelle Bigeard<sup>2</sup>, Marc Sourisseau<sup>1</sup>, Mickael Le Gac<sup>1</sup>, Laure Guillou<sup>2</sup> and Cécile Jauzein<sup>1</sup>

© The Author(s) 2021, corrected publication 2022

Parasites in the genus *Amoebophrya* sp. infest dinoflagellate hosts in marine ecosystems and can be determining factors in the demise of blooms, including toxic red tides. These parasitic protists, however, rarely cause the total collapse of Dinophyceae blooms. Experimental addition of parasite-resistant Dinophyceae (*Alexandrium minutum* or *Scrippsiella donghaiensis*) or exudates into a well-established host-parasite coculture (*Scrippsiella acuminata*-*Amoebophrya* sp.) mitigated parasite success and increased the survival of the sensitive host. This effect was mediated by waterborne molecules without the need for a physical contact. The strength of the parasite defenses varied between dinoflagellate species, and strains of *A. minutum* and was enhanced with increasing resistant host cell concentrations. The addition of resistant strains or exudates never prevented the parasite transmission entirely. Survival time of *Amoebophrya* sp. free-living stages (dinospores) decreased in presence of *A. minutum* but not of *S. donghaiensis*. Parasite progeny drastically decreased with both species. Integrity of the dinospore membrane was altered by *A. minutum*, providing a first indication on the mode of action of anti-parasitic molecules. These results demonstrate that extracellular defenses can be an effective strategy against parasites that protects not only the resistant cells producing them, but also the surrounding community.

ISME Communications; (2021)1:34; <https://doi.org/10.1038/s43705-021-00035-x>

## INTRODUCTION

Parasites, thought to account for half of species richness in some ecosystems, could constitute the unseen majority of species extinctions [1]. The majority of parasites have essential ecological roles by contributing to the balance of ecosystems, limiting invasions and emergence of infectious diseases and contributing to biomass transfer between trophic levels [2–4]. In marine ecosystems, parasites have a predominant role in the planktonic protist interactome, as inferred by sequence-based correlation networks [5], accounting for up to 18% of interactions [6]. Parasites are important contributors to phytoplankton mortality and can sometimes induce the demise of microalgal blooms [7–9].

Amongst marine parasites, the Syndiniales *Amoebophryidae* (also called marine Alveolate group II, or MALVII) is a widely distributed family [10, 11]. This group is ubiquitous in marine waters, including ultra-oligotrophic environments [12] and has been associated with the demise of toxic microalgal species [8, 13–16] in enriched coastal environments. The *Amoebophryidae* life cycle is characterized by a free-swimming stage (dinospores, referred to as zoospores) followed by two, successive, intracellular stages (trophont then sporont) that eventually kill the host and release hundreds of dinospores. Dinospores are flagellated unicellular forms that survive a few hours to a few days in culture [17].

*Amoebophrya* spp. are specialist parasites that require a compatible host to complete their life cycle. The overall consistency in the host spectrum observed within different strains

of the same species suggests a genetic determinism underlying host specialization [18]. Many factors can influence the parasitic population dynamic such as physical (e.g., temperature, water column depth, physical mixing) and chemical (e.g., nutrients) parameters [19]. Optimal abiotic conditions for parasitic infection do not always induce the collapse of targeted dinoflagellate blooms, implicating complex biotic interactions as fundamental to the parasite success [19]. Modeling approaches also indicate that parasitic control of dinoflagellate blooms strongly depends upon the plankton community structure (e.g., cell densities, grazing of free-living stages of parasite stages, competition between cells) [20]. Coexistence between resistant and sensitive hosts could affect parasite propagation through different mechanisms, including dilution effects [20, 21] or through cell signaling as suggested in viral infections [9, 22].

Mechanisms of dinoflagellate host resistance against parasites are poorly known. Different strategies have been described to date, including the production of resting stages [23, 24], the production of intracellular anti-parasitic metabolites [25–29], sometimes released into exudates [29]. The release of anti-parasitic compounds (APC) is a strategy that can be classified within the more general term of allelopathy. The term “allelochemical” refers to any secondary metabolite exuded by a microalga that affects the growth of another co-occurring protist [30]. Whether and how the release of APC can influence the dynamics of parasites remains an open question.

<sup>1</sup>IFREMER, Centre de Brest, DYNECO Pelagos, F-29280, Plouzané, France. <sup>2</sup>UMR 7144 Sorbonne Université & Centre National pour la Recherche Scientifique, «Adaptation and Diversity in Marine Environment», Team «Ecology of Marine Plankton, ECOMAP», Station Biologique de Roscoff, 29680, Roscoff, France. ✉email: marc.florian.long@gmail.com

Received: 25 February 2021 Revised: 21 May 2021 Accepted: 2 June 2021  
Published online: 12 July 2021

This study investigated whether or not co-occurring Dinophyceae, resistant to *Amoebophrya* sp., can affect the dynamics of infection of a sensitive Dinophyceae host. The well-established parasitic couple *Amoebophrya* sp. (A25)—*Scrippsiella acuminata* (ST147) [31] was studied in the presence and absence of resistant dinoflagellate host cells or exudates. Two dinoflagellate species, *Scrippsiella donghaiensis* and *Alexandrium minutum*, were selected for several reasons: (a) they can form recurrent dense blooms [32–34] and are potential competitors of *S. acuminata*, (b) they co-occur with *S. acuminata* and *Amoebophrya* sp. in the same estuaries [10, 18], (c) they are resistant to *Amoebophrya* sp. (A25) [18] and (d) *A. minutum* cells are producers of allelochemicals with lytic activity against competing protists [35, 36]. The production of allelochemicals by *S. donghaiensis* has not been reported. A series of different experimental set-ups were performed to further characterize the interactions. First, we tested the hypothesis that the presence of resistant cells could inhibit the propagation of the infection in cocultures, allowing cell–cell and chemical interactions. To evaluate potential effects of chemical cues upon the interaction, a second set of experiments was performed to study the possible effects of exudates upon the viability of the dinospores and the infection cycle. A third experiment tested the hypothesis that a loss of dinospore viability was linked to *A. minutum* lytic potency.

## MATERIALS AND METHODS

### Biological material

**Origin of strains and culture conditions.** The five hosts and the parasitic strains originated from coastal marine waters of the NE Atlantic Ocean (Table S1). All strains were non-axenic but were cultured under sterile conditions to avoid additional contamination. The parasite *Amoebophrya* sp. strain A25 (RCC4383) was maintained routinely using the sensitive *S. acuminata* clade STR1 (ST147; RCC1627; previously named *S. trochoidea*) as a compatible host. Resistant dinoflagellates used in this study were *A. minutum* (strains CCM11002, Am176 also named RCC749, DA1257) and *S. donghaiensis* (strain Sc39 or RCC4714 sampled during an *A. minutum* bloom). Infected and uninfected host cultures were maintained in a medium prepared with seawater (27 of salinity) from the Penzé estuary (France), stored in the dark for several months before being used, filtered to 0.22 µm, autoclaved, and enriched with modified F/2 nutrients (Guillard's Marine Water Enrichment Solution, Sigma) and 5% (v/v) soil extract [37]. Cultures used for Experiment 3 were prepared using a different medium (K medium [38], seawater from Argenton, France at 35 of salinity) after acclimation of strains. In both cases, a final filtration (0.22 µm pore size filter) under sterile conditions, was done after addition of nutritive solutions. Stock cultures and experiments were incubated under continuous light (90–140 µE m<sup>-2</sup> s<sup>-1</sup>, light bulb Sylvania Aquastar F18W/174 or EASY LED universal light 438 mm) at 21 ± 1–2 °C. All experiments were performed with plastic flasks (CytoOne vented flasks in polystyrene).

Uninfected hosts were kept in exponential growth phase by diluting 5 volumes of stock culture into 8 volumes of fresh medium every 3–4 days. Infections were propagated by diluting 1:5 (vol:vol) of the infected culture into healthy hosts *S. acuminata* (ST147) every 3–4 days.

**Synchronization and collection of *Amoebophrya* dinospores.** Density and infectivity of dinospores decrease rapidly after release (Table S2); therefore the use of freshly released dinospores helps to maximize infections in the flask. To produce freshly released dinospores, cultures of parasites were synchronized (unless specified) following the protocol [39]. During synchronization, infections were initiated with 3-day-old cultures of *Amoebophrya* from which dinospores were collected after a gentle separation from the remaining host cells (*S. acuminata* ST147) using gravity filtration through nylon filter (5 µm, Whatman). These dinospores were incubated with the exponentially growing host *S. acuminata* (strain ST147) using a 1:2 parasite:host (vol:vol) ratio to encourage infection of host cells. After 24 h of incubation, infected hosts were collected by filtration on a 5 µm nylon filter then resuspended in an equal volume of new medium, to remove remaining free-living dinospores. Three days later, freshly liberated dinospores of the same age (i.e., synchronized) were separated from remaining host cells by filtration as described before. In prior experiments, no effect of dilutions on dinospore survival over 24 h was

observed using fresh culture medium, exudates from the healthy host ST147, or exudates from ST147xA25 infected culture (Table S2). Hereafter, filtrates from ST147 cultures in exponential growth were used to adjust densities by dilution.

**Preparation of microalgal filtrates.** Exudates from exponentially growing microalgal strains were collected by filtration (0.2 µm, acetate cellulose membrane, Minisart) using gentle pressure through a syringe. In the present study, dilution of exudates was expressed as equivalent to the microalgal density (corresponding to the theoretical concentration of cells that would have been reached by the initial culture after a similar dilution). Diluted exudates were used immediately for experiments.

### Cell counting methods

**Flow-cytometry (FCM): cell count and membrane permeability.** Densities and individual cell variables (e.g., forward scatter, size scatter, fluorescence signals) were measured using a flow cytometer equipped with 488 nm and 405 nm lasers. A FACSAria flow cytometer (Becton Dickinson) was used in experiments 1 and 2; a Novocyte Advanteon (ACEA Biosciences) was used in experiment 3. Dinophyceae were discriminated from other particles by red chlorophyll autofluorescence. Free-living (dinospores) and late stages of infection of *Amoebophrya* spp. emit a bright green autofluorescence when excited under blue-violet light [23, 40, 41], a proxy of the parasite survival [17]. This natural autofluorescence was used to estimate the density of viable dinospores by FCM using the 405 nm laser.

Intact cell membranes are impermeable to the SytoxGreen (SYTOX Green nucleic acid stain, Invitrogen), but DNA in cells with altered (i.e., permeable) membranes is stained, emitting a bright green fluorescence. Samples were incubated with SytoxGreen (final concentration of 0.05 µM) for 20 min in the dark before measurement.

**Prevalence of infections (CARD-FISH).** CARD-FISH samples were fixed with paraformaldehyde (1% final concentration) for 1 h (4 °C in the dark) before filtration on a 0.8 µm, polycarbonate filter with a vacuum pump (< 200 mm Hg). Filters were then dehydrated using successive 50%, 80%, and 100% ethanol solutions, dried and stored in the dark at –20 °C. FISH staining was then performed according to [8]. The prevalence was estimated from microscope observations with an Olympus BX-51 epifluorescence microscope (Olympus Optical) equipped with a mercury light source, a Wide Blue filter set (Chroma Technology, VT, USA) and fluorescence filter sets for PI (excitation: 536 nm; emission: 617 nm) and FITC (excitation: 495 nm; emission: 520 nm).

Prevalence was determined by averaging infection counts on a minimum of 80 cells per replicate. Prevalence was characterized in: non-infected host cells, early stage (one or more dinospores of *Amoebophrya* sp. in the cytoplasm), and advanced stages (intermediate and beehive stages) as described in [42]. The progeny count (i.e., the number of dinospores per infected host) was estimated by dividing the maximal concentration of dinospores by the concentration of infected hosts in advanced stages.

### Experimental set-ups

**Experiment 1: cocultures.** The dynamic of infection in cocultures was compared when mixing the parasite (*Amoebophrya* sp. A25) with a sensitive host (*S. acuminata* ST147) and a resistant host (*A. minutum* CCM11002 or *S. donghaiensis* Sc39). Mixtures were prepared in triplicates, using a cell ratio of 1:1:1 (parasite:sensitive host:resistant host), with initial concentrations of 4000 cells mL<sup>-1</sup> for each strain (Fig. 1a). Controls consisted of flasks containing: (i) only the compatible host ST147 at 4000 cells mL<sup>-1</sup> or (ii) the host (ST147) at 4000 cells mL<sup>-1</sup> and parasite A25 at a ratio of 1:1. An additional control consisted of mixing the host ST147 and one of the resistant hosts (CCM11002 or Sc39) in parallel, replacing the parasite with 0.2 µm filtrate from the host culture. All cultures and controls were started simultaneously, using the same inoculum cultures. Cell densities were quantified once or twice per day. At the end of the experiment, samples were fixed with non-acidic Lugol's solution (1% final concentration) for microscopic counts and differentiation between *S. acuminata* and *A. minutum* cells.

**Experiments 2 and 3: evaluation of the effects of Dinophyceae filtrates upon *Amoebophrya*.** Filtrates of microalgal cultures were used to analyze the effects of Dinophyceae exudates (from either *A. minutum* or *S. donghaiensis*)

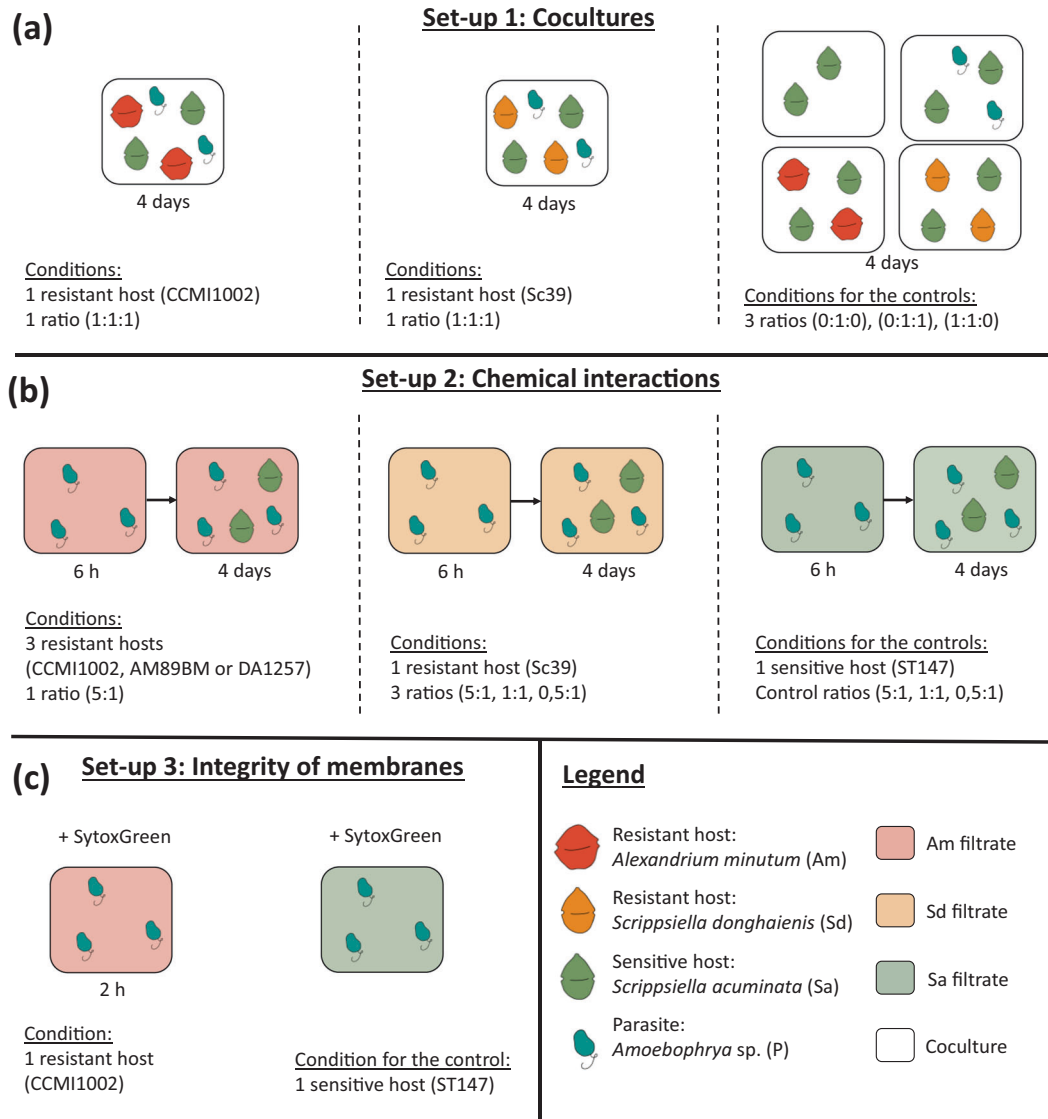


**Fig. 1 Graphical protocol for the study of chemical defenses against *Amoebophrya* sp.** **a** Experimental setup for the coculture experiments. This experiment was conducted over 4 days. The ratios are indicated as (parasite:compatible host:resistant host). **b** Experimental setup for the study of chemical interactions through exudation. This experiment was conducted in two sub-parts, a first pre-exposure to the filtrates over 6 h and an infection of compatible hosts over 4 days. The ratios are indicated as (parasite:compatible host). **c** Experimental protocol for the study of membrane integrity. The exposure to the filtrate was conducted over 2 h and compared to dinospores in their own media.

upon *Amoebophrya*. Experiment 2 was organized into two parts (Fig. 1b): the first to estimate the effect of Dinophyceae exudates upon the abundance of autofluorescent dinospores, and the second to analyze the potential for infection and production of a second generation of dinospores after 6 h of contact with the filtrates. The 6 h pre-exposure was chosen to have a stable density of dinospore (Fig. S1) at the moment of the infection.

First, dinospores from *Amoebophrya* sp. (A25) were exposed to dilutions of dinoflagellate filtrates (equivalent to 1,000 and 5,000 and 10,000 cells mL<sup>-1</sup>) collected from three strains of *A. minutum* (DA1257, AM176, CCMI1002) and for one strain of *S. donghaiensis* (SC39). Counts of autofluorescent dinospores were monitored by FCM. The mortality rate (h<sup>-1</sup>) of autofluorescent dinospores was calculated over the first 3 h according to Eq. 1, where  $N_1$  and  $N_2$  are the respective densities of autofluorescent dinospores before and after 3 h of exposure to the filtrates. Controls consisted of dinospores incubated with exudates from the host ST147. Incubations for controls and using the highest filtrate concentrations (10,000 cells mL<sup>-1</sup>) were performed in triplicates; whereas only one replicate was performed for intermediate

concentrations.

$$\text{Mortality rate} = \frac{\ln(N_1/N_2)}{3} \quad (1)$$

Then, dinospores previously exposed to the maximal concentration of exudates and in the control conditions after 6 h of incubation were used for the second part of the experiment (Fig. 1b). Exposed-dinospores were mixed with the host strain ST147 at a theoretical cell ratio of 5:1 (dinospore:host) for dinospores exposed to *A. minutum* filtrates, and at three different ratios (1:2, 1:1, and 5:1) for dinospores exposed to *S. donghaiensis* filtrate. These ratios were calculated according to the initial dinospore density before exposure to filtrates and did not consider the possible differential losses related to filtrates. The production of dinospores was monitored twice per day during 5 days by FCM, and prevalence was analyzed after 47 h of incubation by CARD-FISH in the controls and with the CCMI1002 and Sc39 filtrate treatments.



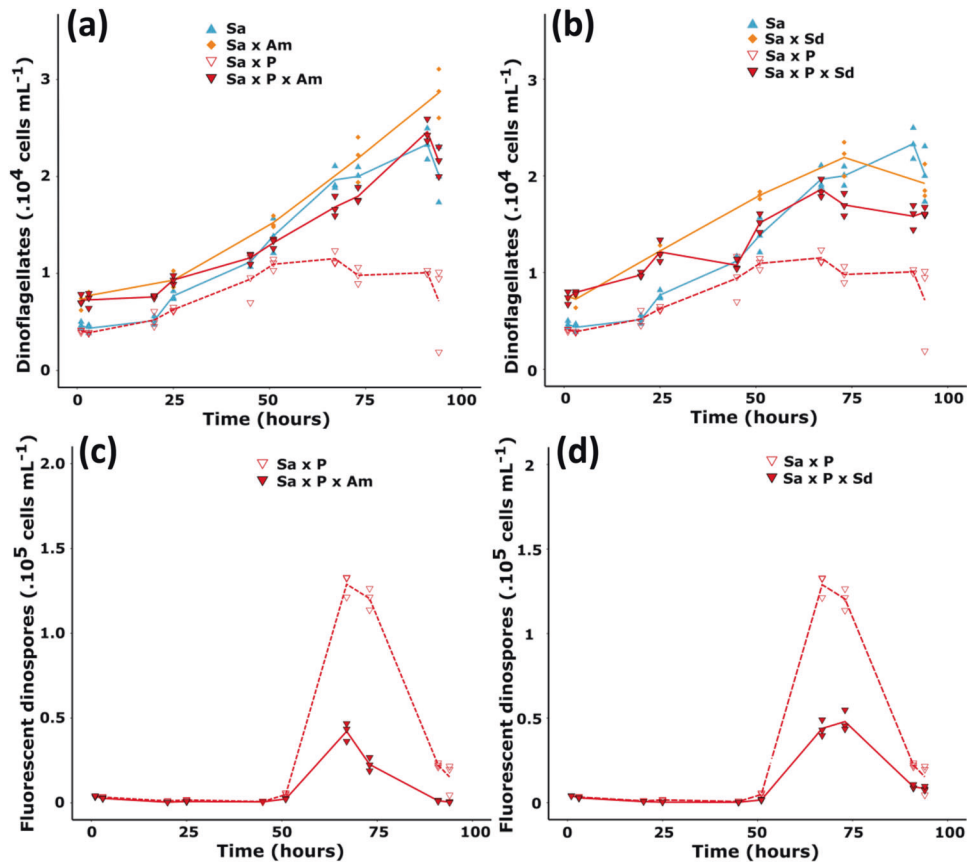


**Fig. 2 Effect of cocultures on the dynamic of infection.** Cocultures of the parasite *Amoebophrya* sp. (P; strain A25) with its compatible host *S. acuminata* (Sa; strain ST147) and a secondary resistant host, either **a, b** *A. minutum* (Am; strain CCMI1002) or **c, d** *S. donghaiensis* (Sd; strain Sc39). Densities of dinoflagellates (*S. acuminata* with *S. donghaiensis* or *A. minutum*) are shown in **(a)** and **(c)**. Densities of autofluorescent dinospores are shown in **(b)** and **(d)**. The same controls (Sa and Sa x P) are shown for both species as experiments were performed at the meantime. Lines represent the mean cell densities while the symbols represent the values of each replicate ( $N = 3$ ).

Experiment 3 was performed to monitor the concentrations of autofluorescent dinospores and their membrane integrity over time when mixed with *A. minutum* exudates compared to the control (Fig. 1c). Dinospores from 3-day-old parasite cultures (non-synchronized) of *Amoebophrya* sp. A25 were harvested by filtration ( $5 \mu\text{m}$ , cellulose acetate, Minisart). Dinospores were exposed in triplicate to *A. minutum* CCMI1002 filtrate at a final concentration of 5,000 theoretical cells  $\text{mL}^{-1}$  in six-well plates (CytOne, polystyrene). In the control, dinospores were diluted in triplicate with *S. acuminata* (ST147) filtrate. The dinospore concentrations and the permeability of their membranes were estimated after 20, 40, 60, and 120 min of incubation with the filtrate.

### Statistics

Statistical analyses were performed using R software [43]. Significant differences in the dependent variables (e.g., concentrations of microalgae and dinospores, prevalence) were assessed with a test of student or one-way ANOVA followed by a post-hoc Tukey HSD, when data met homoscedasticity with a Bartlett test and normality with a Shapiro-Wilk test. When homoscedasticity or normality could not be met, a non-parametric Kruskal-Wallis test followed by a post-hoc Conover with a bonferroni adjustment was applied. All tests were performed with a significance level of  $p$  value = 0.05. Results are expressed as mean  $\pm$  standard deviation.

## RESULTS

**Infections were mitigated by the presence of a resistant host**  
Experiment 1 tested whether or not the co-presence of a resistant host (*A. minutum* or *S. donghaiensis*) could modify *Amoebophrya*

infection dynamics with a sensitive host (*S. acuminata*). In controls and when using fixed experimental culture conditions, a complete infection cycle lasted at least 51 h and ended with the sudden released of freshly produced dinospores. During that period, infected host cells do not divide [13], which explain the lower net growth rates recorded 25 h after the parasite inoculation compared to the controls (Fig. 2a, b). Addition of a resistant host (CCMI1002 or Sc39) did not modify the duration of the parasite development, but always resulted in a significant decrease ( $> 60\%$ ) of dinospore production (Fig. 2c, d). This observation could result from a deleterious effect on the sensitive host, a direct effect upon dinospore survival/infectivity, or both. Cocultivation with *A. minutum* also has a cost for *S. acuminata*. At the end of the experiment, densities of *S. acuminata* in the coculture without parasite were of  $6,900 \pm 1,400$  cells  $\text{mL}^{-1}$  while it reached  $20,000 \pm 3,000$  cells  $\text{mL}^{-1}$  in the control.

### Exudates from *A. minutum* decreased the density of viable dinospores

Autofluorescence of dinospores can be used as a proxy for their viability [17]. In controls, 25% of fluorescent dinospores were lost after 6 h, leading to a natural mortality rate of  $0.07 \pm 0.01 \text{ h}^{-1}$  in tested cultures conditions (Fig. 3). Experiment 2 tested whether or not resistant dinoflagellate exudates affected mortality rate. If exposure to *A. minutum* filtrates significantly increased mortality ( $p$  values  $< 0.02$ ) compared to the control (Fig. 3a), no significant effect using *S. donghaiensis* (Sc39) filtrate was observed (Fig. 3b). For *A. minutum*, this deleterious effect was strain-dependent: the mortality rate of dinospores exposed to strain DA1257 ( $0.11 \pm$



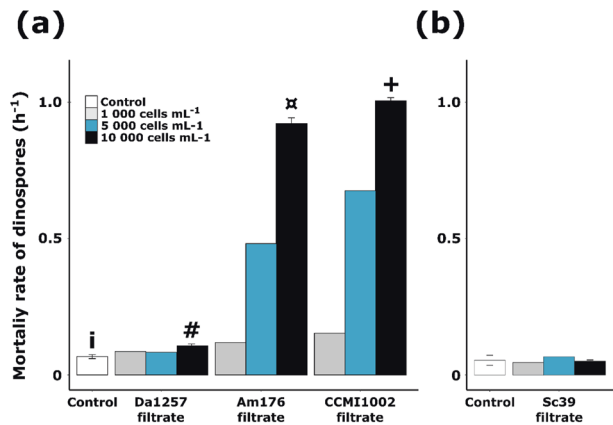


**Fig. 3 Maximal mortality rate of autofluorescent A25 dinospores in the different conditions.** Dinospores were exposed to **a** *A. minutum* and **b** *S. donghaiensis* filtrates during two separate sets of experiment. Results are expressed as the value or the mean  $\pm$  standard deviation when replicates were performed ( $N=3$ ). Significant differences ( $p$  value  $< 0.05$ ) in the mortality rates are indicated by different symbols. The complete dataset, with all sampling points (after 1, 3 and 6 h) is provided in Supporting Information Fig. S1.

$0.01 \text{ h}^{-1}$ ) was much lower than those measured for AM176 ( $0.92 \pm 0.02 \text{ h}^{-1}$ ) or CCMI1002 ( $1.00 \pm 0.01 \text{ h}^{-1}$ ). This resulted in losses of  $32 \pm 1\%$ ,  $96.1 \pm 0.2\%$ , and  $97.2 \pm 0.4\%$ , respectively, of the initial density of autofluorescent dinospores after 6 h of exposure.

#### Exudates from *A. minutum* decreased *Amoebophrya* sp. infectivity

To test whether or not the loss of fluorescence (Experiment 2) was linked to a loss of infectivity, dinospores that were challenged for 6 h with exposure to exudates from three strains of *A. minutum* were then mixed with healthy host cultures. Cell densities were fixed for all treatments before the addition of exudates. However, because of the difference in mortality rates, the starting concentration of autofluorescent dinospores and the dinospores: host ratios differed over treatments:  $41,000 \pm 1,400$  dinospores  $\text{mL}^{-1}$  in the control (ratio 4:1), and  $36,000 \pm 800$ ,  $2,100 \pm 100$ , and  $1,500 \pm 200$  dinospores  $\text{mL}^{-1}$  with exudates of DA1257 (ratio 4:1), Am176 (ratio 1:5), and CCMI1002 (ratio 1:7), respectively. The ability of the remaining autofluorescent dinospores to infect the host, even at low and unfavorable ratios, then was explored.

The growth of the compatible host (*S. acuminata* ST147) was suppressed by the dinospores from the control or previously exposed to DA1257 filtrate (Fig. 4a). This suppression of the host growth in the control was linked to the high prevalence ( $61 \pm 6\%$  in the control; Table 1) of *Amoebophrya* sp. in host cells. In comparison, the compatible host in contact with dinospores previously exposed to AM176 or CCMI1002 filtrates remained able to grow during the first 42 h of incubation (Fig. 4a) as the prevalence was lower (approximately a 35% in the CCMI1002 treatment; Table 1). Between 42 and 80 h, a collapse of the host population was observed in all conditions (Fig. 4a). The degree of the decline in host population was likely related to the prevalence of cells at advanced stages of infection (Table 1). With the CCMI1002 treatment,  $30 \pm 4\%$  of host cell losses were estimated (Fig. 4a) against  $75 \pm 2\%$  of host cell losses in the control.

Novel infections and dinospores releases were observed in all treatments (Fig. 4b). Filtrates of *A. minutum* did not seem to affect the intracellular stage as new progeny were released after 48 h, and the duration of infection was similar over treatments. Progeny (dinospore production per infected host) was 100 times lower with CCMI1002 than in the control (Table 1). As a result of lower

prevalence and lower progeny, the maximal dinospore concentration was drastically lower in the CCMI1002 and AM176 treatment (Fig. 4b') as compared to the control or DA1257 filtrate treatments ( $p$  values  $< 10^{-7}$ ).

The same experiment was conducted with Sc39, results from the 1:1 ratio are shown in Figs. 4c, d, results from cell ratios of 1:2 and 5:1 are presented in Fig. S2. In contrast to *A. minutum* filtrates, infections started with the same density of autofluorescent dinospores in the controls and in Sc39 treatments, as no effect was observed upon the autofluorescence of dinospores. Filtrates of *S. donghaiensis* did not seem to affect the intracellular stage, as novel infections were observed and the duration of infection was similar to control conditions. Release of new progeny started between 48 and 50 h (Fig. 4d). The previous treatment of dinospores with Sc39 filtrate did not significantly affect the prevalence of *Amoebophrya* sp. (Table 1) nor affect the growth rate of the host during the first 48 h (Fig. 4c). With or without the previous treatment with *S. donghaiensis* filtrate, a sharp decline in host population, concomitant with release of new progeny, was observed after 48 h. Overall there was no statistical difference in the percentage of lysed host cells between the treatments ST147 ( $37 \pm 3\%$ ), and Sc39 ( $38 \pm 4\%$ ). The main effect of pre-exposure of dinospores to Sc39 filtrate was observed in the new generation of dinospores: the treatment significantly decreased by 22% the maximum concentration of the new generation of dinospores (Fig. 4d and Supporting Information Fig. S2). This decrease did not seem to be linked to a lower prevalence but was more likely related to a lower number of progeny per infected host, even though the threefold decrease was not statistically significant when compared to the control (Table 1).

#### Exudates from *A. minutum* disrupted membranes of *Amoebophrya* sp

In Experiment 3, it was tested whether or not the loss of autofluorescence from dinospores is concomitant to the loss of membrane integrity when exposed to *A. minutum* filtrate. The most potent strain of *A. minutum* (CCMI1002) was used during this experiment. Following the exposure, a rapid decrease in the count of autofluorescent dinospores was observed, with a 40% decrease within 20 min of exposure and a 98% decrease after 2 h (Fig. 5a). This loss of autofluorescent dinospores was preceded by dinospore membrane permeabilization (Fig. 5b–d). After 20 min of exposure to the filtrate, 68% of the still autofluorescent dinospores were permeable to SytoxGreen.

#### DISCUSSION

Coculture experiments with *A. minutum* showed that co-occurring resistant dinoflagellates could either decrease survival of the free-living stage of the parasite, or limit infectivity during the second generation, or both. Cells and filtrates of *A. minutum* caused similar effects to the infection dynamic, demonstrating that Dinophyceae can remotely affect parasites through the exudation of APC. Although the lytic activity of the genus *Alexandrium* does not seem related to bacteria [44–46], a role of dinoflagellate microbiome upon excreted APC may exist and should be explored for evidence that bacteria can modulate APC bioactivity. Once released, APC are rapidly diluted, highlighting the importance of cell density and ratios. One may expect a particularly efficient protection for cells in close contact with the APC producers. The formation of dense cell patches with concentrations orders of magnitude higher than background [47–50] is likely more protective at micro-scales as this effect is density-dependent. As effects were observed using filtrates from cultures non-exposed to *Amoebophrya* sp. or its chemical cues, the release of APC appears to be a passive. Despite the passive release of APC, the production of toxins and lytic compounds can induce an extra cost for *Alexandrium* spp. cells under certain conditions [51]. To maximize

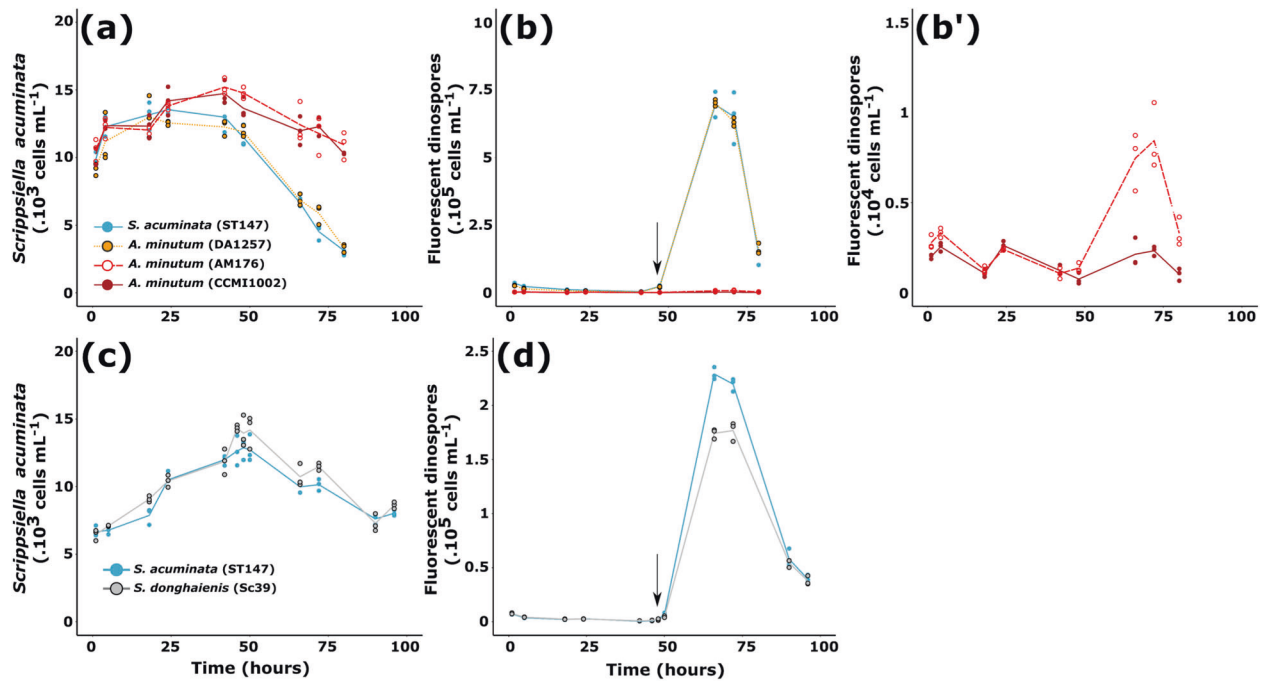


**Fig. 4** Effect of filtrates on the dynamic of infection. Effect of *A. minutum* (a–b') and *S. donghaiensis* (c, d) filtrates (Theoretical cell concentration =  $10^4$  cells  $\text{mL}^{-1}$ ) on infectivity of *Amoebophrya* sp. dinospores on its sensitive host *S. acuminata* (ST147). Cell densities of *S. acuminata* when mixed with A25 dinospores are shown in (a, d). Dynamics of dinospores, previously exposed to the different filtrates, when mixed with the compatible host *S. acuminata* ST147 are shown in (b, b' and c. c is a zoom of (b) with dinospores densities for Am176 and CCMI1002. *S. acuminata* (ST147; blue), *A. minutum* (DA1257; yellow), *A. minutum* (Am176; red) and *A. minutum* (CCMI1002; dark red). In experiments with *S. donghaiensis* (Sc39; gray) filtrate, the graphs show results of the experiment at a dinospore: *S. acuminata* ratio of 1:1; results with other ratios can be found in Supporting Information Fig. S2. The arrow represents the sampling point for prevalence analysis which results are shown in Table 1. Lines represent the mean cell densities while the symbols represent the values of each replicate ( $N = 3$ ).

**Table 1.** Prevalence of *Amoebophrya* sp. (A25) in *S. acuminata* (ST147) during experiment 2 after 47 h of contact.

	Control	CCMI1002 filtrate	<i>p</i> value	Control	Sc39 filtrate	<i>p</i> value
<i>Prevalence (% of host cells)</i>						
Infected	61 ± 6	35 ± 17	NS	24 ± 16	44 ± 23	NS
Early stages	1 ± 2	16 ± 14	NS	5 ± 9	12 ± 20	NS
Advanced stages	60 ± 5	19 ± 4	***	19 ± 7	33 ± 3	NS (0.07)
Progeny	105 ± 28	1 ± 0	**	43 ± 24	14 ± 3	NS

Two controls are shown as the two experiments were performed during two different sets. Results are expressed as the value or the mean ± standard deviation. Significant values between the control and the dinophyceae treatment (CCMI1002 or Sc39) are indicated as followed: “NS” non significant, “\*\*\*” 0.01 > *p* value > 0.001, “\*\*” *p* value < 0.001, ( $N = 3$ ).

the fitness of secondary metabolites production, *Alexandrium* cells can modulate lytic potency against microalgae in response to changing physicochemical conditions [52, 53] and toxicity in response to chemical cues from dead microalgal cells [54] or grazers [55]. Accordingly, *Alexandrium* cells are likely to modulate their toxin profile and quantity (including lytic compounds), in the presence of parasites. This hypothesis is further supported by the fact that *A. fundyense* can respond to waterborne cues of *Amoebophrya* sp. by overexpressing genes associated with defensive responses (i.e. production of reactive oxygen species) [56].

*A. minutum* exudates altered the integrity of the membrane prior to the loss of the natural autofluorescence of *Amoebophrya* sp. dinospores. The loss of cell permeability might eventually lead to an osmotic cell lysis. The release of lytic APC by *A. minutum* cells in the phycosphere (i.e., microenvironment surrounding the cells [57]) would act as a protective “shield” and must, at least partially,

explain the resistance of *A. minutum* against *Amoebophrya* sp. This strategy was evidently ruled out for some *Amoebophrya* cells, as it has already been reported that the genus *Alexandrium* can be infected by *Amoebophrya* sp. [8, 56]. This could be explained by two hypotheses: (i) either *Amoebophrya* sp. infects only clones of *A. minutum* that do not release APC or, (ii) strategies to counteract APC effects exist in *Amoebophrya*. The second hypothesis has already been proven with *Karlodinium* spp., another potential host [26]. *Amoebophrya* cells can acquire “antidotes” that enable them to avoid toxicity [58]. *Karlodinium* cells produce hydrophobic membrane permeabilizing compounds (Karlotoxins) with bioactivities, and molecular targets that are similar to the permeabilizing compounds from *Alexandrium* [36, 59]. The microalgal cells would be protected from their own toxins by their specific sterol membrane composition [60], a hypothesis also proposed to explain the resistance of *Alexandrium* cells to their own allelochemicals [59]. Cells from *Amoebophrya* sp. do not have a

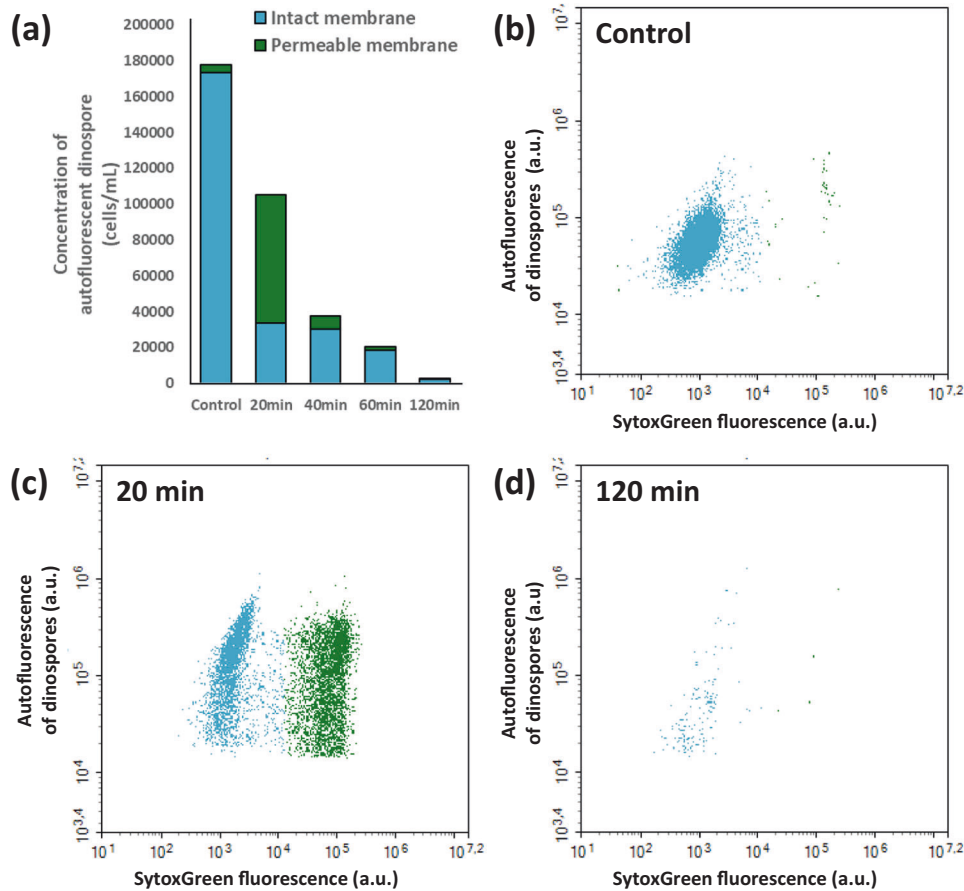


**Fig. 5 Effects of *A. minutum* filtrate on the density of autofluorescent dinospores and their membrane permeability.** Membrane permeability was estimated with the green fluorescence (from 488 nm laser) of cells with SytoxGreen, a stain that only enters cells with damaged permeable membranes. **a** means of the cumulative densities (cells mL<sup>-1</sup>) of autofluorescent dinospores with impermeable (blue) and permeable (green) membranes to the stain. **b** dinospores in the control (stained but not exposed to *A. minutum* filtrate) and exposed to *A. minutum* filtrate for **c** 20 min, **d** 120 min.

specific sterol signature [27, 61], their sterol composition is rather related to the sterols of the host. The parasite is able to retain host lipid content, including the antidote for toxins, during the infection process. This strategy enables the parasite to avoid cell lysis and to infect the host despite defense mechanisms.

Not all potential hosts are hostiles, however. The APC potency was highly variable between *A. minutum* strains and correlated with anti-microbial [62] and ichthyotoxic [63, 64] activities. The mode of action of APC is similar to the mode of action of anti-microbial allelochemicals described from the same strain [36] and from *Alexandrium catenella* (formerly group I of the *A. tamarense/fundyense/catenella* species complex [59]). Both allelochemicals disrupt cell membranes and eventually induce cell lysis. It remains unclear whether APC are the same compounds than the ones described to have anti-microbial or ichthyotoxic effects or distinct. Their characterization is required to answer this essential question.

Similarly, *S. donghaiensis* passively releases APC in the surrounding environment but the potential for active defense remains to be investigated. In comparison with *A. minutum*, a different effect, probably mediated by different molecules, was observed in the presence of *S. donghaiensis*. The former species did not affect the survival of the free-living stage of the parasite infecting *S. acuminata*, but rather decreased infectivity (ability to enter the cells) and/or progeny (ability to develop and produce the next generation of dinospores). The production of extracellular bioactive compounds was reported in *S. acuminata* (formerly identified as *S. trochoidea*) [65, 66] but never tested in

*S. donghaiensis*. APC may also act indirectly as a signaling system for *S. acuminata* that could, in turn, modify its resistance against *Amoebophrya* sp., a compelling hypothesis that requires more investigation. Importantly, these results emphasize that chemical weapons are not limited to harmful algal bloom species.

It was suggested that the presence of genotypes releasing allelochemicals could facilitate the proliferation of non-allelopathic cells and, therefore, the entire population [44, 67]. Here, it was additionally demonstrated that opportunistic (and competitive) species such as *S. acuminata* could be protected from parasitism and could benefit from a few anti-parasitic producers among *A. minutum* and *S. donghaiensis* populations. The cumulative protective effect provided by resistant hosts likely contributes to the survival of a sensitive dinoflagellate species in the presence of parasites, the private good becoming a public good [68]. In cooperative associations, individuals that use common goods produced by others in the absence of feedback are called cheaters. This is the case for non-allelopathic strains of *Prymnesium parvum* that benefit from the exclusion of competitive diatoms by another allelopathic strain [69]. Only the cheaters that are not or weakly sensitive to APC, however, will benefit from the "cure". For some microalgal species, the APC "cure" might have strong deleterious side effects. At least, a negative effect of *A. minutum* cells (but not of the filtrate) was observed on the growth of *S. acuminata* in cocultures. After all, our results highlight a potential protective role of APC for the dinoflagellate but also suggest that the complexity of planktonic community structure in environmental communities may lead to unexpected outcomes.

APC producers never completely eliminated the parasite, as illustrated by the production of a novel generation of dinospores even in the presence of microalgal cells with a strong APC activity. These results suggest that once inside their host, the parasites may be somewhat protected from APC. Eventually, such chemical defenses that moderate infections could contribute to the maintenance of the parasite in time, whilst avoiding the collapse of host populations. More generally, allelopathy prevents competitive exclusion and promotes biodiversity in phytoplankton by favoring weaker competitors for nutrients [67]. Similarly, APC might promote biodiversity of parasites by favoring the most resistant parasite that may not be the most virulent. Indeed, these results well explain the discrepancies between the virulence of parasites that kill 100% of host cells within few days in the laboratory (this study and others; [23, 70]), and the coexistence of hosts and parasites in ecological studies that include sensitive populations [71, 72]. All of these effects contribute to the explanation of the plankton paradox [73]. Chemical interactions between microorganisms tend to promote biodiversity [67, 74]. They limit the effect of competitive exclusion for nutrients (or hosts for parasites) within the plankton community and could partially explain the coexistence of different parasitic cryptic species competing for the same host as reported by [18].

Despite the ubiquity of the genus *Amoebophrya* sp. in marine ecosystems, many open questions remain about regulation of the parasite dynamic. This study highlighted the release of exudates deleterious to free-life stages of *Amoebophrya* sp. by resistant dinoflagellates. Chemical defenses must play a role in the resistance of dinoflagellates to parasites and more largely a role in their competitiveness. The exudation of anti-parasitic metabolites by resistant hosts in the surrounding environment provides a novel mechanistic link between a host–parasite couple and the surrounding community without the need of physical contact. The exudates not only protect the producer against parasitism but also have the potential to affect the entire community by decreasing propagation of the parasite. This study revealed the importance of the plankton community composition during parasite infection as the severity of the effect fluctuated depending on the species and the strains of the resistant partner, concentrations, and/or the ratios between the different partners. Another factor that has not been assessed in this study but requires further consideration is the potential for chemosensing in these interactions. Some parasites such as the generalist parasite *Parvilicifera sinerae*, can “sense” infochemicals from potential hosts [75], even though they cannot actively select a compatible host [21]. Chemosensing of resistant host infochemicals by a parasite may significantly reduce the efficiency of anti-parasitic defenses and should be studied through micro-scale studies. Although “reductionist” experiments are essential to disentangle interactomes [76], -omic tools will be essential in further studies to identify the APC chemical weapons and assess physiological mode of action. Beside their ecological relevance, the use of APC extracted from dinoflagellates could be a mean to mitigate the parasites with devastating effects on algal mass cultures [77].

## REFERENCES

- Carlson CJ, Burgio KR, Dougherty ER, Phillips AJ, Bueno VM, Clements CF, et al. Parasite biodiversity faces extinction and redistribution in a changing climate. *Sci Adv*. 2017;3:e1602422.
- Johnson PTJ, Preston DL, Hoverman JT, LaFonte BE. Host and parasite diversity jointly control disease risk in complex communities. *Proc Natl Acad Sci USA*. 2013;110:16916–21.
- Dougherty ER, Carlson CJ, Bueno VM, Burgio KR, Cizauskas CA, Clements CF, et al. Paradigms for parasite conservation: parasite conservation. *Conserv Biol*. 2016;30:724–33.
- Paseka RE, White LA, Van de Waal DB, Strauss AT, González AL, Everett RA, et al. Disease-mediated ecosystem services: pathogens, plants, and people. *Trends Ecol Evolut*. 2020;35:731–43.
- Lima-Mendez G, Faust K, Henry N, Decelle J, Colin S, Carcillo F, et al. Determinants of community structure in the global plankton interactome. *Science*. 2015;348:1262073.
- Bjorbaekmo MFM, Evenstad A, Røsaeg LL, Krabberød AK, Logares R. The planktonic protist interactome: where do we stand after a century of research? *ISME J*. 2020;14:544–59.
- Brussaard CPD. Viral control of phytoplankton populations—a review. *J Eukaryot Microbiol*. 2004;51:125–38.
- Chambouvet A, Morin P, Marie D, Guillou L. Control of toxic marine dinoflagellate blooms by serial parasitic killers. *Science*. 2008;322:1254–7.
- Vardi A, Van Mooy BA, Fredricks HF, Popendorf KJ, Ossolinski JE, Haramaty L, et al. Viral glycosphingolipids induce lytic infection and cell death in marine phytoplankton. *Science*. 2009;326:861–5.
- Guillou L, Viprey M, Chambouvet A, Welsh RM, Kirkham AR, Massana R, et al. Widespread occurrence and genetic diversity of marine parasitoids belonging to *Syndiniales* (*Alveolata*). *Environ Microbiol*. 2008;10:3349–65.
- de Vargas C, Audic S, Henry N, Decelle J, Mahé F, Logares R, et al. Eukaryotic plankton diversity in the sunlit ocean. *Science*. 2015;348:1261605.
- Siano R, Alves-de-Souza C, Foulon E, Bendif EM, Simon N, Guillou L, et al. Distribution and host diversity of Amoebophryidae parasites across oligotrophic waters of the Mediterranean Sea. *Biogeosciences*. 2011;8:267–78.
- Park M, Cooney S, Yih W, Coats D. Effects of two strains of the parasitic dinoflagellate *Amoebophrya* on growth, photosynthesis, light absorption, and quantum yield of bloom-forming dinoflagellates. *Mar Ecol Prog Ser*. 2002;227:281–92.
- Velo-Suárez L, Brosnahan ML, Anderson DM, McGillicuddy DJ. A Quantitative assessment of the role of the parasite *Amoebophrya* in the termination of *Alexandrium fundyense* blooms within a small coastal embayment. *PLoS ONE*. 2013;8:e81150.
- Li C, Song S, Liu Y, Chen T. Occurrence of *Amoebophrya* spp. infection in planktonic dinoflagellates in Changjiang (Yangtze River) Estuary, China. *Harmful Algae*. 2014;37:117–24.
- Choi CJ, Brosnahan ML, Sehein TR, Anderson DM, Erdner DL. Insights into the loss factors of phytoplankton blooms: the role of cell mortality in the decline of two inshore *Alexandrium* blooms. *Limnol Oceanogr*. 2017;62:1742–53.
- Coats DW, Park MG. Parasitism of photosynthetic dinoflagellates by three strains of *Amoebophrya* (Dinophyta); parasite survival, infectivity, generation time, and host specificity. *J Phycol*. 2002;38:520–8.
- Cai R, Kayal E, Alves-de-Souza C, Bigeard E, Corre E, Jeanthon C, et al. Cryptic species in the parasitic *Amoebophrya* species complex revealed by a polyphasic approach. *Sci Rep*. 2020;10:2531.
- Anderson SR, Harvey EL. Temporal variability and ecological interactions of parasitic marine Syndiniales in coastal protist communities. *mSphere*. 2020;5:e00209–20.
- Alves-de-Souza C, Pecqueur D, Le Floch E, Mas S, Roques C, Mostajir B, et al. Significance of plankton community structure and nutrient availability for the control of dinoflagellate blooms by parasites: a modeling approach. *PLoS ONE*. 2015;10:e0127623.
- Alacid E, Park MG, Turon M, Petrou K, Garcés E. A game of russian roulette for a generalist dinoflagellate parasitoid: host susceptibility is the key to success. *Front Microbiol*. 2016;7:769.
- Vincent F, Sheyn U, Porat Z, Schatz D, Vardi A. Visualizing active viral infection reveals diverse cell fates in synchronized algal bloom demise. *Proc Natl Acad Sci USA*. 2021;118:e2021586118.
- Chambouvet A, Alves-de-Souza C, Cueff V, Marie D, Karpov S, Guillou L. Interplay between the parasite *Amoebophrya* sp. (*Alveolata*) and the cyst formation of the red tide dinoflagellate *Scrippsiella trochoidea*. *Protist*. 2011;162:637–49.
- Pelusi A, De Luca P, Manfellotto F, Thamatrakoln K, Bidle KD, Montresor M. Virus-induced spore formation as a defense mechanism in marine diatoms. *New Phytol*. 2020;229:16951–2259.
- Pouneva ID. Effect of abscisic acid and ontogenic phases of the host alga on the infection process in the pathosystem *Scenedesmus acutus*—*Phlyctidium sceneddesmi*. *Acta Physiol Plant*. 2006;28:395–400.
- Bai X, Adolf JE, Bachvaroff T, Place AR, Coats DW. The interplay between host toxins and parasitism by *Amoebophrya*. *Harmful Algae*. 2007;6:670–8.
- Place AR, Bai X, Kim S, Sengco MR, Wayne, Coats D. Dinoflagellate host-parasite sterol profiles dictate karlotoxin sensitivity. *J Phycol*. 2009;45:375–85.
- Rohrlack T, Christiansen G, Kurmayer R. Putative antiparasite defensive system involving ribosomal and nonribosomal oligopeptides in Cyanobacteria of the Genus *Planktothrix*. *Appl Environ Microbiol*. 2013;79:2642–7.
- Scholz B, Küpper F, Vyverman W, Ólafsson H, Karsten U. Chytridiomycosis of marine diatoms—the role of stress physiology and resistance in parasite-host recognition and accumulation of defense molecules. *Marine Drugs*. 2017;15:26.
- Granéli E, Hansen PJ. Allelopathy in harmful algae: a mechanism to compete for resources? In: Granéli E, Turner JT, editors. *Ecology of harmful algae*. Springer Berlin Heidelberg; 2006. p. 189–201.



31. Farhat S, Le P, Kayal E, Noel B, Bigeard E, Corre E, et al. Rapid protein evolution, organellar reductions, and invasive intronic elements in the marine aerobic parasite dinoflagellate *Amoebophrya* spp. *BMC Biol.* 2021;19:1.
32. Chapelle A, Le Bec C, Amzil Z, Dreanno C, Klouch KZ, Labry C, et al. Etude sur la prolifération de la micro algue *Alexandrium minutum* en rade de Brest (2014).
33. Chapelle A, Le Gac M, Labry C, Siano R, Quere J, Caradec F, et al. The Bay of Brest (France), a new risky site for toxic *Alexandrium minutum* blooms and PSP shellfish contamination. *Harmful Algal News.* 2015;51:4–5.
34. Klouch KZ, Schmidt S, Andrieux-Loyer F, Le Gac M, Hervio-Heath D, Qui-Minet ZN, et al. Historical records from dated sediment cores reveal the multidecadal dynamic of the toxic dinoflagellate *Alexandrium minutum* in the Bay of Brest (France). *FEMS Microbiol Ecol.* 2016;92:fw101
35. Long M, Tallec K, Soudant P, Le Grand F, Donval A, Lambert C, et al. Allelochemicals from *Alexandrium minutum* induce rapid inhibition of metabolism and modify the membranes from *Chaetoceros muelleri*. *Algal Res.* 2018;35:508–18.
36. Long M, Peltekis A, González-Fernández C, Bailleul B, Hégaret H. Allelochemicals of *Alexandrium minutum*: kinetics of membrane disruption and photosynthesis inhibition in a co-occurring diatom. *Harmful Algae.* 2021;103:101997.
37. Starr RC, Zeikus JA. Utex—The culture collection of algae at the university of Texas at Austin 1993 List of cultures. *J Phycol.* 1993;29:1–106.
38. Keller M, Selvin R, Claus W, Guillard RRL. Media for the culture of oceanic ultraphytoplankton 1, 2. *J Phycol.* 1987;23:633–8.
39. Bigeard. Collect of *Amoebophrya* parasite (free-living stage) for genomic and transcriptomic analyses. 2019. [Protocols.io](https://doi.org/10.21203/rs.3.rs-101997).
40. Kim S, Gil Park M, Yih W, Coats DW. Infection of the bloom-forming thecate dinoflagellates *Alexandrium affine* and *Gonyaulax spinifera* by two strains of *Amoebophrya* (Dinophyta). *J Phycol.* 2004;40:815–22.
41. Kim S. Patterns in host range for two strains of *Amoebophrya* (Dinophyta) infecting thecate dinoflagellates: *Amoebophrya* spp. ex *Alexandrium affine* and ex *Gonyaulax polygramma*. *J Phycol.* 2006;42:1170–3.
42. Kayal E, Alves-de-Souza C, Farhat S, Velo-Suarez L, Monjol J, Szymczak J, et al. Dinoflagellate host chloroplasts and mitochondria remain functional during *Amoebophrya* Infection. *Front Microbiol.* 2020;11:600823.
43. R Core Team. R: a language and environment for statistical computing. Vienna: R Foundation for Statistical Computing.
44. John U, Tillmann U, Hülskötter J, Alpermann TJ, Wohlrab S, Van de Waal DB. Intraspecific facilitation by allelochemical mediated grazing protection within a toxigenic dinoflagellate population. *Proc R Soc B.* 2015;282:20141268.
45. Lelong A, Haberkorn H, Le Goïc N, Hégaret H, Soudant P. A new insight into allelopathic effects of *Alexandrium minutum* on photosynthesis and respiration of the diatom *Chaetoceros neogracile* revealed by photosynthetic-performance analysis and flow cytometry. *Microb Ecol.* 2011;62:919–30.
46. Tillmann U, Alpermann T, John U, Cembella A. Allelochemical interactions and short-term effects of the dinoflagellate *Alexandrium* on selected photoautotrophic and heterotrophic protists. *Harmful Algae.* 2008;7:52–64.
47. Durham WM, Stocker R. Thin phytoplankton layers: characteristics, mechanisms, and consequences. *Annu Rev Mar Sci.* 2012;4:177–207.
48. Breier RE, Lalescu CC, Waas D, Wilczek M, Mazza MG. Emergence of phytoplankton patchiness at small scales in mild turbulence. *Proc Natl Acad Sci USA.* 2018;115:12112–7.
49. Wheeler JD, Secchi E, Rusconi R, Stocker R. Not just going with the flow: the effects of fluid flow on bacteria and plankton. *Annu Rev Cell Dev Biol.* 2019;35:213–37.
50. Basterretxea G, Font-Muñoz JS, Tuval I. Phytoplankton orientation in a turbulent ocean: a microscale perspective. *Front Mar Sci.* 2020;7:185.
51. Blossom HE, Markussen B, Daugbjerg N, Krock B, Norlin A, Hansen PJ. The cost of toxicity in microalgae: direct evidence from the dinoflagellate *Alexandrium*. *Front Microbiol.* 2019;10:1065.
52. Martens H, Van de Waal DB, Brandenburg KM, Krock B, Tillmann U. Salinity effects on growth and toxin production in an *Alexandrium ostenfeldii* (Dinophyceae) isolate from The Netherlands. *J Plankton Res.* 2016;38:1302–16.
53. Long M, Holland A, Planquette H, González Santana D, Whitby H, Soudant P, et al. Effects of copper on the dinoflagellate *Alexandrium minutum* and its allelochemical potency. *Aquat Toxicol.* 2019;210:251–61.
54. Brown ER, Kubanek J. Harmful alga trades off growth and toxicity in response to cues from dead phytoplankton. *Limnol Oceanogr.* 2020;65:1723–33.
55. Selander E, Thor P, Toth G, Pavia H. Copepods induce paralytic shellfish toxin production in marine dinoflagellates. *Proc R Soc B.* 2006;273:1673–80.
56. Lu Y, Wohlrab S, Groth M, Glöckner G, Guillou L, John U. Transcriptomic profiling of *Alexandrium fundyense* during physical interaction with or exposure to chemical signals from the parasite *Amoebophrya*. *Mol Ecol.* 2016;25:1294–307.
57. Seymour JR, Amin SA, Raina J-B, Stocker R. Zooming in on the phycosphere: the ecological interface for phytoplankton–bacteria relationships. *Nat Microbiol.* 2017;2:17065.
58. Place A, Harvey H, Bai X, Coats D. Sneaking under the toxin surveillance radar: parasitism and sterol content. *Afr J Mar Sci.* 2006;28:347–51.
59. Ma H, Krock B, Tillmann U, Bickmeyer U, Graeve M, Cembella A. Mode of action of membrane-disruptive lytic compounds from the marine dinoflagellate *Alexandrium tamarense*. *Toxicon.* 2011;58:247–58.
60. Deeds J, Place A. Sterol-specific membrane interactions with the toxins from *Karlodinium micrum* (Dinophyceae) — a strategy for self-protection? *Afr J Mar Sci.* 2006;28:421–5.
61. Leblond JD, Sengco MR, Sickman JO, Dahmen JL, Anderson DM. Sterols of the Syndinian dinoflagellate *Amoebophrya* sp., a parasite of the dinoflagellate *Alexandrium tamarense* (Dinophyceae). *J Eukaryotic Microbiol.* 2006;53:211–6.
62. Long M, Tallec K, Soudant P, Lambert C, Le Grand F, Sarthou G, et al. A rapid quantitative fluorescence-based bioassay to study allelochemical interactions from *Alexandrium minutum*. *Environ Pollut.* 2018;242:1598–605.
63. Borcier E, Morvezzen R, Boudry P, Miner P, Charrier G, Laroche J, et al. Effects of bioactive extracellular compounds and paralytic shellfish toxins produced by *Alexandrium minutum* on growth and behaviour of juvenile great scallops *Pecten maximus*. *Aquatic Toxicol.* 2017;184:142–54.
64. Castrec J, Soudant P, Payton L, Tran D, Miner P, Lambert C, et al. Bioactive extracellular compounds produced by the dinoflagellate *Alexandrium minutum* are highly detrimental for oysters. *Aquat Toxicol.* 2018;199:188–98.
65. Wang Y, Tang X. Interactions between *Prorocentrum donghaiense* Lu and *Scrippsiella trochoidea* (Stein) Loeblich III under laboratory culture. *Harmful Algae.* 2008;7:65–75.
66. Tang YZ, Gobler CJ. Lethal effects of Northwest Atlantic Ocean isolates of the dinoflagellate, *Scrippsiella trochoidea*, on Eastern oyster (*Crassostrea virginica*) and Northern quahog (*Mercenaria mercenaria*) larvae. *Mar Biol.* 2012;159:199–210.
67. Felpeto AB, Roy S, Vasconcelos VM. Allelopathy prevents competitive exclusion and promotes phytoplankton biodiversity. *Oikos.* 2018;127:85–98.
68. Driscoll WW, Hackett JD, Ferrière R. Eco-evolutionary feedbacks between private and public goods: evidence from toxic algal blooms. *Ecol Lett.* 2016;19:81–97.
69. Driscoll WW, Espinosa NJ, Eldakar OT, Hackett JD. Allelopathy as an emergent, exploitable public good in the bloom-forming microalga *Prymnesium parvum*. *Evolution.* 2013;67:1582–90.
70. Rodríguez F, Figueroa RI. Confirmation of the wide host range of *Parvilucifera corolla* (Alveolata, Perkinsozoa). *Eur J Protistol.* 2020;74:125690.
71. Chambouvet A, Laabir M, Sengco M, Vaquer A, Guillou L. Genetic diversity of *Amoebophryidae* (Syndiniales) during *Alexandrium catenella/tamarense* (Dinophyceae) blooms in the Thau lagoon (Mediterranean Sea, France). *Res Microbiol.* 2011;162:959–68.
72. Cosgrove S. Monitoring methods and bloom dynamic studies of the toxic dinoflagellate genus *Alexandrium*. 2014. Doctoral dissertation, National University of Ireland, Galway.
73. Hutchinson GE. The Paradox of the plankton. *Am Nat.* 1961;95:137–45.
74. Czarán TL, Hoekstra RF, Pagie L. Chemical warfare between microbes promotes biodiversity. *Proc Natl Acad Sci USA.* 2002;99:786–90.
75. Garcés E, Alacid E, Reñé A, Petrou K, Simó R. Host-released dimethylsulphide activates the dinoflagellate parasitoid *Parvilucifera sinerae*. *ISME J.* 2013;7:1065–8.
76. Fitzpatrick CR, Salas-González I, Conway JM, Finkel OM, Gilbert S, Russ D, et al. The plant microbiome: from ecology to reductionism and beyond. *Annu Rev Microbiol.* 2020;74:annurev-micro-022620-014327
77. Carney LT, Lane TW. Parasites in algae mass culture. *Front Microbiol.* 2014;5:278.

## ACKNOWLEDGEMENTS

This study was carried out with the financial support of IFREMER, the Centre National de la Recherche Scientifique (CNRS), Sorbonne Université, the Région Bretagne and the GDR Phycotox (a CNRS/IFREMER network on HABs). It results from different projects: the project PARALLAX (IFREMER), the project PARACIDE (SAD2018 Région Bretagne/IFREMER, GDR Phycotox) and the PRC France-Korea MALV-REF. The authors would like to warmly thank Dr. Natalia Llopis Monferrer for the help with the illustrations and Prof. Dianne F. Jolley as well as Dr. Gary H. Wikfors for the constructive comments and English corrections of the manuscript. We also would like to thank Aurore Regaudie de Gioux for her constructive support during the writing of this article.

## AUTHOR CONTRIBUTIONS

ML, LG, CJ, MS, and MLG designed the study. ML, JS, DM, JT, EB and CJ performed the experiments. ML, LG, and CJ performed the data analysis and wrote the manuscript that was discussed and revised by all co-authors.

**COMPETING INTERESTS**

The authors declare no competing interests.

**ADDITIONAL INFORMATION**

**Supplementary information** The online version contains supplementary material available at <https://doi.org/10.1038/s43705-021-00035-x>.

**Correspondence** and requests for materials should be addressed to M.L.

**Reprints and permission information** is available at <http://www.nature.com/reprints>

**Publisher's note** Springer Nature remains neutral with regard to jurisdictional claims in published maps and institutional affiliations.



**Open Access** This article is licensed under a Creative Commons Attribution 4.0 International License, which permits use, sharing, adaptation, distribution and reproduction in any medium or format, as long as you give appropriate credit to the original author(s) and the source, provide a link to the Creative Commons licence, and indicate if changes were made. The images or other third party material in this article are included in the article's Creative Commons licence, unless indicated otherwise in a credit line to the material. If material is not included in the article's Creative Commons licence and your intended use is not permitted by statutory regulation or exceeds the permitted use, you will need to obtain permission directly from the copyright holder. To view a copy of this licence, visit <http://creativecommons.org/licenses/by/4.0/>.

© The Author(s) 2021, corrected publication 2022



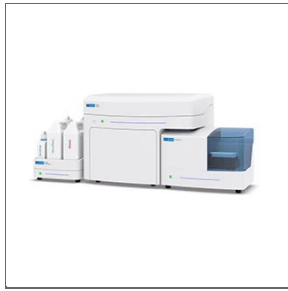
# Thesis Supplementary Document 2

Use of flow cytometry (Novocyte Advanteon) to monitor the complete life cycle of the parasite *Amoebophrya ceratii* infecting its dinoflagellate host

Szymczak, J., Bigeard, E., Guillou, L., 2023.

[www.protocols.io](http://www.protocols.io)





SEP 25, 2023

# Use of flow cytometry (Novocytte Advanteon) to monitor the complete life cycle of the parasite *Amoebophrya ceratii* infecting its dinoflagellate host

Estelle

Jeremy Szymczak<sup>1</sup>, Bigeard<sup>2</sup>, Laure Guillou<sup>2</sup>

<sup>1</sup>AD2M, Station Biologique de Roscoff, CNRS, SU; <sup>2</sup>Station Biologique de Roscoff, France

Ecology of Marine Plankton (ECOMAP) team - Roscoff

Roscoff Culture Collection

1 more workspace ↓



Estelle Bigeard

Station Biologique de Roscoff, France, UMR7144 CNRS Sorbonne...

OPEN ACCESS



DOI:

[dx.doi.org/10.17504/protocols.io.ewov1nrq2gr2/v1](https://dx.doi.org/10.17504/protocols.io.ewov1nrq2gr2/v1)

**Protocol Citation:** Jeremy Szymczak, Estelle Bigeard, Laure Guillou 2023. Use of flow cytometry (Novocytte Advanteon) to monitor the complete life cycle of the parasite *Amoebophrya ceratii* infecting its dinoflagellate host. **protocols.io** <https://dx.doi.org/10.17504/protocols.io.ewov1nrq2gr2/v1>

**License:** This is an open access protocol distributed under the terms of the [Creative Commons Attribution License](https://creativecommons.org/licenses/by/4.0/), which permits unrestricted use, distribution, and reproduction in any medium, provided the original author and source are credited

**Protocol status:** Working  
We use this protocol and it's working

**Created:** Aug 03, 2022

**Last Modified:** Sep 25, 2023

**PROTOCOL integer ID:** 68121

**Keywords:** flow cytometry, cell counting, parasite, coculture, prevalence, parasite life cycle, natural fluorescence, infection dynamics

## ABSTRACT

The parasite belongs to *Amoebophrya ceratii* (Amoebophryidae or MALVII, which stands for Marine Alveolate Group II, Syndiniales, Dinoflagellata, Alveolata), a complex species that includes intracellular marine parasites infecting and ultimately killing other dinoflagellates. During its life cycle, a free-living parasitic cell (known as dinospores, measuring 2-5 μm) penetrates its host, consumes it, and eventually undergoes sporulation. In this study, we present a method for identifying and quantifying the different stages occurring during the entire infective process of this parasite, using flow cytometry (NovoCyte Advanteon, ACEA Biosciences), equipped with two lasers (405 and 488 nm). This document presents the different setup for the acquisition, analysis, and data export.

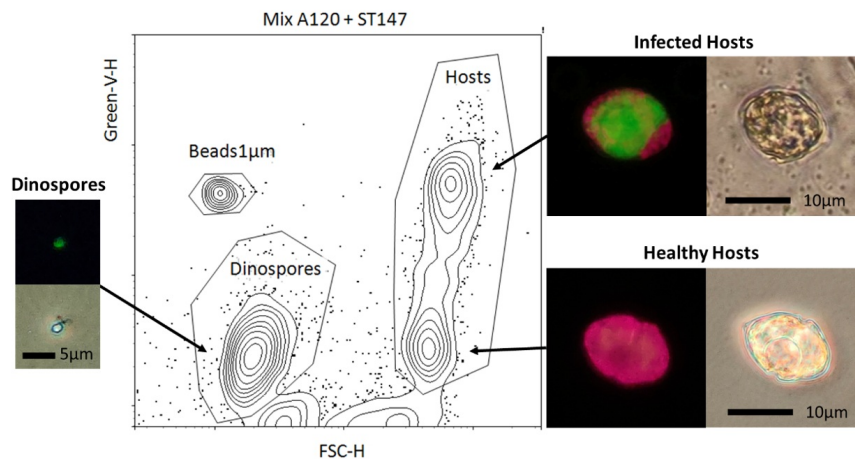


Figure 1: Cytogram displaying three distinct types of cells. The y-axis of the cytogram represents green fluorescence and the x-axis cell size, measured using forward scatter (FSC). The illustrations of the host and parasite cells on the cytogram are captured using an epi-fluorescence microscope (inverted microscope Olympus equipped with the U-MF2 Olympus cube (455/70 excitation, LP 515 emission) and a light microscope (using phase contrast). These visual representations aid in identifying and distinguishing the different cell types present on the cytogram.

## Origin of strains

Strains of both the host and parasite have been isolated from the Penzé estuary, located in the north-west of France in the English Channel (coordinates: 48°37'N; 3°56'W). The *Amoebophrya ceratii* A120 strain (RCC4398) was originally derived from a single infected cell of *Heterocapsa triquetra* collected on June 13th, 2011, and subsequently incubated with exponentially growing *H. triquetra* (primary host HT150, RCC3596). Starting from April 23rd, 2012, A120 has also been

maintained in *Scrippsiella acuminata* (strain ST147, RCC 1627), formerly known as *Scrippsiella trochoidea* as described by Kretschmann et al. in 2015. The host strain ST147 was established from the germination of a single cyst collected from sediment in 2007. Strain A120 is a parasite belonging to MALVII-Clade 2, ribotype 4, based on the nomenclature of Guillou et al. (2008) and Cai et al. (2020).

All strains have been deposited at the Roscoff Culture Collection, <https://roscoff-culture-collection.org/>.

## GUIDELINES

The flow cytometer:

<https://www.agilent.com/en/product/research-flow-cytometry/flow-cytometers/flow-cytometer-systems/novocyte-advanteon-flow-cytometer-1270335>

Novocyte Advanteon flow cytometer manual:

<https://www.agilent.com/cs/library/usermanuals/public/150217-NovoCyte%20Advanteon%20Flow%20Cytometer%20Operator%20Guide.pdf>

## MATERIALS

### Equipments:

Laminar flow cabinet (or biosafety cabinet)  
Micropipette

### Materials for Flow cytometry:

Cytometer tube (haemolysis tube) – Labellians – CML Group – Ref TH5-12PS

Cleaning solution: <https://www.agilent.com/en/product/research-flow-cytometry/flow-cytometers/instrument-consumables-accessories/fluidics-system-solutions-for-flow-cytometry-1320867>

- NovoFlow Sheath Fluid
- NovoClean Solution
- NovoRinse Solution

1µm fluorescent beads for standard: Fluoresbrite® YG Microspheres, Calibration Grade 1.00µm – Polysciences – Ref 18860-1

## BEFORE START INSTRUCTIONS

### Description of the flow cytometer and parameters used

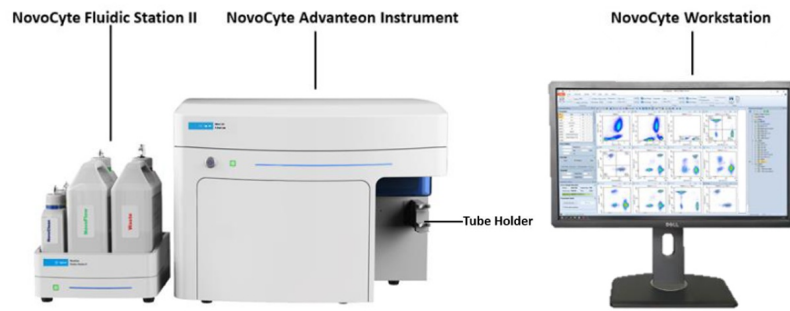


Figure 2: NovoCyte Advanteon (ACEA Biosciences)

We employed the NovoCyte Advanteon flow cytometer (ACEA Biosciences) for our study (Fig. 2), which is equipped with two lasers (488 nm and 405nm wavelengths).

The cytometer's front panel includes the following features:

- A power switch: Steady green indicates the device is powered on, while flashing green signifies a shutdown cleaning procedure.
- An LED status indicator: Green represents normal status, orange indicates a warning (Click on the status bar in the NovoExpress software to review the warning message), and red signals errors (Click on the status bar in the NovoExpress software to review the error message).
- A front panel cover.
- The tube holder.

The NovoCyte Advanteon flow cytometer is equipped with four containers that are positioned in designated locations on the provided NovoCyte Fluidics Station (refer to Figure X). These containers serve various functions in the fluidics system:

- **"NovoFlow" sheath fluid container (green):**  
This container is used for hydrodynamically focusing the sample stream, ensuring precise analysis.
- **"NovoRinse" rinsing solution container (yellow):**  
This container contains a rinsing solution that is employed to wash away protein deposits, adherent cells, various debris, and other contaminants from the fluidics system.
- **"NovoClean" cleaning solution container (blue):**  
This container holds a cleaning solution used to thoroughly clean and maintain the fluidics system, ensuring its proper functioning.
- **Waste container (red):**  
This container is designated for the disposal of waste generated during the flow cytometry process.

The containers are continuously monitored by weight to provide real-time tracking of the remaining liquid volume. This functionality enables the system to issue a warning message when the fluid levels become critically low or when the waste container reaches its capacity.



Figure 3: Reagent containers & Tubing Connections

The host, *Scrippsiella acuminata*, could be detected by its content in chlorophyll, which autofluorescence in red under blue light excitation (488 nm). *Amoebophrya*-like parasites infecting dinoflagellates are detected based on their natural bright green autofluorescence when illuminated under a violet light (405 nm) (Coats and Bockstahler 1994).

Based on that, cell identification by flow cytometry relied on distinctions in cell sizes and fluorescence signals, specifically in the green and red channels.

In our experimental setup, the blue laser (488 nm) serves multiple purposes. Firstly, it is used for the forward scatter measurement, which provides information about the size of cells and other particles. Additionally, the blue laser is responsible for excitation of chlorophyll, which is detected through red fluorescence (695/40). In the schematic representation (Fig. 3), the pathway from the blue laser to the photodetectors is highlighted in red. The default alias for the red fluorescence from the blue laser is "Chl," with the parameter name being B695. However, in this protocol, we modify the alias to "Red-B" to indicate "red fluorescence from the blue laser."

Furthermore, the violet laser (405 nm) is used to excite the parasite, which emits natural autofluorescence detectable in the green channel (525/45). The pathway from the violet laser to the photodetectors is indicated in green on the schematic representation (Fig. 3). The default alias for this fluorescence is "AmCyan," and the corresponding parameter name is V525. In this protocol, we opt to change the alias to "Green-V" to represent the green fluorescence resulting from violet excitation.

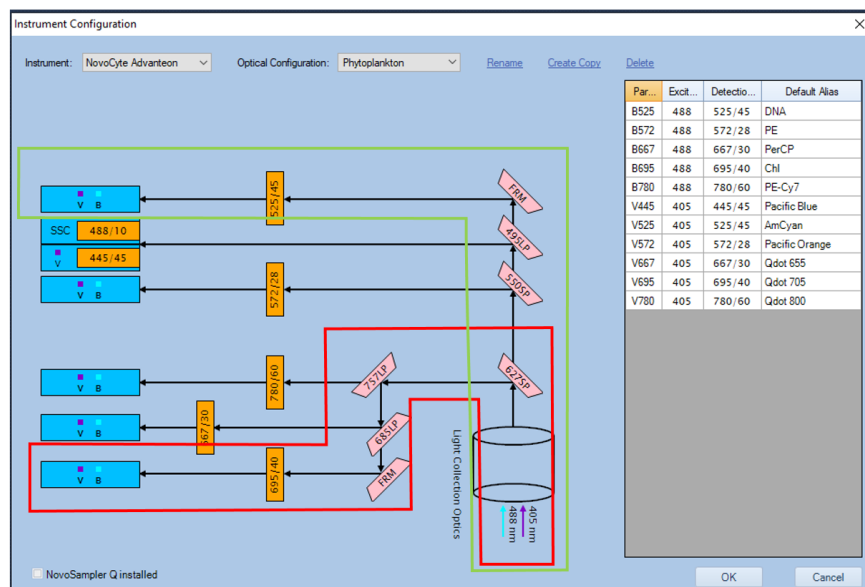


Figure 4: A screenshot of the "Instrument Configuration" in the dedicated software of the flow cytometer is

provided. The two boxed paths represent the filters specifically designed for the detection and counting of the host and parasite. The green path corresponds to the detection of green fluorescence (525/45) emitted by the violet laser (405 nm), while the red path corresponds to the detection of red fluorescence (695/40) emitted by the blue laser (488 nm).

## Flow cytometer startup procedure

1

- Press the power button located on the front of the flow cytometer to switch it on. The flow cytometer will initiate a series of fluidics steps automatically, which typically takes approximately 5 minutes.
- Switch on the computer.
- Launch the cytometer software (NovoExpress).
- Log in to your session.

**Comment 1 :** Once the automatic fluidic startup process is completed, the status displayed at the bottom left of the NovoExpress window should indicate "Ready." This indicates that the flow cytometer is prepared for use. If any other status is displayed, such as indicating a need for maintenance, please contact the platform manager for assistance.

**Comment 2 :** Check cleaning solutions : If there is a warning prompts from the status bar regarding the containers, fill the sheath fluid ("NovoFlow") and/or the cleaning solution ("NovoRince", "NovoClean") containers and/or empty the waste.

## Flow cytometer setup for acquisition

2

### 2.1 Flow cytometer parameters

The NovoExpress software provides access to adjustable parameters and acquisition modes for the flow cytometer. To access these settings, open the "**Cytometer settings**" window (Fig. 4). If the window is not visible, go to the "View" tab at the top and click on "Cytometer settings" to display it.

- **"Parameters":**  
This allows you to select the parameters to be recorded during acquisition and their respective gains. By default, forward scatter (FSC) and side scatter (SSC) are selected in height. Additionally, you must select the Green-V (V525) and Red-B (B695) photodetectors in height, which correspond to the green fluorescence of the parasite and the red fluorescence of the host's chlorophyll. The default gain settings are suitable for analysis, but they can be adjusted if necessary. An underlined gain value indicates a manual change that deviates from the default value.
- **"Stop condition":**  
This allows you to specify the quantity of the sample to be analyzed. The default setting is 1 minute, but this can be adjusted as needed. It is also possible to set a stop condition based on volume, which is useful for analyzing a specific volume of the sample. In such cases, the cytometer will only collect the specified volume from the tube. If the sample volume is limited, you can define a small volume, such as 50µl, for example.
- **"Flow rate":**  
This allows you to select the volume of sample per minute to be analyzed and the core diameter size. NovoExpress provides three preselected flow rates (Slow, Medium, and Fast). For the A120 + ST147 strain combination, a Fast flow rate is suitable, such as 66µl/min with a core diameter of 16.8µm.
- **"Threshold":**  
This parameter allows you to define the value at which an event is considered for analysis and recording by the software.

Setting a threshold is important to avoid recording noise and ensure accurate results. Without a threshold, the cytometer will record all events, leading to incorrect results due to excessive noise. An optimal threshold is a balance between the number of events per second (which should be as low as possible) and the parameter value of the event of interest (such as fluorescence and FSC of a cell). The recommended threshold is based on the Green-V-H parameter with a value of 1000. In cases with a high number of events per second, the threshold can be increased up to 3000. The maximum number of events per second is 4000.

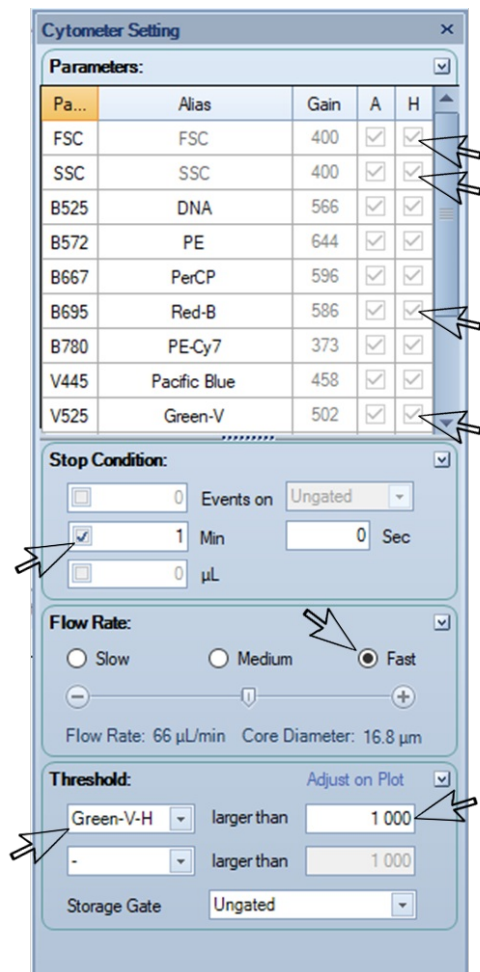


Figure 5: Screenshot from NovoExpress, the cytometer settings, arrows indicate the specific points that need to be settled.

## 2.2 Data management: Samples, specimens, and groups

The data generated during the analysis can be accessed and managed through the "Experiment Manager" window (Fig. 6). If the window is not visible, go to the "View" tab at the top and click on "Experiment Manager" to display it.

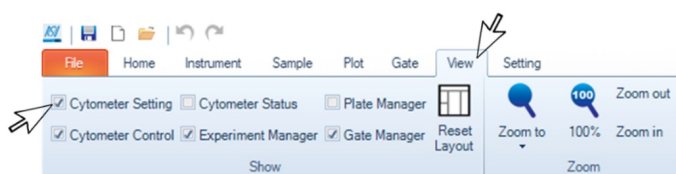


Figure 6: Screenshot of NovoExpress demonstrating how to display the "Cytometer Settings" window.

Terminology:

- A **"sample"** refers to a single acquisition from a tube, representing a measurement.
- A **"specimen"** is a group of samples. Each sample must belong to a specimen.
- A **"group"** is a collection or folder containing multiple specimens. Creating a group is optional.
- An **"experiment"** is the complete file compatible with the NovoExpress software, which includes the analysis. It contains the samples, specimens, groups, and metadata of the analysis (date, analysis template used, gates, etc.). The file is saved on the computer with the ".ncf" file extension.
- A **"population"** in flow cytometry defines a cluster or set of dots or events on a plot or cytogram.

In NovoExpress, analyses are stored in the experiment file. When the software is launched, a new experiment file is automatically created but not yet saved. If the analysis is initiated at this point, the software will prompt to save the experiment file (which will have a ".ncf" file extension) when the first sample is run. Additionally, instead of creating a new experiment file from scratch, it is possible to open an existing ".ncf" file. The "Experiment Manager" is a window within the software that allows for visualization of the list of experiments, samples, and groups, as well as the creation of new ones.

#### ■ Creation of an "experiment"

Click on: File / New / New Blank Experiment (Fig. 7)

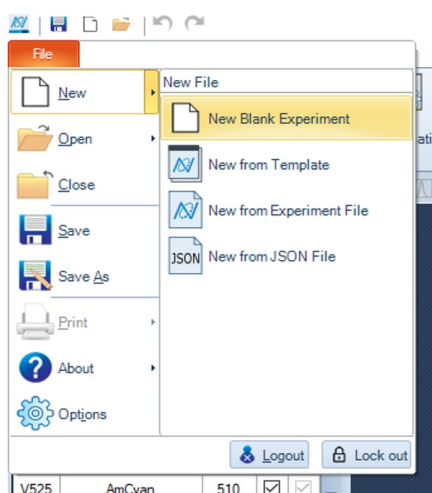


Figure 7: Creation of a new experiment

#### ■ Open an existing "experiment"

Click on: File / Open, then select the file with the browser.

#### ■ Create of a new specimen

Right-click on the first line (file\_name.ncf) in the **"Experiment Manager"** window, then select **"New Specimen"** (Fig. 8). If the **"Experiment Manager"** window is not visible, go to the "View" tab at the top and click on "Experiment Manager" to display it.

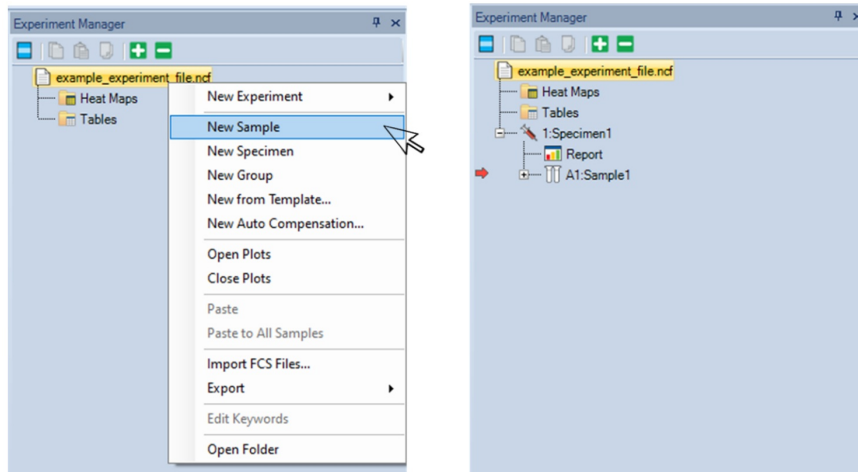


Figure 8: creation of new elements: sample, specimen or group, from the “experiment manager”.

### ■ Creation of a new sample

There are different ways to perform these actions:

1. Right-click on the first line (file\_name.ncf) in the “**Experiment Manager**” window, then select “New Sample” (similar to creating a new sample or group) (Fig.8).
2. If the last sample in the list is selected, click on “Next Sample” at the bottom left (Experiment Control).
3. Right-click on a sample in the list and select “Duplicate” (or after selecting a sample with a left click, press Ctrl+D on the keyboard). This is the fastest method and retains all the parameters and gates.

To move a sample from one specimen to another, right-click on the sample name, then select “Move to Specimen” and choose the desired specimen.

### ■ Creation of a new group

To create a new group, right-click on the first line (“file.ncf”) in the “**Experiment Manager**” window, then click on “**New Group**”.

Please note that the creation of a group is optional and can be done before or after the creation of a specimen.

To move a specimen into a group, right-click on the specimen, then select “Move to Group” and choose the desired group. All the samples contained within the specimen will be moved along with their events.

### • Duplication of groups, specimens and samples

To duplicate an item, right-click on it and select “Duplicate” (Fig.9).

Please note that when duplicating a sample, the cytometer settings (detectors, alias, stop conditions, etc.) and the analysis template (plots and gates) will be preserved. When duplicating a specimen or group, the list of samples will be copied, including their names, cytometer settings, and analysis template, but not the events. Duplicating a specimen is particularly useful when measuring the same type of samples repeatedly over time.



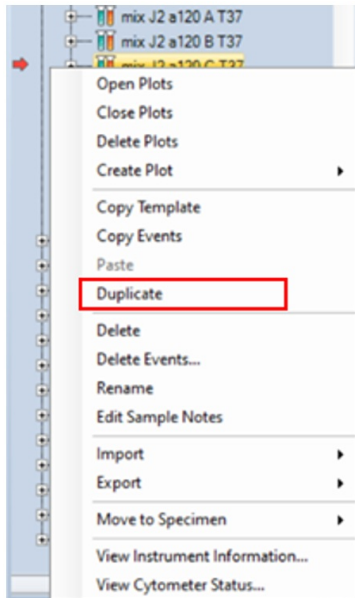


Figure 9: duplication of a sample to create an empty (without events) copy of the sample. Right-click on the item then "Duplicate".

## Sampling of the culture for the analysis

- 3
  - Collect a sample of the culture for analysis by using a laminar flow cabinet (or biosafety cabinet) and extracting approximately 300  $\mu$ l of the fresh co-culture into a specific flow cytometry tube, also known as a hemolysis tube.
  - Vortex the working mix of beads (as the beads have a tendency to settle in the tube) and then add 1% (vol:vol) of 1  $\mu$ m fluorescent beads, which are concentrated at approximately 800,000 beads/ml and are used as a standard during the analysis.
  - Mix the tube manually and place it in the tube holder of the flow cytometer.

**Comment :** The beads serve as stable spatial markers on the cytogram, aiding in the identification of cell populations. Another advantage of using beads is the ability to verify the proper functioning of the cytometer. In fact, the beads' population on the cytogram should appear fairly round, and any deviation from this shape could indicate a fluidic issue in the flow cytometer.

## Running the sample on the cytometer

- 4 In NovoExpress, the "Experiment Control" window enables the initiation of the analysis (Fig. 10).

Before running the sample, select the option "**Recover remaining samples**". This allows for the retrieval of any leftover material and helps prevent clogging of certain parts of the cytometer, thereby facilitating system maintenance. Additionally, ensure that the options "**Absolute Count**" (for calculating cellular densities in number of cells per ml) and "**Rinse after sampling**" (to rinse the sampler needle after each sample) are chosen.

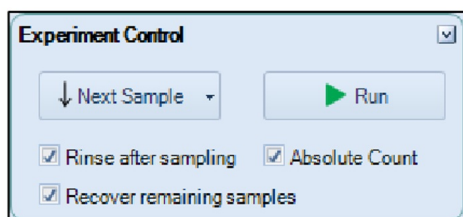


Figure 10: Experiment Control with the three option picked

Once the tube is properly positioned in the tube holder of the flow cytometer and the three options have been selected, click on "Run" to initiate the analysis. The sampler needle will extract the sample from the tube. It is important to keep the tube in its position throughout the analysis. The needle will then return the remaining volume back into the tube due to the selection of the "Recover remaining samples" option.



Figure 11: Active Sample Information: running information are visible during acquisition.

## Data visualisation and creation of the template

- 5 By clicking on the icons in the toolbar (Fig. 12), you can create the corresponding plot and gate.

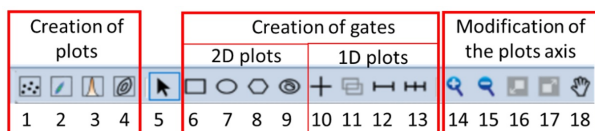


Figure 12: Screenshot of the toolbar in NovoExpress.

Description of the icons for the creation of plots, gates and adjustment of the plots (Fig. 12):

- 1: Dot plot (2D plot)
- 2: Density plot (2D plot)
- 3: Histogram (1D plot)
- 4: Contour plot (2D plot)
- 5: Pointer (basic tool)
- 6: Rectangular gate (for 2D plot)
- 7: Elliptical gate (for 2D plot)
- 8: Polygon gate (for 2D plot)
- 9: Freehand gate (for 2D plot)
- 10: Quadrant gate (for 2D plot)
- 11: Logic gate
- 12: range gate (for histogram)
- 13: Bi-range gate (for histogram)
- 14: Zoom in
- 15: Zoom out
- 16: Auto range of the axis
- 17: Full range of the axis
- 18: Move (pointer type to shift plot)

### • The template: Create density plot and histograms for the analysis of A120+ST147

To create the template for analyzing A120+ST147, follow these steps:

- 5.1 1) Create a 2D plot, such as a contour plot, and two histograms using the buttons in the toolbar.

- 5.2 2) Define the scales for the axes (refer to Fig. 13): Set the parameters' axis scale to "log" and the counts' axis scale (y-axis of the histogram) to "linear". This will enhance the contrast between the populations and improve visibility.
- 5.3 3) Define the axis of the 2D plot (refer to Fig. 13): Set the y-axis as Green-V-H and the x-axis as FSC-H.
- 5.4 4) Draw 2D gates (e.g., polygon gate) around the events corresponding to:
- The beads (located in the middle-left region).
  - The dinospores (below the beads, in the bottom-left region).
  - The hosts (in their respective region).

These gates will help separate and identify the different populations in the analysis.

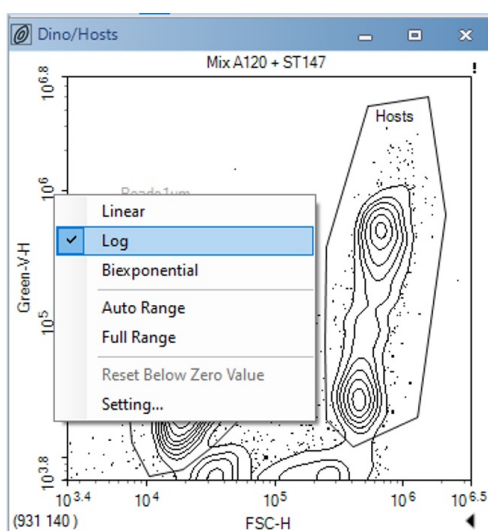


Figure 13: Selection of the scale type of the axis of a plot.

**Comment:** It is indeed easier to identify different populations on the cytogram when working with samples containing only one type. To facilitate this process, the following approach can be adopted:

- Run a blank sample containing only beads as a stable spatial marker. This will provide a reference for identifying the bead population on the cytogram.
- Run a sample containing only healthy hosts. This will allow you to identify the specific population corresponding to healthy hosts on the cytogram.
- Run a sample containing only dinospores. This will enable the identification of the dinospore population on the cytogram.

By conducting several trials and analyzing the resulting cytograms, you will be able to deduce the distinct dot clusters representing each population and assign specific gates accordingly. This iterative process helps in accurately identifying and separating the different populations within the analysis.

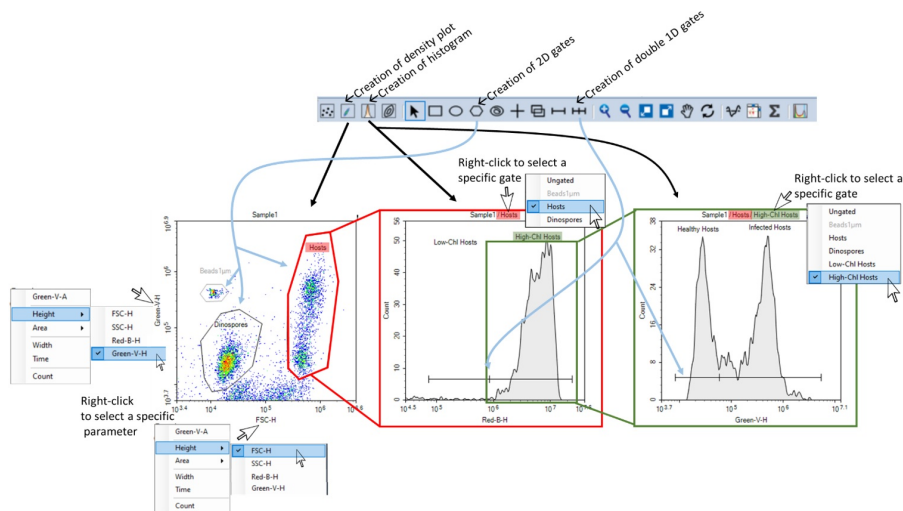


Figure 14: Creation of the template of the analysis with actual data displayed of a co-culture host and parasite with dinospores, healthy hosts and infected hosts.

5.5 5) Define the x-axis for the two histograms:

- a. Set Red-B-H as the x-axis for the first histogram.
- b. Set Green-V-H as the x-axis for the second histogram.

5.6 6) In the second plot (first histogram), select the "hosts" population for gating. This will allow you to focus on the host population in the analysis.

Create a 1D gate or a bi-range gate (a range gate is also suitable) to identify hosts rich in chlorophyll. This gate will help remove cell debris and dead cells from the host population. Name this gate "High-Chl Hosts." If you created a bi-range gate, you can name the other gate "Low-Chl Hosts."

In the third plot (second histogram), select the "High-Chl Hosts" population for gating. This will narrow down the analysis to the hosts with high chlorophyll content.

5.7 7) Create a bi-range gate in the third plot to determine two populations:

- a. The low green hosts, which will be the "Healthy Hosts" gate.
- b. The high green hosts, which will be the "Infected Hosts" gate.

By following these steps, you will be able to define gates and separate different populations, such as healthy hosts and infected hosts, in the analysis of A120+ST147.

**Comment:** You can adjust the upper and lower values of the axis to center the population in the plots by following these methods: Click and drag the extremities of the axis on the plots and/or use the tools in the toolbar for modifying the plot axis.

5.8 8) The template is a file that contains all the information regarding flow cytometer settings and plot visualization. This file should be in the specific format provided by ACEA Biosciences.

To create a template, follow these steps:

1. Right-click on the sample.
2. Click on 'Export,' and then select 'Export as Template...'

### 3. Save the template file.

To upload and use a template, use the following steps:

1. Right-click on a sample.
2. Choose 'Import,' then 'Template.'
3. Browse through the folders to select the desired template.

Alternatively, you can apply the selected template to the targeted sample(s) as followed:

1. Click on the '+' icon in front of the sample listed in the 'Experiment Manager.'
2. Drag and drop the 'Analysis' onto another sample, a specimen, or even onto the experiment (located at the top of the experiment manager).

**Comment:** It is good to know that the "Cytometer Setting" contains "Parameters", the "Stop condition", the "Flow rate" and the "Threshold" and can be dragged and dropped like the "Analysis" section but only to an empty sample because that information will define how the data of the sample will be recorded and cannot be modified after the acquisition.

Also, by double clicking on "Report section", you can have access to information and visualization and most importantly, the date (day and time) of the record of the sample. The date of the sample is also visible in the "statistical table" (See below, "Export data").

## Save and export data

### 6 Before the exportation of the data:

To ensure accurate analysis and proper data management in NovoExpress, please follow these guidelines:

- 1) Ensure well-defined gates around the desired populations: It is important to carefully place the gates on the cytograms to accurately capture the desired populations. Incorrectly placed gates can result in incorrect counts in the statistical tables. If gates are moved during subsequent analyses of the cytograms, the counts will automatically update to reflect the new population definitions.
- 2) Set the density unit to cells per ml: To ensure the unit of density is displayed as cells per ml, navigate to "Setting" > "General" > "Absolute Count" and select "No./ml". This setting will provide cell densities ("Abs. Count") in cells per ml.
- 3) Manually save the experiment file: It is necessary to save the experiment file, which includes all the plots, gates, and statistical tables. To save, either click on "File" > "Save" from the menu or click on the save icon. If you attempt to close NovoExpress without saving, a reminder message will prompt you to save the data. In such cases, click "Yes" to save the data before closing.

By following these guidelines, you can ensure accurate analysis, maintain the desired data settings, and properly save your experiment data in NovoExpress.

#### Creation and export for data table (density of the cell population, mean value of fluorescence...)

All types of data from the analysis, such as cell densities, fluorescence values, and more, can be stored in tables that can be exported as CSV files for use in spreadsheet software.

To create a statistical table in NovoExpress, follow these steps:

- Click on the "Home" tab.
- Look for the option to create a "Statistical Table" (refer to Fig. 15).
- Click on the "Statistical Table" button to create a new table.

By following these steps, you can create a statistical table in NovoExpress to organize and store your analysis data, which can then be exported as a CSV file.

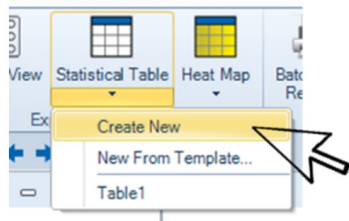


Figure 15: Creation of a data table (statistical table).

Once created, the statistical table is stored within the ".ncf" file and can be accessed from the top section of the "Experiment Manager" window (refer to Fig. 16).

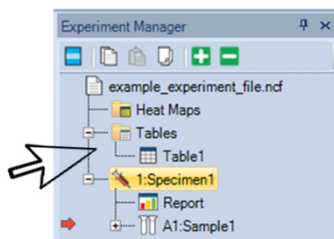


Figure 16: The "statistic table" reachable on the top in the "Experiment Manager" window.

**To set up the statistical table and choose the desired variables, follow these steps:**

- 1) Open the statistical table in NovoExpress.
- 2) In the statistical table window, select the metadata columns you want to include in the table. To do this:
  - a. Click on "Show column" or a similar option.
  - b. Choose the metadata variables you want to display, such as "Specimen", "Sample", and "Run time." These columns will provide metadata information about the samples.
- 3) Next, select the actual data columns you wish to include in the table. To do this:
  - a. Click on "Add column" or a similar option.
  - b. In the "Statistics" section, choose "Abs. Count" to include cell densities in cells per ml.
  - c. Select the gates for which you want to display the data. Hold the Ctrl key on your keyboard to select multiple gates.
  - d. Choose the gates corresponding to "Dinospores," "Healthy Hosts," and "Infected Hosts" (as shown in Fig. 17).

By following these steps, you can set up the statistical table in NovoExpress by selecting the desired metadata columns and adding data columns, including cell densities and specific gate populations, for analysis and further exploration. (Fig. 17).

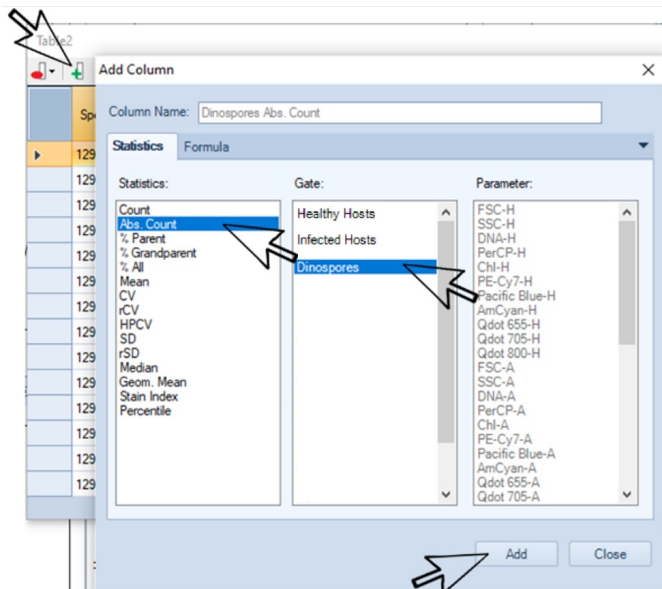


Figure 17: Selection of the types of data and gates of interest.

**Comment:** It is important to ensure that "Abs. Count" is selected in the statistical table, as it provides the density of cell types. This is different from the "Count" column, which simply represents the number of events and does not reflect density.

**To export the statistical table as a CSV file, follow these steps:**

- Open the statistical table in NovoExpress.
- Locate the "export" button, typically located in the upper right corner of the statistical table window.
- Click on the "export" button. This will initiate the export process.
- Choose a location to save the exported CSV file and provide a file name.
- Click "Save" to save the statistical table as a CSV file.

By following these steps, you can export the statistical table in CSV format, allowing you to further analyze and manipulate the data using other software or tools.

## Instrument shutdown

7 To turn off the flow cytometer and initiate the cleaning process, follow these steps:

- Locate the power button on the flow cytometer device.
- Press the power button. This will start the automatic cleaning process.

Note: The computer can be either on or off during this process, as the cytometer will perform the cleaning independently.

Additionally, you have the option to clean and rinse the cytometer without shutting it down, which allows another user to use it afterward. To do this in NovoExpress, follow these steps:

- Go to the "Instrument" tab in NovoExpress.
- Click on either "Cleaning" or "Fluidics Maintenance Sequences." This will open a window where you can create a custom

cleaning sequence.

- Set up the cleaning sequence according to your requirements, such as "Rinse + Cleaning" or "Debubbling + Rinse."

At the bottom left of the window, there should be an option to specify whether or not to shut down the system after cleaning. Select the appropriate choice based on your needs.

NovoExpress will provide an estimation of the time required for the cleaning process.

By following these steps, you can turn off the flow cytometer and initiate the cleaning process automatically or create custom cleaning sequences without shutting down the system in NovoExpress.

**Comment:** In the main window of the software, at the bottom left, there is an indication of the ongoing cleaning process. While the cleaning is in progress, you cannot analyze new samples. However, you can still visualize the samples, access the statistical tables, view the data, and make adjustments to the gates. This allows you to continue working with previously analyzed data and make any necessary modifications during the cleaning process.

**Comment:** it is possible to open several ".ncf" files at the same time. It can be useful if you want to see or export data from an older file during a current analysis (or when another user does an analysis). Also, it is convenient to compare sample between different file or experiments.

**Comment:** You can access the flow cytometer software on the computer even when the flow cytometer itself is turned off. This allows you to manage your samples, specimens, and groups, as well as work on the data before or after analysis.





# Thesis Supplementary Document 3










Comparative biology and ecology of apicomplexans and  
dinoflagellates: a unique meeting of minds and biology

Waller, R.F., Alves-de-Souza, C., Cleves, P.A., Janouškovec, J., Kayal, E., Krueger,  
T., Szymczak, J., Yamada, N., Guillou, L., 2022.

Trends in Parasitology 38, 1012–1019. <https://doi.org/10.1016/j.pt.2022.09.010>

## TrendsTalk

## Comparative biology and ecology of apicomplexans and dinoflagellates: a unique meeting of minds and biology

Ross F. Waller <sup>1,\*</sup>,<sup>@</sup> Catharina Alves-de-Souza <sup>2,@,\*</sup> Phillip A. Cleves <sup>3,@,\*</sup>  
Jan Janouškovec <sup>4,\*</sup> Ehsan Kayal <sup>5,\*</sup> Thomas Krueger <sup>1,@,\*</sup> Jeremy Szymczak <sup>6,\*</sup>  
Norico Yamada <sup>7,\*</sup> and Laure Guillou <sup>6,\*</sup>,<sup>@</sup>

The commonalities and convergences shared in apicomplexans and dinoflagellates are continually becoming more and more apparent, yet researchers across this myzozoan supergroup seldom meet at scientific meetings. The Conférence Jacques Monod meeting entitled ‘From Parasites to Plankton and Back: Comparative Biology and Ecology of Apicomplexans and Dinoflagellates’ sought to change this. Held at the Roscoff Marine Station in France on September 5–9, 2022, researchers spanning organisms, disciplines, and perspectives met to immerse themselves in the latest developments and discoveries across the group. The outcome was an exciting and stimulating view of the synergies, revelations, and opportunities enabled by expanding one’s view and network across this vast, spectacular and important biological group. In this TrendsTalk, the conference organizers and several young researchers present a synthesis of the key outcomes of this meeting of minds and biology.



Ross F. Waller



Catharina Alves-de-Souza

## The meeting’s rationale

The development of tunnel vision is a natural, almost inescapable phenomenon in most scientific fields. The complexities of biological systems and the tools and theories used to investigate them often lead us towards increasingly exclusive research communities, bodies of literature, and suites of technologies. But this comes with the danger of also constraining our thoughts, ideas, and conclusions. The constant challenge of scientists is to work against such forces that can limit our work, its vision, and opportunities.

Addressing this challenge was the overarching aim of the Conférence Jacques Monod meeting ‘From Parasites to Plankton and Back: Comparative Biology and Ecology of Apicomplexans and Dinoflagellates’ held in early September at the Roscoff Marine Station on the beautiful Brittany coast in France. Apicomplexans (including chromerids and colpodellids) and dinoflagellates (including perkinsids and syndinians) represent two major sister lineages of unicellular eukaryotes that have far-reaching impacts on both human and environmental health and function, particularly on a changing planet. Collectively they form the Myzozoa whose name is derived from the common apical complex structures known to be used for host cell invasion and myzocytotic feeding within both lineages. However, the research communities that study these two important groups seldom meet due to their general focus on either human and animal parasitic diseases or the biology and ecology of aquatic systems, respectively. But as both lineages are derived from a common ancestor, they maintain many shared traits. The meeting addressed six major themes to capture and explore this common biology: (i) diversity, phylogeny, and biogeography, (ii) life cycles and sexual reproduction, (iii) genome and organelle evolution, (iv) cell biology and host–symbiont interactions, (v) functional ecology, and (vi) new model systems, tools, and databases. Under these umbrellas, a remarkable spread of organisms, techniques, questions, and discoveries were presented and discussed (Figure 1).



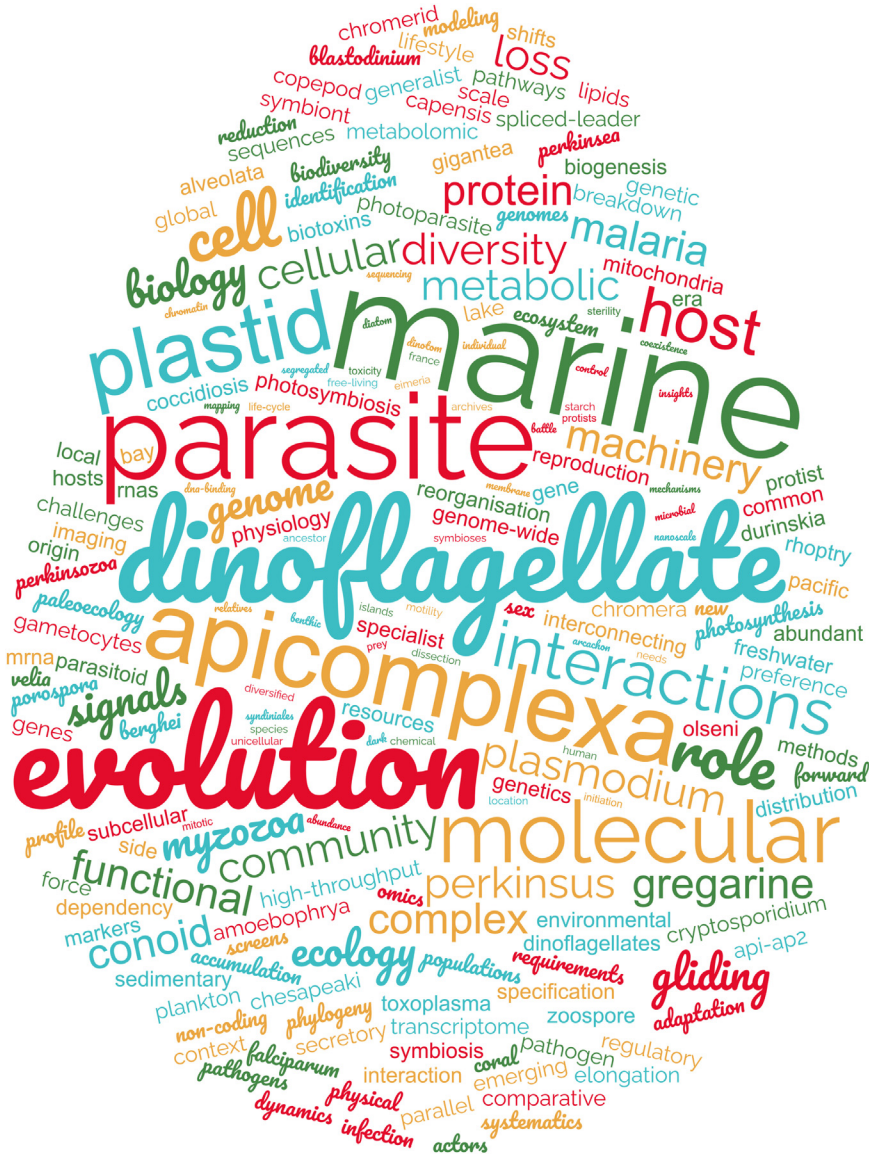
Phillip A. Cleves



Jan Janoušek



Ehsan Kayal



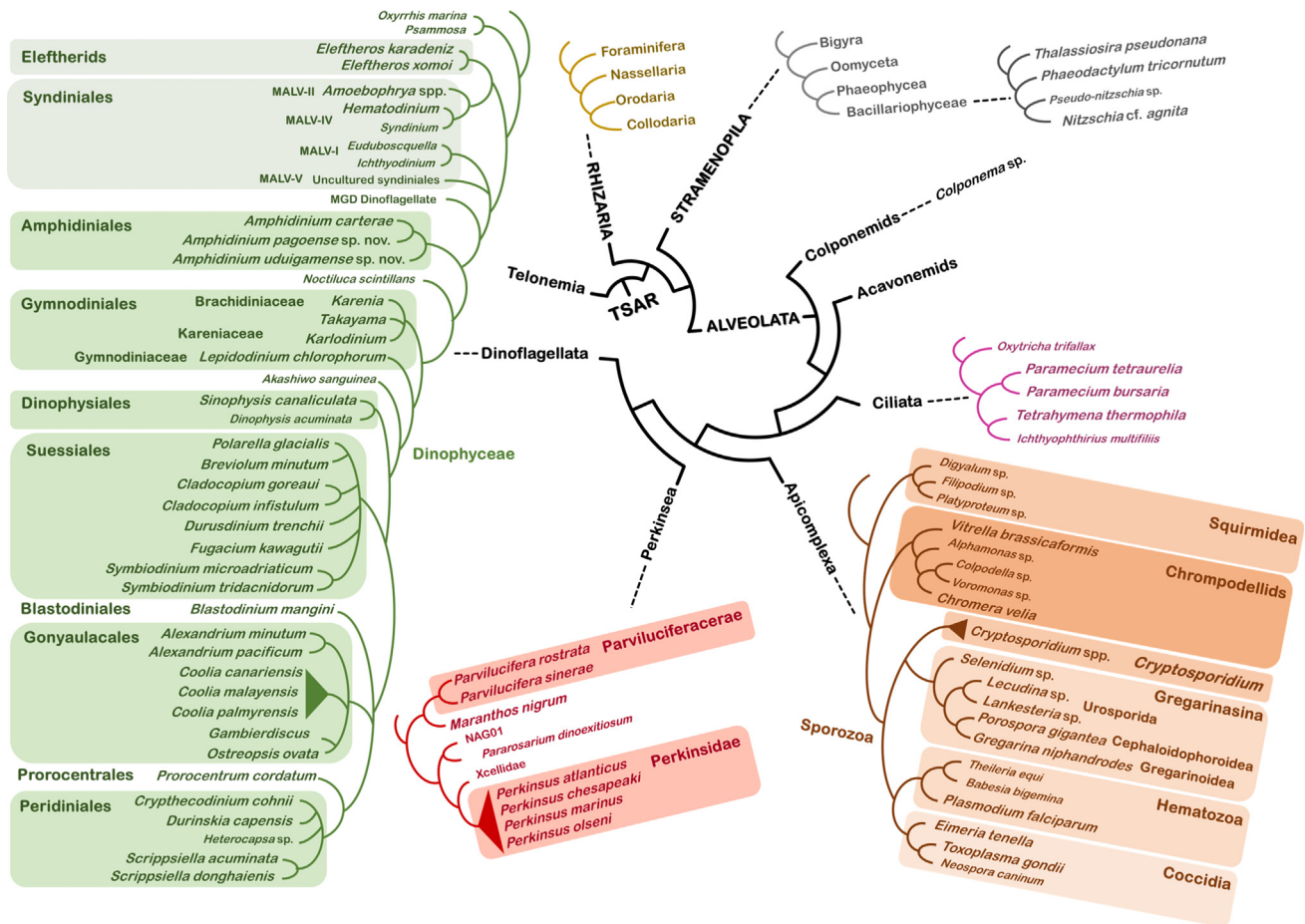
Trends in Parasitology

Figure 1. Word cloud of key terms listed in titles and abstracts from across the meeting. Figure created with [wordclouds.com](http://wordclouds.com).

**Diversity is the key to understanding Myzozoa**

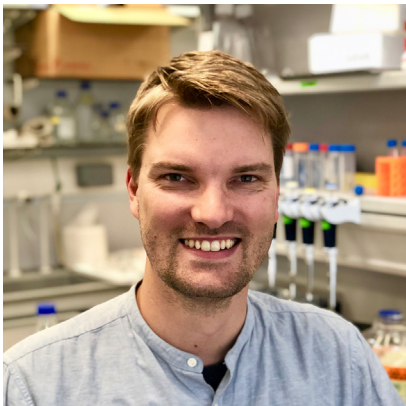
A clear theme that emerged during the meeting was how dependent our understanding of myzozoan biology is on our knowledge of the diversity of organisms found in these lineages. [Figure 2](#) represents the spectacular diversity of organisms presented as study subjects during the meeting – which demonstrated how much we draw on this breadth for our insights. But there are still many gaps yet to fill. The keynote address by Patrick Keeling (University of British Columbia) illustrated recent notable gains that have been made in our knowledge of both apicomplexans, where gregarines are emerging as major components of diversity, and dinoflagellates, where new heterotrophic species are also revealing significant new evolutionary trajectories. Further talks





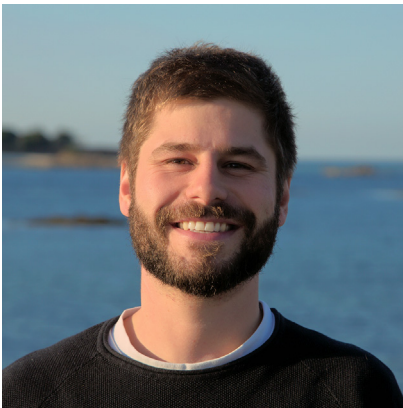
Trends in Parasitology

Figure 2. The diversity of a meeting. Phylogeny of major clades of Myzozoa: dinoflagellates (green), perkinsids (red), and apicomplexans (orange), showing in enlarged bold font all the organisms that were subjects of presentations during the course of the meeting. Even further diversity was presented in the form of undescribed but major myzozoan clades currently known only from metagenomic sequence data.

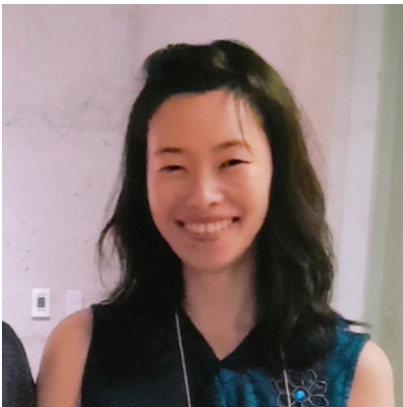


Thomas Krueger

illustrated how the deep-branching lineages of both groups are also expanding, with squirmids and eleutherids, both recently discovered as new basal groups that inform on additional diversity within each major lineage. Collectively, these new organisms are redefining our understanding of the relationships within these groups. For example, gregarines are now recognised as multiple lineages, whereas *Cryptosporidium*'s true relationship within Apicomplexa remains uncertain. Further major myzozoan diversity was revealed by both Cécile Lepère (Université Clermont Auvergne) and Sebastian Metz (Station Biologique de Roscoff) who showed that perkinsids, best known as parasites of marine molluscs and phytoplankton, are also much more diverse than previously appreciated. Evidence of perkinsids is now widely found in freshwater habitats as well as soil, which represent new diverse and often habitat-specific lineages. A common theme for much of the new diversity is the lack of culturability of these organisms, or even their physical observation where environmental (e)DNA surveys are the only evidence of their existence. This challenges our understanding of ecological roles that this myzozoan diversity fulfils, and points to much work still to be done.



Jeremy Szymczak



Norico Yamada



Laure Guillou

### Ancestral states and parallelisms

From the appreciation of Myzozoan diversity, two further themes of the meeting emerged: (i) how pervasive common characters are, but also (ii) how parallelisms have repeatedly occurred across the group. The common perception of parasitism evolving only once early in apicomplexans is overturned by the discovery of the repeated emergence of parasitism in Apicomplexa presented by both Patrick Keeling and Jan Janouškovec (University of Southampton). Furthermore, Sonja Rueckert's (Edinburgh Napier University) address explored if some gregarines might actually be mutualists providing positive benefits to their hosts rather than negative ones. Of course, parasitism is also found throughout perkinsids and dinoflagellates. Laure Guillou (Station Biologique de Roscoff) illustrated how the dinoflagellate parasite *Amoebophrya* displays superb adaptations for parasitism where it invades its host, initially establishes a parasitophorous vacuole, and then remodels the host's nucleus where it ultimately resides, feeds, and replicates. This dinoflagellate even selectively sustains the energy-producing capacity of its photosynthetic host to achieve greater parasite replication. The sophistication of this parasite–host interaction, and its parallels to the better-studied apicomplexans, reveal how dispersed such complex traits are across the group. Indeed, versatility of trophic modes was a central theme of myzozoan biology and evolution explored at the meeting, with multiple shifts between phototrophy, heterotrophy, and parasitism found. Victoria Jacko-Reynolds (University of British Columbia) showed examples of photoparasitic dinoflagellates of the genus *Blastodinium* in the throes of conversion from autotrophy to parasitism, showing that these shifts are contemporary and ongoing.

A common element of myzozoan cells that might explain these core themes of their biology is the ancestral apical complex structure linked to both feeding and invasion. Dominique Soldati-Favre (University of Geneva) and Markus Meissner (Ludwig Maximilians Universität) both presented superb studies of the assembly, structure, and function of the *Toxoplasma* conoid and apical complex using the molecular and cell biology tools that only such a well-developed model organism can allow. Maryse Lebrun (Université de Montpellier) further revealed the molecular machinery for rhoptry apical secretion during *Toxoplasma* invasion. Notably, her group discovered elements of this machinery through its conservation with ciliates, hinting that these processes are ancient rather than new. Moreover, Jeremy Szymczak (Sorbonne Université) tantalized us with images of similar apical complex structures in the parasitic dinoflagellate *Amoebophrya*, and such structures have been widely observed in all myzozoan groups including both parasites, predatory heterotrophs, and even autotrophs. Collectively, these studies reveal the deep ancestry of these common cellular machineries for interactions with other cells and organisms and that serve multiple different lifestyles. In turn, the theme of mixotrophy, cells that are both photosynthetic and heterotrophic, was discussed as greatly understudied in Myzozoa but is likely central to both the ecological functions of this group and its propensity to oscillate between different trophic modes.

Symbiosis is another topic where parallelism was a clear theme. Fabrice Not (Station Biologique de Roscoff) illustrated how the perception of Symbiodiniaceae being the primary dinoflagellate symbiotic group is misleading, with lineages found across dinoflagellate diversity forming partnerships with a wide variety of other organisms. Both he and Senjie Lin (University of Connecticut) touched on some of the cellular and genomic adaptations seen upon entering into such relationships, but both showed that this is an

underexplored area where much further work is needed. Myzozoan organisms as the hosts of endosymbiotic partners is another major theme of diversity and parallelism in this group. The plastid in both photosynthetic and nonphotosynthetic myzozoans has been a topic of strong interest for several decades, but still new discoveries and revisions are being made. Elisabeth Hehenberger (Czech Academy of Sciences) showed that parallel loss of plastid function is ever more apparent than was realized when wider surveys of taxa are made. Even parallel loss of the organelle genome or the organelle itself, both considered exceedingly rare events, are now evident. Miroslav Obornik (University of South Bohemia) illustrated how we still cannot even be sure of a simple ancestry of the myzozoan plastid(s). His group's work argues for lateral gain of a chlorophyll *c*-containing plastid from eustigmatophytes, and possible subsequent early parallel plastid replacement in dinoflagellates, as still credible possibilities. From ancient to new, Noriko Yamada (University of Konstanz) demonstrated how much we can learn from recent cases of plastid uptake in dinoflagellates. She has developed multiple cell models bearing nascent diatom endosymbionts offering new insights into the patterns and processes of these developing relationships. Similar to plastids, mitochondrial evolution in Myzozoa also follows these patterns of parallelism. Varsha Mathur (University of Oxford) exploited single-cell transcriptomics of unculturable gregarines to illuminate patterns of parallel functional loss in mitochondria, notably of complex III and IV of the electron transport chain. Moreover, mitochondrial parallel adaptations also span the group, with independent fragmentation and relocation of *cox1* seemingly having occurred in some gregarines (Varsha Mathur) as well as the dinoflagellate *Amoebophrya* (Ehsan Kayal, Station Biologique de Roscoff).

In this backdrop of parallelism, resolving the state of ancestral features can be challenging. Gliding motility is closely associated with parasitism in Apicomplexa, and Isabelle Tardieux (Université Grenoble Alpes) dazzled us with her biophysical studies of force-delivery mechanisms driving the well-studied gliding patterns of *Toxoplasma*. However, some of the champions of gliding speed are found in the gregarines, and genomic analysis of *Porospora* by Isabelle Florent (Muséum National d'Histoire Naturelle) showed that the identifiable molecular signatures of gliding are relatively limited when considered more broadly. The fascinating but open questions of when and how gliding developed in Myzozoa is thus a challenge to investigate by genomics alone. Complex cell cycles are another trait that reaches across all groups. Differentiated sexual stages are often key to transmission and persistence, and Oliver Bilker (Umeå University) showed his use of genetic screens in *Plasmodium* to identify a wide range of fertility-related genes. While sex in the nearest photosynthetic relatives, *Chromera* and *Vitrella*, is less well understood, the generation of motile zoospores was shown by Jitka Richtová (Czech Academy of Sciences) to be equally carefully controlled and likely responsive to both metabolic and environmental signals. Jeremy Szymczak also demonstrated that transmissive stages of parasitic dinoflagellates can employ two distinct differentiated spore forms, although the significance of these is also yet to be elucidated. Similarly, Rosa Figueroa (Instituto Español de Oceanografía) summarized the life-cycle complexities of bloom-forming dinoflagellates in general, and how much is still to be learned of the strategies and control of the different sexual and life-cycle stages in this group. Finally, Shauna Murray (University of Technology, Sydney) discussed secondary metabolite production in dinoflagellates and how both gene expansion and lateral gene transfer contribute to the wide range of toxins that many produce, often with major impacts on food chains and ecosystems. The complex evolution of these traits, however, remains difficult to unpick, and the

secondary metabolism in apicomplexans is substantially unexplored, further confounding comparisons or the derivation of common principles.

### Tools and technologies and the path forward

A final core theme of the meeting was how new tools and technologies are driving the opportunities for discovery and understanding in Myzozoa. Of course, not all organism systems are equal, and the disparity was stark between those that can be cultured and genetically manipulated, versus those that must be field-isolated for samples or are even only detectable as meta-genomic traces from the environment. Dominique Soldati-Favre championed the role of observation in scientific discovery, and her group's use of ultrastructure expansion microscopy (U-ExM) demonstrated how new resolution should be achievable across the field where cells can be collected. Markus Meissner's engineered filamentous actin-detecting chromobodies have also unveiled a new era for understanding actin dynamics and function, and testing for conservation of these processes should also now be available in all genetically transformable groups. A noteworthy breakthrough in model organism development has been that for *Cryptosporidium* led by Boris Striepen's group (University of Pennsylvania). Through this they provide a revised understanding of this important parasite's life cycle, including sexual commitment, and knowledge of new cell compartments driving host-interactions, all of which can now be interrogated through reverse genetics.

Sequencing technologies remain at the heart of much of myzozoan research, particularly where cells cannot be cultured. Single-cell genomics and transcriptomics have enabled remarkably penetrating insights, in some cases where only a few tens of cells have ever been seen and collected (e.g., the eleutherids presented by Elisabeth Hehenberger). Single-cell RNAseq of cell populations is also giving stunningly resolved detail of the transcriptional programs of life cycles and differentiated states, and these were shown in several presentations. A common challenge, however, is the 'dark genetic matter', the unique genes and proteins either within myzozoan groups as a whole or in individual lineages. Isabelle Florent lamented this challenge in interpreting gregarine genomes, and Lucie Bittner (Muséum National d'Histoire Naturelle) and others are tackling it with sequence similarity networks (SSNs), structure similarity networks (e.g., via AlphaFold), gene correlation with ecosystems and biogeography, and machine learning to shed light on the 'dark proteome'. A different strategy to illuminate the function of new, derived, and unstudied proteins is the 'LOPIT' method of spatial proteomics employed by Ross Waller's group (University of Cambridge). This method is limited only by the culturability of an organism and provides genome-level resolution of the subcellular distribution of a cell's proteins, and it enables comparative cell biology across Myzozoa and beyond. Forward genetic screens to identify the molecules of function are also starting to be applied more widely in Myzozoa. While the use of targeted mutations in *Toxoplasma* and *Plasmodium* allowed screening for proteins involved in actin networks and sex functions by Markus Meissner and Oliver Billker, respectively, Ugo Cenci (University of Lille) demonstrated that lack of experimental genetics is not a barrier to forward genetics. Using UV-based mutation and genome sequencing in *Chromera*, he is identifying the genes for starch synthesis in this otherwise genetically intractable system. The wide potential of 'omics' data, and increasingly its correlation with 'metadata', was reinforced by David Roos's (University of Pennsylvania) eloquent description of the origins and current state of the [VEuPathDB.org](https://veupathdb.org) databases and tools. The challenge for Myzozoa, however, is to span this entire group with integrated tools, and the importance of this was recognised by all.



In a changing planet where myzozoan ecosystems are literally as vast as the oceans, computational tools are also essential and being applied to understanding and predicting organism dynamics and responses. Catharina Alves-de-Souza (University of North Carolina Wilmington) showed us how she is tackling the question of how two parasites with very different parasitic strategies (*Amoebophrya* and *Parvilucifera*) are able to coexist while exploiting overlapping hosts. Drawing on experimental data, she showed how population modelling is required to identify the complex roles of both biotic and abiotic factors that shape the dynamics of these systems. Cécile Jauzein (IFREMER) further explored how host programmed cell death and generation of allelopathic compounds might be further incorporated into these models. Both presentations stress the importance of assessing host–parasite dynamics in plankton assemblages from a community point of view instead of relying on the pairwise comparison based on networking analyses of metabarcoding data. Even Garvang (University of Oslo) similarly built epidemiological models to predict the best experimental strategies to study the impacts of parasitic dinoflagellates on copepods. In doing so, he reminded us that copepods are the most abundant arthropods on the planet and enormously important for ocean food webs. Finally, Raffaele Siano (IFREMER) stunned the audience by describing how he has developed methods to revive dinoflagellate cysts from sediments that are over 150 years old. His group pursue palaeoecology studies that integrate revived dinoflagellates and their physiology examination, with sediment DNA sequencing and metabolomics. Using these tools, they have been able to determine the impacts on coastal protist communities of major historical environmental disturbances such as World War II and changing agricultural practices affecting the Brittany coast.

### Perspectives and outstanding challenges

While this report cannot comprehensively cover all the wonderful biology and science that was presented at this meeting, nor fully convey the excitement of many for this convergence of systems and minds, it seeks to illustrate the success of bringing diverse researchers working across myzozoan biology together. The wealth of shared biology was obvious when viewed en masse. But it was also clear that the interpretations that we make in individual groups are rarely complete without recognition of equivalent or differing states amongst the relatives. It was powerful to see how different tools have been developed, adapted, and exploited across different systems, and there is clear potential for the wider application of many of these tools and techniques across this group. New partnerships were formed, and it was pleasing to observe one *Plasmodium* researcher slipping a dinoflagellate culture in their luggage before departure. But the challenges were also brought into focus. There is vast diversity still to be discovered and/or identified at an organism level, and gaps in our interpretation of this important group will remain while this is the case. For example, much of the Marine Alveolate (MALV) groups remain completely uncharacterized, and predatory heterotrophs are also shown to be under-sampled and under-studied in general. The limited culturability of many taxa is a huge challenge, as is the lack of widely available experimental genetic tools, and these are challenges that we must continue to tackle. While much biology is shared, the lineage-specific differences must also be accounted for and understood, with challenges of interpreting the aberrant molecular genetics of dinoflagellates and perkinsids one example and theme of several presentations. This field is exciting and spectacular, and there is still so much work to be done. And it is with great excitement that we announce that the organizers of Conférence Jacques Monod have proposed to host this meeting on an ongoing 3-year cycle. If you missed out this time, be sure not to for the next one in 2025.

### Acknowledgments

We thank the Gordon and Betty Moore Foundation for sponsoring this meeting.

<sup>1</sup>Department of Biochemistry, University of Cambridge, Cambridge, CB2 1QW, UK

<sup>2</sup>Center for Marine Science, University of North Carolina Wilmington, Wilmington, NC 28409, USA

<sup>3</sup>Department of Embryology, Carnegie Institution for Science, Baltimore, MD, USA

<sup>4</sup>School of Biological Sciences, University of Southampton, Southampton, SO17 1BJ, UK

<sup>5</sup>Department of Ecology, Evolution, and Organismal Biology, Iowa State University, Ames, IA, USA

<sup>6</sup>Sorbonne Université, CNRS, UMR7144 Adaptation et Diversité en Milieu Marin, Ecology of Marine Plankton (ECOMAP), Station Biologique de Roscoff, 29680 Roscoff, France

<sup>7</sup>Department of Biology, University of Konstanz, Konstanz, 78457, Germany

\*Correspondence:

[r1w26@cam.ac.uk](mailto:r1w26@cam.ac.uk) (R.F. Waller), [cathsouza@gmail.com](mailto:cathsouza@gmail.com) (C. Alves-de-Souza), [cleves@carnegiescience.edu](mailto:cleves@carnegiescience.edu) (P.A. Cleves),

[janjan.cz@gmail.com](mailto:janjan.cz@gmail.com) (J. Janouškovec), [ehsan.kayal@sb-roscoff.fr](mailto:ehsan.kayal@sb-roscoff.fr) (E. Kayal), [tk556@cam.ac.uk](mailto:tk556@cam.ac.uk) (T. Krueger),

[jeremy.szymczak@sb-roscoff.fr](mailto:jeremy.szymczak@sb-roscoff.fr) (J. Szymczak), [norico.yamada@uni-konstanz.de](mailto:norico.yamada@uni-konstanz.de) (N. Yamada), and [lguillou@sb-roscoff.fr](mailto:lguillou@sb-roscoff.fr) (L. Guillou).

<sup>®</sup>Twitter: [@RossWaller3](https://twitter.com/RossWaller3) (R.F. Waller), [@C\\_AlvesDeSouza](https://twitter.com/C_AlvesDeSouza) (C. Alves-de-Souza), [@pacleves](https://twitter.com/pacleves) (P.A. Cleves), [@CoratTKrueger](https://twitter.com/CoratTKrueger) (T. Krueger), and [@guillou\\_laure](https://twitter.com/guillou_laure) (L. Guillou).

<https://doi.org/10.1016/j.pt.2022.09.010>

© 2022 Elsevier Ltd. All rights reserved.



# Thesis Supplementary Document 4

*Amoebophrya ceratii*

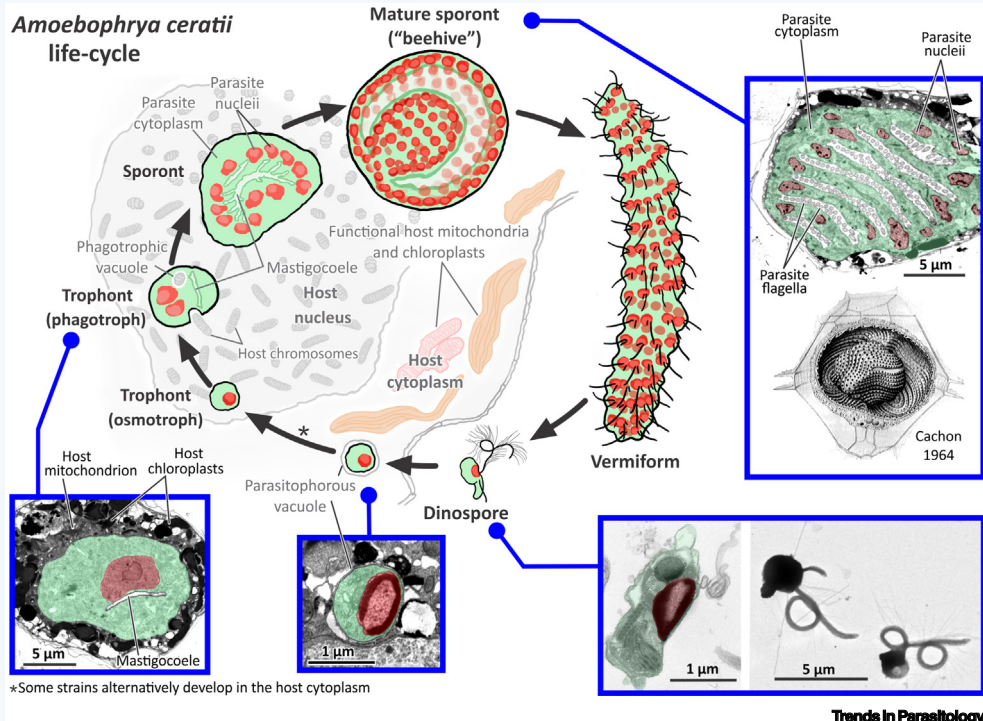
Guillou, L., Szymczak, J., Alves-de-Souza, C., 2023. *Amoebophrya ceratii*.

Trends in Parasitology 39, 152–153. <https://doi.org/10.1016/j.pt.2022.11.009>

# Amoebophrya ceratii

Laure Guillou <sup>1,\*</sup>, Jeremy Szymczak <sup>1</sup> and Catharina Alves-de-Souza <sup>2,@</sup>

<sup>1</sup>Sorbonne Université, CNRS, UMR7144 Adaptation et Diversité en Milieu Marin, Ecology of Marine Plankton (ECOMAP), Station Biologique de Roscoff, 29680 Roscoff, France  
<sup>2</sup>Algal Resources Collection, Center for Marine Science, University of North Carolina Wilmington, Wilmington, NC 28409, USA



**KEY FACTS:**

*A. ceratii* is haploid, with V-shaped permanently condensed chromosomes during most of its life cycle. Genomes are rather small (hundreds of Mb) compared with other dinoflagellates (~3–245 Gb).

Genes are grouped into unidirectional clusters, and mRNAs are trans-spliced. In two strains, introns were predominantly non-canonical (differing from the GT-AG motif) and partly composed of introns acting as transposable elements.

The complex III of the oxidative phosphorylation (OXPHOS) pathway is missing, breaking the mitochondrial electron transport chain into two independent operating subchains.

**DISEASE FACTS:**

Infection occurs either in the nucleus or cytoplasm. Once inside the host, the *A. ceratii* nutrition mode starts with osmotrophy and then shifts to phagotrophy. Predigested host chromosomes are sucked into feeding tubes and consumed in food vacuoles.

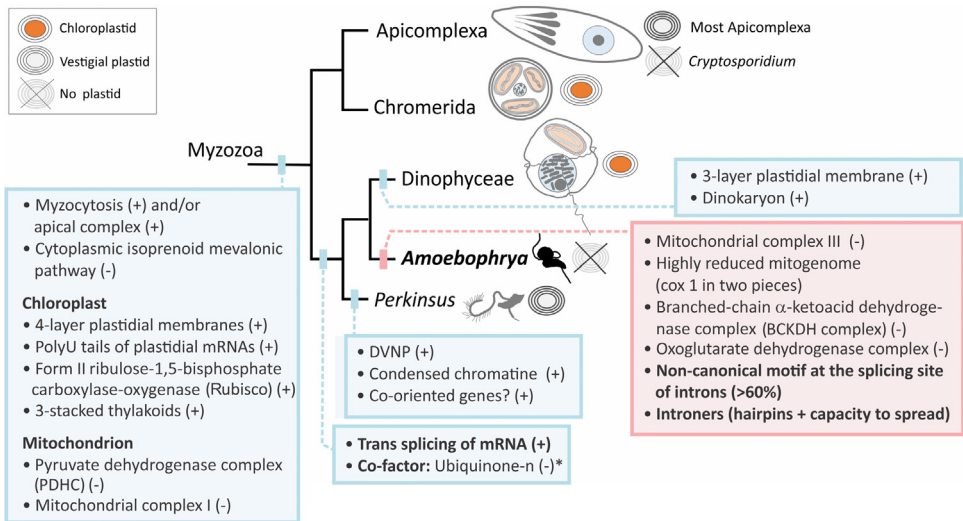
Dinoflagellates are one of the most abundant and diverse components of marine plankton. Many of them, if not all, are infected by the endoparasitoid *Amoebophrya ceratii* (Syndiniales, Marine Alveolate Group II), an early emerging dinoflagellate group. As these parasitoids frequently display narrow host ranges, they are believed to be as diversified as their hosts and are composed of cryptic species. Infections last 2–4 days and end with the host's death and the release of a transient fast-swimming colony (the vermiform) that fragments within a few hours into hundreds of infective cells (dinospores). Due to this exponential growth, *A. ceratii* exerts striking potential on top-down control of planktonic dinoflagellate blooms in natural waters. Both *A. ceratii* and their dinoflagellate hosts share the same common ancestor, a red myzozoan microalga. *A. ceratii* is rather atypical by having lost its plastid and having an extremely reduced mitochondrial DNA. It can be cocultivated with its host but not cryopreserved.

During the infection, the host is 'zombified': it still swims, with functional mitochondria and chloroplasts, despite the complete digestion of its nucleus. The energy produced by the host organelles likely benefits the parasitoid.

The lifespan of spores is only a few days. *A. ceratii* is able to enter dormancy simultaneously with its host resting cyst, emerging months later to propagate novel infections.

**TAXONOMY AND CLASSIFICATION:**

- PHYLUM:** Myzozoa
- CLASS:** Dinoflagellata
- ORDER:** Syndiniales
- FAMILY:** Amoebophryidae
- GENUS:** *Amoebophrya*
- SPECIES:** *A. ceratii* (species complex composed of multiple cryptic species)



\*Correspondence: [lguillou@sb-roscoff.fr](mailto:lguillou@sb-roscoff.fr) (L. Guillou).  
 @Twitter: [@guillou\\_laure](https://twitter.com/guillou_laure) (L. Guillou) and [@AC\\_AlvesDeSouza](https://twitter.com/AC_AlvesDeSouza) (C. Alves-de-Souza).



## Acknowledgments

This research is funded by the ANR (ANR-21-CE02-0030-01 EPHEMER). Electron microscopy images were provided by Sophie Lepanse (MERIMAGE platform, Station Biologique of Roscoff) and Gérard Prensier (in memory). Estelle Bigeard (Station Biologique of Roscoff) is in charge of parasitic strains within the Roscoff Culture Collection (RCC).

## Declaration of interests

The authors declare no competing interests.

## Resources

[www.aquasymbio.fr/en/amoebophrya-ceratii-species-complex](http://www.aquasymbio.fr/en/amoebophrya-ceratii-species-complex)

[www.roscoff-culture-collection.org/](http://www.roscoff-culture-collection.org/)

## Literature

1. Cachon, J. (1964) Contribution à l'étude des péridiniens parasites. Cytologie, cycles évolutifs. *Ann. Sci. Nat. Zool.* 6, 1–158
2. Cai, R. *et al.* (2020) Cryptic species in the parasitic *Amoebophrya* species complex revealed by a polyphasic approach. *Sci. Rep.* 10, 2531
3. Chambouvet, A. *et al.* (2008) Control of toxic marine dinoflagellate blooms by serial parasitic killers. *Science* 322, 1254–1257
4. Chambouvet, A. *et al.* (2011) Interplay between the parasite *Amoebophrya* sp. (Alveolata) and the cyst formation of the red tide dinoflagellate *Scrippsiella trochoidea*. *Protist* 162, 637–649
5. Coats, D.W. and Park, M.G. (2002) Parasitism of photosynthetic dinoflagellates by three strains of *Amoebophrya* (Dinophyta): parasite survival, infectivity, generation time and host specificity. *J. Phycol.* 38, 520–528
6. Decelle, J. *et al.* (2022) Intracellular development and impact of a marine eukaryotic parasite on its zombified microalgal host. *ISME J.* 16, 2348–2359
7. Farhat, S. *et al.* (2021) Rapid protein evolution, organellar reductions, and invasive intronic elements in the marine aerobic parasite dinoflagellate *Amoebophrya* spp. *BMC Biol.* 19, 1
8. John, U. *et al.* (2019) An aerobic eukaryotic parasite with functional mitochondria that likely lacks a mitochondrial genome. *Sci. Adv.* 5, eaav1110
9. Kayal, E. and David, R.S. (2021) Is the dinoflagellate *Amoebophrya* really missing an mtDNA? *Mol. Biol. Evol.* 38, 2493–2496
10. Kayal, E. *et al.* (2020) Dinoflagellate host chloroplasts and mitochondria remain functional during *Amoebophrya* infection. *Front. Microbiol.* 11, 600823



## Résumé long en français

Les interactions symbiotiques parasitaires ont un impact significatif sur l'écologie et l'évolution des espèces impliquées, ainsi que sur la dynamique des écosystèmes. Cependant, il est rare de bien connaître le cycle de vie de ces parasites et encore plus rare de comprendre les stratégies qu'ils développent pour optimiser leur survie et leur capacité d'infection.

La communication chimique, qui repose sur production et la détection de substances sémiachimique, telles que les phéromones, les kairomones ou les messagers chimiques, etc., joue un rôle prépondérant dans les interactions intra et inter-espèces. Cette forme de communication est fréquemment utilisée dans le règne animal pour diverses fonctions, telles que l'attraction sexuelle, la délimitation du territoire, la recherche de nourriture et l'alarme en cas de danger. Dans un environnement aquatique, ces signaux sont directement libérés dans l'eau et se propagent depuis leur point d'émission, créant ainsi un gradient chimique.

En première approche, ces molécules font partie du métabolome, et les approches métabolomiques sont cruciales pour comprendre ces interactions symbiotiques avant, pendant et après l'interaction. C'est le concept central de ce travail de thèse, où je me suis intéressé non seulement au cycle de vie d'un parasite aquatique, mais également à la production de molécules susceptibles d'influencer l'infectivité du parasite ou la résistance de l'hôte.

Le modèle de parasite utilisé au cours de cette thèse, *Amoebophrya ceratii*, appartient à un groupe de parasites largement répandus et diversifiés au sein du plancton marin, connus sous le nom d'Amoebophryidae ou Marine Alveolate Group II (MALVII). Ces parasites ciblent principalement les dinoflagellés, y compris des espèces hôtes toxiques ou nuisibles. Un aspect caractéristique de ce parasite est son mode de vie : il tue inévitablement son hôte pour accomplir son cycle infectieux, mais maintient en même temps son hôte en vie pendant la majeure partie de son développement intracellulaire, fonctionnant ainsi comme un parasitoïde biotrophe.

Les Amoebophryidae ont un spectre d'hôte relativement restreint, étant capables d'infecter seulement quelques espèces hôtes. En culture, le stade intracellulaire de ce parasite a une durée d'environ 36 heures, après quoi il aboutit à la production de spores libres. Ces spores n'ont que quelques jours pour détecter et pénétrer un nouvel hôte au sein d'une communauté complexe et en constante évolution.



## Abstracts

Ce projet de thèse avait donc pour but d'améliorer la compréhension de ce stade libre et d'étudier ses capacités sensorielles, notamment en ce qui concerne le chimiotactisme envers son hôte. Pour cela, j'ai utilisé un large éventail de techniques, allant de la cytométrie de flux à la transcriptomique et à la métabolomique. J'ai travaillé au plus près de l'interaction en utilisant des approches de cellules isolées ou de microfluidique. Enfin, j'ai également réalisé de nombreux tests expérimentaux en batch qui m'ont permis de tirer des conclusions statistiques sur certains processus clés.

Globalement, ce travail a servi à : 1) une meilleure compréhension du cycle de vie de ce parasite, en particulier la reconnaissance formelle d'une reproduction sexuée ; 2) la production du métabolome associé à l'infection à différents stades de développement du parasite (intra- et extracellulaire) ; 3) la réalisation des tout premiers tests en microfluidique afin de tester les capacités de chimiotactisme du parasite envers son hôte.

Le premier chapitre de cette thèse a révélé la présence de deux morphotypes de spores grâce à la cytométrie en flux. Des techniques telles que la microscopie électronique, la métabolomique et la transcriptomique, ainsi que des tests expérimentaux, ont permis d'identifier que le morphotype plus petit est le stade infectieux, tandis que le morphotype plus grand est non infectieux et lié à la reproduction sexuée du parasite. Ces deux types de spores se distinguent par leur capacité de nage, leur durée de vie, leur cytologie, et des caractéristiques moléculaires.

Nous avons pu démontrer qu'une cellule hôte infectée produisait un type de spores unique (soit infectieux, soit sexuelle), suggérant que la décision de produire l'une ou l'autre des spores se fait en amont, potentiellement en fonction de la densité des spores infectieuses dans la génération précédente. En résumé, cette étude identifie le premier exemple de cellules sexuelles chez les Amoebophryidae, ainsi que les conditions environnementales nécessaires pour déclencher le processus de reproduction sexuée. Le type de reproduction, ainsi que le moment de la fusion et de la méiose restent cependant encore obscures.

Dans le deuxième chapitre de notre étude, nous avons observé des modifications significatives des métabolites internes (endométabolites) et des métabolites potentiellement sécrétés (exométabolites) au cours de l'infection de l'hôte par les parasites. Ces modifications sont associées à des changements physiologiques notables chez les parasites, se traduisant par des altérations morphologiques et transcriptionnelles visibles. Cependant, notre compréhension des changements métaboliques associés, tels que l'accumulation ou la sécrétion de métabolites, demeure limitée, bien que ces métabolites puissent jouer un rôle essentiel dans la

virulence du parasite ou la défense chimique de l'hôte. Pour tester cette dernière hypothèse, nous avons réalisé des essais biologiques. Lorsque nous avons pré-incubé l'hôte avec les exsudats du parasite, nous avons observé une réduction de la prévalence de l'infection après 8 heures, bien que cet effet ait disparu après 24 heures. De plus, nous avons étudié l'impact de l'incubation de l'hôte avec de l'acide azélaïque, un métabolite dont la corrélation avec l'infection est négative, mais positive avec la production de spores impliquées dans la reproduction sexuelle. Les résultats ont montré que le pourcentage d'hôtes infectés par un seul parasite a diminué avec 200  $\mu\text{M}$  de ce composé après 8 heures, sans effet notable après 24 heures. Bien que ces résultats aient soulevé des questions méthodologiques, ils ont clairement révélé un mécanisme de défense potentiel que l'hôte dinoflagellé utilise contre le parasite.

Dans le dernier chapitre de cette étude, nous avons examiné la capacité chimiotactique des dinospores d'une souche de ce parasite. La survie de ce parasite obligatoire dépend en grande partie de sa capacité à localiser un hôte compatible. Pour cela, nous avons utilisé le *test de chimiotaxie in situ* (ISCA) pour créer des micro-gradients d'extraits chimiques provenant de l'hôte. Les dinospores ont montré des réponses chimiotactiques modérées mais significatives, ce qui représente une étape préliminaire pour comprendre comment le parasite parvient à rejoindre son hôte et ainsi initier le processus d'infection.

Dans l'ensemble, cette thèse de doctorat apporte un nouvel éclairage sur la biologie d'un parasite largement répandu mais encore méconnu. La description des différentes spores nous permet de mieux comprendre son cycle de vie et ses capacités en matière de reproduction sexuelle, même si les modalités précises de cette reproduction restent à découvrir. Il serait bénéfique d'établir un contrôle total en laboratoire pour favoriser la production majoritaire de ces spores sexuées en vue de futures recherches.

Ce travail ouvre de nombreuses perspectives. Nous avons constaté que ce modèle de parasite est particulièrement intéressant pour améliorer notre compréhension de phénomènes majeurs tels que la reproduction sexuelle, la communication chimique, les interactions avec l'hôte et la modulation de la virulence au sein du plancton marin. Les bases de données recueillies au cours de cette thèse, notamment en transcriptomique et en métabolomique, offrent des informations précieuses, bien que leur potentiel demeure largement sous-exploité. Malgré certaines limites techniques, les progrès dans le domaine de la cytométrie en flux et de la microfluidique ont contribué à surmonter certains de ces obstacles et devraient continuer à le faire à l'avenir.

## Résumé

La communication chimique, impliquant la production et la détection de signaux moléculaires, joue un rôle essentiel dans les interactions entre les espèces. Cette communication est cruciale pour des fonctions telles que l'attraction sexuelle, la délimitation du territoire, la recherche de nourriture et la défense. Au cours de cette thèse, nous avons exploré cette communication entre un parasite répandu au sein du plancton marin, mais encore mal compris, *Amoebophrya ceratii*, et son hôte, *Scrippsiella acuminata*, un dinoflagellé capable de produire des efflorescences colorées. Ce parasite est un modèle intéressant car il tue inévitablement son hôte pour accomplir, en moins de deux jours, son cycle infectieux, et possède un spectre d'hôte très restreint.

Ce travail de thèse s'est initialement concentré sur l'étude du stade libre du parasite. Le premier chapitre révèle l'existence de deux types de spores, l'une infectieuse et l'autre dédiée à la reproduction sexuée. Nous montrons également qu'une cellule hôte infectée produit un type unique de spore, et que le déterminisme de produire l'une ou l'autre de ces spores est certainement induit bien avant l'infection. Le deuxième chapitre décrit les changements métaboliques chez les parasites pendant l'infection, suggérant un potentiel mécanisme de défense de l'hôte. Le troisième chapitre évalue la capacité chimiotactique des spores, une étape cruciale pour l'infection par l'utilisation de la microfluidique.

Dans l'ensemble, cette thèse apporte de nouvelles perspectives sur la biologie de ce parasite, mettant en lumière des aspects clés de sa biologie, de sa communication chimique, et de son interaction avec les hôtes. Elle a généré énormément de données qui restent encore à exploiter, ouvrant la voie à des recherches futures pour mieux comprendre la reproduction sexuée, la chimiotaxie et d'autres aspects de la biologie de ces parasites dans le plancton marin.

# Abstracts

Chemical communication, involving the release and detection of signaling molecules, plays a crucial role in species interactions. This communication is essential for functions such as sexual attraction, territory marking, food foraging, and defense. In this thesis, we have explored this communication between a widespread yet poorly understood parasite, *Amoebophrya ceratii*, and its host, *Scrippsiella acuminata*, a dinoflagellate capable of producing colorful blooms. This parasite is an interesting model as it inevitably kills its host to complete its infectious cycle in less than two days and has a very limited host range.

This thesis first focused on studying the free-living stage of the parasite. The first chapter reveals the existence of two types of spores, one infectious and the other dedicated to sexual reproduction. We also demonstrate that an infected host cell produces a unique type of spore, and the determinism to produce one type or the other is certainly induced well before infection. The second chapter describes metabolic changes in parasites during infection, suggesting a potential host defense mechanism. The third chapter evaluates the chemotactic ability of spores, a crucial step for infection, using microfluidics.

Overall, this thesis provides new insights into the biology of this parasite, shedding light on key aspects of its biology, chemical communication, and interactions with hosts. It has generated a wealth of data that remains to be further explored, paving the way for future research to better understand sexual reproduction, chemotaxis, and other aspects of the biology of these parasites in marine plankton.